Novel dimeric aporphine alkaloids from the West African

medicinal plant, *Enantia chlorantha* are potent anti-trypanosomal agents.

Thesis submitted by

Adesokan, Adedapo (MD, MSc)

In fulfilment of the requirements of the Degree of Doctor of Philosophy,

Institute of Cardiovascular and Medical Sciences,

College of Medical, Veterinary and Life Sciences,

University of Glasgow.

Matriculation number: 0808123a

January 2015.

Supervisors: Prof Matthew Walters (University of Glasgow)

Prof Alexander I. Gray (SIPBS, University of Strathclyde)

Dr John Igoli (SIPBS, University of Strathclyde)

Declaration of originality and copyright

Adesokan, Adedapo (2014) Novel dimeric aporphine alkaloids from the West African medicinal plant, *Enantia chlorantha* are potent anti-trypanosomal agents (PhD thesis). Copyright and moral rights of this thesis are retained exclusively by this author.

The author of this thesis declares that this thesis does not include work forming part of a thesis presented for another degree other than his Master's degree thesis of the University of Glasgow Adesokan (2009), without proper citation. All details presented represent the author's own work except when referenced to others *for example the first part of Molecular modelling studies was done in India by Rajeev K Singla of the Netaji Subhas Institute of Technology, India. The second part was supervised by Dr Blair Johnston, Dr Murray Robertson and Dr Nahoum Anthony of SIPBS, University of Strathclyde with hands-on efforts by the author using their software under guidance to model the "alkaloids" ligands and protein targets. Normal Phase HPLC studies were carried out by Gavin Bain with the author by his side having prepared the samples and solutions , dither to for Reveleris chromatography, Reverse phase HPLC, Flash Chromatography,anti-parasitic activity studies, NMR Mass Spectroscopy studies   and several chromatographic techniques employed in this study, were either done by the author with guidance or in cases where specialised equipment were used by Post-doctoral scholars and technicians (as detailed in the acknowledgements on the next page) with the author engaging hands-on.*

 This thesis complies with the regulations set for the degree of Doctor of Philosophy by the University of Glasgow. The copyright of this thesis belongs to the author under the terms of the UK Copyright Acts as qualified by the University of Glasgow. Due acknowledgement must always be made when referring to any material within or derived from this thesis.

I confirm this has a word count of about 40,150 words in 258 pages complying with the 255-360 pages as required by the University of Glasgow.

Adedapo Adesokan.

Institute of Cardiovascular and Medical Sciences,

College of Medical, Veterinary and Life Sciences,

University of Glasgow, G12 8QQ Scotland, United Kingdom.

2015.

sourced for the herb for this study. To my loving and caring Dad, Professor Ayoade Adesokan and my late mum Mrs Funke Adesokan I dedicate this thesis for their unconditional love, support and encouragement all through my life. My loving wife Dr Yetunde Adesokan I can't say thank you enough for your moral support, unrelenting care and love. To my wonderful family I am most sincerely grateful, THANK YOU ALL!!

CONTENTS

Chapter 2: MATERIALS AND METHODS

List of Tables

List of Figures

List of abbreviation

1D   One Dimensional Nuclear magnetic Resonance Spectroscopy

2D   Two Dimensional Nuclear magnetic Resonance Spectroscopy

3D   Three dimensional space

CC   Open Column Chromatography

$CDCl_3$ Deuterated Chloroform

COSY   Correlation Spectroscopy

DMSO-d_6 Deuterated dimethyl sulfoxide

ESI MS

Electrospray Ionisation Mass Spectroscopy

FC   Flash Chromatography

HAT   Human African Trypanosomiasis

HMN Heptamethylnonane granules

LDL Low Density Lipoproteins

MIC Minimum Inhibitory Concentration

NCE New clinical entities

NMR Nuclear Magnetic Resonance

PDB Protein Data Bank

RP Reverse Phase column Chromatography with C-18

SSA   Sub-Saharan Africa

UV Ultraviolet light

VLC Vacuum Liquid Chromatography

Summary

This thesis describes the isolation, structure elucidation, anti-trypanosomal activity and molecular modelling of the aporphine alkaloids obtained from *Enantia chlorantha.*

Phytochemical studies on the *Enantia chlorantha* stem bark yielded six dimeric and one monomeric aporphine alkaloid along with one protoberberine type alkaloid, palmatine. Three dimeric aporphine alkaloids were novel namely: 1,1',2,2',3-pentamethoxy-6-methyl-5,5',6,6'-tetrahydro-4H,4'H-7,7'-bidibenzo[de,g]quinoline, **ECP-19** (**89**),8-(1,2,3-trimethoxy-5,6-dihydro-4H-dibenzo[de,g]quinolin-7-yl)-6,7-dihydro-5H-[1,3]dioxolo[4',5':4,5]benzo[1,2,3-de]benzo[g]quinoline, **ECHE-45** (**90**), and 7-methyl-8-(1,2,3-trimethoxyl-5,6-dihydro-4H-dibenzo(*de,g*)quinolin-7-yl)-6,7-dihydro-5H-(1,3)dioxolo(4'5':4,5)benzo(1,2,3-d*e*) benzo(*g*)quinoline **ECH-56** (**91**). The structures of the alkaloids were determined using 2D NMR experiments and their masses confirmed using ESI Mass Spectrometer.

Anti-trypanosomal screening of these alkaloids for activity against the non-virulent bloodstream form of *T.brucei brucei* ,carried out using a modified microplate Alamar blue ™ assay revealed that these alkaloids had excellent anti-trypanosomal activity, with MICs 1.27 to 10.96 nanomolar compared to the positive control Suramin with MIC of 9.6 nanomolar. Of the three novel dimeric alkaloids, ECP**-19** (**89**) was the most active with MIC of 1.27 nanomolar.

Molecular modelling was carried out for all of these alkaloids as well as their derivatives monomeric aporphine alkaloids using the GRIP technique with Vlife molecular Design Suite (V life MDS 4.2) on seven validated *Trypanosoma brucei* protein targets from the Protein Data Bank (PDB). These protein targets were: *T. brucei Glutathione Synthetase , Glutathione peroxidase-type tryparedoxin peroxidase,* oxidized form ,*Glutathione peroxidase-type tryparedoxin peroxidase,* reduced form *, Sterol 14-alpha demethylase (CYP51)* from *T. brucei* in complex with the *tipifarnib derivative 6-(4-chlorophenyl)(methoxy)(1-methyl-1H-imidazol-5-yl)methyl)-4-(2,6-difluorophenyl)-1-methylquinolin-2(1H)-one , T. brucei Ornithine Decarboxylase , Riboflavin kinase ,*and *Trypanothione reductase* from *T. brucei.*

The inhibition of *T. brucei ornithine decarboxylase* was the most significant, hence the possibility of it being a likely mechanism of action for these alkaloids. Further molecular modelling studies of the eight alkaloids whose structure were elucidated in this thesis, as well as six derivate monomeric alkaloids were carried out to pinpoint the "best fit "alkaloids to *Ornithine decarboxylase's* active site Lysine 69 using the GOLD 5.5.2 software. This revealed the dimeric aporphine alkaloids isolated in this study had docking score as a function of GOLD.PLP.Fitness which ranged from -95.1384 to 27.8819 for dimers,which is not as good as the docking scores ranging from 26.5959 - 38.4616 for monomers

isolated in this study, as well as monomeric derivatives of the dimers. Derivative monomer, Compound 95 had the best docking score of 38.4616.

This set of results in terms of the novelty of the dimeric alkaloids, their excellent anti-trypanosomal activity *in vitro*, significant results in molecular models and the fact that anecdotal evidence of use of *Enantia chlorantha* extracts *in vivo* for treatment of ailments traditionally in rural West Africa for centuries may form a basis for further drug development studies. As it is the norm in drug discovery synthetic analogues developed from a natural product scaffold tend to provide a vast number of molecules to test and develop further, therefore future molecular modelling studies are currently being tailored to optimising the "best fit" monomeric alkaloids to hybrid modelled synthetic analogues for further drug development studies beyond the scope of the PhD study.

Introduction

Humans have since time immemorial relied on nature to cater for their basic needs, including traditional medicines for the treatment of a wide variety of diseases. Plants, most especially, have formed the basis of age-long traditional medicine systems. Newman et al., (2000) reported the people of Mesopotamian times recorded use of drugs using clay tablets in cuneiform writings around 2600 BC. Among which were *Cedrus* species (cedar) and *Cupressus sempevirens* (cypress) oils, *Glycyrrhiza glabra* (licorice),*Commiphora* species (myrrh), and *Papaver somniferum* (poppy juice), all of which are still used today in traditional medicine for the treatment of ailments ranging from coughs, colds to parasitic infections and inflammation. Newman et al., (2000) also documented the Egyptians reported Pharmaceutical agent called "Ebers Papyrus" from 1500 BC comprising of over 700 medicines. Also in India as far back as 1000 BC writings of Indian Ayurvedic medicine reported 394 Charaka medicines and 516 Sushruta medicines according to Kapoor (1990). The Chinese Materia Medica documented records dating from about 1100 B. C. by Wu Shi Er Bing Fang, containing 52 medicines, followed by works such as the Shennong Herbal at about 100 B. C containing 895 drugs and the Tang Herbal 659 A. D containing 850 drugs as reported by Huang (1999).

More recently, the Greeks and Romans contributed immensely to the use of herbal drugs in the ancient western world. Dioscorides, a Greek physician (100 CE), documented the collection, storage, and use of medicinal herbs during his travels with Roman armies throughout the then "known world", whilst Galen (130–200 CE.), a practitioner and teacher of pharmacy and medicine in Rome, was well known for his complex prescriptions and formulae used in compounding medicines according to NIH report (2002).

West Africa, the westernmost part of Africa comprises of seventeen countries namely Benin, Burkina Faso, Cape Verde,Cote d'Ivoire,Gambia, Ghana, Guinea, Guinea-Bissau, Liberia, Mali, Mauritana, Niger, Nigeria, Island of Saint Helena, Senegal, Sierra Leone, Sao Tome and Principe, Togo. *Enantia chlorantha* also known as "African Yellow Wood" is a dense forest tree found in the coastal and rainforest areas of several of the listed West Africa countries.

Human African Trypanosomiasis (HAT) comprises of two forms: *T.brucei gambiense* which is found in Western and Central Africa, *T.brucei rhodesiense* in Eastern and Southern Africa. There is also the South American variety known as Chagas disease. They continue to place a huge health burden on millions of lives in Sub-Saharan Africa, North and Latin American countries. Present treatment regimens are hardly effective and saddled with severe adverse side effects; hence the need for new therapeutic agents to combat this deadly scourge, one from natural sources such as *Enantia Chlorantha* could be a

possible option. It is a medicinal herb that belongs to the family Annonaceae, which has been in traditional use in West and Central Africa for several centuries.

1.1. Aims and objectives of the study

Aims and Objective of the study

Research aims

To investigate the phytochemistry and bioactivity of compounds derived from traditional Nigerian medicine herb, *Enantia chlorantha* known for its potential anti-parasitic traditional uses in Africa using various chromatographic separation and molecular modelling techniques.

Objectives

1. To test the initial extracts for anti-cancer, anti-parasitic, and anti-microbial activity to decipher which activity the extracts have, this turned out to be anti-trypansomal with no carcinogenic activity, see Masters' thesis summary in the appendix.

2. To determine which class of bioactive compounds among tannins, fats, alkaloids, flavonoids, sugars and saponins had the anti-trypanosomal activity of interest, this turned out to be the alkaloids.

3. To use a bioassay guided approach in isolating alkaloids obtained from *Enantia chlorantha*, by testing the extracts as well as alkaloids obtained from the extracts for their anti-trypanosomal properties. An earlier study on *Enantia Chlorantha* was carried out on aqueous extracts, Adesokan *et al.,* (2007*)* investigated the anti-bacterial effects of the stem bark extract on *Staphylococcus aureus, Bacillus subtilis*, *Escherichia coli*, *Salmonella typhi* and *Pseudomonas aeruginosa.* However aqueous extracts tend to be non-specific in extraction of compounds, thus necessitating a gradient approach for extraction based on polarity of constituents. Hexane extracted the non-polar compounds; ethyl acetate extracted the medium polar compounds, while methanol extracted the highly polar compounds.

4. To see if there is variation in types of alkaloids isolated based on season of collection of the plant materials. It is a known fact among traditional herbalists in Africa and Amazon that their herbs tend to contain different bioactive extracts at different time of the year . This is based on the premise that different parasites, weather or similar challenges are poised at different times of the year. In response to these different kinds of stress, plants are known to synthesize different bioactive substances for survival based on seasonal variation. Thus this study was tailored along similar lines to see if there were differences in the kinds of compounds isolated in plant materials collected in summer, compared to those collected in winter.

5. To use different separation techniques to attempt to purify the alkaloids obtained from the *Enantia chloratha* extracts. The intention was to try several methods to see those that would yield the purest fractions for further bioactivity studies

6. Subject the isolated bioactive alkaloids to molecular modelling studies to determine which one were best bound to protein trypanosomes targets . We modelled the alkaloids ligands against several protein targets, picked the best of the lot of the protein targets in terms of binding affinity and proceeded to further model the alkaloids and their derivative alkaloids to see which ones would have the best fit into the pocket of the active site of the most actively bound protein trypanosomes target, *Ornithine decarboxylase.*

7. To attempt to optimise the best docked "best perfect fit" alkaloid (ligand) into the active site of *Ornithine decarboxylase* (Lysine 69) to generate hybrid alkaloid(s) for synthesis and further in-vivo activity and pharmacokinetics studies.

Thus these lead bioactive alkaloids isolated in this study could serve as leads with potential to treat human diseases. This is especially in the area of antimicrobials and anti-parasitic agents in the face of common evolving drug resistance and intolerable severe side effects of presently available treatment regimens especially for neglected diseases like HAT (see section 1.11 on page 53 for more information on present drugs for treating HAT).

Study's step-wise action plan in a flowchart

Extraction from plant material using the soxhlet extractor

⇓

Various anticancer, antimicrobial, and anti-parasitic activity testing of extracts for activity

⇓

Isolation of bioactive compounds from *Enantia chlorantha* extracts.

⇓

Structure elucidation and molecular weights determination using NMR and Mass Spectroscopy.

⇓

Purification of the isolated alkaloids using various chromatographic techniques and subsequent anti-trypanosomal activity testing

⇓

Molecular modelling and other Translational Chemistry approaches to define drug targets in terms of most potent alkaloid's binding affinity for proven anti-trypanosomal enzyme target(s).

⇓

*Synthesis of the novel modelled lead compounds and analogues

⇓

*In-vivo parasitized mouse model activity studies

⇓

*Further parasitic activity screening looking at the synthesized compounds activity against a variety of parasitic infections bioassay templates like malaria, leishmaniasis in addition to trypanosomiasis.

⇓

*Pharmacokinetics and lead compounds safety studies using stem cell models to predict the bioactive alkaloids' metabolism and toxicity profile in vivo and vitro (this technology is extremely efficient and is now replacing the laborious use of animals to a large extent in pre-clinical activity, toxicity and pharmacokinetics screening)

*Written in blue beyond scope of the PhD study

1.2 The plant: *Enantia chlorantha*

Enantia chlorantha according to the Thesaurus of Agricultural Organisms (1990) is otherwise known as 'African whitewood'. It is an ornamental tree found in the rainforests of Nigeria, Liberia, and Cote

d' Ivoire, Gabon, Democratic Republic of Congo and Cameroun among others. The tree grows to about 30m high with dense foliage and spreading crown with fluted stem which produces a sulfurous yellow dye as reported by Iwu (1993). It is used locally across Africa to make unpainted furniture and veneers. It is referred to locally by the Nigerian Yoruba tribe as "*Dokita Igbo*" which literally means "Doctor of the forest" due to medicinal use in rural West Africa to treat several ailments. In Nigeria, traditionally it is used in the treatment of malaria as reported by Gbadamosi and Oni (2005).

Gill and Akinwunmi (1986) also reported the use of the infusion of *E. chlorantha* stem bark for the treatment of pulmonary tuberculosis and infected wounds. The stem bark is made up of an inner bark which is bright yellow and an outer cork which is dark brownish.

Figure 1.1 Cork of *Enantia chlorantha* used for the study.

In the 1980s, Virtanen *et al.,* (1988) showed that a mixture of protoberberines from *Enantia chlorantha* had preventive and curative effects on CCl_4- and glucosamine – induced liver injury. Adjanohoun *et al., (*1996) reported the extract's effectiveness in treating jaundice and urinary tract infections. Agbaje and Onabanjo (1998) also documented the potential of *E. chlorantha*stem bark in relieving pyrogen-induced fever *in vivo* in albino rats. Oyewopo *et al.,* (2012) reported the testiculo-protective effect of stem bark extract of *E. chlorantha* on lead induced toxicity in adult wistar rats (*Rattus norvergicus*). It has also been documented by Hutchings *et al.,* (2003) that sick animals tend to forage plants rich in tannins and alkaloids such as *E. chlorantha.*

In the Western world, *E. chlorantha* stem bark extract has been included in dermatologic preparations like Dermalogica Clean Start Kit, cosmetics like Ultra Beauty and anti-acne preparations; this is due to the protoberberine content which act on the pilosebaceous units by inhibiting growth of hair follicles of the face and /or the body.

1.3 **Alkaloids**

 Alkaloids are a class of unique naturally occurring organic nitrogen-containing bases. They are well known for their diversity and role in important plants, animal and humans physiologic functions.

About 3,000 different types of alkaloids have been identified in a total of more than 4,000 plant species. In general these alkaloids belong to unique families notable among them are *Papaveraceae* from which the opium poppy plant was derived, the *Claviceps* from which ergot fungus was obtained. Other are the Ranunculaceae which gave rise to buttercups, *Solanaceae* from which nightshades arise, and *Amaryllidaceae* which gave rise to amaryllis. Few alkaloids have also been reported to be derived from animal species notable examples are New World beaver (*Castor canadensis*) and poison-dart frogs (*Phyllobates*).

Despite been around for umpteenth years the function of alkaloids in plants is still yet to be fully understood. They are believed to serve specific biologic functions, it has been suggested that they are simply waste products of plants' metabolic processes. In some plants, the concentration of alkaloids increases just prior to seed formation and then drops when the seed is ripe, suggesting that alkaloids may play a role in this process. Alkaloids may also protect some plants from being infested by certain parasitic insect species.

In terms of chemistry the structures of alkaloids are extremely variable. Generally, an alkaloid contains at least one nitrogen atom in an amine fashion, that is one derived from ammonia by replacing hydrogen atoms with hydrogen-carbon groups called hydrocarbons. This or another nitrogen atom can be active as the base in acid-base reactions. The name alkaloid ("alkali-like") was originally used because they react with acids as bases to form salts. Most alkaloids have one or more of their nitrogen atoms as part of a ring of atoms in cyclic systems. Alkaloid names generally end in the suffix -ine, a reference to their original chemical classification as amines. In their pure form most alkaloids are colourless, non-volatile, crystalline solids. Majority of them tend to have a bitter taste.

The first alkaloid to be isolated and crystallized was morphine (1) in 1804 as the potent active constituent of the opium poppy plant.
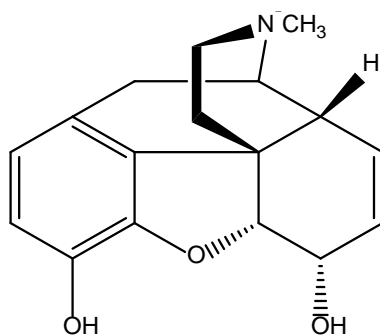
(**1**)

Alkaloids are generally are classified based on of their chemical structures. For example Indole alkaloids contain a ring system are known as Indole (2).
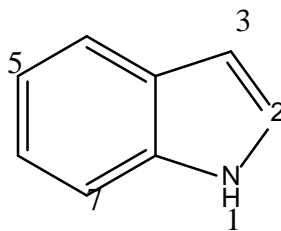
(**2**): Indole core of alkaloids

On this basis, other notable principal classes of alkaloids are the pyrrolidines, pyridines, tropanes, pyrrolizidines, isoquinolines, indoles, quinolines, and the terpenoids and steroids.

Alternative means of classification of alkaloids is along the biological system in which they occur. For example, the opium alkaloids occur in the opium poppy (*Papaver somniferum*).

Despite belonging to the same class of compounds alkaloids are known to have diverse biologic functions. Morphine (1) is a powerful narcotic used for severe pain relief but used with caution because of its addictive and sedating properties. Codeine (3) is a methyl ether derivative of morphine, it is an excellent analgesic however is non-addictive.
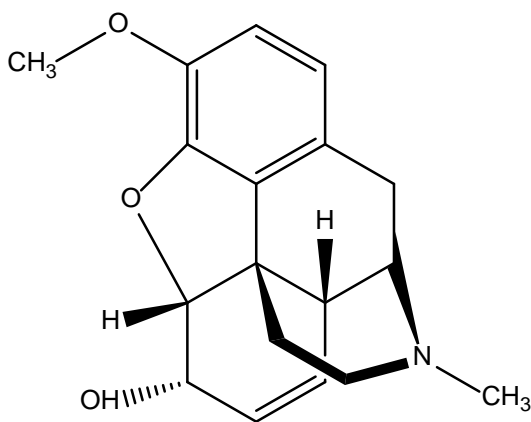
(**3**)

Certain alkaloids are used clinically as cardiac or respiratory stimulants. Quinidine (4) from the plant genus Cinchona is used to treat arrhythmias.
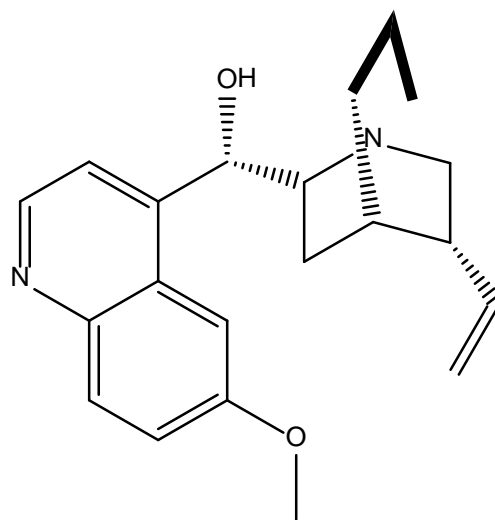
(**4**)

Ergonovine also known as Ergometrine (**5**) is used to reduce uterine haemorrhage after childbirth was derived from the fungus Claviceps *purpurea* and Ephedrine (**6**) used in many anti-cold preparation was derived from *Ephedra* species, both have vasoconstriction properties. Ephedrine (**6**) is commonly used to relieve the discomfort of common colds, sinusitis, hay fever, and bronchial asthma.
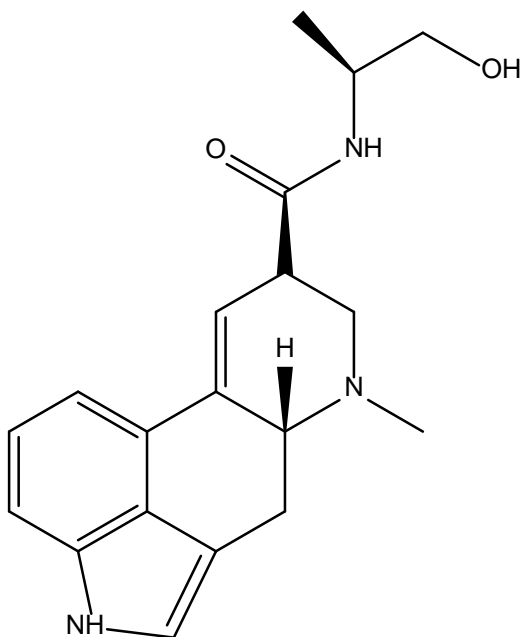
(5)
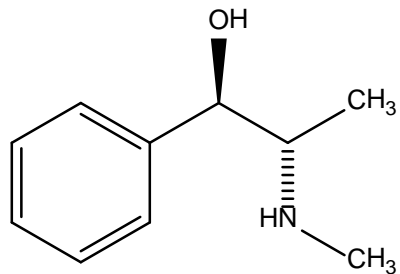
(**6**)

Many alkaloids possess local and general anaesthetic properties, though clinically they are seldom used for this purpose. D-tubocurarine (7) derived from South American poison curare, is used as a muscle relaxant in surgery. Quinine (8) derived from *Cinchona* species is a powerful antimalarial agent especially in the paediatric age group, though this has been largely replaced by Artemisinin based Combination Therapy (ACT). Vincristine (9) and Vinblastine (10) from *Vinca rosea* are widely used as chemotherapeutic agents in the treatment of breast, ovarian and other types of cancer.

(**7**)

[25]

(**8**)

(9)

[26]
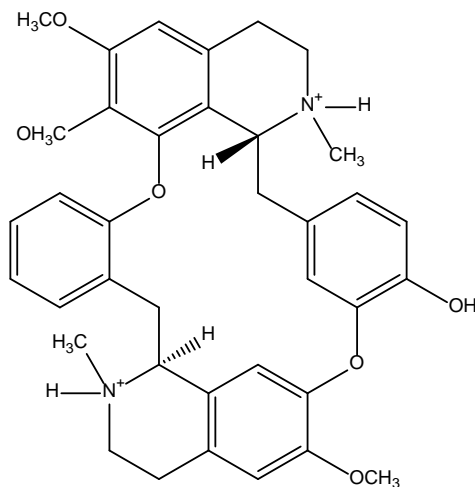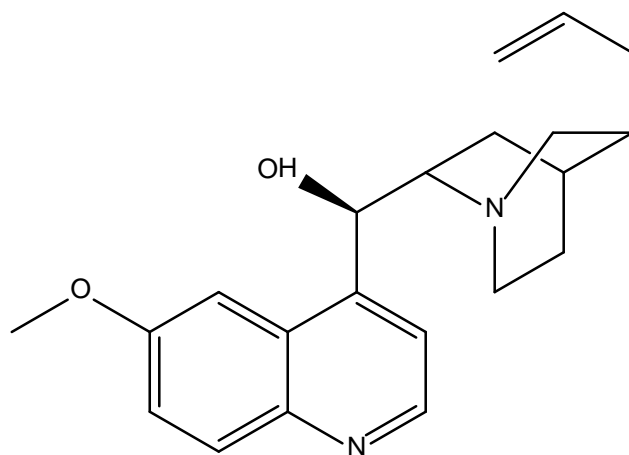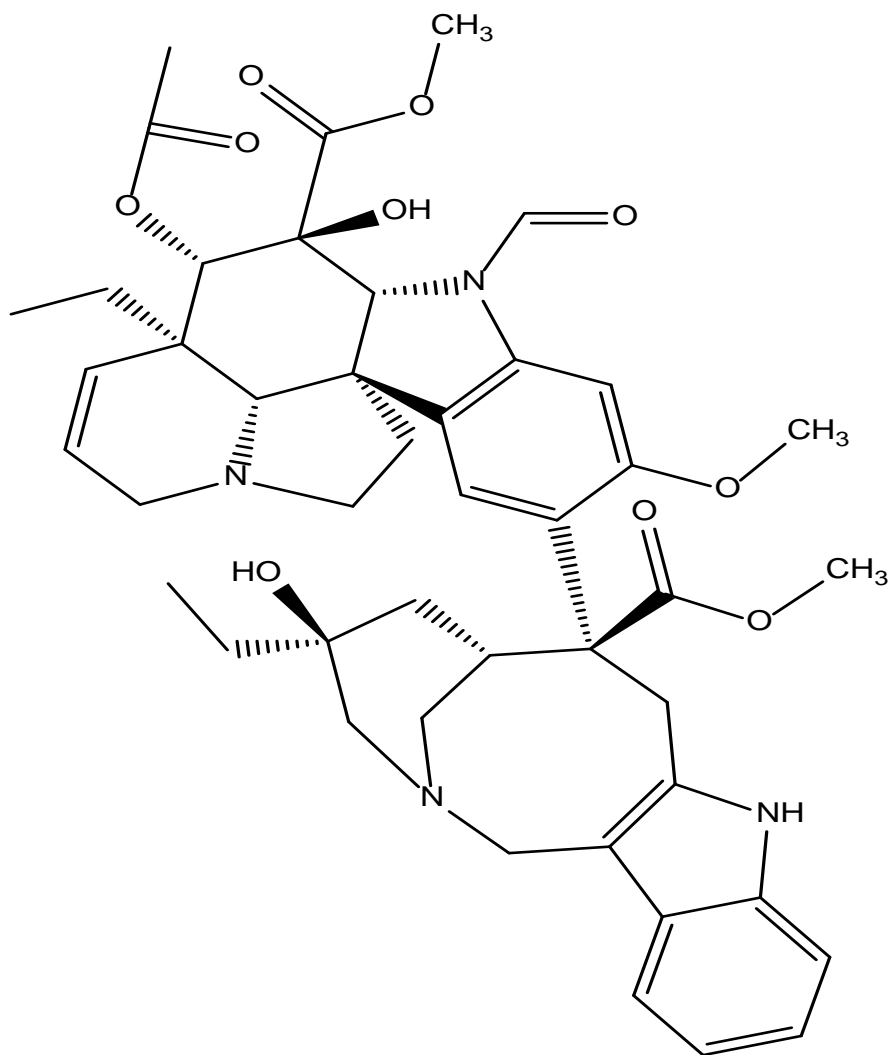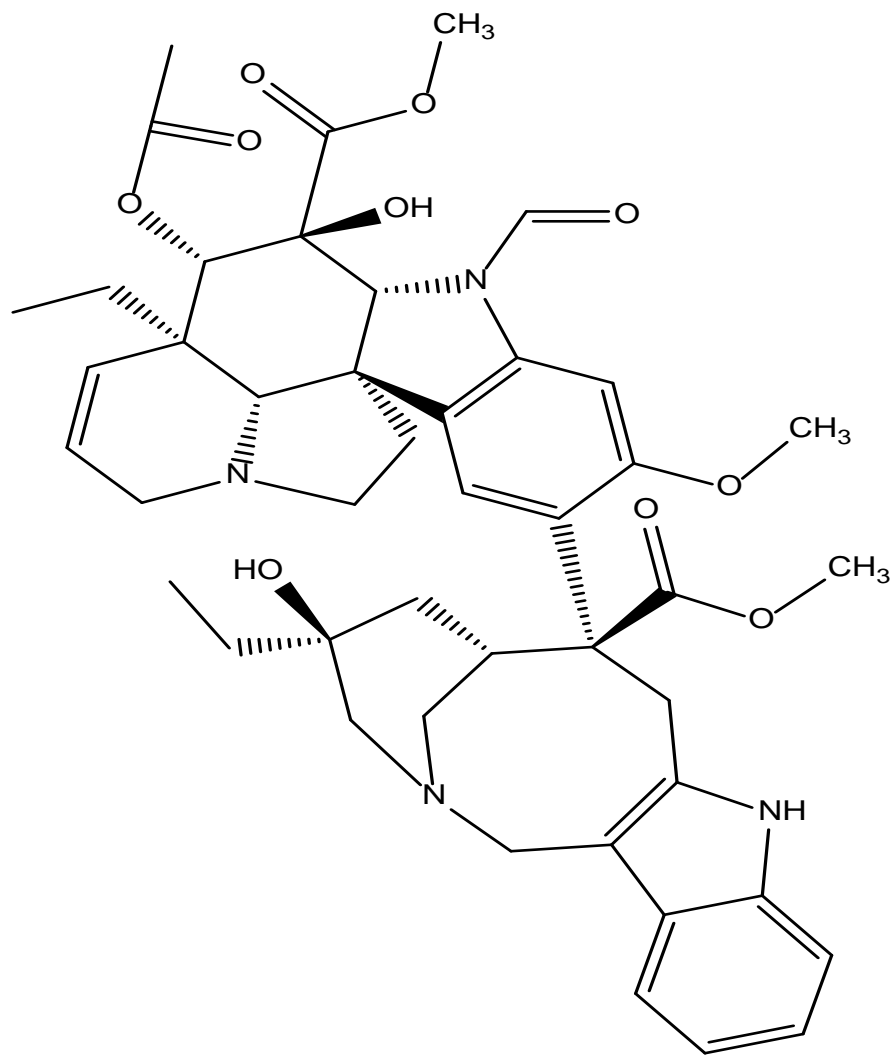
(**10**)

The tobacco plant (*Nicotiana tabacum*) gave rise to Nicotine (11), which is the principal alkaloid and chief addictive ingredient of the tobacco smoked in cigarettes, cigars, and pipes. This unique molecule contains both pyridine benzene-like and pyrrolidine ring as shown below in Compound 11.
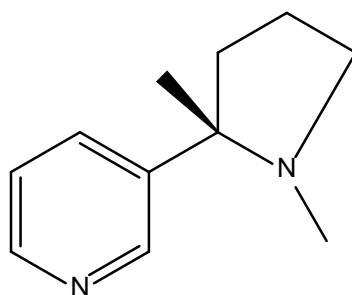
(**11**)

[27]

Some alkaloids are well known illicit drugs, these include the hallucinogenic drugs such as mescaline (12) from *Anhalonium* species and psilocybin (13) from *Psilocybe mexicana*. Synthetic derivatives of the alkaloids morphine (1) and lysergic acid (14) were derived from *C. purpurea* which gave rise to heroin (15) and LSD (14) respectively.

(**12**)

(**13**)

(**14**)

[28]
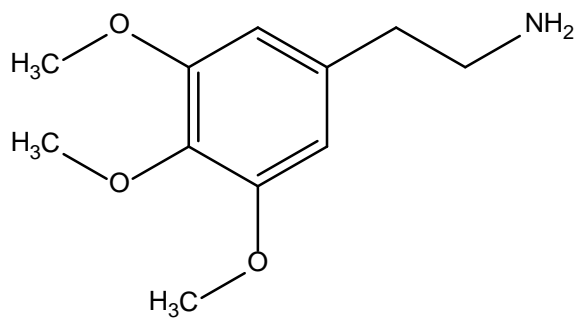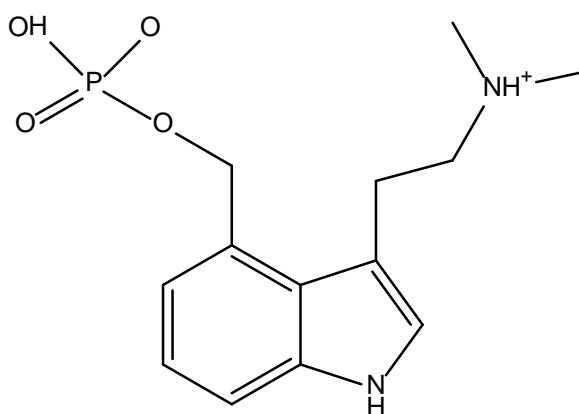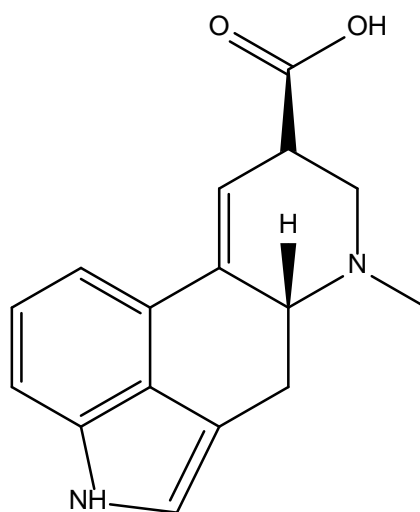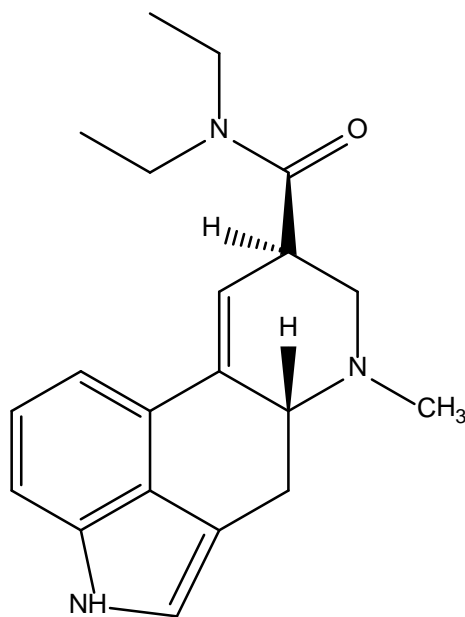
(**15**)

In terms of monomeric alkaloids common classes include:

1. Pyrrolidines (16) a good example is Strachydrine (17)

(**16**)

(**17**)

[29]
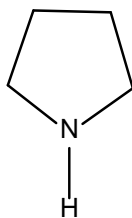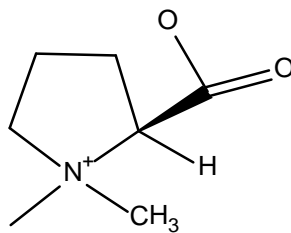
2. Tropane derivatives (18) good examples are the common used drug to treat symptomatic bradycardia, that is atropine (19) and narcotic cocaine (20)
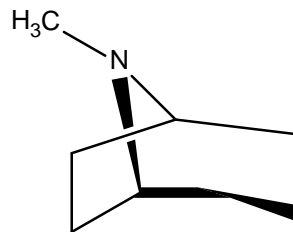
(**18**)
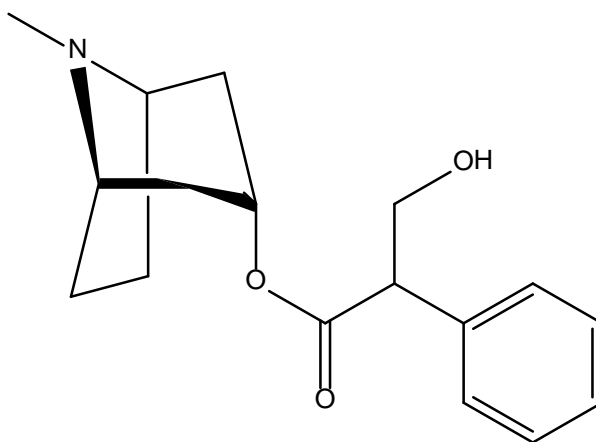
(**19**)
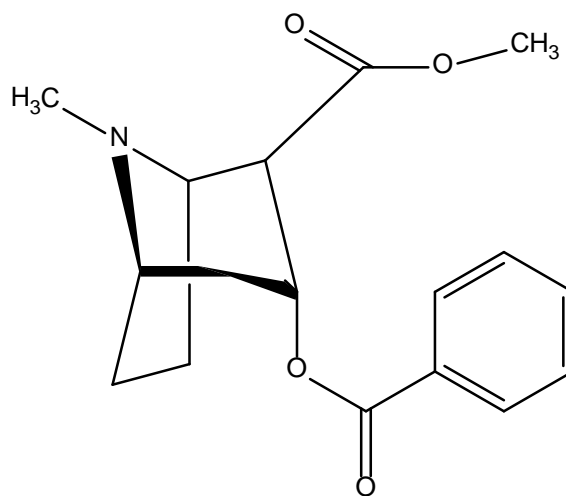
(**20**)

Other monomeric classes include pyrrolizidine derivatives (21), Piperidine derivatives (22), Quinolizidine derivatives (23), Indolizidine derivatives (24), Pyridine derivatives (25), the Isoquinoline (26) which the aporphine alkaloids described in detailed in this thesis belong. Other notable classes are Oxazole derivatives(27),Thiazole derivatives(28), Quinazoline derivatives(29) , Acridine derivatives(30), the Quinoline derivatives(31) to which the antimalarial ,Quinine(8) belongs: oth-

ers are Imidazole derivatives(32), Purine derivatives(33), Colchicine alkaloids(34) to which conventional anti-gout agent colchicine(35) belongs and the Benzylamine derivatives(89) from which analgesic capsaicin(90) cream widely used for knee and hand osteoarthritis was derived.
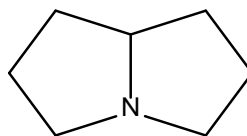
(**21**)
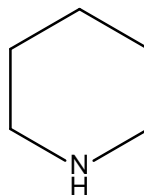
(**22**)
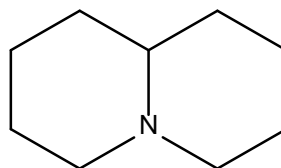
(**23**)
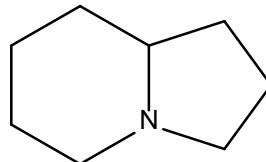
(**24**)
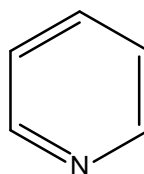
(**25**)
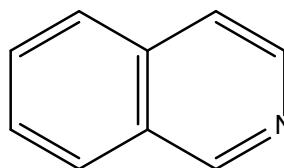
(**26**)

(**27**)

(28)

(29)

(30)

(31)

(32)

(33)

[32]

(34)

(35)

(89)

(90)

[33]
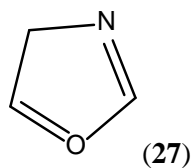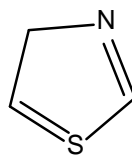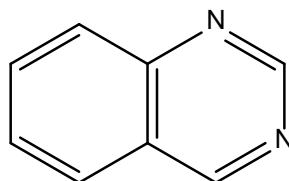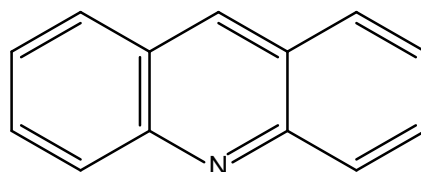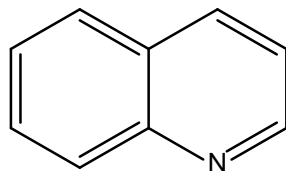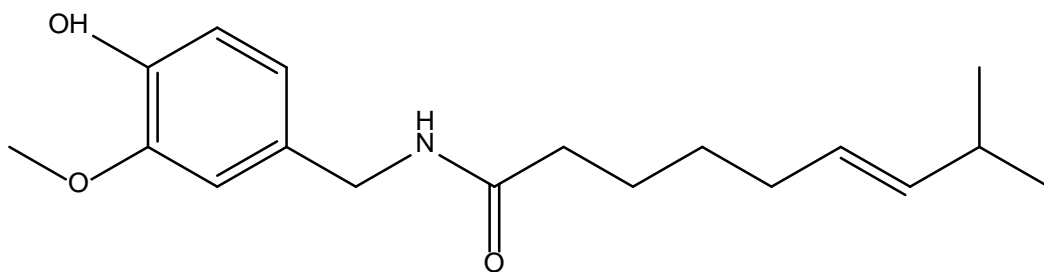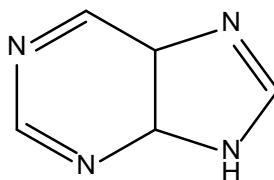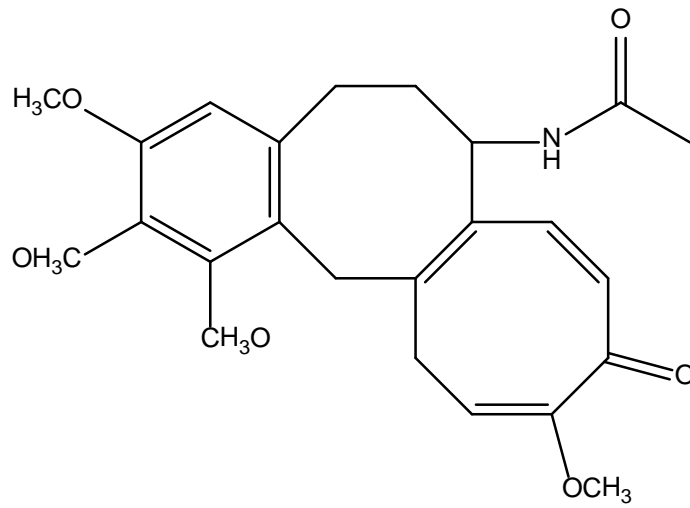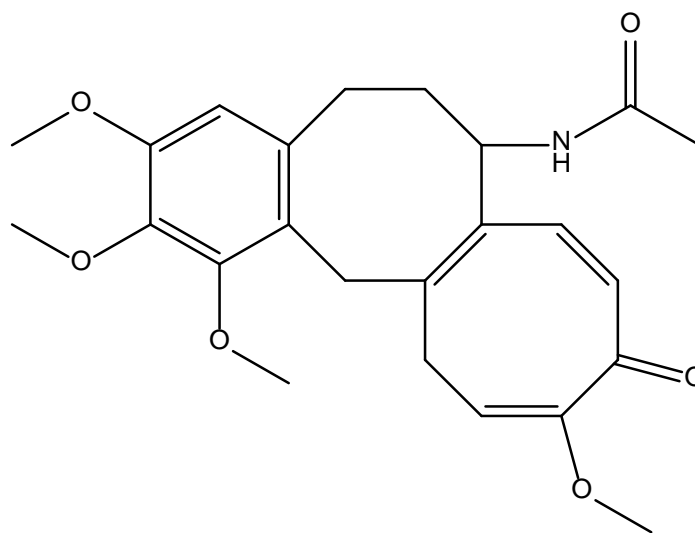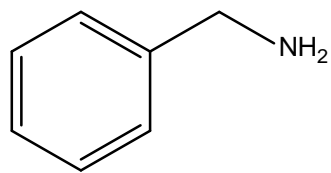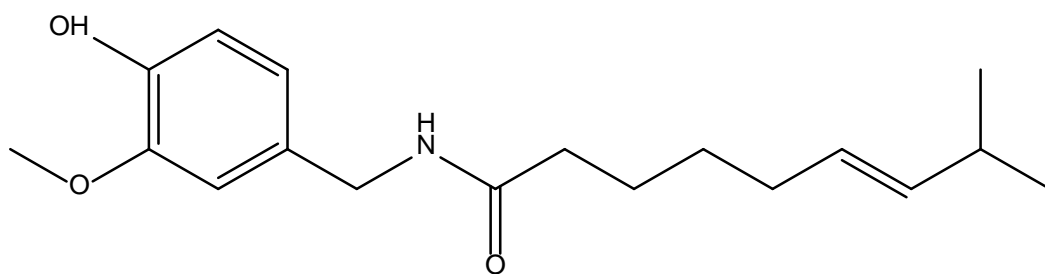
In majority of cases there is need to extract, isolate and purify alkaloids from their plants sources. Special methods have been developed for isolating commercially useful alkaloids. In most cases, plant materials are subjected to extraction in aqueous or appropriate solvent system. The alkaloids are thereafter be separated and purified from the mixture of alkaloids in solution using appropriate separation techniques such as chromatography. Chromatography tend to take advantage of the different degrees of adsorption of the various alkaloids on solid material such as alumina or silica.

Alkaloids are usually obtained in crystalline form using appropriate solvents.

1.4 Alkaloids and activities previously reported from *E. chlorantha* stem bark

A protoberberine alkaloid 7, 8 -dihydro -8-hydroxy palmatine (**91**) was isolated from *E.*

chlorantha stem bark. It demonstrated some *in vivo* activity against *Helicobacter pylori* in mice as reported by Tan (2000).
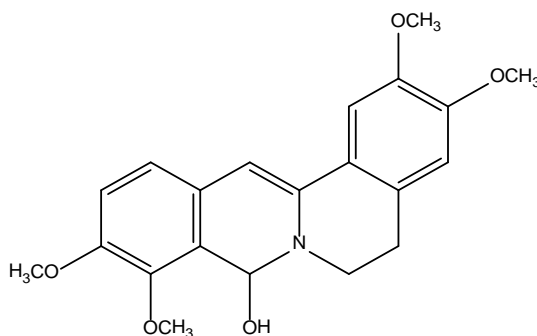
(**91**)

Two aporphine alkaloids; 6a, 7-dihydro-1, 2-dimethoxy-7-hydroxy-*N*-methyl aporphine (**92**) and 6a, 7-dehydro-1, 2-dimethoxy-7-hydroxyaporphine (**93**) were also reported to have been isolated from the stem bark of *E. chlorantha* by Wafo *et.al.* (1999).

(**92**) R= CH₃, (**93**) R=H

[34]
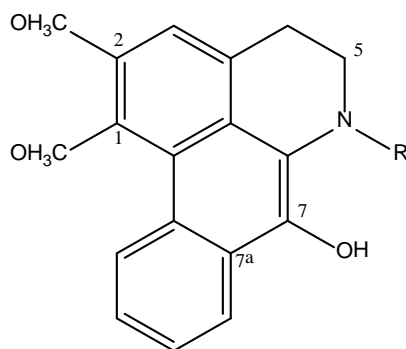
1.5 The Family Annonaceae

The *Annonaceae* is a large family of trees, shrubs or climbers generally pantropic according to Oliver (1868). The *Annonaceae* family comprises of about 130 genera with more than 2,000 species. The family is commonly known for production of isoquinoline type alkaloids, though non-alkaloidal compounds have also been isolated from the family by Yang-Chang Wu (2006) and many others. To the local people where this family species are found economically, it is an important source of edible fruits and oils, as well as raw material for perfumery.

1.6   Reported anti-parasitic properties in *E. chlorantha* protoberberine alkaloids

Palmatine (**41**) and berberine derivatives have been reported to possess anti-leishmanial properties by Vennerstrom *et al.,* (1990).
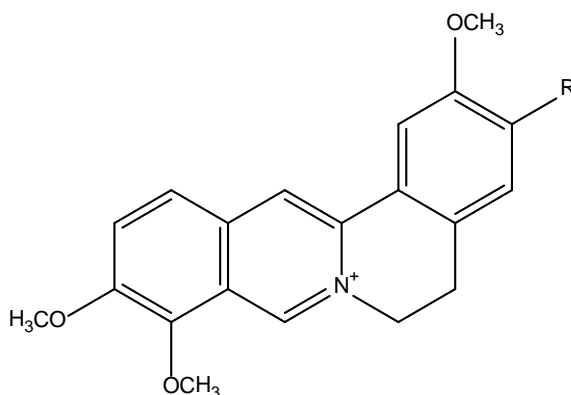
(**941** R= OCH$_3$

(**42**) R= OH

128 plants extracts were screened for anti-leishmanial and anti-trypanosomal activities, isolating proto-berberine-type alkaloids; jatrorrhizine (**42**) and palmatine (**41**) which were found to be active Bahar (2012). Jatrorrhizine (4**2**) has been reported with palmatine to have potent anti-malarial properties Vennerstrom and Klayman (1988). Anti-babesial activity has also been reported Subeki *et al.,* (2005), for palmatine and other protoberberine alkaloids isolated from an Indonesian medicinal plant *Arcangelisia flava* ,used in the treatment of malaria.

1.7 Bisbenzylisoquinolinealkaloids: pharmacological properties

Aporphine alkaloids of the bisbenzylisoquinoline class represent a large group among the Isoquinoline alkaloids. This interesting group of alkaloids comprises of compounds like the Non-

depolrizing neuromuscular blocking agent tubocurarine (**7**) discovered as a toxic alkaloid found to have skeletal muscle relaxant properties, thus it's use in clinical medicine as an adjunct anaesthetic agent in surgery and mechanical ventilation. There are also a wide range of others with important pharmaceutical pharmacological activity like thalicarpine (**43**) an aporphine-benzyltetrahydroisoquinoline alkaloid found to have tumour inhibitory activity Kupchan et al., (1963), tetrandrine (**44)** and cepharanthine (**45**) as reported by Wu and Huang (2006). Isolated as natural products, this group of alkaloids as leads have led to synthesis of much improved analogues in clinical use today such as atracurium (**46**).

Atracurium (**46**) was synthesized in 1981 by Stenlake and his colleagues at the University of Strathclyde Stenlake *et. al.,* (1981).
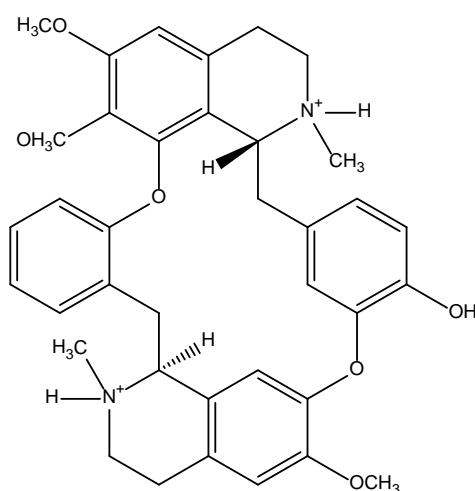
(**7**)
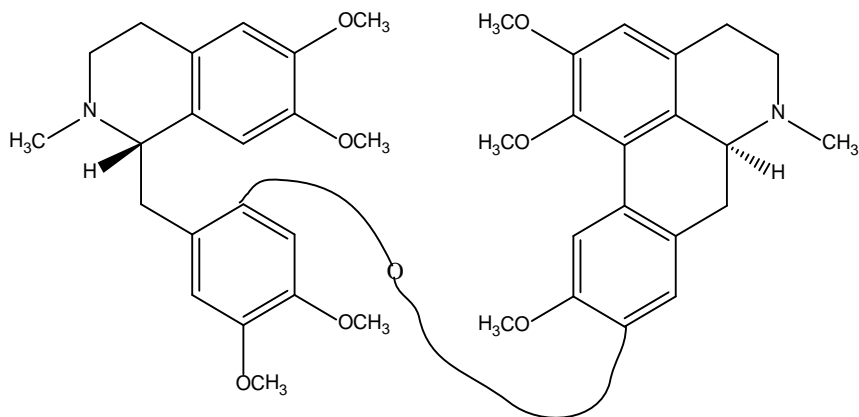
(**43**)
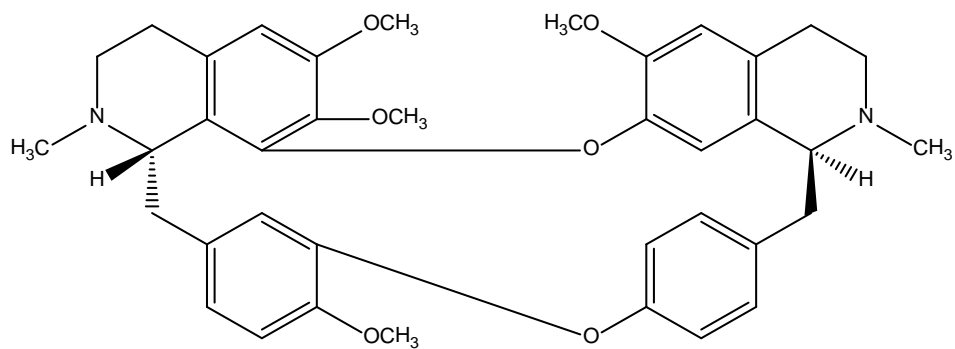
(**44**)
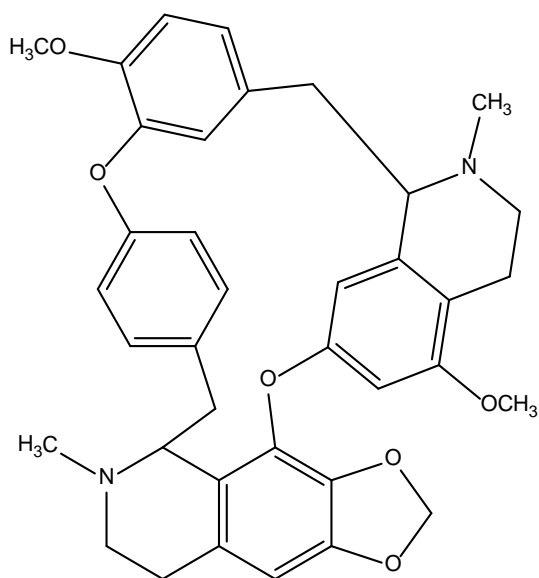
(**45**)
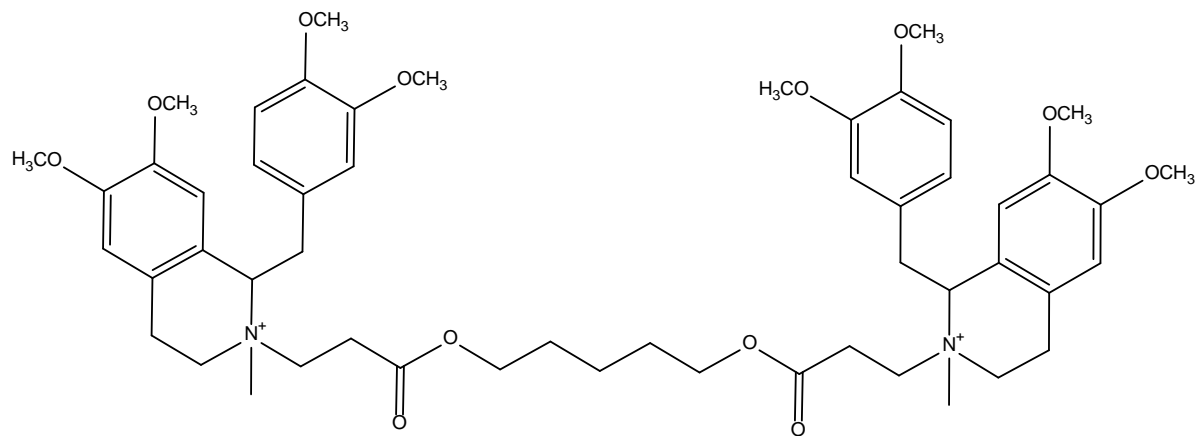
(**46**)
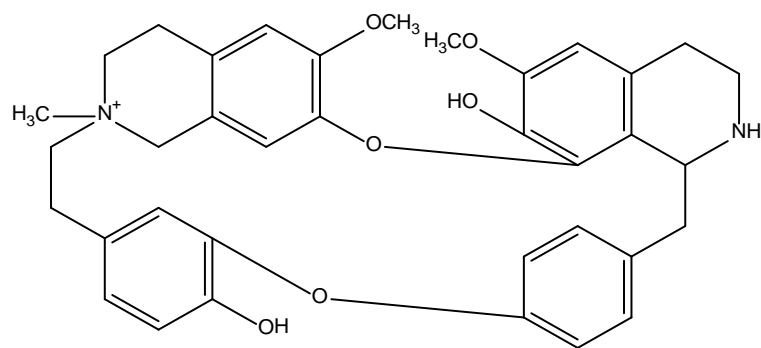
(**47**)

Other notable bisbenzylisoquinolines like daphnoline (**47**) and an anti-parasitic agent benznidazole (**48**) have been reported as active against *Trypanosoma cruzi* through *trypanothione reductase* inhibition by Fournet *et al.,* (2000).
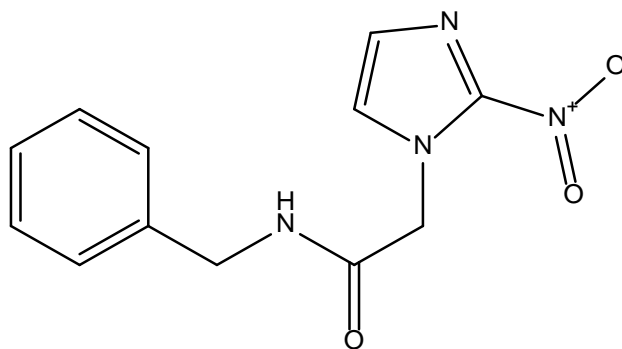
(**48**)

Several other bisbenylisoquinolines have been reported with skeletal muscle relaxant, anti-inflammatory, platelet aggregation inhibition and antimicrobial properties by Schiff (1987).

1.8 Natural products in drug discovery

The World Health Organisation (WHO) 2008 states that approximately 25% of modern drugs used in the United States of America were developed from plants. It is worthy to note that many drugs in

clinical use today are from natural products. Examples include digoxin (**49**) obtained from foxglove (*Digitalis lanata*) for treatment of cardiac arrhythmia and congestive heart failure.
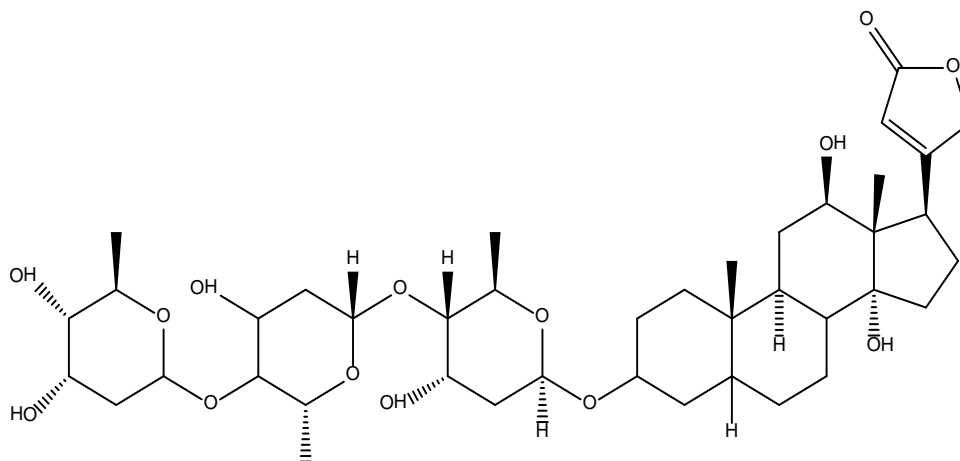
(**49**)

Morphine from the Opium poppy plant, *Papaver somniferum* is clinically used for alleviating severe pain (**1**). Malaria remains a global health challenge with its huge mortality and morbidity profile. The isolation of the antimalarial drug, Quinine (8) from the bark of *Cinchona officinalis*, was reported in 1820 by the French pharmacists, Caventou and Pelletier, however cinchona's bark have documented to in use by indigenous people in the Amazon region for the treatment of fevers for a long time, and was

in early 1600s first introduced into Europe for the treatment of malaria. Subsequently Quinine (8) formed the basis for the synthesis of the commonly used antimalarial drugs, chloroquine (**50**) and mefloquine (**51**) which largely replaced Quinine (8) in the mid-20th century as reported by Wongsrichanalai et al.,(2002). However due to the emergence of resistance, another plant long used in the treatment of fevers and malaria in Traditional Chinese Medicine (TCM), *Artemisia annua* gave rise to a new antimalarial Artemisinin (**52**) and its derivatives according to O'Neil and Posner (2004) widely used today in combating resistance in form of ACT (Artemisinin-based Combination Therapy) .
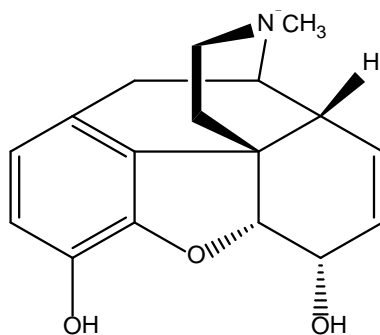
+   (**1**)
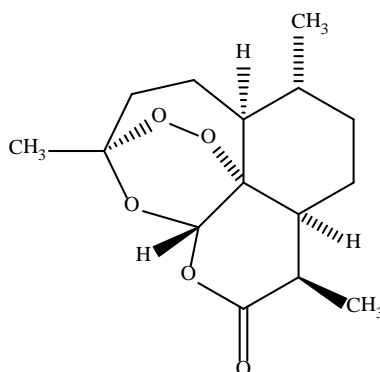
(**52**)

Another good example is paclitaxel (**53**), the anti-cancer agent which was obtained from the Pacific Yew tree , *Taxus brevifolia* as reported by Stierle A *et al*.,(1995). About 56% of the leading compounds used for medicines in the British National formulary (BNF) are either natural products or their derivatives as reported by Pitchaimani (2012). For example, vincristine (**9**) and vinblastine (**10**), well known anti-cancer agents are from the plant *Catharanthus roseus* (Madagascar periwinkle), formerly known as *Vinca rosea.*
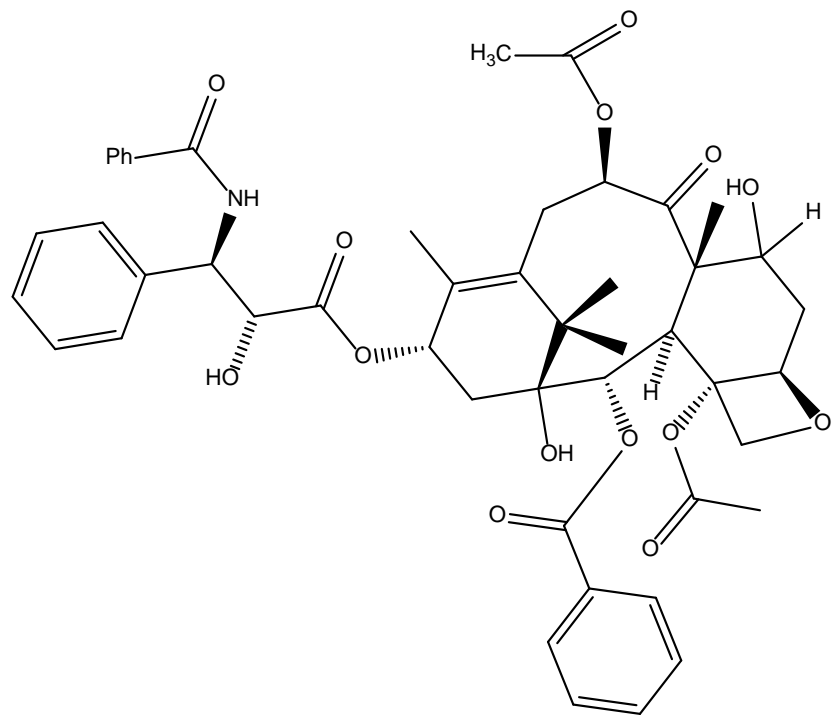
(**53**)
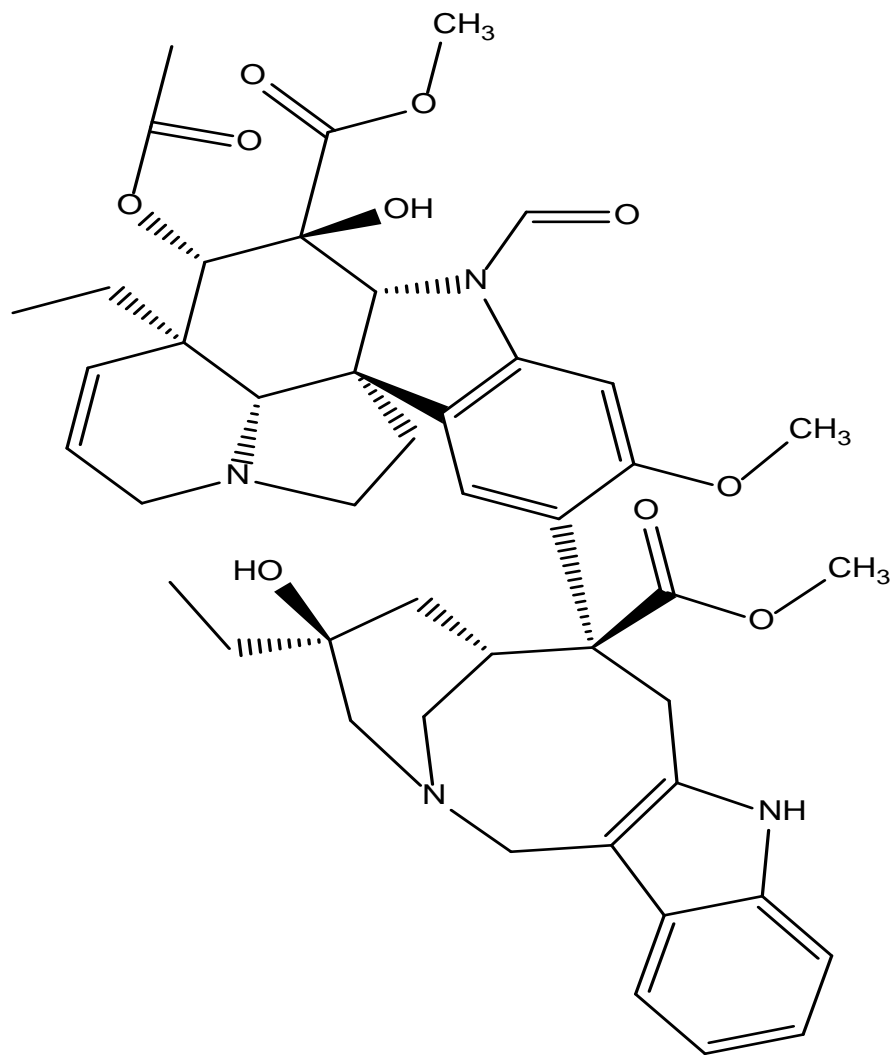
(**9**)
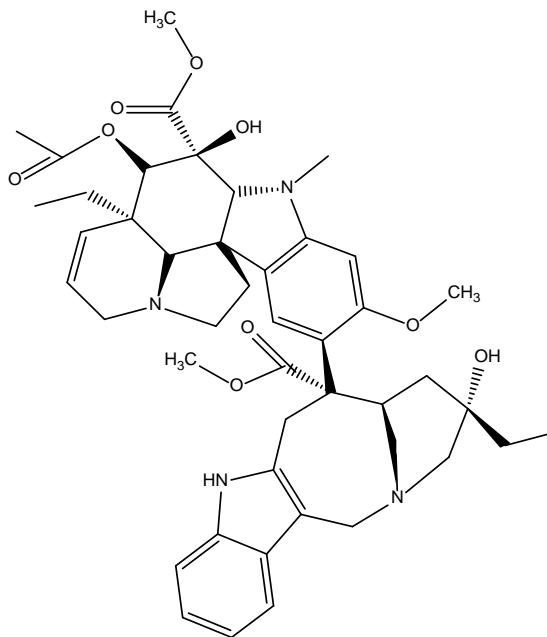
(**10**)

Other notable examples are khellin, from *Ammi visnaga* (L) Lamk., which led to the development of chromolyn widely known as sodium chromoglycate (**54**) used clinically as a bronchodilator; galegine, from *Galega officinalis* L., which was the lead source for the synthesis of metformin (**55**) and other bisguanidine-type antidiabetic drugs. Papaverine from *Papaver somniferum* formed the basis for vera-pamil (**56**) synthesis used in the treatment of atrial fibrillation. Other notable clinical entities developed from traditional medicinal plants include: the antihypertensive agent, reserpine (**57**), isolated from *Rauwolfia serpentina* and ephedrine(6) isolated from *Ephedra sinica* (Ma Huang), a traditional Chinese medicinal plant and this formed the basis for the synthesis of the widely used anti-asthma agents Beta2-adrenergic agonists: salbutamol (**58**).

Microorganisms over the year have been a rich sources of antimicrobials, notable examples include: antibacterial agents, such as the penicillin (**59**) from *Penicillium* species, cephalosporin (**60**) from *Cephalosporium acremonium*. Widely used drugs in clinical use like cholesterol lowering agents, statins such as mevastatin (**61**) were developed from *Penicillium* species, lovastatin (**62**) was developed from *Aspergillus* species. Other natural products derived clinical entities includes: ACE inhibitors cap-topril (**63**) used in the treatment of cardiovascular disease derived from Teprotide, isolated from the venom of the pit viper, *Bothrops jaracaca*. A further notable example are incretin mimetics extenatide polypeptide, Byetta (**64**), a parenteral drug used as an adjunct to improve glucose (blood sugar) control in adults with type 2 diabetes which was developed following the isolation of exendin-4 from the ven-om of the Gila monster, *Heloderma suspectum*.

(54)

(6)

(55)

(**56**)

(**57**)

[45]
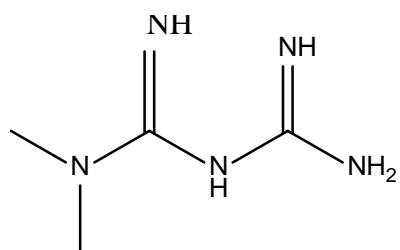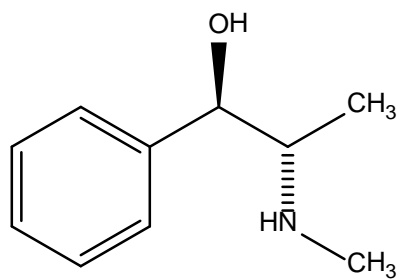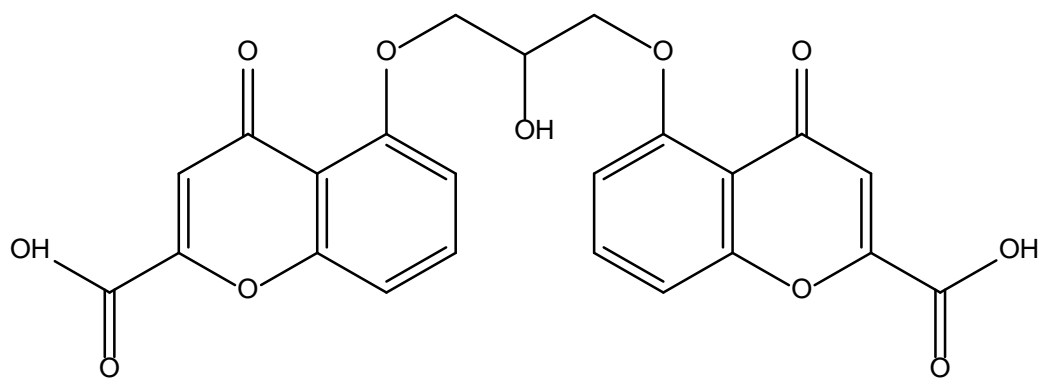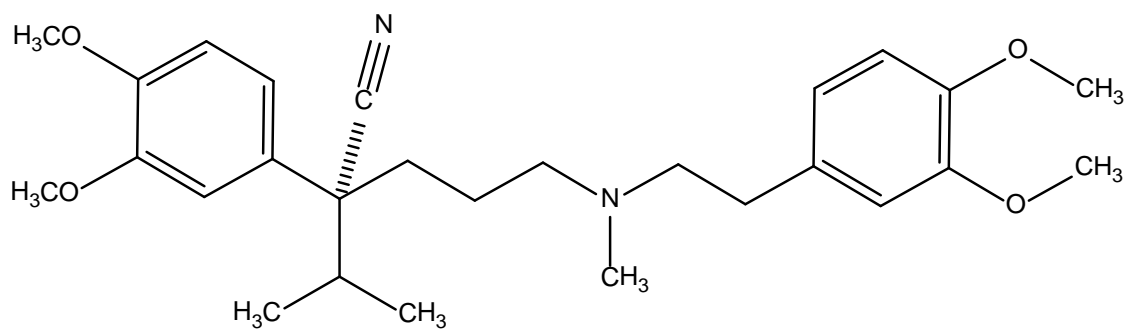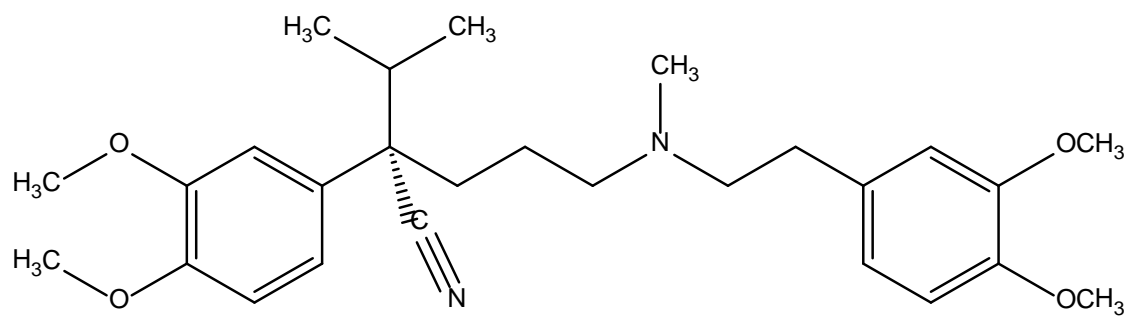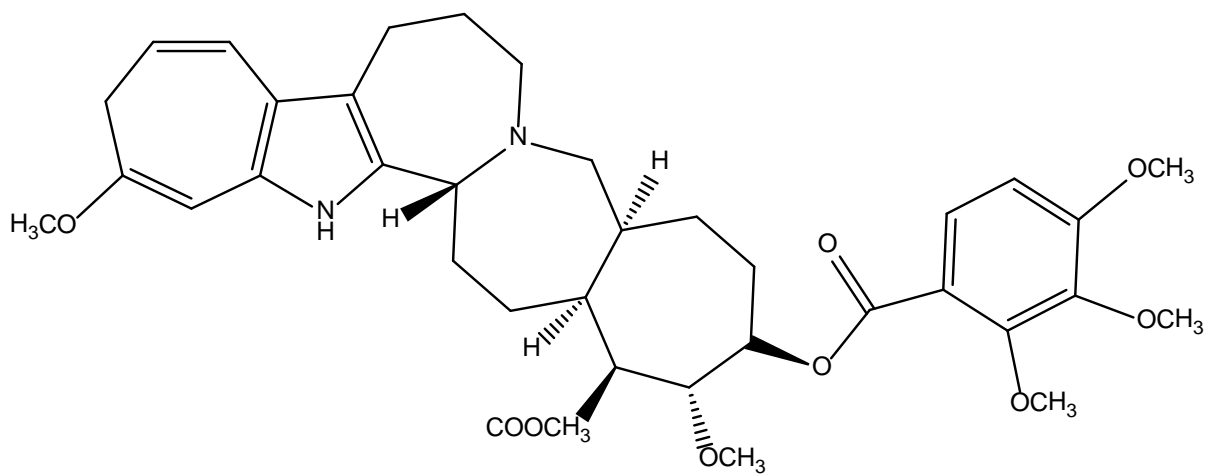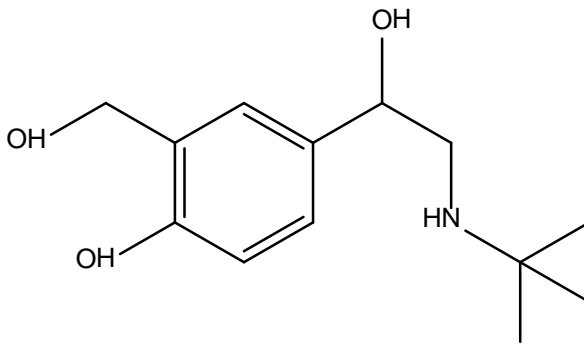
(58)
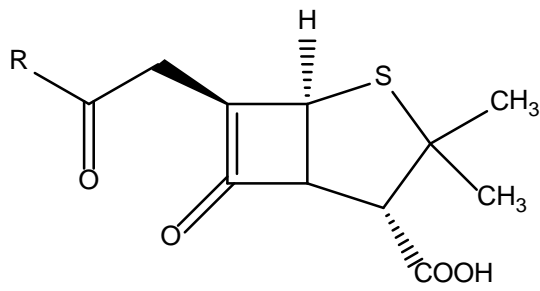
R= PhO in Penicillin V

(59)

(60)

[46]

(**61**)

(**62**)

[47]
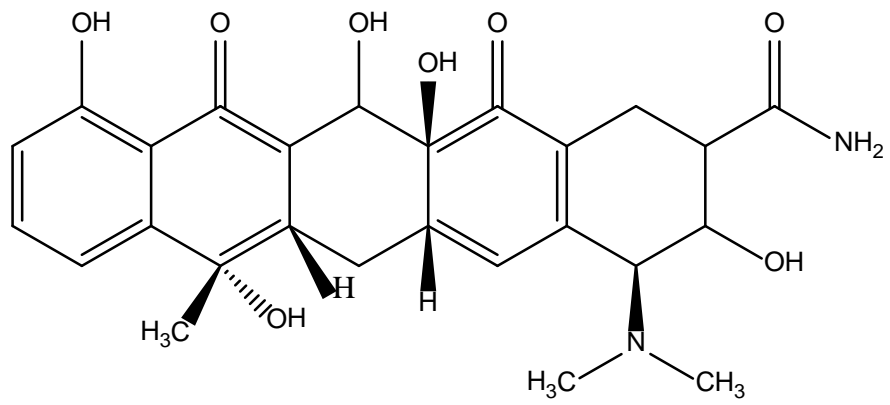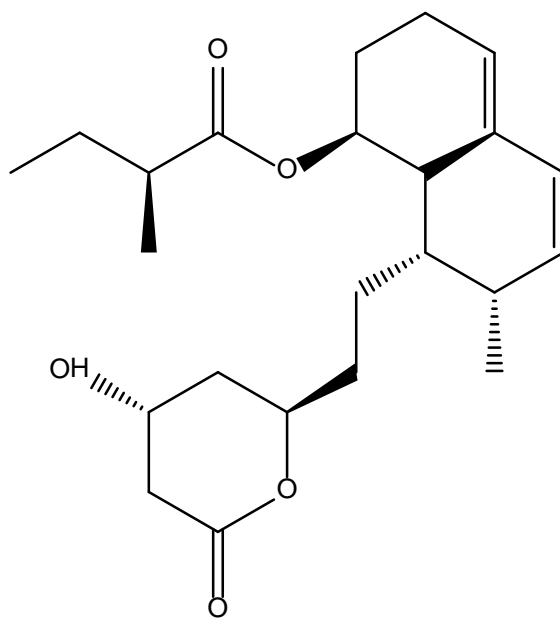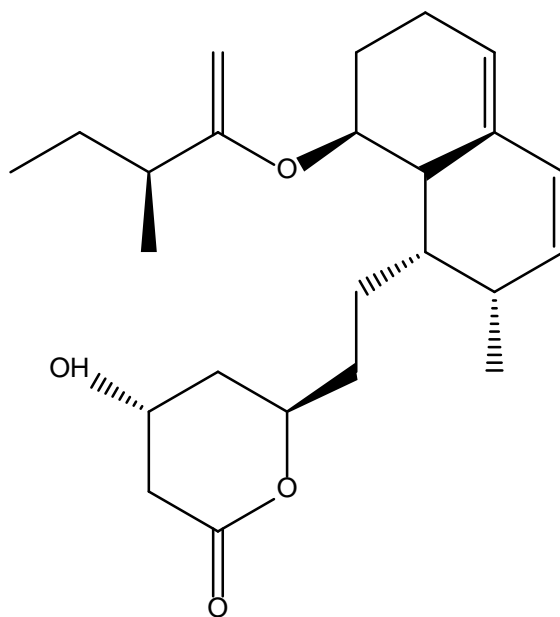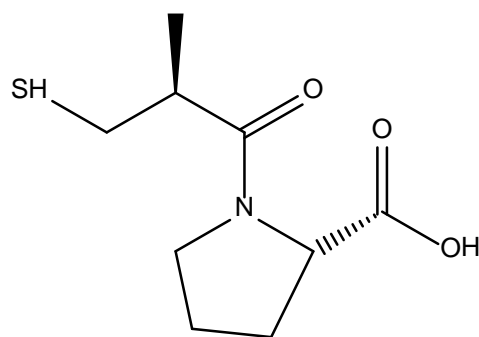
(63)

H-His-Gly-Glu-Gly-Thr-Phe-Thr-

Ser-Asp-Leu-Ser-Lys-Gln-Met-

Glu-Glu-Glu-Ala-Val-Arg-Leu-

Phe-Ile-Glu-Trp-Leu-Lys-Asn-

Gly-Gly-Pro-Ser-Ser-Gly-Ala-

Pro-Pro-Pro-Ser-NH

(64)

Drugs from natural sources still have a role in the present day drug discovery, as the search for new therapeutic clinical entities from natural products have yielded appreciable successes in the last thirty years. **Table 5.11** on page 245 in the appendix shows a list of twenty four natural products-derived clinical entities discovered since 1970 and approved between 1981-2006 (Ganesan,2008).

1.9 Human African Trypanosomiasis (HAT): Health burden, clinical course, and current therapy.

Seventy million people are said to be at risk of contracting HAT in sub-Saharan Africa (SSA) as reported by Simarro *et al.,* (2012), while an estimated 7-8 million people worldwide mostly in Latin America are infected with *Trypanosoma cruzi* according to the World Health Organisation (WHO) 2014.

Chagas disease occurs through Vector-borne transmission. The insect vector is a triatomine bug that carries the parasite *Trypanosoma cruzi,*the disease causative agent. Unlike HAT, Chagas disease is curable if treatment is initiated soon after infection. According to WHO report (2014) up to 30% of chronically infected people develop cardiac complications and up to 10% develop digestive, neurological or mixed manifestations which may require specific treatment.Vector control is the most useful method to prevent Chagas disease in Latin America. It is important to prevent infection through transfusion and organ transplantation by blood screening. It runs a more severe course in infections in pregnant women and their newborns, so diagnosis of infection is of paramount importance in this suspectible group. Also infected persons shoud have contact particularly siblings tested WHO report (2014). HAT, otherwise known as sleeping sickness is caused by infection with one of two extra-cellular protozoan parasites: *Trypanosoma brucei rhodesiense* or *brucei gambiense.*

.
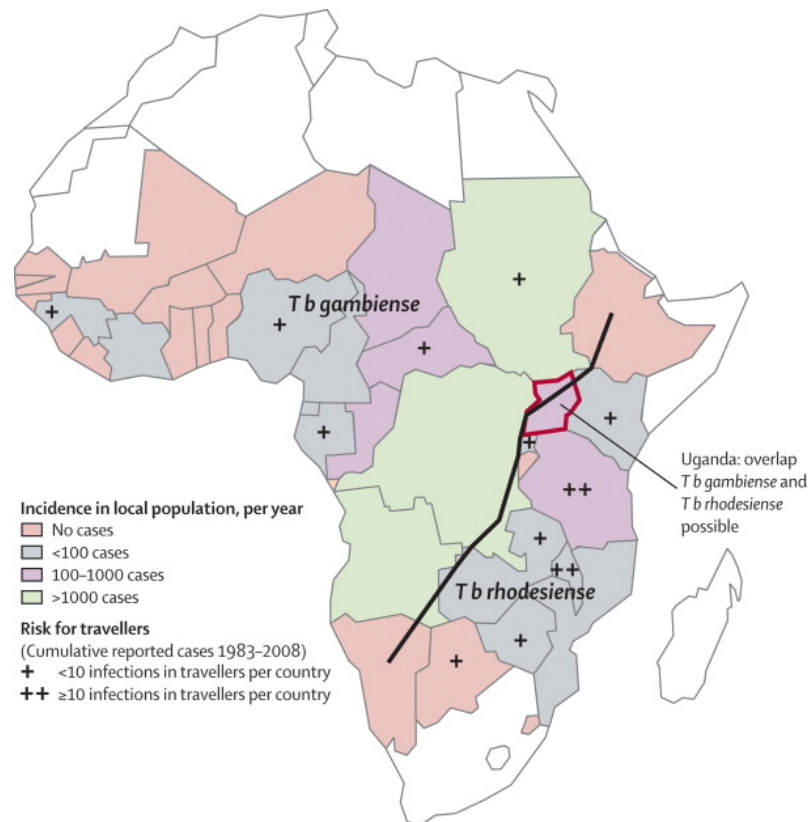
Figure 1.2: Distribution of Human African Trypanosomiasis with incidences and risk for

Travellers. The black line divides the areas in which *Trypanosoma brucei gambiense* prevails from areas in which *Trypanosoma brucei rhodesiense* predominates: Blum(2009).

The causative parasites of HAT are transmitted by Tse tse flies; the insect vectors of the genus *Glossnia* mainly in Sub-Saharan Africa (SSA) where the vector, the parasite, reservoir hosts and humans co-exist. HAT creates a huge public health and economic burden in SSA. It accounts for over 1.5 million

Disability-Adjusted Life Yearly (DALY) in 2002, affecting mainly the rural poor. DALY is a measure of overall disease burden, expressed as the number of years lost due to pre mature death, ill-health or disability. It is becoming an increasingly important concept in public health and health impact assessment (HIA). It defines the concept of potential years of life lost due to premature death poor health or disability. Prevalence estimates from the World Health Organization (WHO) are 50,000–70,000 cases, based on a total number of 17,500 new cases reported per year worldwide by the WHO report (1998).

Of the three major forms of human disease causative trypanosome parasites known: *T.brucei gambiense* found in Western and Central Africa, accounts for 95% of cases, running a chronic infection course. *T.brucei rhodesiense* found in Eastern and Southern Africa; accounts for 5% of cases, causing acute infection which rapidly invades the central nervous system. *T.cruzi* is the only other form of human trypanosomiasis, it is prevalent in twenty one Latin American countries causing Chagas disease. It typically causes inflammation of the heart known as myocarditis.

The name "sleeping sickness" stems from the typical clinical presentation of drowsiness during the day, and insomnia at night, victims are known to have frequent REM (Rapid Eye Movement) sleep at onset of the disease and this helps to determine the stage of the disease and evaluate the effectiveness of new treatments. REM sleep is one of the five stages of sleep humans experience at night which is characterized by quick, random movements of the eyes and paralysis of the muscles. In stage 2 of HAT , as shown in **Figure 1.4**, the parasites proliferate in the haemolymphatic system (haemolymphatic stage). In stage 3 in **Figure 1.4** (meningoencephalitic stage), they invade the central nervous system and brain provoking progressive neurological dysfunction leading to symptoms that include the disrupted sleep wake patterns that typify HAT, thus the common name of "sleeping sickness".

When the Tsetse fly bites "chancre" appears on the skin, this has a typical characteristic appearance as shown in **Figure 1.3** below. Three weeks later trypanosomes invade the bloodstream, lymph glands and other internal organs, so the victim manifests swollen lymph nodes commonly cervical, other manifestations though rare include myocarditis and eventually heart failure. Less commonly it affects the endocrine system to cause loss of libido and impotence in males, other less common features are orchitis, gynecomastia in men, abortion and infertility in women. Common symptoms include fever, headache, hirsutism, anxiety and coma.

HAT occurs predominantly in rural populations dependent on farming, fishing and animal husbandry. The health burden is worsened by the fact that diagnosis and treatment of the disease are complex.

Figure 1.3: Tse tse fly and characteristic skin appearance "chancre" following infected fly's bite :Fidssa bulletin (2012)

1.10. Life cycle of Trypanosoma parasite

The unique lifecycle of the trypanosome parasite correlates to the clinical features of HAT. There is an immune response causing inflammation at site of bite, this is the basis for the skin appearance known as "trypanosomal chancre". Trypomastigotes move via the host lymphatics to the lymph nodes before proceeding into the bloodstream , in the process swollen cervical lymph nodes manifest as what is known as "Winterbottom's sign" named after the physician; Dr. Thomas Masterman.

Winterbottom (1766-1859), born in England, studied in Edinburgh, later Glasgow, who discovered the sign ('small glandular tumours' in the neck) in weak and less productive slaves later found to be infected in Sierra Leone's native population in 1803. He termed it 'negro lethargy' Kennedy (2007)[2].

HAT causative trypanosomes reside exclusively in the bloodstream. When an infected host is bitten by Tsetse fly of the *Glossinia* species, the blood-sucking fly takes a 'blood meal', the parasites exist as bloodstream trypomastigotes. In the fly's midgut they become procyclic trypanomastigotes, undergo a complex series of changes in shape and metabolism to become epimastigotes as they leave the fly's midgut. Initially the ingested trypanosomes which are long and slender are not infective until they reach the mid-gut of the fly, where they become short and stumpy becoming infective before moving on to the fly's salivary gland as epimastigotes to multiply. These complex changes take three weeks from the blood meal on an infected human host to become infective in the fly. It should be noted that less than 10% of all Tsetse flies in an endemic area are infected with trypanosomes

Kennedy (2007)[3]

Tsetse fly Stages

Epimastigotes multiply in salivary gland. They transform into metacyclic trypomastigotes.
8

1 Tsetse fly takes a blood meal (injects metacyclic trypomastigotes)

7 Procyclic trypomastigotes leave the midgut and transform into epimastigotes.

6

Bloodstream trypomastigotes transform into procyclic trypomastigotes in tsetse fly's midgut. Procyclic tryposmatigotes multiply by binary fission.

5 Tsetse fly takes a blood meal (bloodstream trypomastigotes are ingested)

Human Stages

2 Injected metacyclic trypomastigotes transform into bloodstream trypomastigotes, which are carried to other sites.

3 Trypomastigotes multiply by binary fission in various body fluids, e.g., blood, lymph, and spinal fluid.

4 Trypomastigotes in blood

$\triangle$ i = Infective Stage
$\triangle$ d = Diagnostic Stage

http://www.dpd.cdc.gov/dpdx

Figure 1.4: A schematic diagram of the lifecycle of the trypanosome distinguishing between the Infective and Diagnostic stages.

1.11 Drugs used in treatment of HAT:

Polyanionic compound Suramin (**65**) developed by Oskar Dressel and Richard Kothe of Bayer, Germany in 1916 as reported by Black and Seed (2001). Pentamidine (**66**) formulated as aerosolized salt developed in 1994 was originally an insulin mimetics, later discovered to possess anti-parasitic properties Elliot (2011). Melarsoprol (**67**) developed by Friedheim in 1949 by reacting melarsen oxide with 2,3-dimercaptopropanol, however it was not until 1990 before it became the drug of choice for second stage (CNS infections) with *T.b.gambiense* Seed and Hall (1992). Eflornithine (**68**) developed in 1990 in the US by Sanofis-Aventis under the trade name Ornidyl as a parenteral antitrypanosmal agent. It also has a topical form useful in treatment of facial hirsutism, and most recently Nifurtomox (**69**) useful in treatment of Chagas disease. A safer and more effective combination therapy with Nifurtimox (**69**) and Eflornithine (**68**) was developed in 2009, it is now the goal standard treatment for second-stage African Trypanosomiasis infection Priotto (2009).
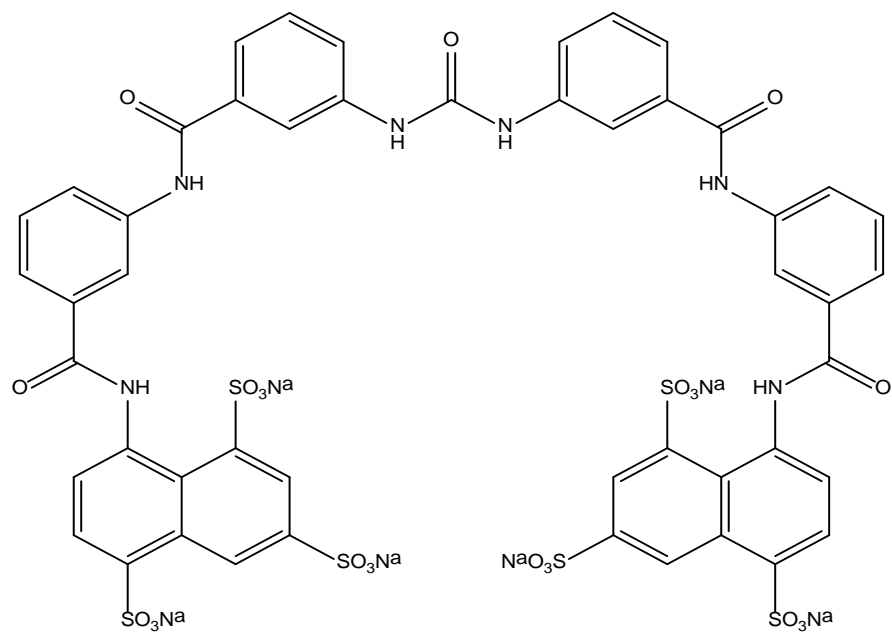
(**65**)
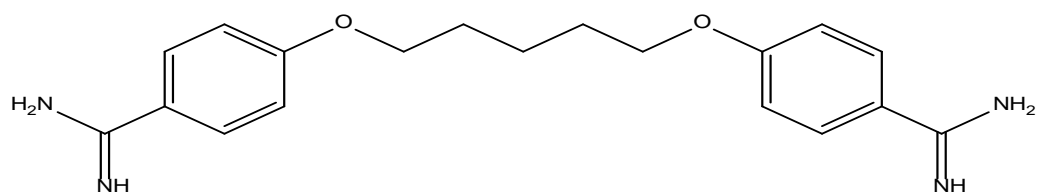
(**66**)
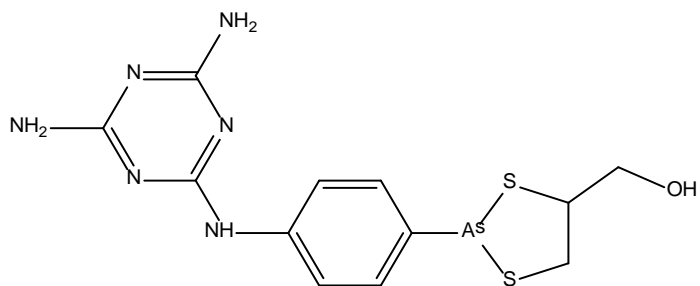
(**67**)
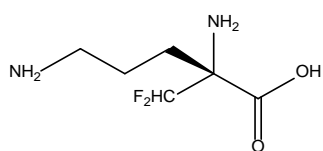
(**68**)

[53]
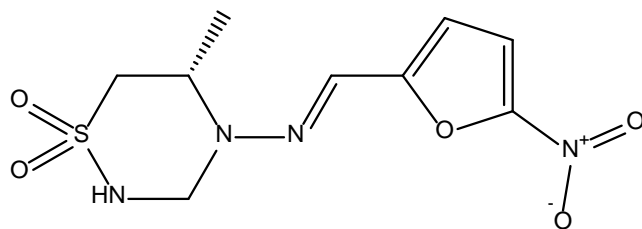
(**69**)

Suramin (**65**) is a polysulphonated symmetrical naphtylamine derivative with urea in the centre. It contains eight benzene rings, amide and sulfone groups and is used in the treatment of HAT parenterally, as it is highly hydrophilic, that is a molecule that is polar and thus dissolves in water. It is ionic in nature, possessing six negative charges. It is administered as a single weekly intravenous injection once for 6 weeks. This involves an initial administration of 200 mg test dose which if well tolerated is followed by 1 g per day dosages on day 1,3, 7 , 15 and 21 or 1 g weekly for 6 weeks. It is highly bound to plasma proteins and Low Density Lipoproteins (LDL). It was hypothesized that uptake of Suramin (**65**) is through endocytosis when bound to LDL, which explains the slow accumulation of the drug in trypanosomes Vansterkenburg *et al*., (1993). Several trypanocidal mechanisms of action have been proposed, but not proven. It is believed to inhibit a number of glycolytic enzymes Wierenga*et al*., (1987). It does not enter the central nervous system, thus is not effective in treatment of advanced disease. It is pharmacokinetics is complex, it has a short initial half-life as well as a lengthy terminal half-life of about 50 days, and it is slowly cleared from the body by renal excretion Katzung (2004).

The other licensed use of Suramin (**65**) is in the treatment of onchocerciasis. Clinical use is however associated with 50% chance of developing drug-induced adrenal cortical damage capable of triggering anaphylaxis, as well as fever, rash, headache, paraesthesia, neuropathies, seizures, severe GI upset, haemolytic anaemia, agranulocytosis and kidney damage. With these worrisome adverse side effects, it is imperative to attempt to develop new anti-trypanosomal agents.

The second anti-trypanosomal agent in line of development was pentamidine (**66**). It is formulated as an anti-microbial salt which acts through uptake of parasite purine receptors, accumulating within the parasite to inhibit essential enzymes and infer with DNA to kill the parasite. Its dosage parenterally is 2-4 mg/kg daily up to 15 doses and sometimes a second course might be needed. It is a highly toxic drug and 50% of patients receiving 4mg/kg of the drug tend to experience severe side effects Katzung (2004). These side effects includes sever hypotension, tachycardia, dizziness and dyspnoea so the drug is administered slowly usually over 2 hours with patient in recumbent position and monitored closely drug treatment. Other common side effects includes pancreatic toxicity as well as hypoglycaemia secondary to inappropriate insulin release which often occurs 5-7 days after treatment. Reversible acute

kidney injury has also been reported. Other less severe side effects includes fever, rash, metallic taste, gastrointestinal upset, deranged liver function tests, acute pancreatitis, hypoglycaemia, thrombocytopenia, hallucinations and cardiac arrthymias. Other type of preparation of pentamidine, Inhaled pentamidine has documented side effects such as cough, dyspnea and bronchospasm.

Pentamidine (**66**) other licensed uses include prevention and treatment of Pneumocystis pneumonia (PCP) caused by *Pneumocystis jirovecci* previously known as *Pneumocystis carinii*; Visceral leishmaniasis, Leukaemia, as well as parasitic infections like Acanthamoeba granulomatous encephalitis in immunocompromised persons. As an anti-trypanosomal agent for *Trypanosoma brucei gambinese* infections predominantly, it is only effective for early stage infection.

Melarsoprol (**67**) is an organo-arsenic compound which crosses the blood brain barrier, making it particularly effective against late stage of *T .brucei gambiense* in the CNS, as well as late stage of *T. brucei rhondinese* infection. The mechanism of action of Melarsoprol (**67**) is not totally understood, but it is believed to kill the parasite by inhibiting an essential energy metabolism pathway. It is administered intravenously at dosage of 3.6 mg/kg/day for 3-4 days with repeated courses weekly should the need arise. Clinical use is limited in humans due to the life-threatening encephalopathy: Sub- acute Sclerosing Panencephalitis (SSPE) it possesses, this occurs within the first week of therapy with clinical features like cerebral edema, seizure, coma and eventually death. Other common side effects include fever, vomiting, abdominal pain, and arthralgia. This accounts for mortality in 20% of patients receiving Melarsoprol (**67**) for treatment of the two varieties of HAT. Recently high failure rates to treatment have been reported raising the possibility of drug resistance

Eflornithine (**68**) also known as DFMO, is only effective in the treatment of *T brucei gambiense.* It is administered intravenously and has good central nervous system penetration, peak plasma concentration is achieved rapidly and elimination half-life is about 3 hours. The dosage is usually about 100 mg/kg every 6 hours for 1-2 weeks. It acts by inhibiting *ornithine decarboxylase*. *Ornithine decarboxylase* is essential in the survival of the parasite as it catalyses the synthesis of essential amine-based compounds involved in cell division and cell differentiation. Reported side effects notably are diarrhoea, vomiting, anemia, thrombocytopenia, leucopenia and seizures. These side effects are usually reversible Katzung (2004).

To combat this limitation, combination therapy of Eflornithine-Nifurtimox was developed in 2009. Niturtimox (**69**) is a nitrofuran compound effective in the treatment of South American variety of the human disease, Chagas disease. It is well absorbed orally and eliminated with plasma half-life of 3 hours. It is administered at a dose of 8-10 mg/kg/day divided into 3-4 doses orally for 3-4 months, it has poor central nervous system penetration. Reported adverse effects includes nausea, vomiting, abdominal pain, fever, rash, restlessness, insomnia, neuropathies and seizures as documented by Katzung (2004).

It has been noted that one in every 20 patients suffering from African Trypanosomiasis taking the current first line drug Melarsoprol (**67**), tend to die from the side effects rather than the disease itself Kennedy (2007)[1]. With all these limitations in mind, the need to find new anti-trypanosomal agents to combat these huge burden diseases (HAT and Chagas disease) is of paramount importance.

Table 1.1 showing stages and their effective drugs in the treatment of HAT, Kennedy (2013).

Stage	HAT specie	1st line treatment	2nd line treatment
Early stage (Haemo-lymphatic)	*T.brucei rhondesiense* *T. brucei gambiense*	Suramin IV (**65**) Pentamidine IM (**66**)	Pentamidine IM (**66**) Suramin IV(**65**)
Late stage (Meningoencephalitic)	*T.brucei rhondesiense* *T. brucei gambiense*	Melarsoprol IV (**67**) Eflornithine IV(**68**) plus oral Nifurmatox (**69**)	None Melarsoprol IV (**67**)

NB: IV Intravenous, while IM is Intramuscular.

1.12 Potential anti-trypasomal drug targets

1) Enzymes

a.Trypanosomes contain an essential reductant known as trypanothionine which has two gluthathione peptides conjugated to spermidine. This reduction is NADPH-dependent and mediated by *trypanthionine reductase* which is a prime drug target. Blocking production of glutathione which is essential for survival of trypanosomes is a proven target for anti-trypanosomal drugs.

b. *Ornithine decarboxylase*: Inhibition of *ornithine decarboxylase* in the parasite makes it unable to make critical substances called polyamines that are essential to the survival of the parasites.

2. Glucose metabolism: Metabolism of the infective procyclic trypanosomes in the fly's mid-gut

requires glucose metabolism, that is these blood stream forms are totally dependent on glycolysis

regulated by glycolytic enzymes through the Tricarboxylic Acid (TCA) cycle, and oxidative

phosphorylation. The inhibition of these glycolytic enzymes can be targeted by potential drugs as a mechanism of action

3. Essential proteins like proline, alanine and so on are important for the survival of the trypanosomes as these proteins are energy sources for the parasite; they are regulated by proteases which can also be good drug targets.

4. Reactive oxygen intermediates and free radicals. Trypanosmes are sensitive to high levels of

 reactive oxygen intermediates and free radicals; this is the mechanism through which Nifurtimox works.

5. Cell membrane disruption: Interfering with synthesis of key fatty components of the parasite's cell membrane is another probable anti-trypanosomal drug mechanism of action.

6. Target *T. brucei rhondesiense*'s natural defence system: By blocking the serum resistance factor (SRA) which is used by *T brucei rhondesiense* to resist natural ability of the human serum to destroy it, robs the parasite of one of the most important innate defence mechanism it has against human host.

7. Targeting the Blood Brain Barrier (BBB): The normal course of the CNS-type East African variety Human Trypanosmiasis is for the trypanosomes to cross the BBB within weeks of infection, targeting and preventing this essential stage in the course of the human disease is another probable mechanism of action potential anti-trypanosomal drugs could exploit.

1.13 Molecular modelling

Molecular modelling describes the theoretical methods and computorial techniques used to model or mimic the behaviour of bioactive molecules. It forms the bedrock of fields such as computorial chemistry, computorial biology and drug design. Methods used include molecular mechanics, which utilise classical and Newtonian mechanics to describe the physical basis of molecules by analysis of spring-like interactions which represent chemical bonds and Van der Waals forces. As an effective drug development tool; molecular modelling investigates protein folding, enzyme catalysis, protein stability, conformational changes associated with bimolecular functions and molecular recognition of proteins, DNA, and membrane complexes.

1.13.2 Molecular modelling studies on phytochemical compounds for anti-trypanosomal activity

Ogungbe and Setzer (2012) reported a molecular docking study carried out on phytochemical compounds used traditionally to treat parasitic infections or known to have *in vitro* anti-trypanosomal activity. 916 compounds from 19 Nigerian medicinal plants were investigated using in-silico molecular docking technique on validated *Trypanosoma brucei* protein targets that were available from the Protein Data Bank (PDB): *Adenosine kinase* (TbAK), *pteridine reductase* 1 (TbPTR1), *dihydrofolate re-*

ductase (TbDHFR), *trypanothione reductase* (TbTR), *cathepsin B* (TbCatB), heat shock protein 90 (TbHSP90), *sterol 14α-demethylase* (TbCYP51), *nucleoside hydrolase* (TbNH), *triose phosphate isomerase* (TbTIM), *nucleoside 2-deoxyribosyltransferase* (TbNDRT), UDP-*galactose 4' epimerase* (TbUDPGE), and *ornithine decarboxylase* (TbODC). The study revealed anthraquinones, xanthones, and berberine alkaloids docked strongly to pteridine reductase 1 (TbPTR1), chromenes, pyrazole and pyridine alkaloids docked notably to *triose phosphate isomerase* (TbTIM), while indole alkaloids showed significant docking energies with UDP-*galactose 4' epimerase* (TbUDPGE). *E. chlorantha* compounds investigated in the molecular modelling studies include atherosperminine (**70**), columbamine (**78**), jatrorrhizine (**42**), lanuginosine (**72**), liriodendronine (**73**), palmatine (**41**), isololdine (**74**), isocorydine (**75**), 7, 8-dihydro-8-hydroxypalmatine (**38**), O-methylmoschatoline (), pseudocolubamine 79**6**), pseudopalmatine (**80**).

(**70**)

(**78**)

(**72**)

(**73**)

(**74**)

(**75**)

(**82**)

[59]
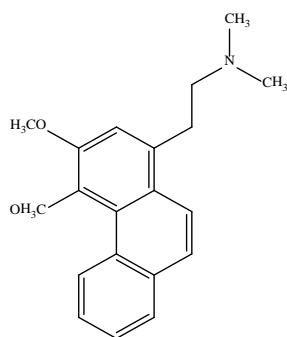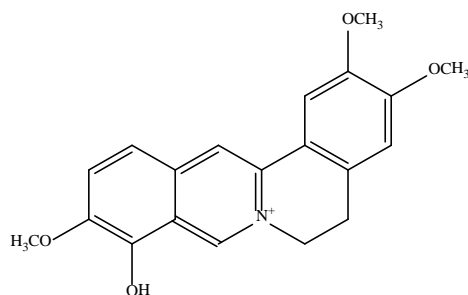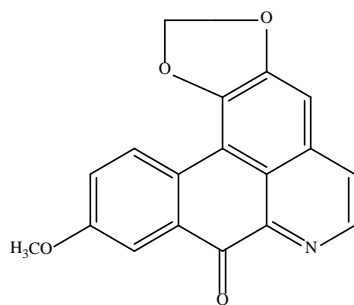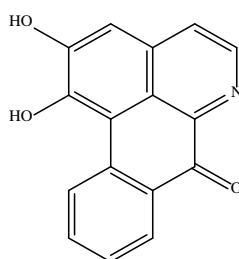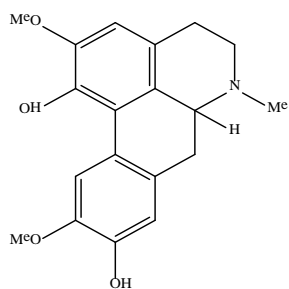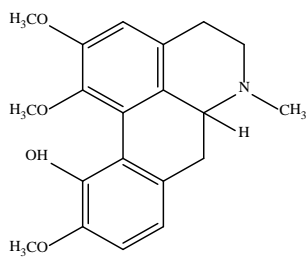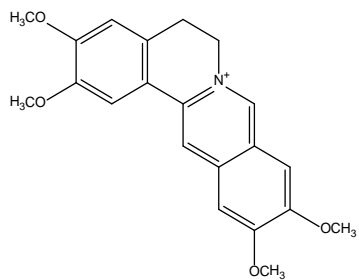
1.14 Previous phytochemical studies on *E. chlorantha*

The *Annonanceae* family are known to produce a wide range of phytochemicals including alkaloids and non-alkaloidal compounds. In terms of production of alkaloids they are particularly known to produce benzylisoquinoline alkaloids. Some of such alkaloids previously isolated from *E.chlorantha* are outlined below in **Table 1.2.**

Table 1.2 Benzylisoquinline alkaloids previously isolated from *E. Chlorantha*

Compound	Structure and molecular formula	Reference
Atherosperminine	$C_{20}H_{33}NO_2$ (**72**)	Leboeuf *et al.,*(1980)
Atherospermidine	$C_{18}H_{11}NO_4$ (**71**)	Leboeuf *et al.*, (1980)
Columbamine	$C_{20}H_{21}NO_4$ (**78**) **(78) R = OH**	Hamonniere *et al.*, (1990)
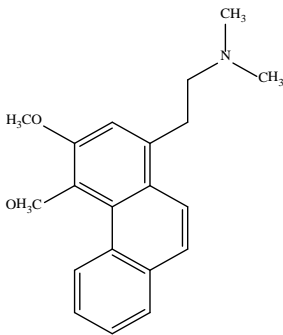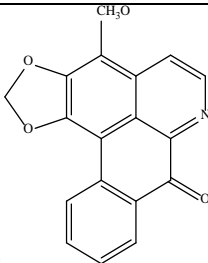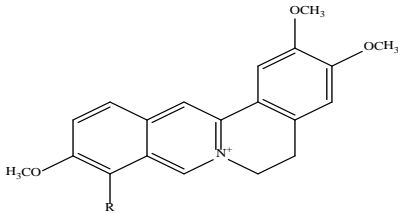
Jatrorrhizine	$C_{20}H_{20}NO_4$ (**42**) (5) R=OH	Hamonniere et al., (1990)
Lanuginosine	$C_{18}H_{11}NO_4$ (**72**) 	Guinaudeau *et al.,* (1994)
Liriodendronine	$C_{16}H_9NO_3$ (**73**) 	Guinaudeau *et al.,* (1994)
Lysicamine	 $C_{18}H_{13}NO_3$ (**77**)	Guinaudeau *et al.,*(1994)
Palmatine	$C_{21}H_{24}NO_4$ (**41**) **R**= OCH_3 	Hamonniere *et al*.,(1990)
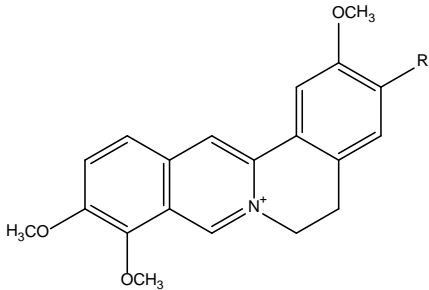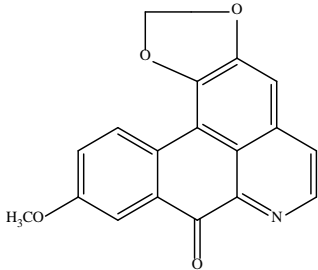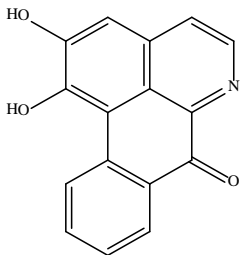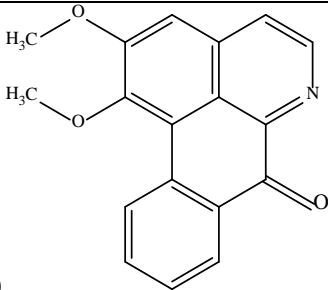
[61]

Isoboldine	C$_{19}$H$_{21}$NO$_4$ (**74**) 	Leboeuf *et al.*, (1980)
6a,7-dehydro -7-hydroxy-1,2-dimethoxy-7-hydroxy-N-methyl-aporphine	C$_{19}$H$_{19}$NO$_3$ (**39**) (**39**) R= CH$_3$	Wafo *et al.,*(1990)
6a,7-dehydro -7-hydroxy-1,2-dimethoxy-7-hydroxyaporphine	C$_{18}$H$_{17}$NO$_3$ (**40**) **R=H** 	Wafo *et al.,*(1990)
Isocorydine	C$_{20}$H$_{23}$NO$_4$ (**76**) 	Leboeuf *et al.,* (1980)
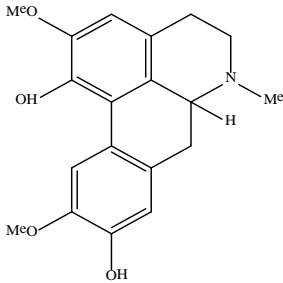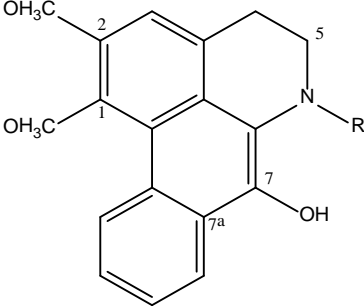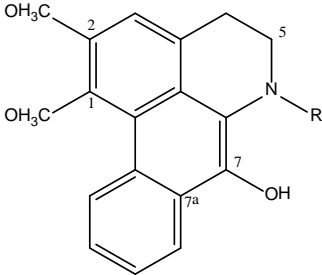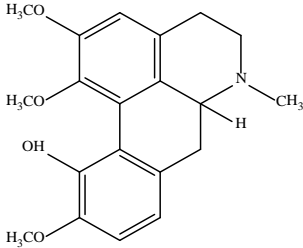
7,8-dihydro-8- hydroxypalmatine	$C_{22}H_{22}NO_4$ (**38**)	Tan *et al.,* *(2000)*
O-Methylmoschatoline	$C_{18}H_{13}NO_4$ (**85**) 1,2,3-trimethoxy-7*H*-dibenzo[*d*e,*g*]quinolin-7-one	Guinaudeau *et al.*,(1994)
Pseudocolumbamine	$C_{20}H_{20}NO_4$ (**79**) (**79**) R= H₃CO	Hamonniere *et al.*,(1990)
Pseudopalmatine	$C_{21}H_{22}NO_4$ (**82**)	Tan *et al.,(2000)*
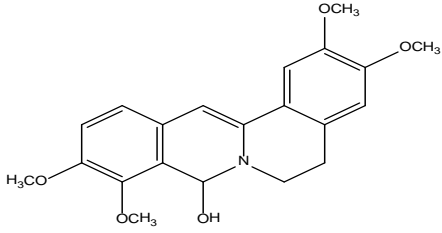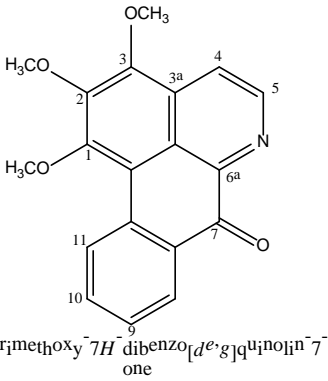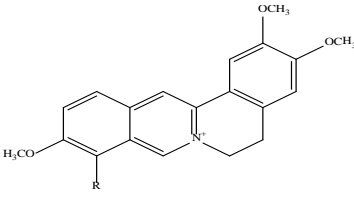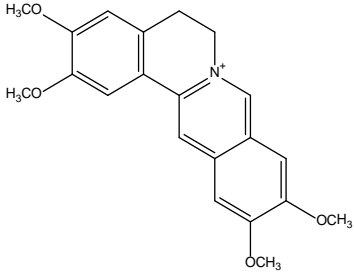
1.14.2 Protoberberine alkaloids reported from *E. Chlorantha* stem bark and their pharmacological properties.

Four similar protoberberine alkaloids namely; palmatine (**41**), jatrorrhizine (**42**), and columbamine (**78**) and pseudocolumbamine (**79**) were isolated from stem bark of *E. chlorantha* Hamonniere *et al*., (1990).
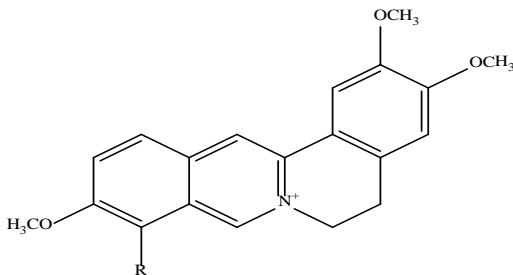
(**78**) R = OH

(**79**) R = H₃CO

Palmatine(**41**), jatrorrhizine(**42**) and columbarine (**78**) isolated from stem bark of *E. chlorantha* have been reported to have preventive and curative effects on artificially provoked liver injury Virtanem *et al.,* (1988). Palmatine(**41**) was investigated as a pharmaceutical drug for treatment of viral hepatitis as reported by Virtanen *et al.,* (1993) ; the reduced form, tetrahydropalmatine (**80**) is one of the major bioactive components in *Corydalis yanhusuo*W.T Wang, a well-known traditional Chinese medicine with potent analgesic, sedative-tranquilizing and hypnotic properties Hsu (1962).
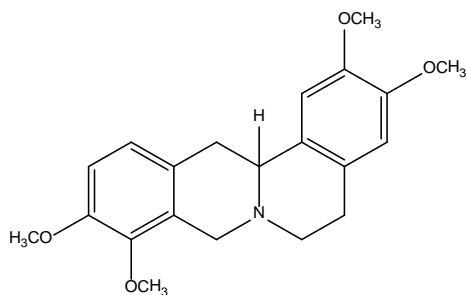
(**80**)

Bourdat-Deschamps (2004) had reported the isolation of the four very polar quaternary protoberberine alkaloids: palmatine (**41**), jatrorrhizine (**42**), columbarine (**78)** and pseudocolumbamine (**79**), as very challenging, because their adsorption on silica was very high and their chemical structures very closely related. Hence, the need to use High Performance Centrifugal Partition Chromatography (HPCPC) to isolate the four protoberberine alkaloids from *E. chlorantha*.

Isolated protoberberine alkaloids from *E. chlorantha* with their interesting properties have been reported to attract attention of medicinal chemists to synthesize derivatives of these alkaloids for structure activity relationships studies McCall *et al*., (2002) Vennerstrom *et al*., (1998) and Iwasa *et al*., (1996). A bioactivity based fractionation of *E. chlorantha* root and stem bark led to the isolation of palmatine chloride and jatrorrhizine chloride as the major antimicrobial constituents. Minimum Inhibitory Concentrations of these isolated compounds were found to be superior to those of well established broad antibiotics like ampicillin and ciprofloxacin against some of the organisms tested Moody *et al., (*1995).

Chapter 2: Materials and Methods

2.1 Materials

2.1.1 Plant Materials

Stem bark samples of *E. chlorantha* were obtained from the suburbs of Ile Ife, Osun State in South Western Nigeria. The botanical identification and authenticity of samples were carried out at the herbarium of Department of Plant Biology, University of Ilorin, Nigeria with voucher specimen NM 325 kept for purpose of reference. The plant materials were collected in summer and winter to see variation in the types of compounds synthesized by plants in different parts of the year.

2.1.2 Chemicals, Reagents and Laboratory wares

2.1.2.1 Solvents used for extraction, chromatographic separation, TLC and isolation purposes:

1. Ethyl Acetate (HPLC grade)

2. n-Hexane (HPLC grade)

3. Methanol (HPLC grade)

4. n-Pentane (HPLC grade)

5. Acetone (HPLC grade)

6. Acetic acid (Analytical grade)

7. Dragendorff reagent (Sigma-Aldrich)

The solvents were obtained in 2.5 L bottles from Fisher Scientific UK limited and VWR UK Limited.

2.1.2.2 Chromogenic reagents

1. Anisaldehyde-Sulfuric acid spray solution was used for identification of sugars, steroids, terpenes and phenols in mixtures on TLC plates.

2. Drangendorff spray solution was used for identification of alkaloids

2.1.2.3: Table 2.1: Deuterated solvents used for NMR

Solvent	Chemical formula	^{1}H shift (ppm)	^{13}C shift (ppm)	Peak trace for water (ppm)
Deuterated chloroform	$CDCl_3$	7.26	77.00	1.50
Deuterated Acetone	$(CD_3)_2CO$	2.05	29.92	2.80
Deuterated DMSO	$(CD_3)_2SO$	2.50	92.43	3.30

2.1.3 Laboratory wares

TLC Plates and Tank

Pre-coated TLC aluminium plates (Merck, Silica gel PF_{254}) were cut to appropriate sizes to fit into a TLC tank, containing the solvents for separation of the extract mixtures into components compounds.

UV lamp

Mineral light Lamp used: Model UVGL -58, Multiband UV 254/896 nm (Upland CA91786 USA)

Heat Gun

Model: Power Craft 5969 (Clobaltronics GmbH & Co KG, China)

Rotary evaporator (Buchi)

Column Chromatography

1. Glass columns: (1a) diameter (3 cm), length (60 cm), (1b) diameter (2.5 cm) length (90 cm).

2. Column grade silica gel (silica gel 60, mesh size 20-200 µm, Merck, Germany)

3. Weighed sample(s): crude extracts.

Gel Filtration Chromatography (Sephadex)

1. Glass column: diameter (1.5 cm), length (90 cm)

2. Sephadex LH-20 (GE Health Lifescience UK)

Preparative TLC

1. Glass plates 20 cm by 20 cm.

2. TLC grade silica gel (60H, Merck, Germany)

Reverleris IES Flash Chromatography

Reveleris® X2 Flash Chromatography System

Reverse phase HPLC

Reverse phase HPLC gradient system:

1. Degasser

2. HPLC Pump mixer (Spectra System P2000)

 3. Auto Sampler (Spectra System AS3000)

 4. Column (ACE 3 C18 dimension 150 X 3.0 mm internal diameter, Batch No: V10-2659)

5. Detector (Spectra System UV2000)

6. 2.5 L bottles to collect waste

7. Computer to record and analyse the data using the Chromquest Software version 2.53 (ThermaQuest Corporation, UK).

Normal Phase HPLC system

Normal Phase HPLC System:

1. Nylon 66 membrane.

2. 1ml loop on Rheodyne injection valve where all samples were manually injected into.

3. Pump Gilson Model 302 Isocratic HPLC Pump (Model 802C manometric module).

 4. Column (ACE 3 C18 dimension 60 X 21.20 mm 10 u Luna silica Part No 03R-9391-P0,S/N 324722G.

5. Detector Waters 2487 Dual λ Absorbance detector at 254 nm.

6. 2.5 L bottle to collect waste.

7. Computer to record and analyse the data using the Dionex PeakNet Software version 4.30.

2.2 Methods

2.2.1 Pre- extraction sample preparation

The outer portion (dark brown) cork of the stem bark was peeled with aid of a knife to separate the inner (green yellow) bark to differentiate compound(s) isolated from the cork to those of the bark.

Figure 2:1: Ground bark of *E. chlorantha* stem bark.

Figure 2.2: Bark of stem bark of *E. chlorantha.*

Subsequently, they were cut into small pieces (about 2 by 4 cm) and air-dried (spread on paper to become drier through contact with room air under a fume hood for 72 h. This was to ensure the plant materials were free from water which could constitute a source of impurity. It was however worthy of note there was hardly any difference in the weights of the plant material after 72 h under the fume hood and before, as they were brought from Nigeria already dry.

The plant material was ground to become fine powdered materials (cork and bark) and weighed to obtain cork (735.8 g) and bark (804.5 g).

Extraction and Isolation

2.2.2 Extraction and partitioning

Soxhlet Extraction: Soxhlet extraction is a method developed in 1879 by Franz von Soxhlet. In the case of this present study. Soxhlet extraction was carried out at 50°C for hexane and ethyl acetate extracts and 70 $^{\circ}$C for methanol extracts at 2 cycles per hour.

The finely ground (cork and bark) samples were loaded in cellulose 'thimble' and placed in the main chamber of the Soxhlet extractor. Solvent of choice was poured into the main chamber using a funnel.

Hexane, ethyl acetate and methanol were used successively for the extraction. This is based on the premise that hexane will extract mostly the non-polar compounds, ethyl acetate the medium polar and methanol the polar compounds.

As the chamber flowed compounds dissolve in the solvent, thereafter the chamber was emptied through the side arm and the cycle was then repeated several times until exhaustive extraction was achieved (usually 48-72 h) as reported by Saleem et al.,(2013). For hexane extracts they were run at 2 cycles per hour lasting 18 hours (36 cycles), ethyl acetate (24 cycles) and methanol (18 cycles). At the end of this process the liquid extract was then decanted from the round bottom flask of the extractor for further processing.

2.2.3 General analytical methods

2.2.3.1 Post-Extraction separation and analysis.

Rotatory evaporation

The rotatory evaporator was used to evaporate the extracts obtained from the Soxhlet extraction close to dryness. Concentrated extracts were thereafter collected in small labelled vials and kept in the fume cupboard to evaporate to dryness for weighing.

Thin Layer Chromatography (TLC) development

TLC is a simple and quick method of defining the number of compounds in a mixture and to identify a single pure compound using pre-prepared TLC plates (Merck Precoated Silica gel PF_{254}). It works by capillary action when immersed in the appropriate solvent mixture in a TLC tank to separate components.

Thin Layer Chromatography (TLC) was carried out on the extracts to determine the possible number and types of compound(s) in the crude extracts. Plant extracts, chromatographic fractions or pure compounds were initially dissolved in appropriate solvent e.g. chloroform for non-polar samples, methanol for very polar samples. They were thereafter spotted approximately 1 cm above the bottom edge of a TLC plates using capillary tubes. Spots were applied as band and kept narrow to reduce chance of overlapping as well as aid easy identification of resulting components of the mixture(s). Filter paper was placed in the tank to aid saturation. 10 ml mixtures of hexane and ethyl acetate in ratio 50/50, 60/93, 70/30, 80/20 or as appropriate was poured into the TLC tank using a measuring cylinder to obtained a good resolution of bands which was achieved at R_f value of 0.3. The prepared TLC plates were gently placed into the appropriate hexane/ethyl acetate solvent system in the TLC Tank. The appropriate solvent systems were allowed to ascend from the bottom of the plate to near the top by capillary action to develop of the spotted TLC plates.

Thereafter, the TLC plates were removed from the tank and dried with a stream of warm air using the heat gun. The developed TLC plates were initially visualized with the naked eye, under UV light and

finally sprayed with appropriate chromogenic reagent; Anisaldehyde and Dragendorff reagents. This was because some of the compounds on the developed TLC plates were UV active, thus were not visible to the naked eye and had to be observed under UV using the UV lamp at shortwave length 254 nm and/or long wave 896 nm Stahl and Mangold(1975), Stock and Rice (1974). Shortwave length was particularly useful for the detection the aromatic alkaloids isolated in this study.

Choosing appropriate mobile phase for TLC plates development

Mixtures of solvents were used for developing spotted TLC plates. Different combinations of solvent systems were tried until a desirable resolution between bands was obtained. For analysis of fractions from Open column or Flash chromatography separation techniques R_F value of 0.4-0.5 as shown in **Table 3.1** was used, while for HPLC fractions R_F value of 0.3 was used.

2.2.3.2 Nuclear Magnetic Resonance (NMR) Spectroscopy

It is a method which uses the magnetic properties of certain nuclei of compounds. Two types are of immense importance in Organic chemistry: 1D Proton NMR and [13] Carbon NMR. It is programmed to produce information useful in identifying functional groups in a mixture or pure compound. The number and types of chemical entities in a molecule can also be detected from it. 2D NMR spectral in form of HMBC, HSQC and COSY were also carried out in the process of structure elucidation.

All NMR experiments were carried out using a JOEL (JNM LA400 MHz and Bruker (Avance) 600 MHz using 5 mm NMR tubes (Wilmad-Labglass). Samples were dissolved in about 1 ml of deuterated solvents and pipetted into NMR tubes for the experiments. Too much or too little volume was avoided to prevent shimming problems. Samples of low yield had NMR experiments carried out in Shigemi tubes (Sigma-Aldrich UK Limited) using about 0.2 ml of deuterated $CDCl_3$ or DMSO solvents. While for 1 ml TMX tubes 1 mg of the fractions were dissolved in 0.1 ml of deuterated solvent for 1D and 2D NMR spectroscopic studies. Structure elucidations were carried out using 1D and 2D NMR spectroscopy for known compounds spectral data were compared with published spectral data for compounds identification, while the NMR spectral were processed using the MNOVA software. ^{1}H NMR experiment was the primary means of 1D NMR experiment used for structure elucidation, using the chemical shifts and integrations to determine the number and type of protons present in the compound. The other ID experiment was ^{13}C NMR which was useful in determining the number of carbons present in the compounds.

The 2D NMR experiments carried out were COSY (Correlation Spectroscopy) which showed [1]H-^{1}H correlations. Heteronuclear Single Quantum Coherence (HSQC) spectroscopy, the ^{1}H-^{13}C NMR experiment showing one-bond [1]J correlations and NOESY (Nuclear Overhauser Enhancement Spectroscopy) which recorded all [1]H-^{1}H NOE correlations in the molecule of interest, this helped in determining protons in close proximity to one another. Lastly HMBC (Heteronuclear Multiple-Bond Correlation), it

is the NMR experiment which is set with time delay (1/2J) with pulse sequence programmed in a way that J value is in the range of $^3J_{CH}$ and $^2J_{CH}$ correlations Breitmaier (1993).

As an effective analytical chemistry technique Nuclear Magnetic Resonance (NMR) spectroscopy is used in for determining the constituents and purity of a sample, as well as its molecular structure. NMR can be used quantitatively for analysing known compounds from mixtures. For unknown compounds, with the aid of vast spectral libraries, NMR can either be used to match them to attempt to determine what they are or to infer the basic structure directly. After the basic structure is determined, NMR can be used analyse physical properties such as conformational exchange, phase changes, solubility, and diffusion. It can also be used to determine molecular conformation in solution as well as.

The basis of NMR

NMR operates on the basis that all nuclei are electrically charged ,most nuclei have spin, thus when an external magnetic field is applied, an energy transfer occurs between the base energy to a higher energy level . This energy transfer takes place at a wavelength that corresponds to certain radio frequencies and when the spin returns to its base level, energy is emitted at the same frequency. The signal that matches this transfer is measured and processed to produce an NMR Figure for the nucleus concerned. This leads to the concept "Chemical shift".

Chemical shift

At the nucleus the precise resonant frequency of the energy transition is dependent on the effective magnetic field. This field is affected by electron shielding which depends on the chemical environment. Therefore analysis of the resonant frequency can give information about the nucleus' chemical environment. As a general rule, the more electronegative the nucleus is, the higher the resonant frequency. Other factors which affect the frequency shifts are ring currents (anisotropy) and bond strain affect. The norm is to adopt tetramethylsilane (TMS) as the proton reference frequency. This is because the magnetic field used determines the precise resonant frequency shift of each nucleus. However frequencies are not easy to remember (for example, the frequency of benzene might be 400.132869 MHz), so chemists decided to define chemical shift to yield a more convenient number such as 7.17 ppm.

$\delta = (\nu-\nu0)/\nu0$

Using this equation the chemical shift is not dependent on the magnetic field and it is convenient to express it in ppm where (for proton) TMS is set to $\nu0$ thereby giving it a chemical shift of zero. For other nuclei, $\nu0$ is defined as Ξ νTMS, Ξ (Greek letter Xsi) is the frequency ratio of the nucleus, for example it is 25.145020% for ^{13}C.

In analysing ^{1}H NMR Figure electronegative functional groups resonate at low frequencies and therefore the most electronegative would resonates at the lowest chemical shift. Aromatic groups such as phenol which are highly electron donating (electropositive) would have the highest chemical shift. However, if the chemical shift of the aromatics were due to electropositivity alone, then they would resonate between four and five ppm.

Factors affecting chemical shifts

Chemical shifts of the same sample differ when under different conditions such as solvent, temperature, etc. Chemical shifts are also affected slightly by isotopic substitution. This leads to the concept known as Spin-spin coupling

Spin-spin coupling

The orientation of neighbouring nuclei affects the effective magnetic field. This effect is known as spin-spin coupling. It causes splitting of the signal for each type of nucleus into two or more lines. The size of the splitting (coupling constant or J) is measured as an absolute frequency in (Hertz), it is independent of the magnetic field. The number of chemically bonded nuclei in the vicinity of the observed nucleus is indicated by the number of splitting.

Ortho, para and Meta coupling

"Ortho" substitution the two substituents are next to one another, while in "Meta" it is position 1 to 3 and in "Para" substitution it is position 1 and 4 with the two substituents occupying opposite ends.

Two Dimensional NMR Spectroscopy

The invention of multi-dimensional spectral (2D NMR Spectroscopy) was a major leap in NMR Spectroscopy as it has led to additional spectral dimensions which gives extra information to make elucidation of structures of unknown compounds much easier. In addition to 1D experiments' preparation and detection, the 2D experiment has an indirect evolution time t_1 and a mixing sequence. This can be simplified in four stages as: a. preparation b. evolution c. mixing d. detection.

Preparation is the first step, thereafter the spins process freely for a given time t_1 where the magnetization is labelled with the chemical shift of the first nucleus. During the third stage, the mixing time's magnetization is transferred from the first nucleus to a second one. This mixing sequences for magnetization transfer involves two mechanisms: scalar coupling or dipolar interaction (NOE). Direct evolution time are collected as data are acquired at the end of the experiment in the detection phase, the chemical shift of the second nucleus during this time labels magnetization. 2D FT yields the 2D Figure with two different frequency axes.

[73]

A diagonal of signals divides the Figure in two equal halves. Symmetrical to this diagonal, there are more signals (X), called cross signals, these cross signals contain the really important information useful in intrepreting 2D NMR spectra.

Homonuclear 2D experiments:

There are three homonuclear 2D spectra which are widely used for the structure elucidation 2D COSY, 2D TOCSY and 2D NOESY.

2D COSY:

Unique to 2D COSY experiments is the fact that scalar coupling transfers magnetization. Protons that are more than three chemical bonds apart show no cross signal because the 4 coupling constants are close to 0. Thus, only signals of protons which are two or three bonds apart appear in a COSY Spectral.

2D TOCSY:

Whereas in the TOCSY experiment, magnetization is dispersed over a complete spin system of the functional group by successive scalar coupling. The TOCSY experiment correlates all protons of a spin system. Therefore, in addition to signals that are visible in a COSY Spectral, there are also additional signals from the interaction of all protons of a spin system that are not necessarily connected via three chemical bonds.

2D NOESY:

The NOESY experiment is particularly useful in elucidation of structure of compounds with close protons in spatial arrangement. The Nuclear Overhauser effect, NOE using the dipolar interactions of spins is used for correlation of protons. The intensity of the NOE is in first approximation proportional to 1/r6, where r is the distance between the protons: The correlation between two protons depends on the distance between them, usually a signal is only observed if their distance between two protons is smaller than 5 Å. The NOESY experiment correlates all protons which are close enough. It also correlates protons close in space due to tertiary structure. Therefore it is a very useful spectral for the determination of protein structures.

Heteronuclear NMR spectroscopy:

The use of these hetero nuclei allows some new features in NMR which facilitate the structure determination especially of larger molecules (> 100 AA). Therefore, two strategies are used for Heteronuclear NMR Spectroscopy includes Isotopic enrichment of these nuclei in proteins and enhancement of

the signal to noise ratio by the use of inverse NMR experiments in which the magnetization is transferred from protons to the hetero-nucleus.

Thus the most important inverse NMR experiment is the HSQC (heteronuclear single quantum correlation) correlates the nitrogen atom of an NH group/ the carbon atom in CH with the directly attached proton. Each signal in a HSQC Figure represents a proton that is bound to a nitrogen atom or carbon atom as the case may be.

2.2.3.3 Column Chromatography (CC)

Depending on the quantity of crude extract(s), 100-300 g of silica gel packed glass columns containing a slurry of column grade silica gel (silica gel 60) prepared using the appropriate solvent system. The glass column was filled to half capacity with the chosen solvent system, and then the slurry applied as a thin stream allowing for gradual flow of solvent to ensure homogenous packing of the silica gel. The plant extract had previously been dissolved in an appropriate solvent system mixed with column grade silica gel to give smooth flowing powder, which was then applied gently onto the top of the packed column to allow for elution isocratically or gradient-wise. Hexane-ethyl acetate and ethyl acetate-methanol solvent systems were used for hexane and ethyl acetate extracts, while ethyl acetate and ethyl acetate -methanol mixture were used for the methanol extracts. The fractions obtained were subsequently subjected to TLC, visualized under UV lamp and sprayed with appropriate chromogenic reagents Braithwaite and Smith (1996)

Subsequently, NMR and Mass spectroscopy studies to determine the type of compounds in the resulting fractions were carried out. Further attempts to isolate the alkaloids as pure compounds were carried out using Flash Chromatography(C-18 Reversed Phase Flash Chromatography), Gel Filtration Chromatography , Prep TLC, Reveleris IES Flash Chromatography, Reverse Phase and Normal Phase HPLC.

2.2.3.4 Gel Filtration Chromatography

This chromatographic method separates molecules such as proteins, peptides, alkaloids, oligonucleotides and so on, based on their sizes as the molecules move through beds of porous beads (Sephadex, in this case). Small molecules tend to move slower through the beds, while large molecules move faster. Molecular weight and 3-dimensional shape also contributes to the movement through the beds and degree of retention of compounds in the column.

Forty grams (93 g) of sephadex LH 20 was soaked overnight in methanol and subsequently packed into a column. A TLC guided solvent system of 90% chloroform and 10% methanol was used to elute the column Determann and Brewer (1975). Fractions obtained were submitted for NMR experiments and anti-trypanosomal activity determination.

2.2.3.5 C-18 Reverse Phase Flash Chromatography

Separation of *Enantia chlorantha* extracts using the reverse phase flash chromatography method works on the principle of reversible adsorption of molecules using a stationary phase which is hydrophobic. It is a modification to traditional column chromatography in such a way that the solvent is driven through the column by applying positive pressure. This allowed most separations to be performed faster, in less than 30 minutes as it is the case of this study. It has pre-packed plastic cartridges, and the solvent is pumped through the cartridge, with the system linked with detectors and fraction collectors. The introduction of gradient pumps in this chromatography system has resulted in quicker separations and less solvent usage. While this chromatographic system is dependent on pressure it differs from Gel filtration system where separation is based on effective size of analyte molecules as they pass through the pores of the stationary phase, silica.

For this study the Initial Thin layer Chromatography (TLC) on reverse phase C-18 plates showed good separation of the mixtures in a solvent system of 95% methanol 5% water to 75% methanol and 25% water. So the solvent system of 85% methanol and 15% water was chosen as mobile phase for possible Flash Chromatographic separation of *E. chlorantha* extracts Braithwaite and Smith (1996)[2].

300 mg of the mixture was dissolved in 20 ml methanol and added to 93 g of HMN granules. The vial was covered with a small piece of musin and secured with rubber band before placing in the Turbo Vap (50 degree Celsius) to remove the solvent under nitrogen for about two hours.

Thereafter, a pre-primed flash master plunger was attached to the Isolute Flash C-18 pre-packed cartridge which had *E. chlorantha* extracts adsorbed HMN granules loaded onto it gently, a frit was then placed on top and pushed slowly to sit directly on the granules and positioned using the frit applicator,before securing the set up using the pre-primed flash master plunger. The set-up was then switched on to elute and collect fractions in pre-labelled vials in appropriate volumes according to the ELSD/UV Vis detector.

Operating conditions of C-18 Reverse Phase Flash Chromatography

Instrument: JONES Flash (Flash Master Personal)

Column: Isolute Flash C18

Sample loading method: Pre-loaded on C18 pre-packed cartridge

Mobile phase: solvent A: water, solvent B: methanol

Flow rate: Initially 5 ml/min; later 15 ml/min

Solvent bottle: Containing 85% methanol and 15% water in a total combined volume of 500 ml

Collected fractions, fifty in totals had similar fractions pooled based on TLC and appearance under UV light for subsequent NMR experiments.

This experiment was supervised by Carol Clements, she operated the C-18 Reverse Phase Flash Chromatography, while I loaded the extracts and developed appropriate solvent system.

2.2.3.6 Preparative Thin layer Chromatography

Preparative Thin Layer Chromatography is another useful method in the separation of mixtures. It is carried out on a glass (as in this study) plastic, or aluminium foil coated with adsorbent material which acts as the stationary phase and are developed in large tanks with solvents previously determined from normal TLC.

The plate in this present study was prepared by mixing silica gel with water, stirred into thick slurry form, poured and spread on the TLC glass plates 20 cm by 20 cm using a manual plate spreader, heated at 120°C for one hour to fix it. Activated resultant plates had thickness of the dry adsorbent layer of about 2.5 mm. With a margin of 1 cm from the bottom of the TLC plates, the alkaloid-rich mixtures were applied in a straight continuous line on the adsorbent material and subsequently immersed in a TLC tank with an appropriate solvent system Braithwaite and Smith (1996).

The four samples (column fractions); DCM 35, ECEB 19-22, ECH 12-26 and ECH 1 had 100 mg weighed and dissolved in dichloromethane.

1. DCM 35 applied on the Prep TLC plate was placed in the preparative TLC tank containing the solvent system; 98% dichloromethane and 2% methanol and subsequently allowed to separate.

The DCM 35 plate gave eight bands; their edges were sprayed with Dragendorf's reagent. Three bands gave positive results (orange colour) indicative presence of alkaloids. These three bands; DCM 35-1, DCM 35 -2, DCM 35-4 were scrapped off the fifteen plates into a beaker and dissolved in 50% chloro-form: 50% methanol and allowed to stand overnight. The supernant was decanted and air-dried in the fume cupboard to give; 12 mg of DCM 35-1, 8 mg of DCM 35-2 and 10.1 mg of DCM 35-4

The same procedures were repeated for ECH-1, ECH 12-16, ECEA 19-22. 1D and 2D NMR experiments were subsequently carried out for structure elucidation.

Extraction and various chromatography separation techniques were carried out by myself under supervision of John Igoli, NMR analysis under supervision of Professor Sandy Gray.

2.2.3.7 Reversed-Phase High Performance Liquid Chromatography (RPHPLC)

RPHPLC has a column made of modified silica, making it non-polar by attaching long hydrocarbon chains to the silica's surface- typically with either 8 or 18 carbon atoms. Polar solvent such as

methanol is commonly used as the solvent system. Because of Van der Waals 'dispersion forces, non-polar compounds in the mixture tend to form strong bond with the hydrocarbon groups, while the

Polar compounds form strong bond with the polar solvent.

Retention time is an important concept in HPLC, it is the time it takes a reference compound to travel through the column to the detector. It is the measured time from which the sample is injected to the point at which the display shows a maximum peak height for that compound. Different compounds have different retention times, thus retention time can be used to identify compounds Clark (2007)

Reverse Phase HPLC conditions

Geng and Regnier (1984): The mobile phase used was:

A. 0.1% Formic acid   B. Acetonitrile

The flow rate 0.3 ml/min, wavelength: 254 nm. Injection volume was 20 µl. 12 samples were run for about 45 minutes apiece with the gradient system in the table below:

Table 2.2: Reverse Phase HPLC conditions

Time	A % (0.1% Formic acid)	B% (Acetonitrite)
0	70	30
5	70	30
30	0	100
40	0	100

This experiment was supervised by Lorraine Allen, she operated the Reverse Phase HPLC Chromatography, while I loaded the fractions and developed appropriate solvent system.

2.2.3.8 Normal Phase High Performance Liquid Chromatography (HPLC)

Chromatography can be described as a differential migration process where sample compounds (in this case *E. chlorantha* alkaloid-rich mixtures) were dissolved in appropriate mobile phase and separated by being selectively retained by a stationary phase. Differences in equilibrium distribution between the phases will result in components being separated as components as they migrate in the mobile phase.

The column of the chromatograph contains tiny silica particles, which is the stationary phase, and the solvent system used is commonly non-polar. This ensures polar compounds in the mixture as they pass through the column will stick longer to the polar silica than non-polar compounds. The non-polar ones will therefore pass more quickly through the column. The resultant signal is processed by a recorder or data handling device i.e. Integrator and the computer with the processing software, that is as the each component (in this case alkaloids, sugars and fats elute through the detector, a change in the electrical output is produced and displayed as graphs on the PC monitor with peak(s), heights and areas directly proportional to the quantity of each components in the mixtures.

Normal Phase HPLC conditions

An appropriate solvent system with TLC guided R_f value of 0.3 was used in this study to determine the appropriate solvent system to separate the benzylisoquinoline alkaloids mixtures into the various constituents, comprising of alkaloids and impurities mainly fats and sugars.

Mobile Phase: 20% Ethyl acetate in Hexane

Flow; 7.5 ml/min

Wavelength (λ): 254 nm

Pressure: 120 psi

Injected volume: 900 ul of 20 mg/ml using 80 mg in 4 ml Li *et al*., (2013).

This experiment was supervised by Gavin Bain, he operated the Normal Phase HPLC Chromatography, while I loaded the fractions and developed appropriate solvent system.

2.2.3.9 Reverleris IES Flash chromatography

Reverleris IES flash chromatography system is a system designed to facilitate increased speed of isolation of bioactive molecules from natural products for pharmaceutical, agro-chemical and other relevant industries.

Reveleris IES Flash chromatography conditions

1. Flow Rate: 25 ml/min   2. ELSD Carrier: Iso-propanol

3. UV1 Wavelength 254 nm, UV2 Wavelength 280 nm.

4. Cartridge equilibration 30 minutes.

5. Extract type: *E.chlorantha* hexane, ethyl acetate and methanol extracts

6. Extract solvent: A. Hexane   B.Ethyl acetate

7. Solvent volume 93 ml   8. Ultar-sonification: 20 minutes

Operating conditions as reported by Bose, Anderson and Lawrence (2010).

This experiment was supervised by Neil Herbert, he operated the **Reveleris IES Flash chromatography** *, while I loaded the extracts and developed appropriate solvent system.*

2.2.3.10 Mass spectrometry

A known method useful in elucidating the elemental composition of a sample or molecule with mechanism of action based on ionizing the chemical compound(s) of interest to generate charged fragmented molecules whose flight of path is dependent on the mass/electric charge ratio in an electromagnetic field.

MS is made up of:

1. An ion source which converts compound or sample of interest into charged ions after bombarding high energy electrons.

2. A mass analyser which sorts the ions out by their masses

3. A detector measures the value in terms of quantity of the fragmented ions making MS an invaluable method of quantitative and qualitative analysis in some cases for identifying unknown compounds. It measures mass and identifies corresponding structure by matching the obtained spectra to a library of similar compounds.

In the present study EI mass spectra was obtained on a JOEL JMS-7- high resolution mass spectrometer using a direct probe at 70 eV. Positive ion and negative ion mode ESI experiments were carried out on Orbitrap HRESI mass spectrometer. Samples were dissolved in methanol, water or acetonitrite (HPLC grade and analytical grade) to obtain a concentration of 100 µg/ml. Sample solutions of 10 µl was injected with 0.1% formic acid in acetonitrite: water (90:10) at flow rate 200 µl/min.

Operating conditions were Tube lens of 90 V for positive mode,-145 V for negative mode, capillary temperature of 220 degree Celsius, Sheath Gas flow (bar) 0f 30, Auxiliary Gas flow (bar) of 10. Others were source voltage in kV, 4.00 for positive mode and 3.00 for negative mode, source current of 100 µA and capillary voltage of 35.5 V for positive mode and -48 V for negative mode.

This experiment was carried out by Dr Tong Zhang, while I loaded the fractions in appropriate solvent system.

2.2.3.11 Minimum Inhibitory Concentration (MIC)

MIC is the least concentration of a drug or compound to inhibit the growth of target microbes after overnight incubation. MICs are important to confirm the resistance of microbes to a drug or Compound, and to monitor the activity of a new drug. MICs are used by diagnostic laboratories mainly to confirm resistance, but most often as a research tool to determine the *in vitro* activity of new antimicrobials, and data from such studies have been used to determine MIC breakpoints Andrews (2001).

Determination of MIC using Almar ^{TM} Blue assay for anti-trypanosomal activity screen

Anti-trypanosomal activity of the alkaloids was determined using modified Almar blue ^{TM} 96 well microplate assays. The *Trypanosome brucei brucei* parasites (CMP strain) were isolated from previously infected CD1 female mice using method reported by Raz *et al*., (1997) and Franzblau (1998).

At concentration of 20 µM, an initial screen was carried out, subsequently the samples were prepared at 10 mg/ml solutions in 100% DMSO and diluted to a concentration of 1 mg/ml using HMI-9 medium.

Assay wells had 4 µl of test sample added to 96 µl of HMI-9 media to obtain a final concentration of 1:1 dilution of 20 µM. As control DMSO was in column 1, test samples in 2-11 and positive control Suramin (**19**) in column 12. The non-virulent strain *T.brucei brucei* S427 (a bloodstream form of the parasite) /mL was incubated at humidified 5% CO_2 atmosphere for 48 h. using HMI 9 media, Almar blue indicator, measuring the fluorescence. The surviving trypanosomes were counted using a haemocytometer. MICs were carried out in triplicates to ensure reliability and MIC concentrations were calculated as the concentrations which had <5% of control values.

This experiment was carried out by Carol Clements, while I supplied the extracts and fractions in appropriate developed solvent system.

2.2.3.12 Molecular modelling studies

Eight alkaloids of interest comprising of seven aporphine-derived alkaloids and one protoberberine type (palmatine) were investigated using GRIP molecular docking technique on Vlife molecular

Design suite (Vlife MDS 4.2) on seven validated *Trypanosoma brucei* protein targets that were available from the Protein Data Bank (PDB). The validated targets were. *Brucei Glutathione*

Synthetase, Glutathione peroxidase-type tryparedoxin peroxidase, oxidized form*, Glutathione*

peroxidase-type tryparedoxin peroxidase, reduced form*, Sterol 14-alpha demethylase (CYP51)* from *T. brucei* in complex with the *tipifarnib derivative 6-(4-chlorophenyl) (methoxy) (1-methyl-1H-*

imidazol-5-yl) methyl)-4-(2, 6-difluorophenyl)-1-methylquinolin-2(1H)-one, T. brucei Ornithine

Decarboxylase, Riboflavin kinase, Trypanothione reductase from *T. brucei.*

Vlife engine module was used for the alkaloids drawn in 3D forms for their energy minimization to achieve the most stable conformations. Five best conformers from each alkaloid were subjected to docking studies using the GRIP technique of Vlife Biopredicta module, the resulting multiple

 Interactions with the seven validated proteins were subsequently reported and analysed. Subsequently the Discovery Studio 3.5 visualizer and OpenBabel 2.3.2a Microsoft windows_installer were used to generate 2D forms of key protein-ligand interactions. Gold 5.3.2 software was thereafter used to model *ornithine decarboxylase* as protein target against the alkaloids as ligands to generate 3D interactions and docking scores used to evaluate the alkaloids' binding affinity for their most potent proven protein target.

This experiment was carried out by myself and Murray Robertson

Log P values for the eight aporphine-derived alkaloid and palmatine were also calculated. Log P is the Partition coefficient used in estimating the distribution of drugs within the body. It gives an idea of how hydrophilic "water-attracting" or hydrophobic "water-resistant" a compound is.

2.3.2.13 ChemBioDraw

Structures elucidated from 1D and 2D NMR spectral interpretation were drawn using the software ChemBioDraw in a 2D fashion. *I draw all 2D structures myself*

2.3.2.14 Lipinski's rule of 5

Bioactive molecules in the initial stages of drug development that conform to Lipinski's rule of 5 tend to have low attrition in clinical trials later. Therefore the rule acts as a guide in pursing further drug development studies considering the cost involved.

Lipinski's rule states that to be an orally active drug a bioactive molecule in development should not violate more than one of the following criteria:

1. Have not more than 5 hydrogen bond donors (the total number of nitrogen–hydrogen and oxygen–hydrogen bonds)

2. Have not more than 10 hydrogen bond acceptors (all nitrogen or oxygen atoms)

3. The ideal molecule should have a molecular mass less than 500 daltons

4. The ideal molecule should have an octanol-water partition coefficient [5] log P not greater than 5

Chapter 3: Results

Separation techniques and yield

In this study 805.4 g of ground bark of *Enantia.chlorantha* was extracted in Soxhlet to give three extracts from ground plant material. The three extracts obtained had their solvent removed at reduced pressure to give solid residues. The three extracts solid residues were subsequently subjected to column chromatography and other appropriate separation techniques to give fractions, which were weighed to give percentage yield of based on the dry plant material weight of 804.5 g as shown below in **Table 3.1**. Following soxhlet extraction and evaporation under pressure using the rotatory evaporator of 804.5 g of starting stem bark plant material ,ethyl acetate crude extract 16.5 g (2.05%) methanol 88.7 g (11%) and Hexane 17.6 g (2.2%) were obtained.

 Weighed 10 mg of the fractions from the various separation techniques were dissolved in 1 ml of deuterated Methyl sulfoxide-d_6 (DMSO) or chloroform ($CDCl_3$) for 2D NMR studies to characterize the alkaloids described in this chapter. In most cases 1-120 vials were collected from each column run over a period of 4 weeks. For the initial 1-25 vials fractions, NMR analysis revealed they were fats, sugars, while vials number 60-120 were tannins, sugars and likes indicating the termination of collection of vials from the column chromatography. This was based on result of initial anti-trypanosomal screen which revealed fats, sugars, tannins, saponins did not possess any anti-trypanosomal activity.

On TLC ECP-17 and other alkaloids described here below gave had different R_f values as shown above in **Table 3.1**, as well as one prominent spot in UV at λ 254 nm with blue fluorescence. On spraying with Dragendorff's reagent, the spots were positive, indicating they were alkaloids. The same findings were observed in other alkaloidal fractions to be described later in this chapter. 8 alkaloids isolated with their structures elucidated were: **(ECP-17)** 7,7'- Bisdehydro-*O*-methylisopiline,**(ECM-1)**; the protoberberine alkaloid palmatine,**(ECP-19)** 1,1',2,2',3-pentamethoxy-6-methyl-5,5',6,6'-tetrahydro-4H,4'H-7,7'-bidibenzo[de,g]quinoline and **(ECHE-45) :** 8-(1,2,3-trimethoxy-5,6-dihydro-4H-dibenzo[de,g]quinolin-7-yl)-6,7-dihydro-5H-[1,3]dioxolo[4',5':4,5]benzo[1,2,3-de]benzo[g]quinoline. Others were (**ECH-56**)7-methyl-8-(1,2,3-trimethoxyl-5,6-dihydro-4H-dibenzo(*de,g*)quinolin-7-yl)-6,7-dihydro-5H-(1,3)dioxolo(4'5':4,5)benzo(1,2,3-d*e*) benzo(*g*)quinoline, (**ECF 5-10)** O-methyl moschatoline,**(ECP-23)**7-dehydro-nornuciferinyl-7'-dehydro-O-methylisopiline, and (**ECH-B 17-18**) Urabaine**.**

Table 3.1: Extracts, separation techniques, F_{ry} values and % yields.

Extract	Fraction	Separation Technique	Solvent System	R_f value	Yield
Ethyl acetate(EC)	ECP-17(88)	Column chromatoraphy(CC)	Hexane/EC 50:50	0.42	0.0002%
Methanol	ECM-1(41)	CC	EC/Methanol 95:5	0.45	0.28%
Ethyl acetate(EC)	ECP-19(89)	CC	Hexane/EC 35:65	0.93	0.00029%
Ethyl acetate(EC)	ECHE 45(90)	CC	Hexane/EC 60:93	0.50	0.00062%
Hexane	ECH 56(91)	CC	Hexane/EC	0.44	0.00062%
Hexane	ECF 5-10(92)	CC/FC	Hexane/EC 85:15	0.42	0.00082%
Ethyl acetate(EC)	ECP 23(93)	CC	Hexane/EC 30:70	0.50	0.0026%
Hexane	ECH-B 17-18(94)	CC/Normal Phase HPLC	Hexane/EC 55:45	0.45	0.002%

The yields in % were obtained by dividing the resultant chromatography fractions weight by the starting ground plant material weight, for example 20 mg obtained from a chromatography fraction was divided by 804.5 g starting plant material and the result expressed in percentage to obtain the yield percentages in the table above.

3.1.1: Characterization of Compound 88: ECP-17

The ^{1}H NMR spectrum of ECP-17 (**Figure 3.1**) gave sufficient information for it to be identified as a dehyroaporphine system. The NMR spectral were processed used Mnova software.

Figure 3.1: ^{1}H NMR (400MHz, CDCl3) of ECP

A11875
person manager
ECP-17
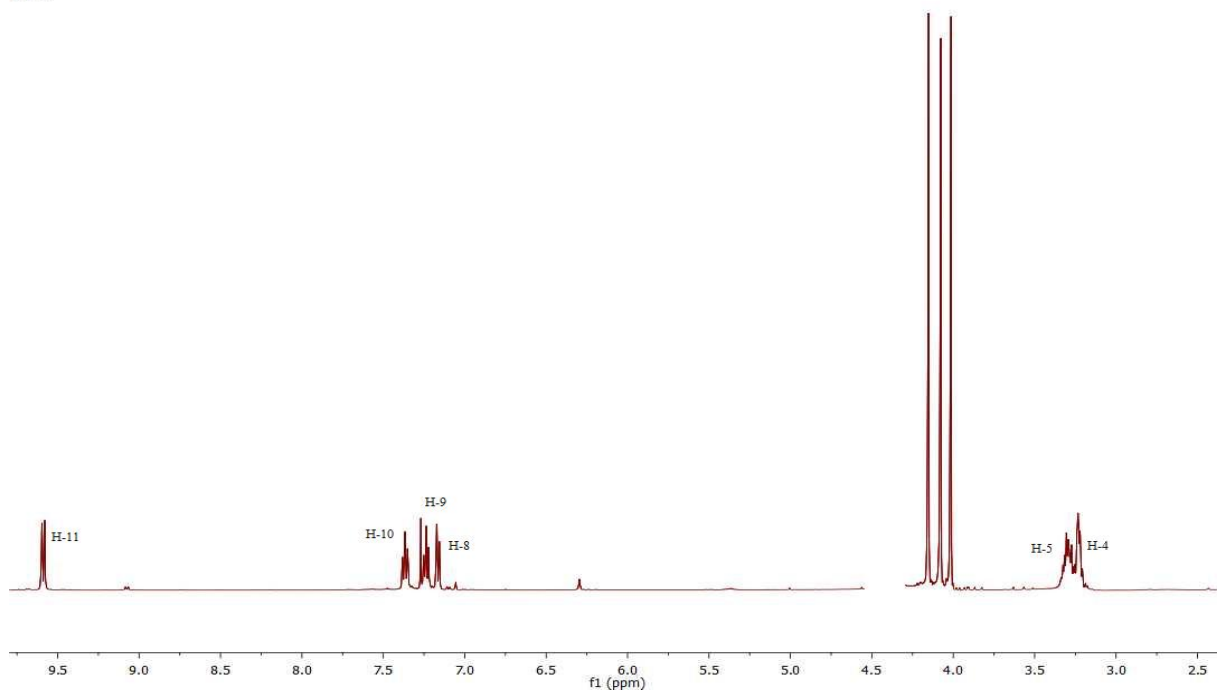
^{1}H NMR Spectrum showed the aporphine alkaloid had a strongly deshielded proton δ_H 9.59 ppm (doublet, *J= 6.8 Hz,H-11*), completing the four-spin aromatic system were δ_H 7.90 ppm (doublet of doublet of doublet *J*=6.8,5.6,0.8 Hz , H-10), 7.24 ppm (doublet of doublet of doublet ,*J* = 6.8Hz,5.6Hz,0.8Hz ,H-9), 7.17 ppm (doublet of doublet, *J*= 6.8,0.8Hz ,H-8). The fact that there are only these four aromatic protons, three methoxy signals (4.01 ppm, 4.08 ppm, 4.15 ppm) and aliphatic methylene resonances which appeared as a complex multiplex between δ_H 3.23 ppm (H-4) and doublet of doublet H-5 (*J= 6.24Hz, 9.28Hz*) at 3.29 ppm completed the structure of an aporphine alkaloid as shown in (**81a**) below, implying that there is no proton at position 7 as described by Connolly JD et al., (1996).

OCH₃
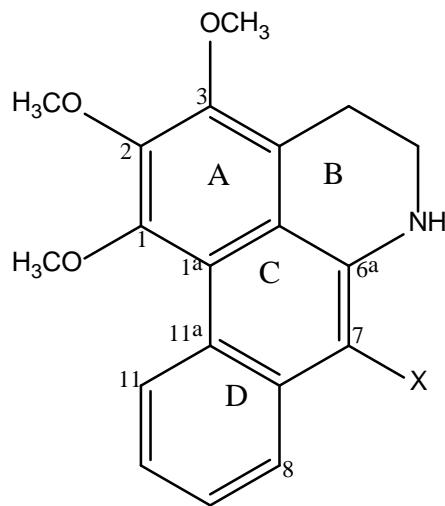
(**88a**)

X-Unknown.

X is stated as unknown because structure elucidation was done in such a way that one could build piece by piece the full structure of ECP-19 in a sequential manner.

The [13] C NMR Spectrum (**Figure 3.2**, **Table 3.2**) was as expected for an aporphine alkaloid with 19 carbons. It had four aromatic methines (123.1 ppm, 123.8 ppm, 126.8 ppm, and 127.2 ppm), two

methylene (23.9 ppm and 93.8 ppm), and three methoxy carbons (60.4 ppm, 60.9 ppm and 61.3 ppm)

together with ten quaternary carbons (120.5 ppm, 121.8 ppm,122.1 ppm,122.8 ppm,125.8 ppm,132.9 ppm, 192.4 ppm 146.9 ppm,148.8 ppm and 151.4 ppm).
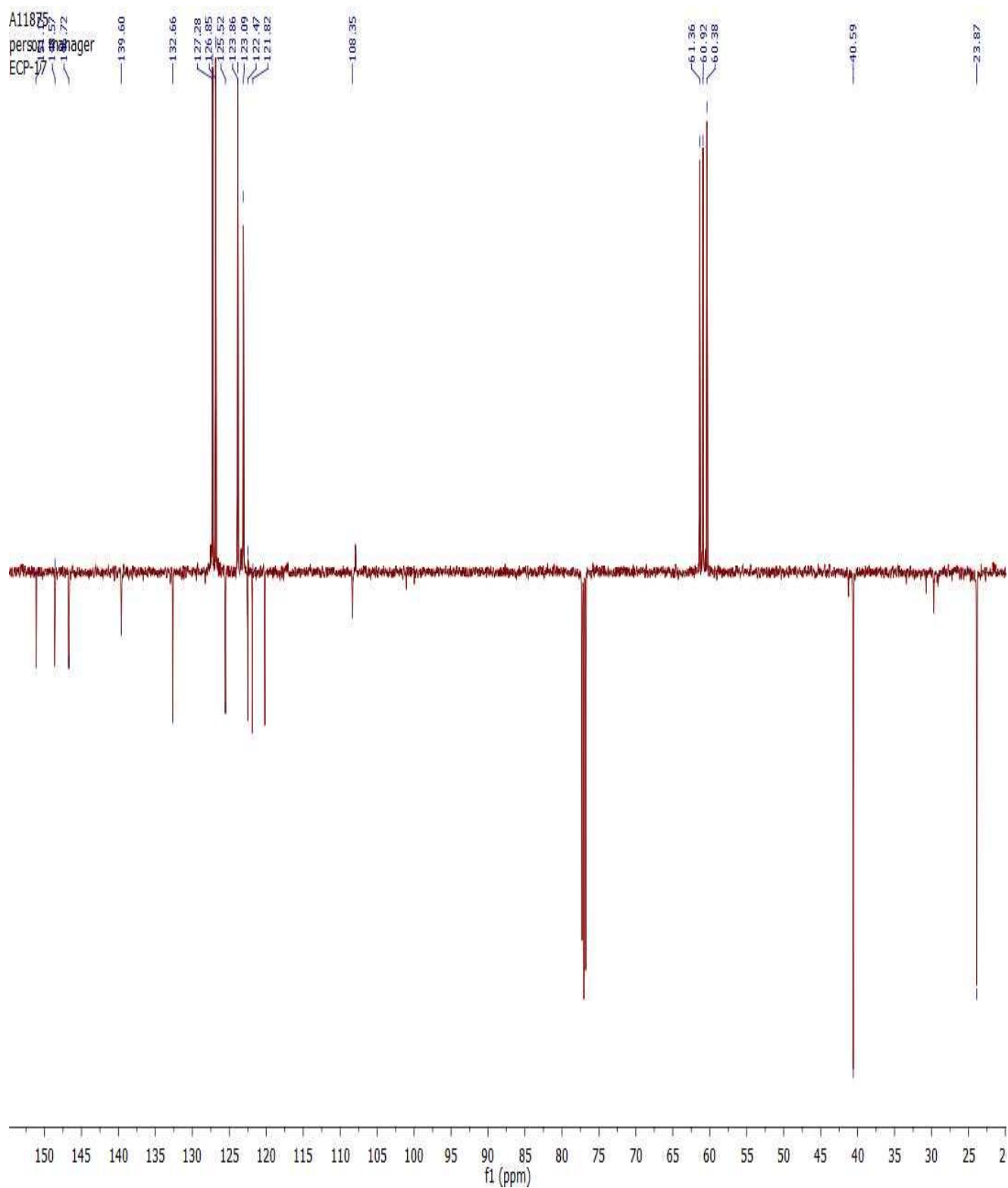
Figure 3.2: ^{13}C NMR Spectrum (400MHz, CDCl3) of ECP 17. It is a J –modulated spectrum like other 13 C spectral discussed in this thesis, C-1 and C-3 carbons were facing upwards, while C (quaternary carbon) and C-2 were facing downwards.

The ^{1}H-^{1}H COSY NMR Spectrum (**Figure 3.3**) showed 9.59 ppm (H-11) was ortho-coupling to (H-10) 7.90 ppm, while the latter was further coupled (ortho) to 7.24 ppm (H-9) and 7.17 ppm (H-8) (Meta).
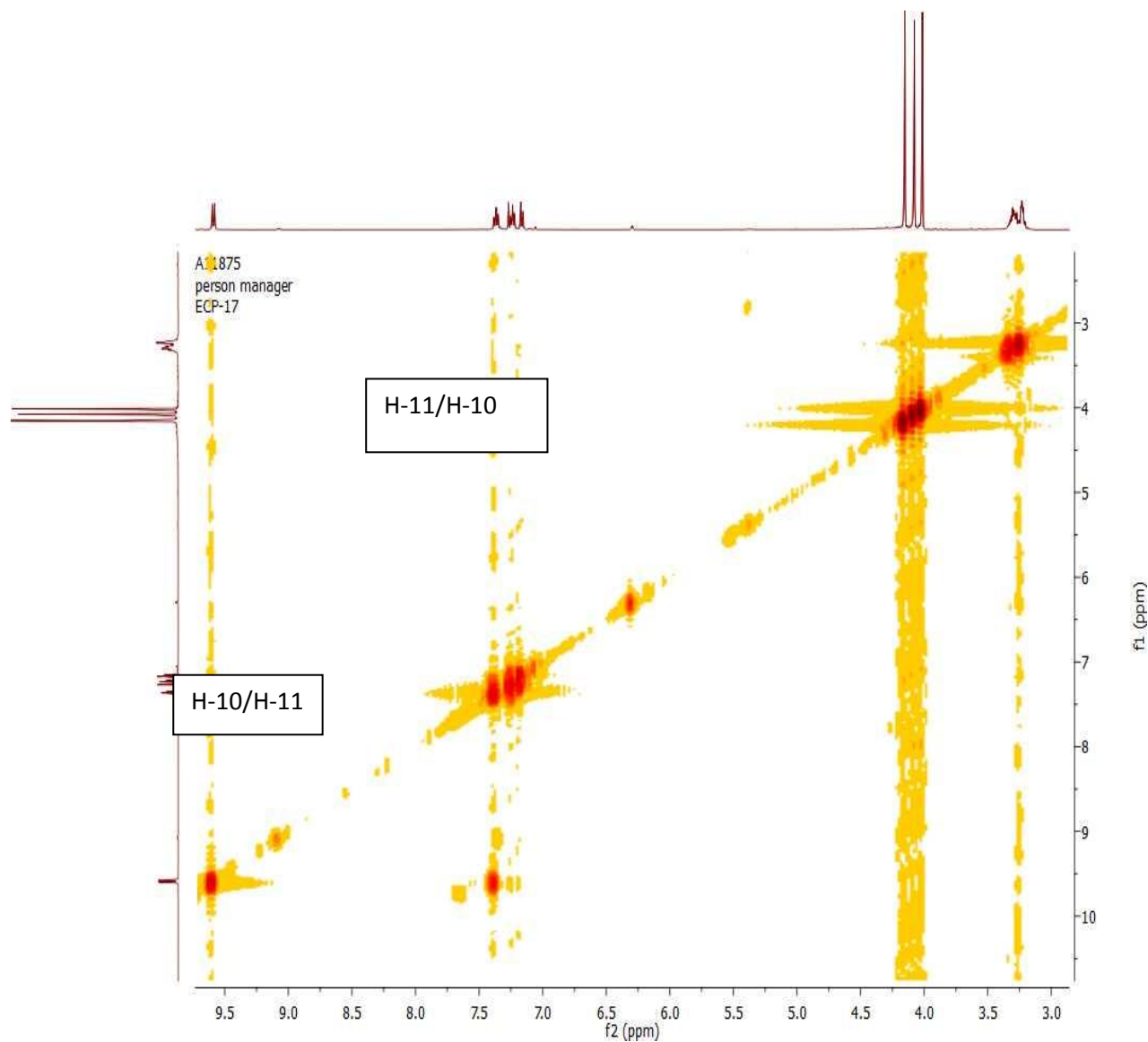
Figure 3.3: COSY NMR (400MHz, CDCl$_3$) of ECP 17

The HSQC Spectrum as shown below was consistent with an aporphine with three methoxys, two aliphatic methylenes and four aromatic protons as listed in **Table 3.4.**

Figure 3.4: HSQC NMR (400MHz, CDCl$_3$) of ECP 17
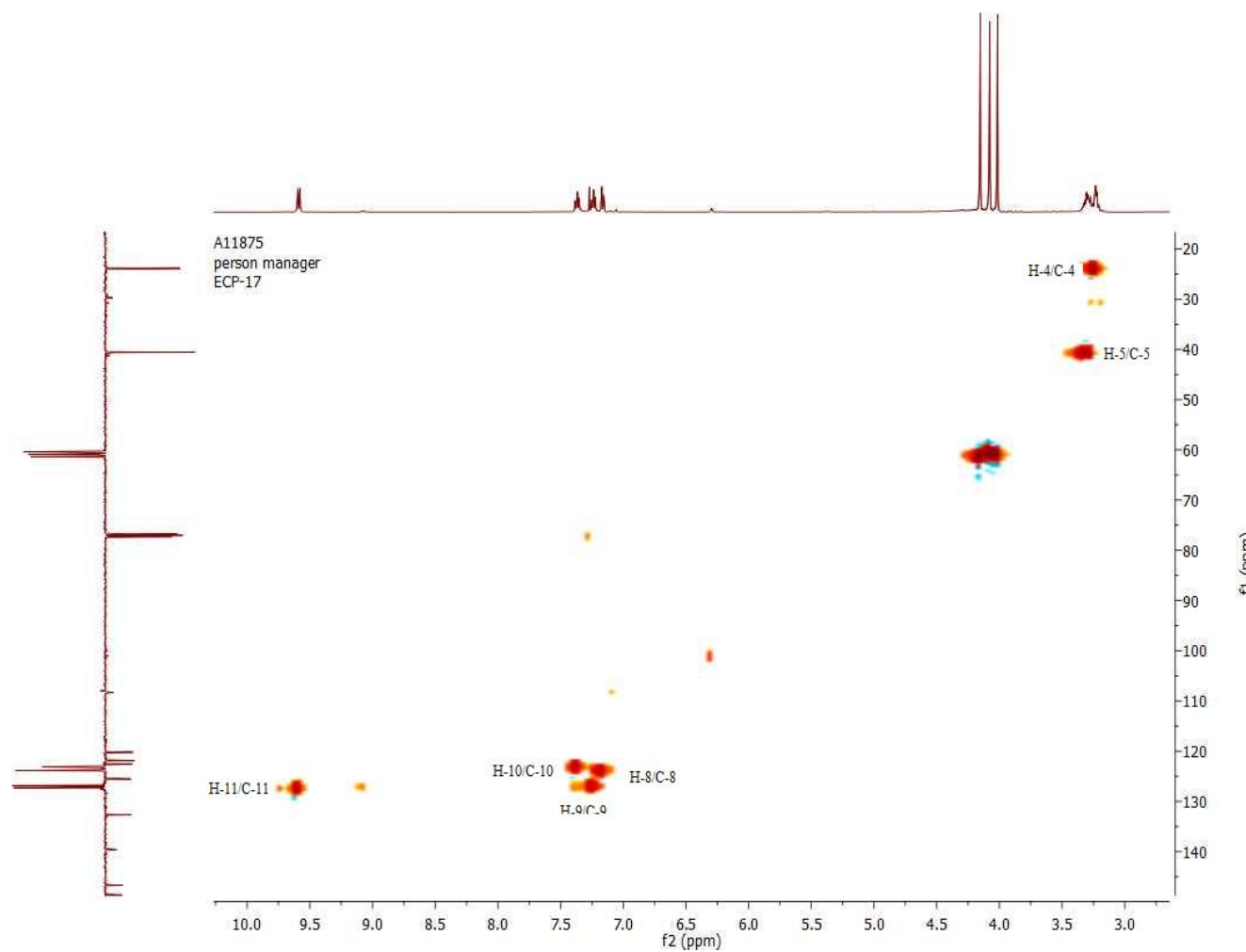
The HMBC Spectrum as shown in **Figure 3.5a and 5b,** the most deshielded aromatic proton δ_{11} 9.59 had ^{3}J coupling in ring D with carbon at 126.8 ppm (C-9) and 132.7 ppm (C-7a). Proton 11 is the most deshielded proton because it is the most stearically hindered of the four aromatic protons. The latter

carbon also showed strong ^{3}J coupling with H-9 (δ 7.24) and this proton was coupled to C-11(127.3 ppm). The other correlations within ring D involving H-8 and H-10 are given in **Table 3.2.**

[91]
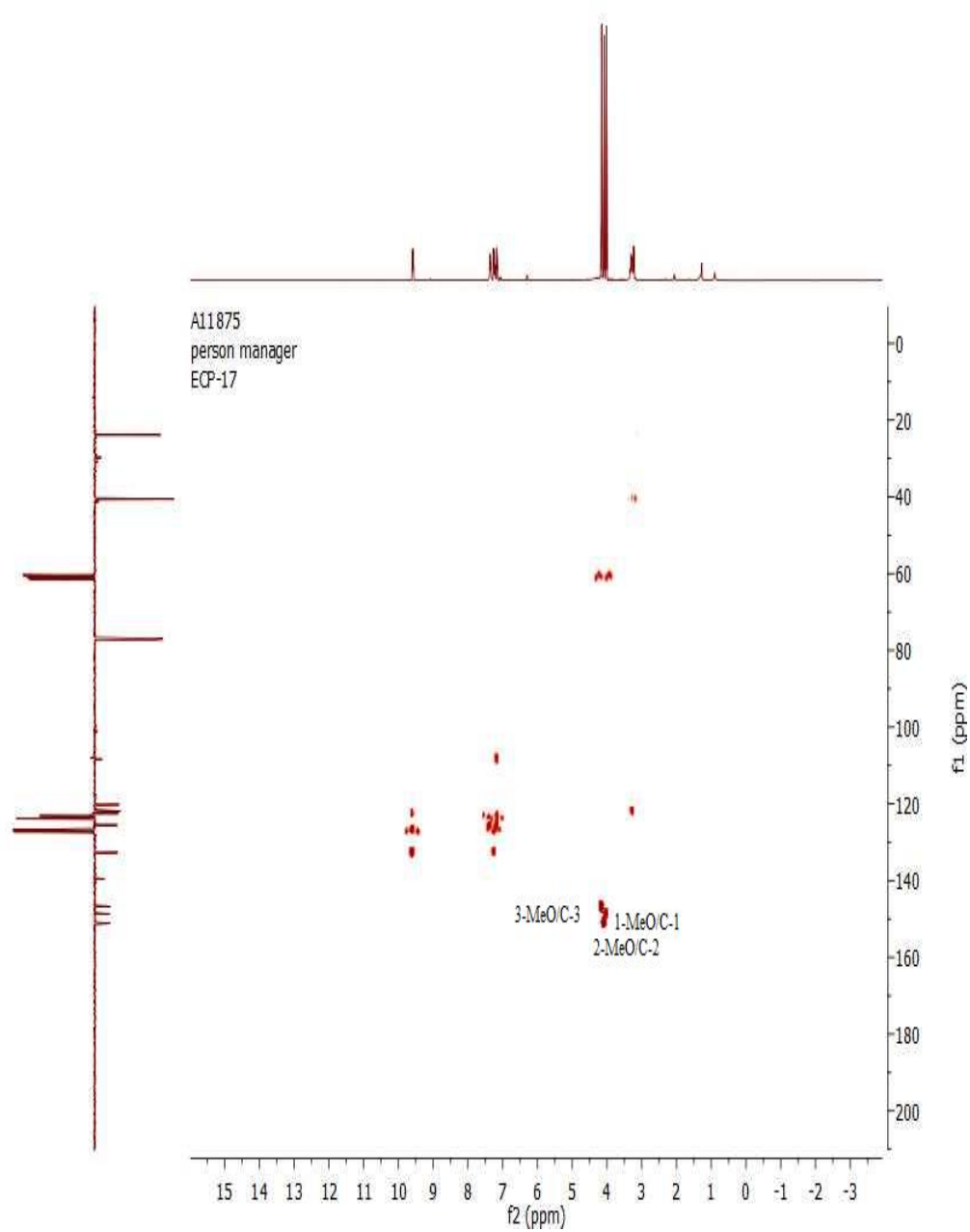
Figure 3.5a: HMBC NMR (400MHz, CDCl$_3$) of ECP 17
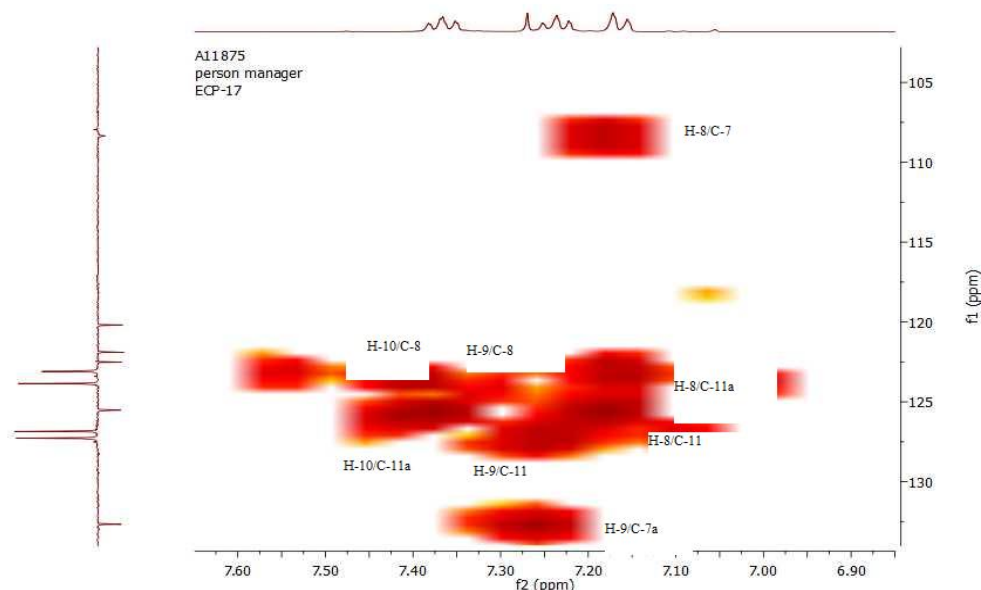
Figure 3.5b: HMBC NMR Spectrum (400MHz, CDCl₃) of ECP 17 (aromatics)

H-11(δ 9.59) correlated with a carbon outside ring D at 122.5 ppm which must be C-1a on the ring junction between ring A and C. In a similar fashion H-8 (δ 7.17) showed further strong (^{3}J) coupling with carbon-7 (108.3) in ring C.

Each of the three methoxys showed ^{3}J correlations to their respective aromatic oxygenated carbons (see **Table 3.2**). The methylene protons of C-4 and C-5 had correlations to each other's carbon and both showed strong correlations to a single aromatic carbon which could only be C-3a (122.9 ppm). The methoxy protons of position-3 (δ_H 4.01) had an NOE with the protons at δ_H 3.23 (H-4), while the methoxy δ_H 4.08 (C-1 OMe) NOEed a proton at δ_H 9.59 (H-11). This confirmed the assignments of the methoxys and their associated chemical shifts. There was a very weak correlation with a quaternary carbon at 192.6 ppm which must be C-6a carrying the nitrogen. This set of data implies an aporphine alkaloid but with C-7 as a quaternary carbon (108.3 ppm), it was not clear what was attached at that position.

The expected mass of dehydro-O-methylisopiline would be 308. However the ESI MS Figure of Compound 35 gave a quasi-molecular ion in positive ion mode at 615.20 (M+H)$^+$ indicating that this was actually a symmetrical dimer connected via C-7/C-7'.
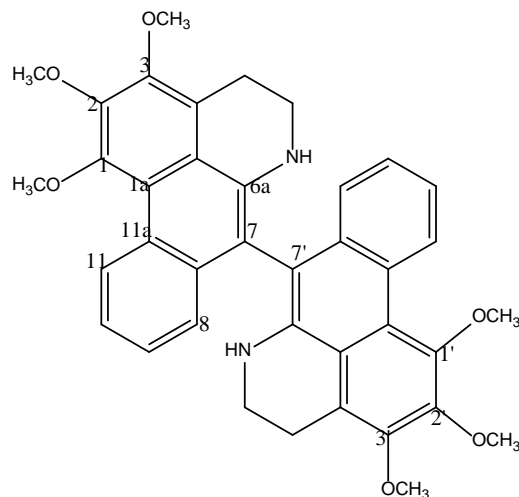
(**81**)

This compound, 7, 7'- Bisdehydro-*O*-methylisopiline obtained from column chromatography was

previously isolated from Malaysian peninsula *Polyalthia bullata* ethyl acetate extract as reported by

Connolly JD *et al*., (1996), although there are some differences between the assignments of some

proton/carbon shifts made by the above authors and those reported in this thesis. For example, the C-7

carbon assignment in the current data based on 2D NMR correlations, was 108.3 ppm [compared with

120.1 ppm reported by Connolly JD *et al*., (1996) as well as C-8 at 123.8 ppm [127.2 ppm],C-10

at123.1[123.8 ppm], C-11 at127.3 ppm [123.1],1-OMe at 60.9 ppm [60.4 ppm],2-OMe at 60.4 ppm

[60.9 ppm],C-1 at 151.1 ppm[148.6 ppm] and C-3 at148.6 ppm [151.1 ppm].

Thus ECP-17 (**81**) was identified as 1,1',2,2',3,3'-hexamethoxy-5,5,6,6'-tetrahydro-4H,4'H-7,7'-

bidibenzo[de,g]quinoline also known as 7,7'- Bisdehydro-*O*-methylisopiline and this is the first report

of this compound in *E. chlorantha*.

Table 3.2: ^{1}H and ^{13}C chemical shifts of ECP-17

Position	^{1}H (ppm)	^{13}C (ppm)
1-OMe,1-MeO'	4.01	60.9
2-OMe,2-MeO'	4.08	60.4
3-OMe,3-MeO'	4.15	61.4
C-1,C-1'	-	151.1
C-1a,C-1a'	-	125.5
C-1b,C-1b'	-	123.4
C-2,C-2'	-	146.7
C-3,C-3'	-	148.6
C-3a,C-3a'	-	121.9
C-4,C-4'	3.23	23.9
C-5,C-5'	3.29	93.6
C-6a,C-6a'	-	192.6
C-7,C-7'	-	108.3
C-7a,C-7a'	-	132.7
C-8,C-8'	7.90	123.8
C-9',C-9	7.24	126.8
C-10,C-10'	7.14	123.1
C-11,C-11'	9.59	127.3
C-11a,11a'	-	122.5

Table 3.2 HMBC correlations of ECP-17

Position	^{1}H(ppm)	^{13}C(ppm)
1-OMe	4.08	1 (151.1)
2-OMe	4.15	2 (146.7)
3-OMe	4.01	3 (148.6)
4	3.23	5(93.6) 3a(121.9)
5	3.29	4(23.9),3a(121.9)
8	7.90	8(123.84) 11a(125.5)
9	7.24	7a(132.7),8(123.1)11(127.3)
10	7.17	11(127.3),11a(125.5)7(108.3)
11	9.59	7a(132.7),9(126.8),1a(122.5)

3.1.2: Characterization of ECM-1, Compound 41, as the protoberberine alkaloid Palmatine.

ECM-1 was obtained from column chromatography as described in Table 3.5 and mass was

confirmed by ESI-MS Figure which gave a quasi-molecular ion $(M+H)^+$ at region m/z 352.30 with predicted molecular formula of $C_{21}H_{22}NO_4$.
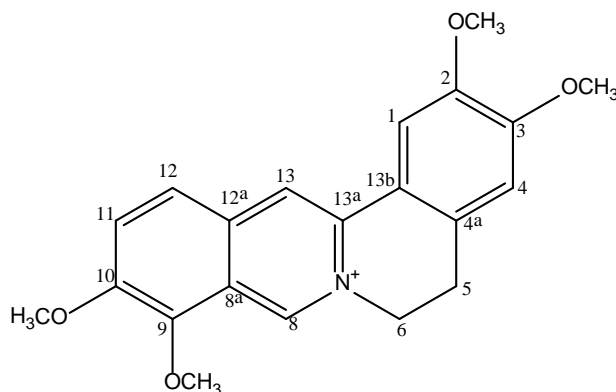
2, 3, 9, 10-tetramethoxy-5, 6-dihydroisoquinolino [2, 1-b] isoquinolin-7-ium

(**41**)

The ^{1}H NMR Spectrum (**Figure 3.6a- b** (500 MHz in DMSO-d$_6$) indicated a protoberberine system as previously described by Wafo (1998) with four deshielded methyl groups at δ_H3.85 (3-OMe),3.92 (2-OMe), 4.05 (10-OMe) and 4.09 (9-OMe).
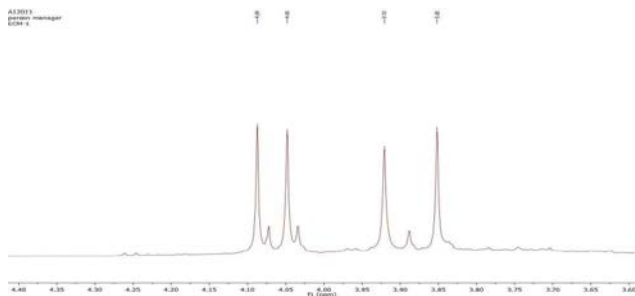
Figure 3.6a: ^{1}H NMR (500 MHz, CDCl3) Figure of ECM-1 (methoxys)
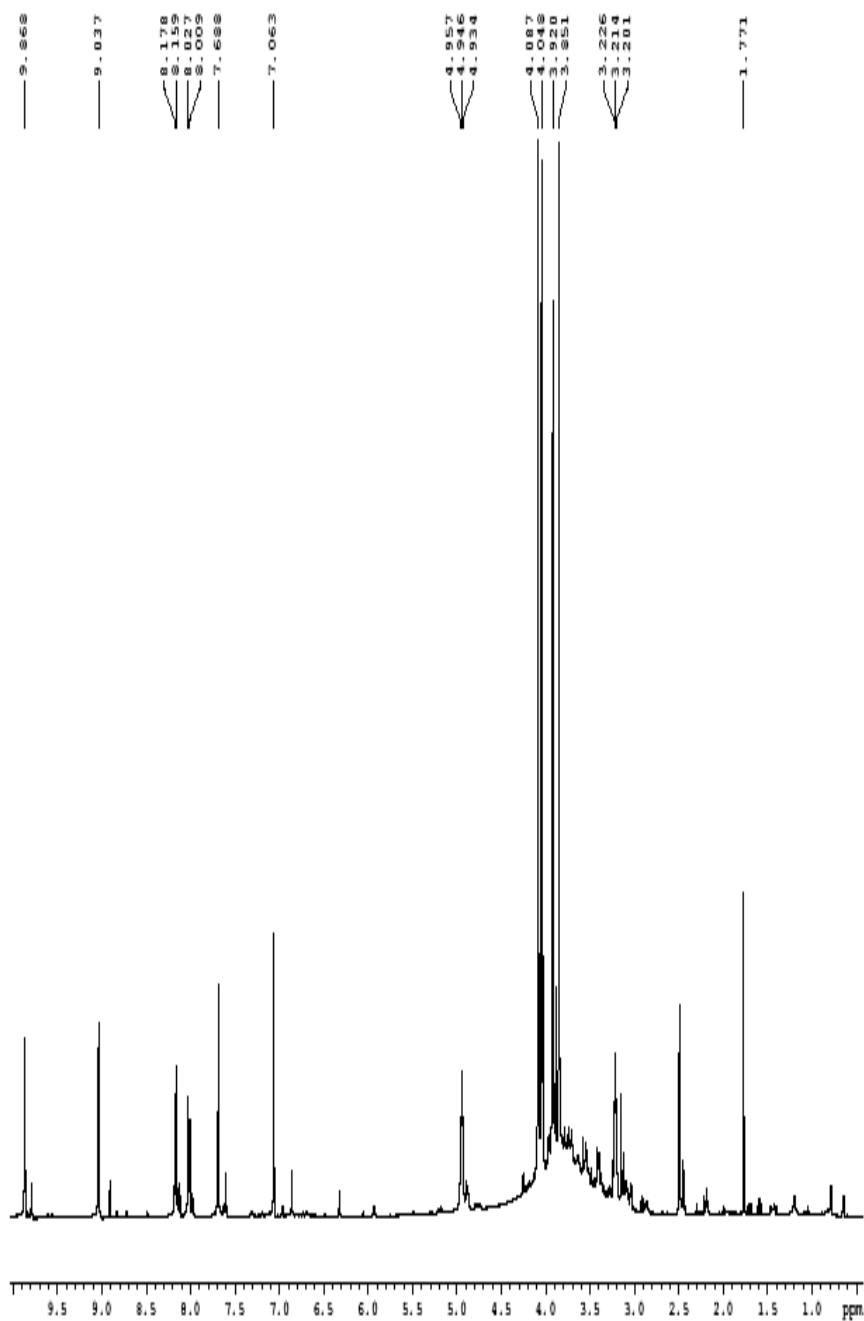
NAME   A12011
EXPNO   1
PROCNO   1
Date_   20090826
Time   11.54
INSTRUM   DRX500
PROBHD 5 mm DUL 13C-1
PULPROG   zg30
TD   65536
SOLVENT   DMSO
NS   32
DS   2
SWH   10288.065 Hz
FIDRES   0.156983 Hz
AQ   3.1850996 sec
RG   80.6
DW   48.600 usec
DE   6.00 usec
TE   300.0 K
D1   1.00000000 sec
TD0   1

======= CHANNEL f1 =======
NUC1   1H
P1   12.00 usec
PL1   -2.70 dB
SF01 500.1330885 MHz
SI   32768
SF   500.1300084 MHz
WDW   EM
SSB   0
LB   0.30 Hz
GB   0
PC   1.00

Figure 3.6b ^{1}HNMR (500 MHz, CDCl$_3$) of ECM 1 (**41**)

The protoberberine unit had strongly deshielded protons δ_H 9.87 (singlet , H-8), and 9.04 (singlet, H-13), two deshielded ortho -substituted protons 8.18 ppm (doublet J= 9.08 Hz,H-11) and 8.02 ppm(doublet „J= 9.08 Hz,H-12) on ring D as shown in the ^{1}H/ ^{1}H COSY Spectrum (**Figure 3.7**), while aromatic ring A had two protons para- substituted 7.69 ppm (singlet, H-1), and 7.06 ppm (

singlet, H-4) with the two methoxys attached to complete the ring. Completing the protoberberine unit were two vicinal methylene groups at 3.22 ppm (H-5) and 4.95 ppm (H-6) shown to be coupling in the ^{1}H/ ^{1}H COSY Spectrum (**Figure 3.7**).
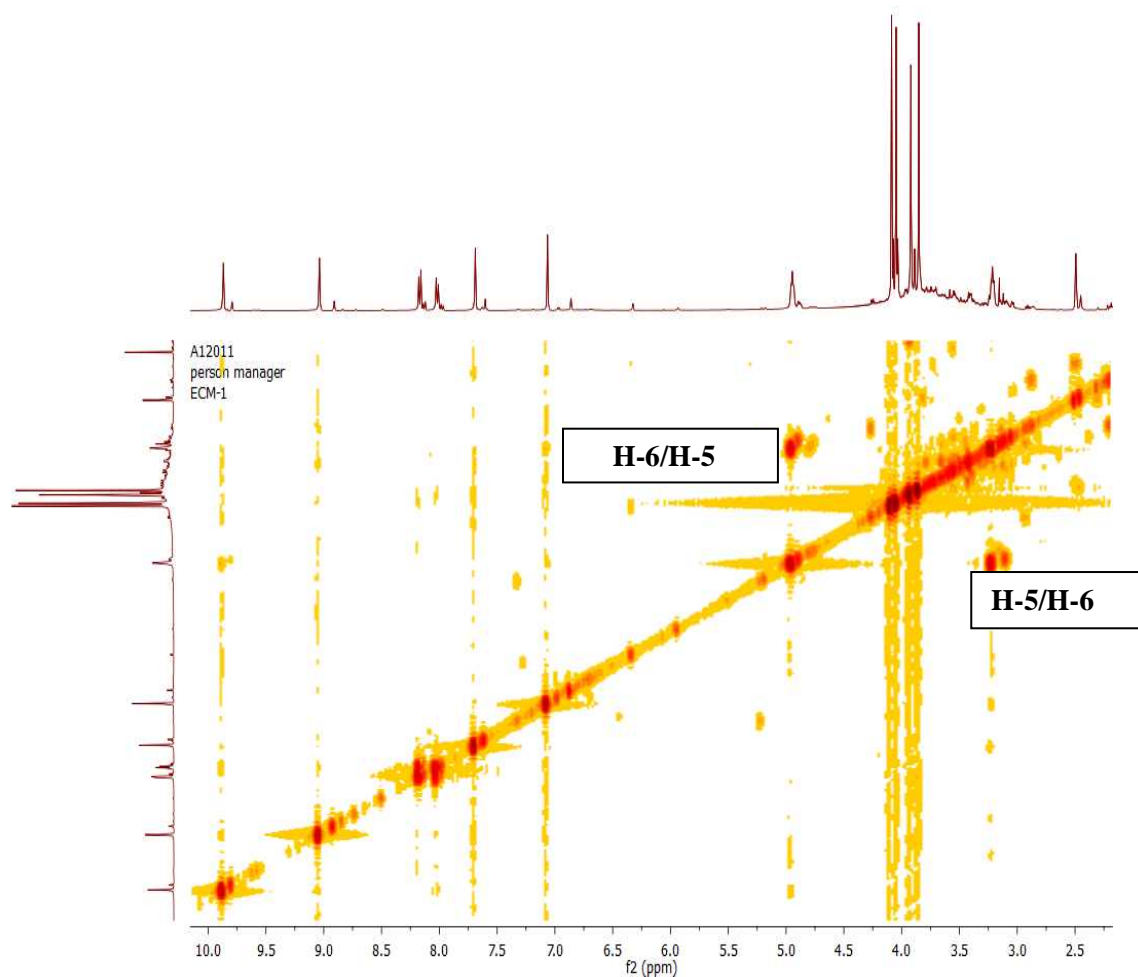
Figure 3.7: ^{1}H-^{1}H-COSY NMR (500MHz, CDCl$_3$) of ECM-1(**41**)

The ^{13}C NMR Spectrum (**Figure 3.8**) with ^{13}C chemical shifts as shown in Table 3.4 correlates as expected for a protoberberine.
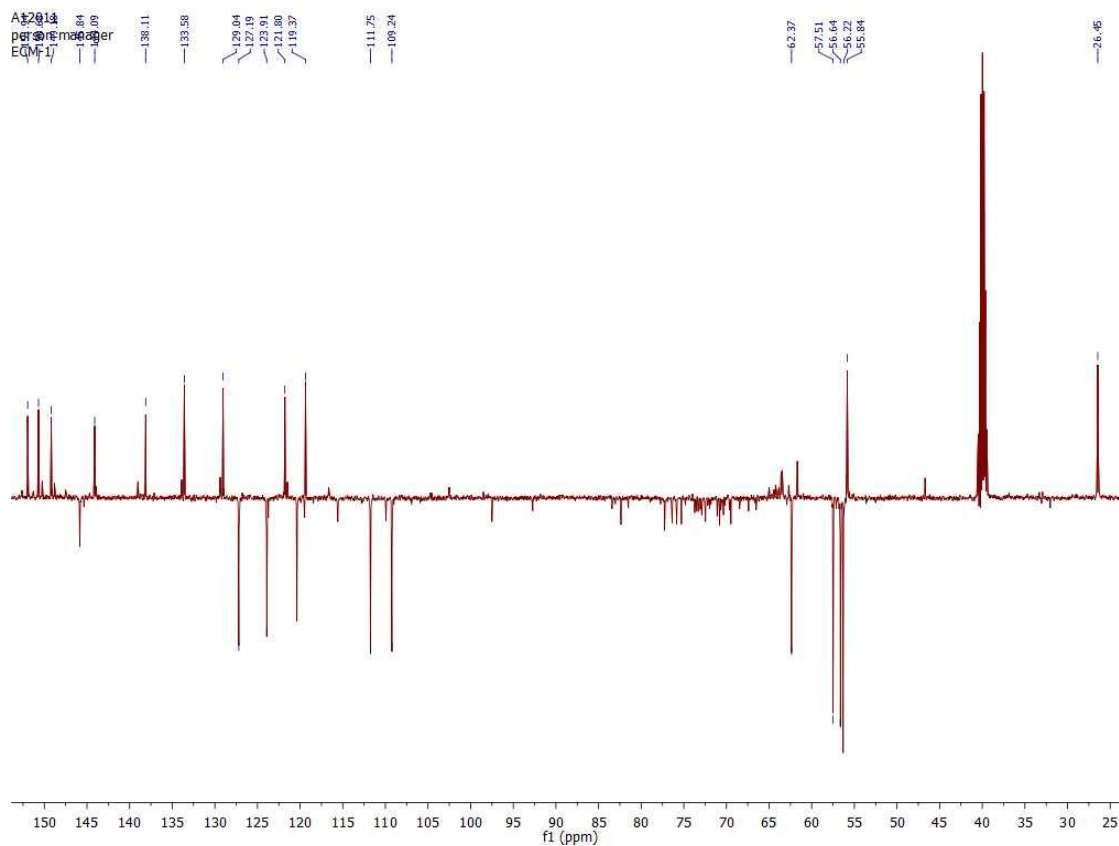
Figure 3.8: ^{13}C NMR (500MHz, CDCl3) Spectrum of ECM-1(**41**)

This spectrum like its ^{1}H spectrum indicated that this is not a pure compound, as it has an associated protoberberine alkaloid tagging along as source of impurity.

The HSQC Spectrum (**Figure 3.9**) confirmed the methoxy protons were attached to ^{13}C carbons 2-MeO, 3-MeO, 10-MeO and 9-MeO at 56.6, 56.4, 57.5 and 62.4 ppm, respectively, and the fact that the

9-MeO methoxy was the most deshielded methoxy indicated it was sterically hindered.
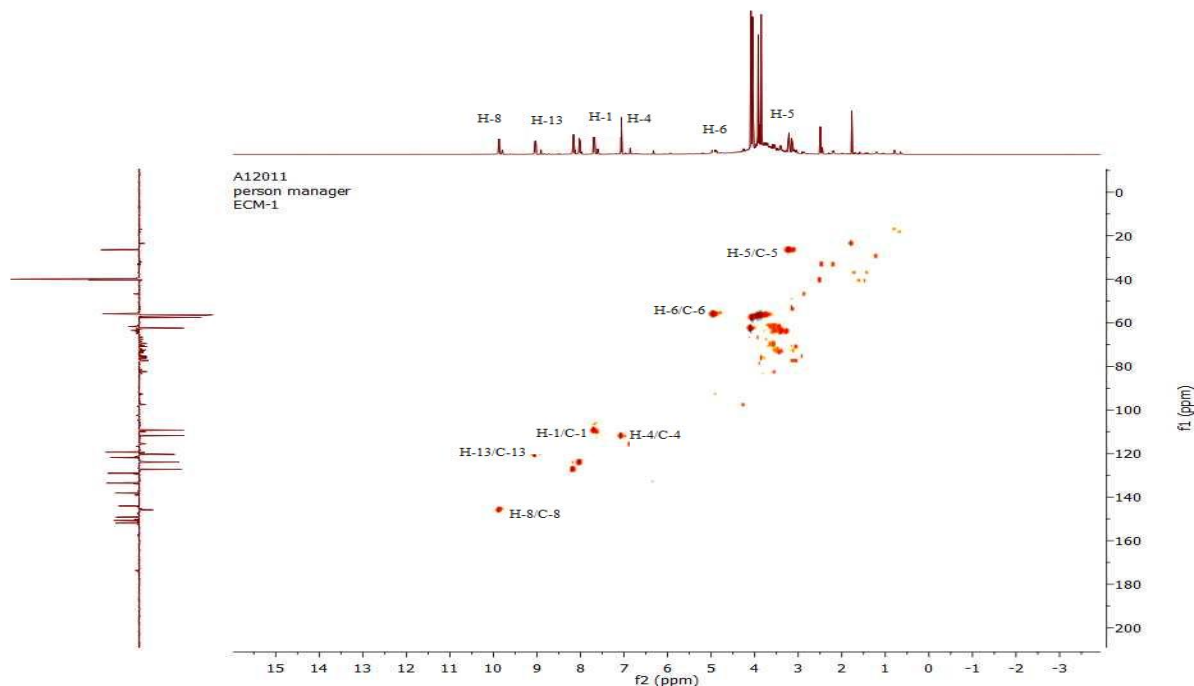
Figure 3.9: HSQC NMR (500MHz, CDCl3) Spectrum of ECM-1(**41**)

The HMBC Spectrum (**Figure 3.10a**) revealed the four methoxys showed strong ^{3}J couplings to their respective aromatic oxygenated carbons. The proton δ_H 8.02 showed a strong ^{3}J coupling to a carbon at 150.7(C-10) as well as carbons 121.8 ppm (quaternary carbon, C-8a) and aromatic methine 120.4 ppm (C-13). It also had weak correlations to aromatic methine 127.2 ppm (C-11) and quaternary carbon 133.6 ppm (C-12a).

The proton δ_H 8.17 showed strong ^{3}J coupling to the quaternary carbons 133.6 (C-12a) and 144.1 (C-9). The latter carbon was coupled to the methoxy δ_H 4.09 which bore the sterically hindered methoxy. The proton δ_H 8.17 also showed weak ^{2}J coupling to the neighbouring aromatic carbons 123.9 (C-12) and quaternary carbon 150.7 (C-10). The proton δ_H 9.04 showed strong ^{3}J couplings to quaternary carbon 121.8 ppm (C-8a) and aromatic carbon 123.9 ppm(C-12). This proton also had further correlations to carbons at 119.4 ppm (C-13b) and 191.1 ppm (C-13a).
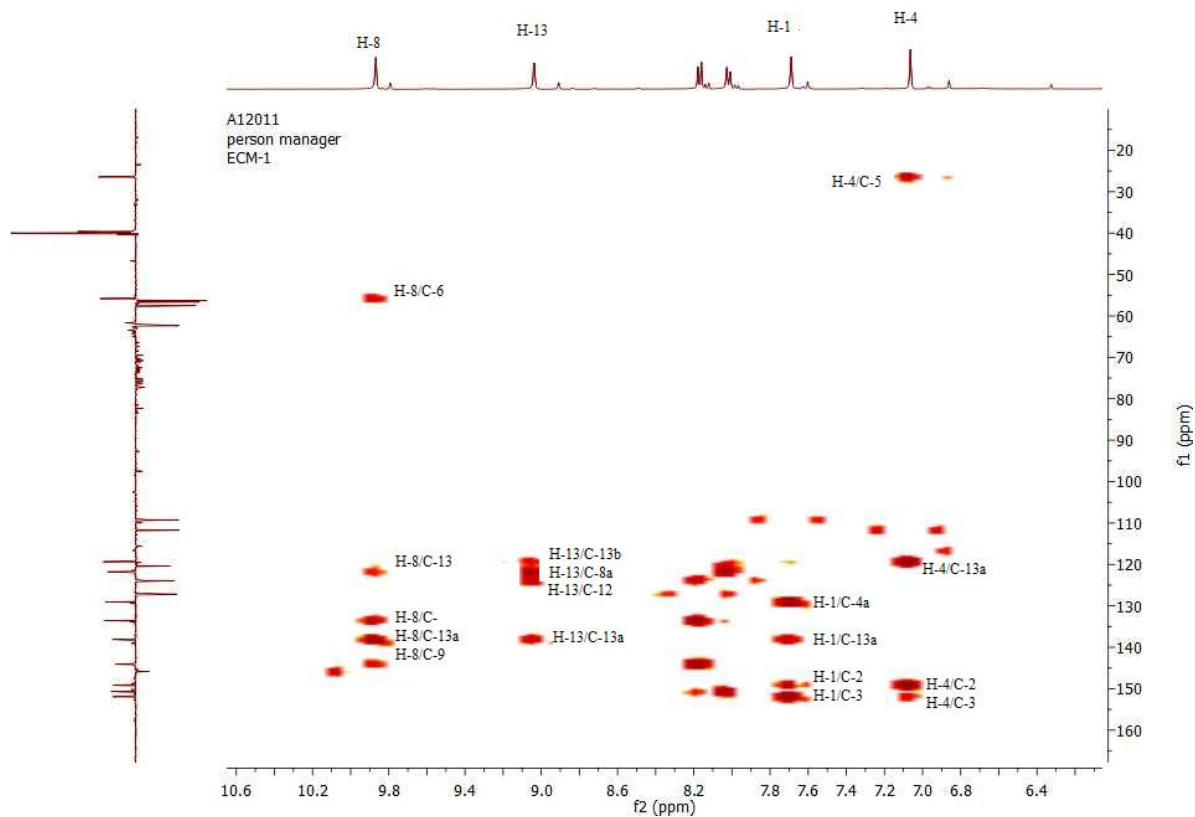
Figure 3.10a: HMBC NMR Spectrum (500MHz, CDCl$_3$) of ECM-1(deeper levels)

Another highly deshielded aromatic proton singlet δ$_H$ 9.87(δ$_C$145.8 ppm from the HMBC

Spectrum also showed strong ^{3}J coupling to two carbons 133.6 ppm (C-12a), 144.1 ppm (C-9) as well as quaternary carbon 191.1 ppm (C-13a) and an aliphatic methylene carbon at 55.8 ppm. The presence of a further aromatic ring bearing two non-sterically hindered methoxy groups and two proton singlets was supported by the following: the proton δ$_H$7.06 ppm (δ$_C$111.7 ppm) had strong ^{3}J couplings to quaternary carbon 119.4 ppm (C-13b) and quaternary carbon which bore the methoxy at δ$_H$ 3.92, as well as an aliphatic methylene (CH$_2$) at 26.4 ppm (δ$_H$3.22). The proton at δ$_H$ 7.69 showed strong couplings with carbon at 129.0 ppm(C-4a), 152.0 ppm (C-3) and a further carbon at 191.1 ppm which was already seen to be coupling with δ$_H$ 9.87 and 9.04 the most deshielded protons in the molecule. These data allow the assignment of the structure to the known protoberberine alkaloid palmatinepreviously isolated   from a methanol: chloroform extract of *E. chlorantha* by Wafo (1998). The strong deshielding of one set of methylene signals at δ$_H$ 4.95(t) and the proton δ$_H$

[101]

9.87 manifesting the presence of the quaternary ammonium nitrogen in position-6. The natural counter ion to this quaternary alkaloid is not known. Palmatine was the major alkaloidal secondary metabolite found in this study on *Enantia chlorantha (0.28 %* yield) and is possibly the main constituent responsible for the strong yellow-orange colour of the stem bark.

Table 3.4 ECM-1 (Palmatine's) ^{1}H and ^{13}C chemical shifts

Position	[1]H (ppm)	[13]C (ppm)
1	7.69	109.2
1a	-	119.4
1b	-	191.1
2	-	149.2
3	-	152.0
4	7.06	111.7
4a	-	129.0
5	3.22	26.5
6	4.95	55.8
7	-	-
8	9.86	145.8
8a	-	121.8
9	-	144.1
10	-	150.7
11	8.18	127.2
12	8.02	123.9
12a	-	133.6
13	9.04	120.4
2-MeO	3.92	56.6
3-MeO	3.85	56.2
9-MeO	4.09	62.4
10-MeO	4.05	57.5

Table 3.5: ECM-1 (Palmatine) HMBC correlations

Position	^{1}H (ppm)	^{13}C (ppm)
1	7.69	(3) 152.0,(2) 149.2,(13a)191.1 ,(4a)129.0,(5)26.5,
4	7.06	((2)149.2, 13a)191.1(13b)119.4, (5) 26.5
5	3.22	(4a) 129.0 ,(13b) 119.4,(6) 55.8,
6	4.95	(4a) 129.0
8	9.87	(8)145.8,(9)144.1,(13a) 191.1,(12a)133.56,(13)120.4
11	8.18	(10)150.7, (9)144.1, (12a)133.6,(13) 120.4
12	8.02	(10) 150.7, (9) 144.1, (12a) 133.6, (8a) 121.8.
13	9.04	(13b) 191.1(8a) 121.8, (1a)119.4
2-MeO	3.92	(2)149.2
3-MeO	3.85	(3) 152.0
9-MeO	4.09	(9) 144.1
10-MeO	4.05	(10) 150.7

3.1.3: Characterisation of Compound 89: ECP-19 as 1,1',2,2',3-pentamethoxy-6-methyl-5,5',6,6'-tetrahydro-4H,4'H-7,7'-bidibenzo[de,g]quinoline.

ECP 19 was obtained by column chromatography over silica gel as illustrated in Table 3.1. It was highly suggestive from the ^{1}H NMR Spectrum that ECP-19 (Compound **89**), unlike ECP-17 (

Compound **88**) which was symmetrical with two identical sets of NMR data, was likely to be an asymmetric dimer. ECP-19 showed two strongly deshielded aromatic protons at 9.73 ppm H-11' (broad doublet, J=8.49Hz) and 9.57 ppm H-11(broad doublet, J=8.91Hz), also there was an aromatic proton a singlet H-3' at 7.18 ppm. The other aromatic protons were doublet of doublet H-8 at 7.23 ppm(J= 1.58,8.50),H-8' at 7.14 ppm, H-9 at 7.28 ppm ,H-9' at 7.25 ppm H-10 at 7.34 ppm, H-10' at 7.45 ppm,as well as five methoxys (4.15 ppm ,4.09 ppm,4.08 ppm,4.02 ppm and 4.00 ppm). The aliphatic protons were at 3.23 ppm H-4', 3.21 ppm, H-4 and multiplet at 3.32 ppm H-5.
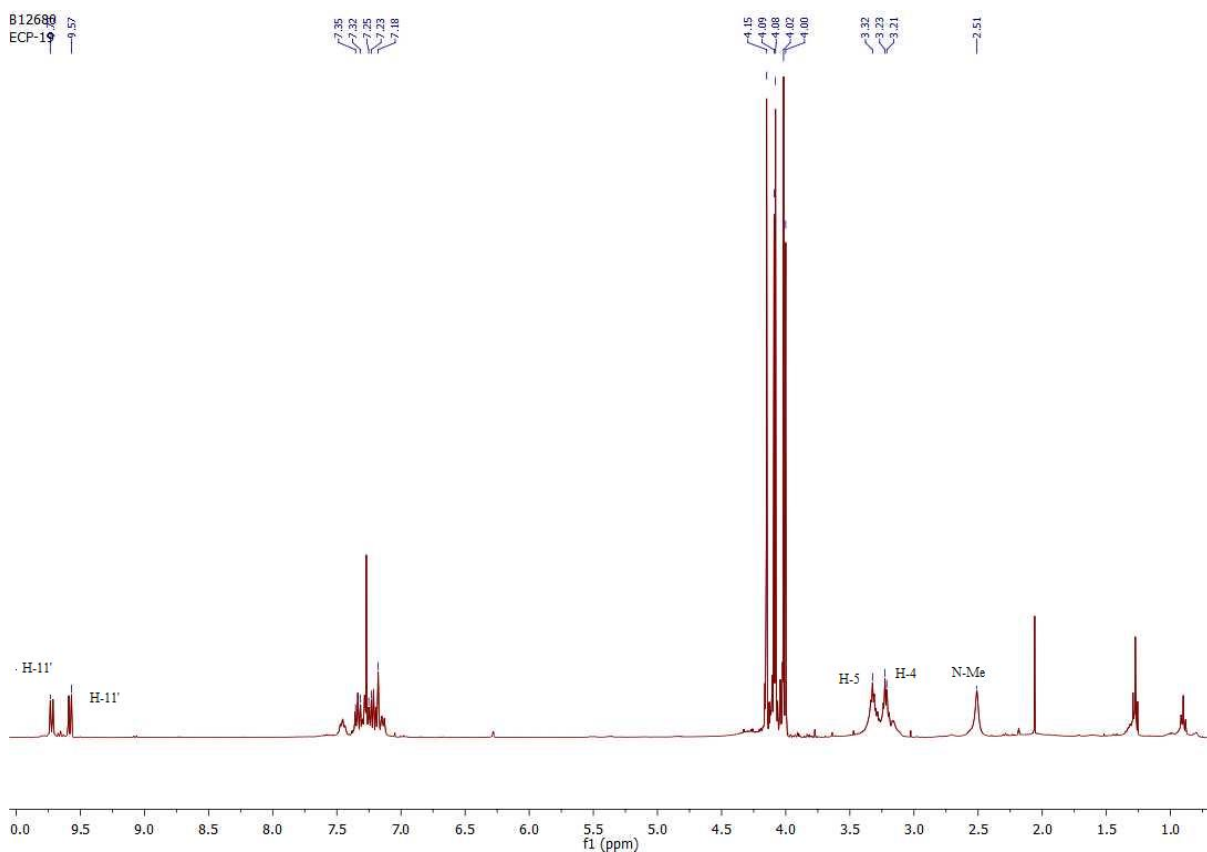
Figure 3.11: ^{1}H NMR Spectrum (400MHz, CDCl3) of ECP-19

The ^{1}H-^{1}H-COSY 2D NMR Spectrum (**Figure 3.12**) showed the highly deshielded proton 9.57 ppm was ortho-coupling with position 10's ^{1}H (7.34 ppm), of the 1st A,B,C, D spin system and the highly deshielded proton 9.73 ppm H-11'of the A',B',C',D' spin system was ortho-coupled to H-

10'(7.45 ppm) .
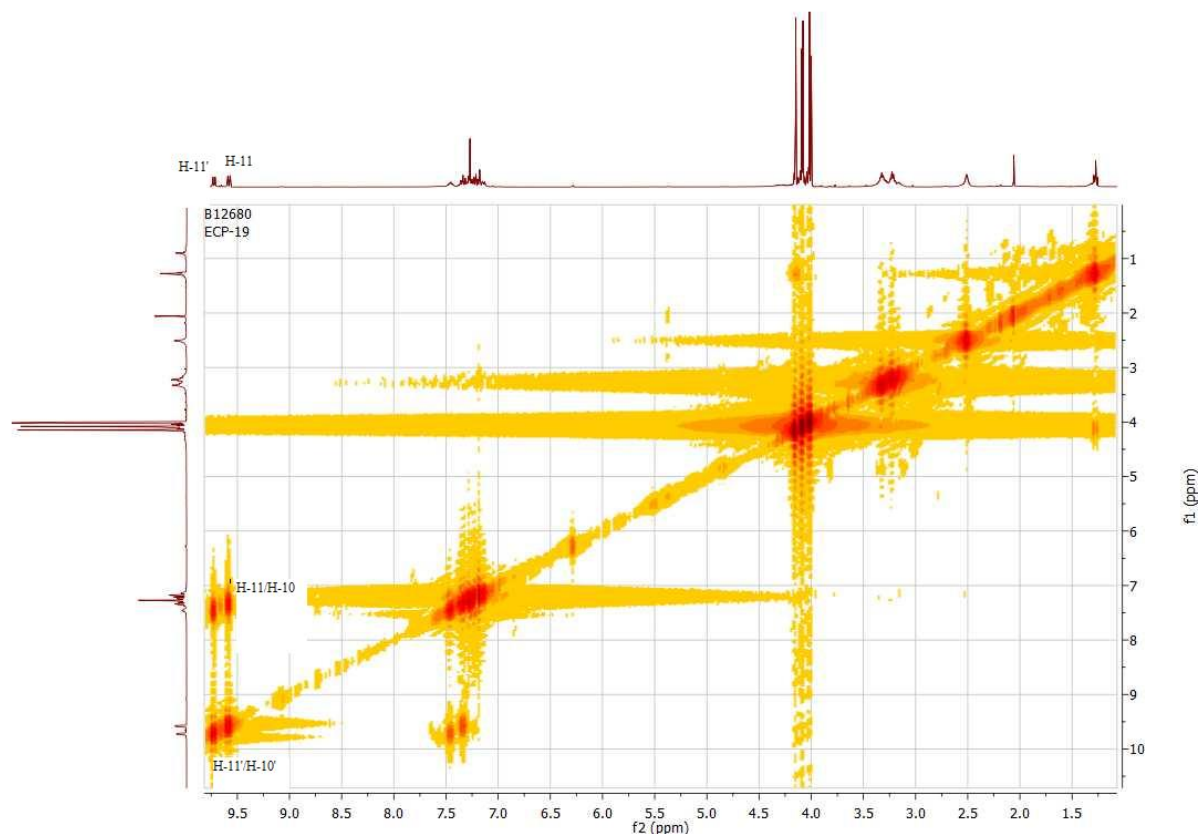
Figure 3.12:   COSY NMR Spectrum (400MHz, CDCl3) of ECP-19

The 2D NMR HSQC Spectrum (**Figure 3.13**) showed ^1J ^1H -^{13}C coupling as shown in **Table 3.7**. There was a singlet at 2.51 ppm (42.0 ppm) for N-Methyl group, three aliphatic methylenes: H-4' (δ_H 3.23, δ_C24.1), H-4 (δ_H 3.21, δ_C23.98), a complex multiplet H-5(δ_H 3.32,δ_C93.6). There were also five methoxys(δ_H 4.15,4.09, 4.08,4.02 and 4.00), nine aromatic methines H-11' (δ_H 9.73, δ_C127.9),H-11 (δ_H 9.57, δ_C127.2),H-10 (δ_H 7.34, δ_C122.5),H-10'(δ_H 7.45, δ_C125.4),H-9 (δ_H 7.28, δ_C127.1)H-9' (δ_H 7.25, δ_C 126.9),H-8(δ_H 7.14, δ_C123.8),H-8' (δ_H 7.23, δ_C126.3),H-3' (δ_H 7.18, δ_C112.5).
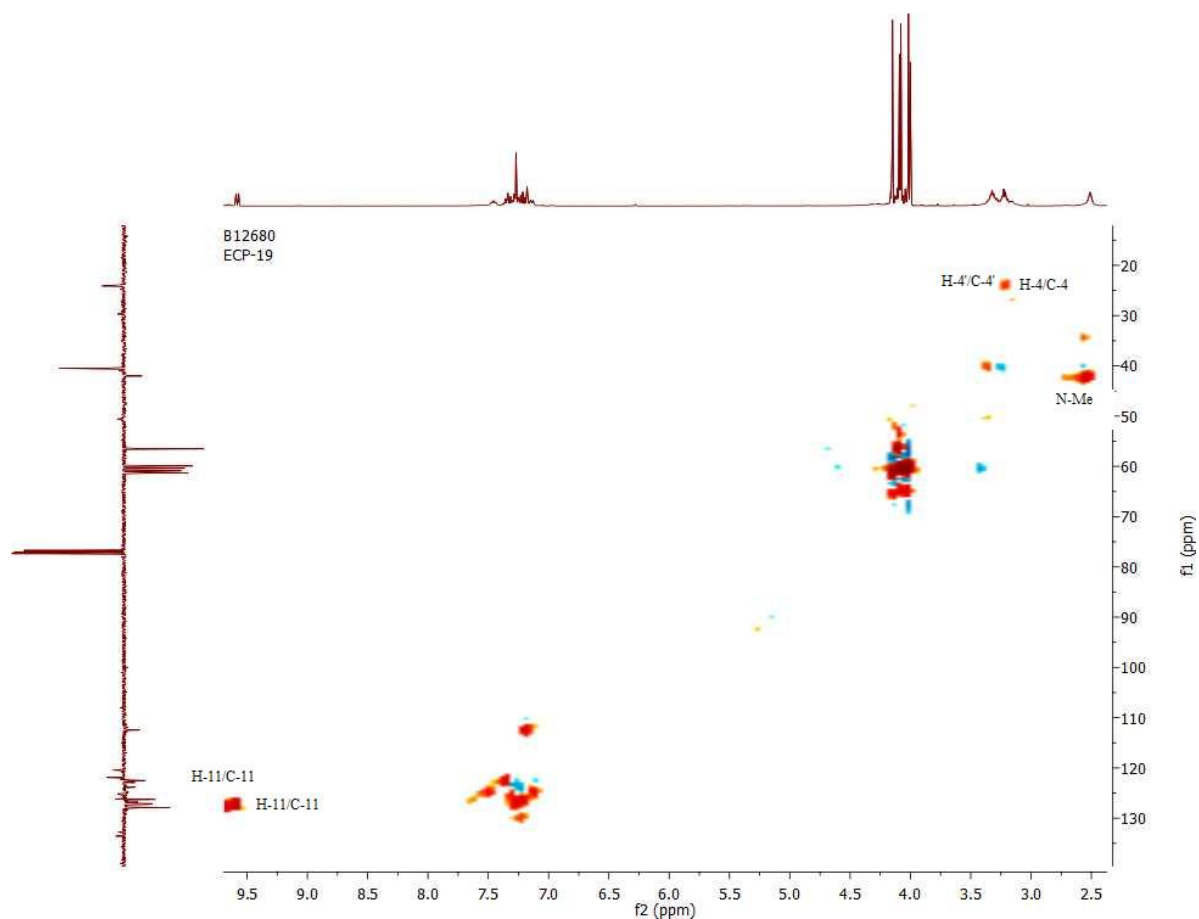
Figure 3.13: HSQC NMR Spectrum (400MHz,CDCl$_3$) Spectrum of ECP-19

Completing the 2D NMR analysis of this aporphinoid alkaloid was the HMBC Spectrum (**Figure 3.14a**) which showed that H-11 (δ_H 9.57) had strong ^{3}J coupling to a quaternary carbon C-7a (133.6 ppm) and ^{2}J couplings to aromatic carbon C-10 (122.5 ppm) and weak ^{2}J coupling to quaternary carbon C-11a (125.4 ppm). The most deshielded aromatic methine for the A', B', C', D' spin system H-11'δ_H 9.73 showed 3J coupling to quaternary carbon C-7a' (133.6 ppm) and aromatic methine C-9' (126.8). While the aromatic proton H-10 δ_H 7.34 had weak ^{2}J coupling to aromatic carbon C-9 (127.1 ppm) and ^{3}J coupling to quaternary carbon which can only be C-11a (191.9).
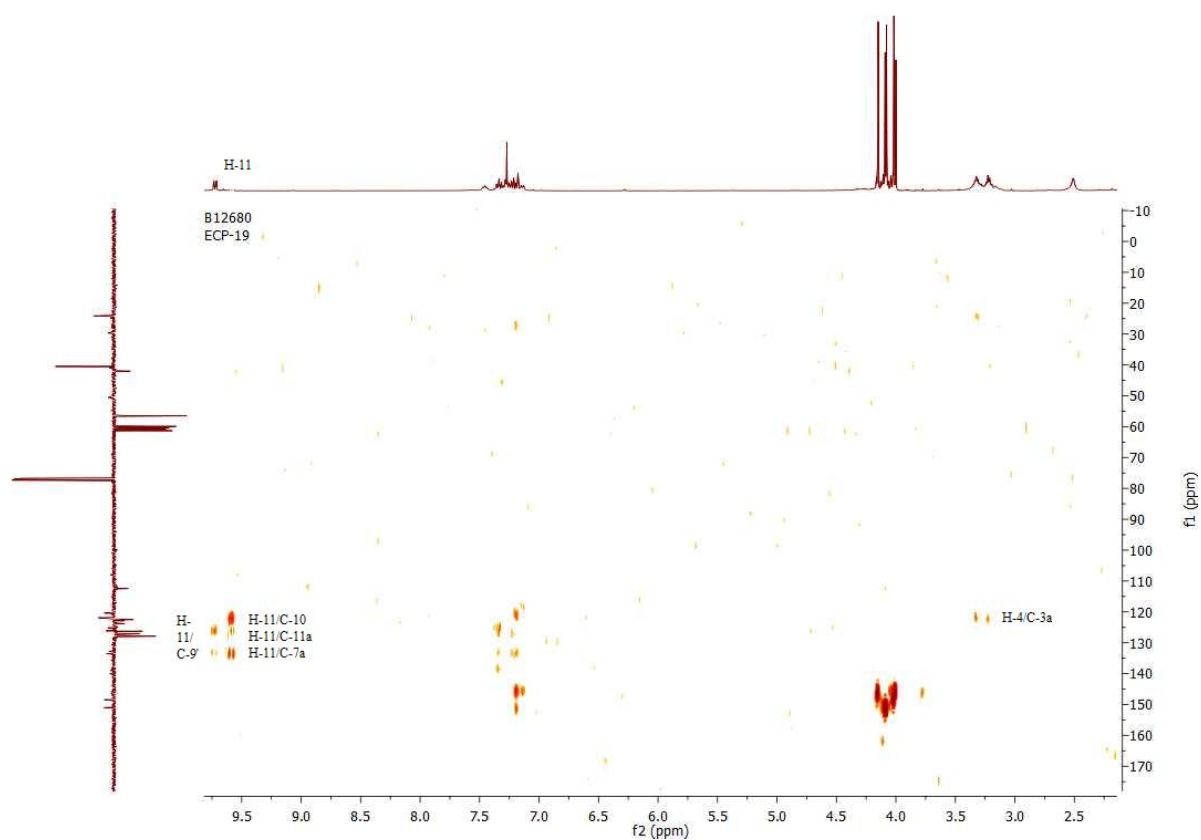
Figure 3.14a: HMBC NMR Spectrum (400MHz, CDCl3) of ECP-19

The HMBC Spectrum also showed aromatic proton H-9 δ_H 7.28 to have a ^{3}J correlations to quaternary carbon C-7a (133.6 ppm). The aromatic ring D aromatic proton H-8 δ_H7.23 showed strong ^{3}J couplings to carbons C-7a (133.6 ppm) and C-11 (127.2 ppm). It also showed a weak ^{2}J coupling to aromatic methine C-9 (127.1 ppm). The none sterically hindered methoxy on the aromatic spin system A', B', C', D' δ_H 4.09 (2-MeO) had a strong ^{3}J correlation to aromatic carbon (C-3', δc 112.4). For the aliphatic CH$_2$; H-4'δ_H 3.23, it showed weak ^{2}J correlation to quaternary carbon C-3a (122.3), while H-4 δ_H 3.21 showed weak correlation to C-5 (93.5 ppm). While the aliphatic proton H-5 showed weak couplings to the neighbouring methylene carbon C-4 (24.1 ppm) , and ^{3}J couplings to quaternary carbons C-6a (192.98 ppm), and C-3a (122.3 ppm).

1,1',2,2',3'-pentamethoxy-6-methyl-5,5',6,6'-tetrahydro-4H,4'H-7,7'-bidibenzo[de,g]quinoline
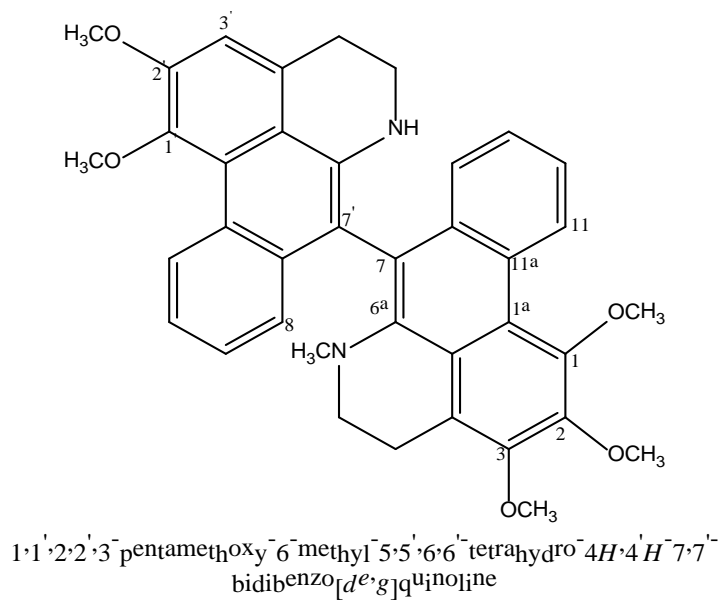
(**82**)
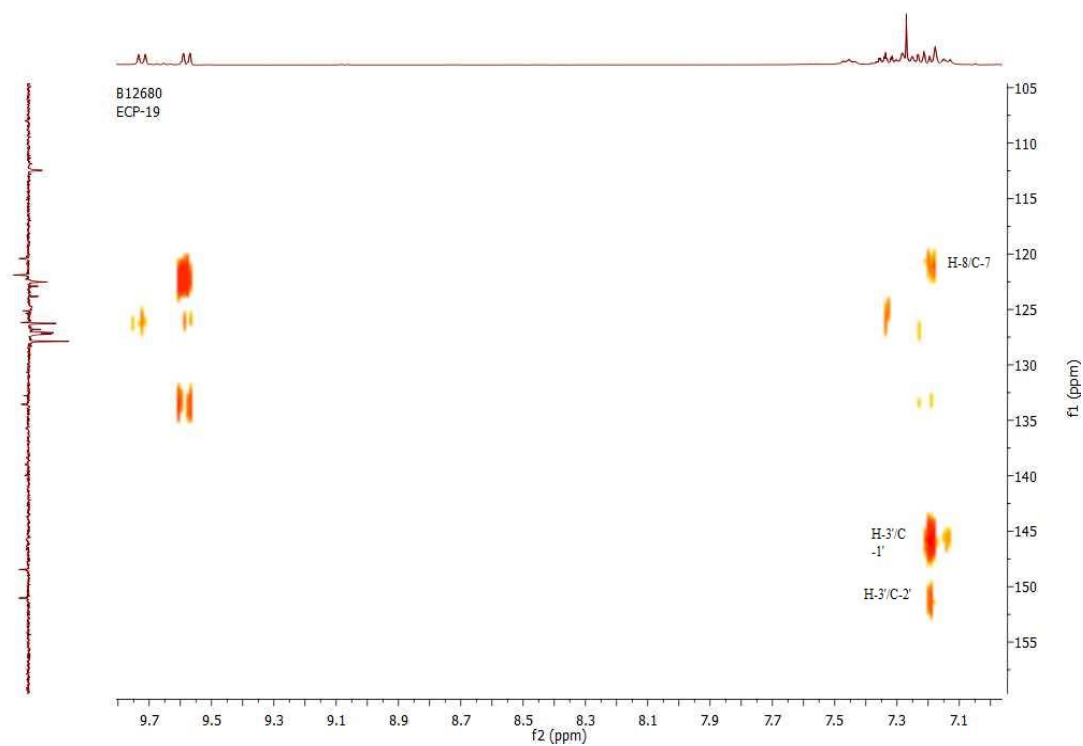
Figure 3.14: HMBC NMR Spectrum (400MHz,CDCl$_3$) of ECP-19 (deeper levels aromatics)

The HMBC Spectrum also revealed the five methoxys showed strong [3]J couplings to their respective aromatic oxygenated carbons, see **Figure 3.14b** below. The methoxys other correlations are showed in **Table 3.6**.
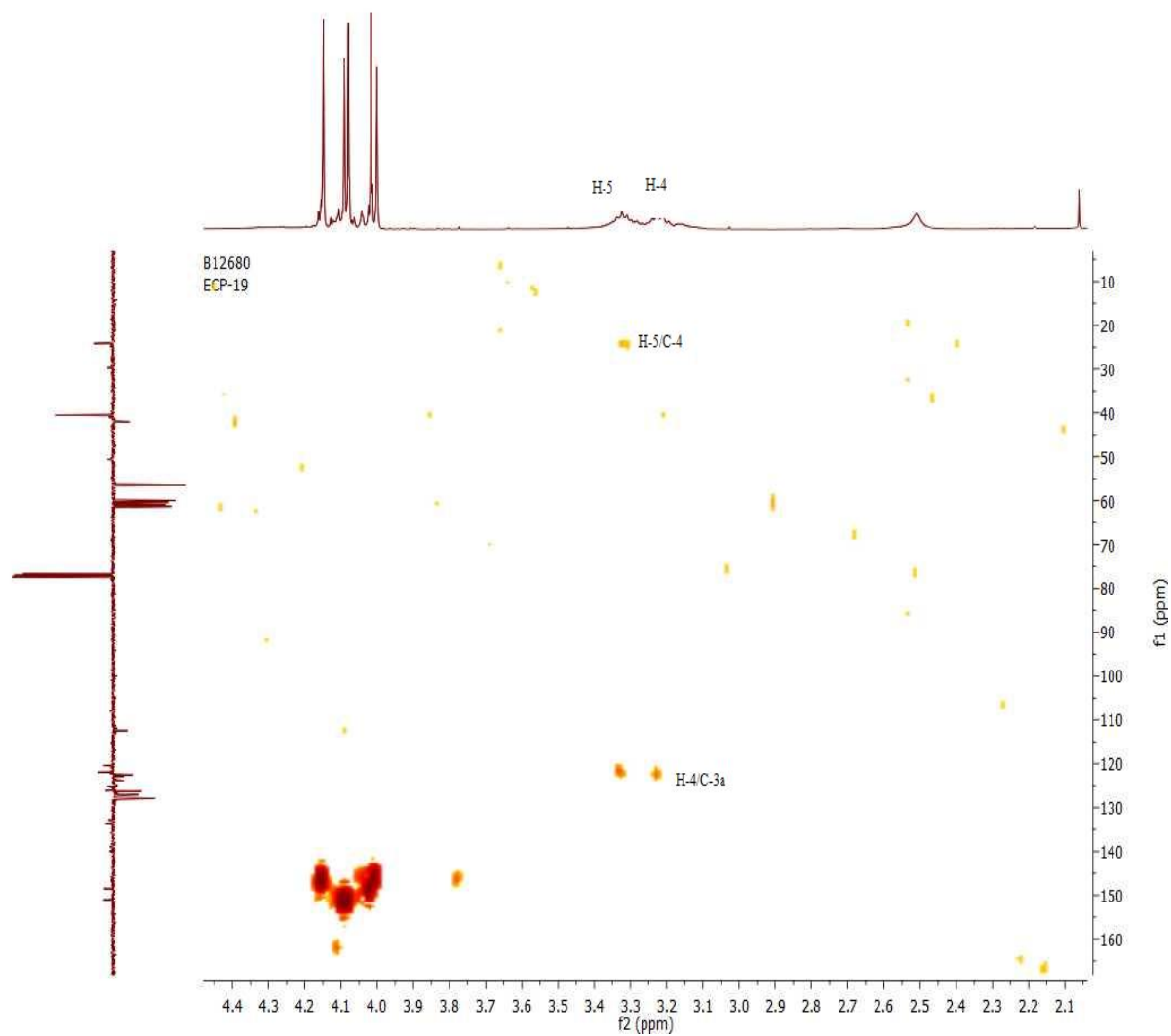
Figure 3.14c: HMBC NMR Spectrum (400MHz,CDCl$_3$) of ECP-19 (deeper levels aromatics 2)

The ^{13}C NMR Spectrum as shown in **Figure 3.15** and correlations shown in **Table 3.7** below.
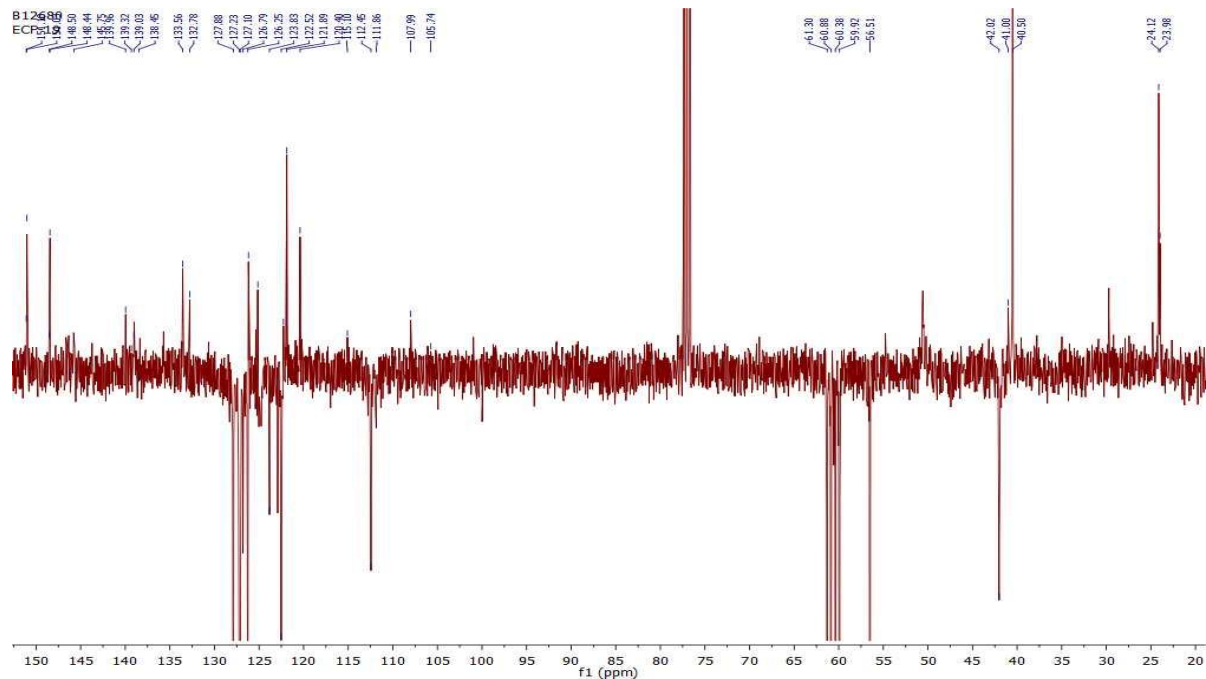
Figure 3.15: ^{13}C NMR Spectrum (400MHz, CDCl3) of ECP-19

Table 3.6: HMBC correlations of ECP-19

Position	^{1}H (ppm)	^{13}C (ppm)
3'	7.18	1-MeO (151.2), 2-MeO (145.8), 121.8(1b').
4	3.21	93.4(5)
4'	3.23	122.3(3a')
5	3.32	24.1(4)122.5(3a),192.98(6a)
8	7.23	120.4(7) 127.1(9),127.2(11),133.6(7a)
9	7.25	133.6(7a) 127.2(11),126.3(8)
10	7.35	127.1(9),133.6(7a)
11	9.58	122.5(10),133.6(7a),125.4(11a)
11'	9.73	126.8(9'),133.6(7a')
1-OMe	4.02	148.3(1)
1'-OMe'	4.00	145.3(1')
2-OMe	4.08	151.1(2)
2-OMe'	4.09	151.1(2),112.4(3')
3-OMe	4.14	146.4(3),

Table 3.7 showing ^{13}C chemical shifts of ECP-19

Position	^1H (ppm)	^{13}C (ppm)
C1	-	148.4
C-1'	-	145.3
C-1a	-	125.1
C-1a'	-	125.3
C-1b	-	121.8
C-1b'	-	121.9
C-2	-	151.0
C-2'	-	151.1
C-3	-	146.4
C-3'	7.18	112.4
C-3a	-	122.3
C-3a'	-	122.3
C-4	3.21	23.98
C-4'	3.23	24.1
C-5,C-5'	3.32	93.5
C-6a'	-	192.01
C-6a	-	192.96
C-7	-	108.3
C-7'	-	105.8
C-7a	-	133.6
C-7a'	-	132.8
C-8	7.23	126.3
C-8'	7.14	123.8
C-9	7.28	127.1
C-9'	7.25	126.9
C-10	7.34	122.5
C-10'	7.45	125.4
C-11	9.58	127.2
C-11'	9.73	127.9
C-11a,C-11a'	-	191.99
1-OMe	4.02	60.4
1'-OMe	4.00	59.9
2-OMe	4.08	60.9
2'-OMe	4.09	56.5
3-MeO	4.14	61.3
N-Me	2.51	42.0

ECP 19 was obtained also as yellow brown powder, with predicted molecular formula as $C_{90}H_{34}O_5$ N_2, mass confirmed by ESI-MS Spectrum which gave a molecular ion M^+ at region m/z 601 with two units ;$C_{18}H_{16}O_2$ N and $C_{20}H_{20}O_3$ N ;suggesting an asymmetric dimer, It is **novel.**

3.1.4: Characterization of Compound 90 ECHE-45 :8-(1,2,3-trimethoxy-5,6-dihydro-4H-dibenzo[de,g]quinolin-7-yl)-6,7-dihydro-5H-[1,3]dioxolo[4',5':4,5]benzo[1,2,3-de]benzo[g]quinoline.

ECHE-45 was obtained as yellowish powder from the hexane's extract with conditions as described in **Table 3.1.**

The ^{1}H NMR Spectrum (**Figure 3.16**) had nine aromatic protons , one highly deshielded proton at 9.59 ppm forming part of the ring D aromatic spin system (9.59 ppm,7.89 ppm,7.25 ppm and 7.20 ppm) of the 1st A,B,C, D spin system. The 2nd spin system A',B',C',D's ,Ring D four aromatic protons (9.06 ppm,7.33 ppm,7.23 ppm,7.10 ppm). Ring A' had an aromatic singlet H-3'δ 7.05, as well as methylenedioxy at 6.28 ppm C-1' and C-2' substitutions. The ring D of the 1st A,B,C,D spin system had C-1,C-2 and C-3 substitution in form of three methoxys groups(1-MeO, 2-MeO and 3-MeO) all these data were characteristic of 7,7'-dehyroaporphine system, indicative of an asymmetric dimer.
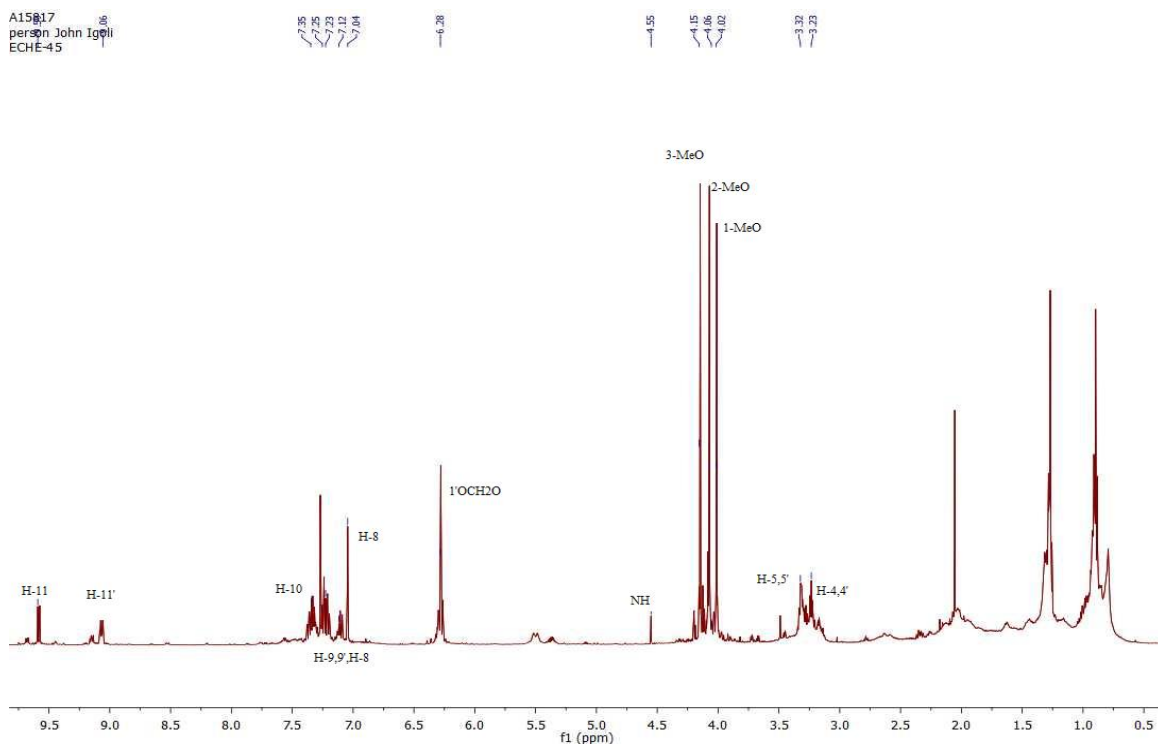
Figure 3.16: ^{1}H NMR Spectrum (400MHz, CDCl$_3$) of ECHE 45

The 2D NMR HSQC Spectrum (**Figure 3.17**) showing [1]J [1]H -^{13}C couplings revealed   1'OCH$_2$O at 101.0 ppm, as well as seven aromatic methines H-11 δ_H 9.59, δ_C 127.3 ,H-11' δ_H 9.06,δ_C 127.3 ,H-10 δ_H 7.35,δ_C 122.9,H-10' δ_H 7.33,δ_C122.4, H-9 δ_H 7.22,δ_C 126.8 ,H-9' δ_H 7.25,δ_C 127.5 ,H-8 δ_H 7.20,δ_C 123.8, H-8' δ_H 7.12,δ_C 123.4 and H-3' δ_H 7.05, δ_C 107.9. There were also the three methoxys 1-MeO (4.02 ppm δ_C 60.4), 2-MeO (4.08 ppm δ_C 60.9), 3-MeO (4.16 ppm δ_C 61.4) and four aliphatic meth-

ylene H-4 δ_H 3.25,δ_C 23.9 ,H-4' δ_H3.23,δ_C 30.8,H-5 δ_H 3.33,δ_C 93.6 and H-5' δ_H3.31,δ_C 94.2 as shown in **Table 3.9**.
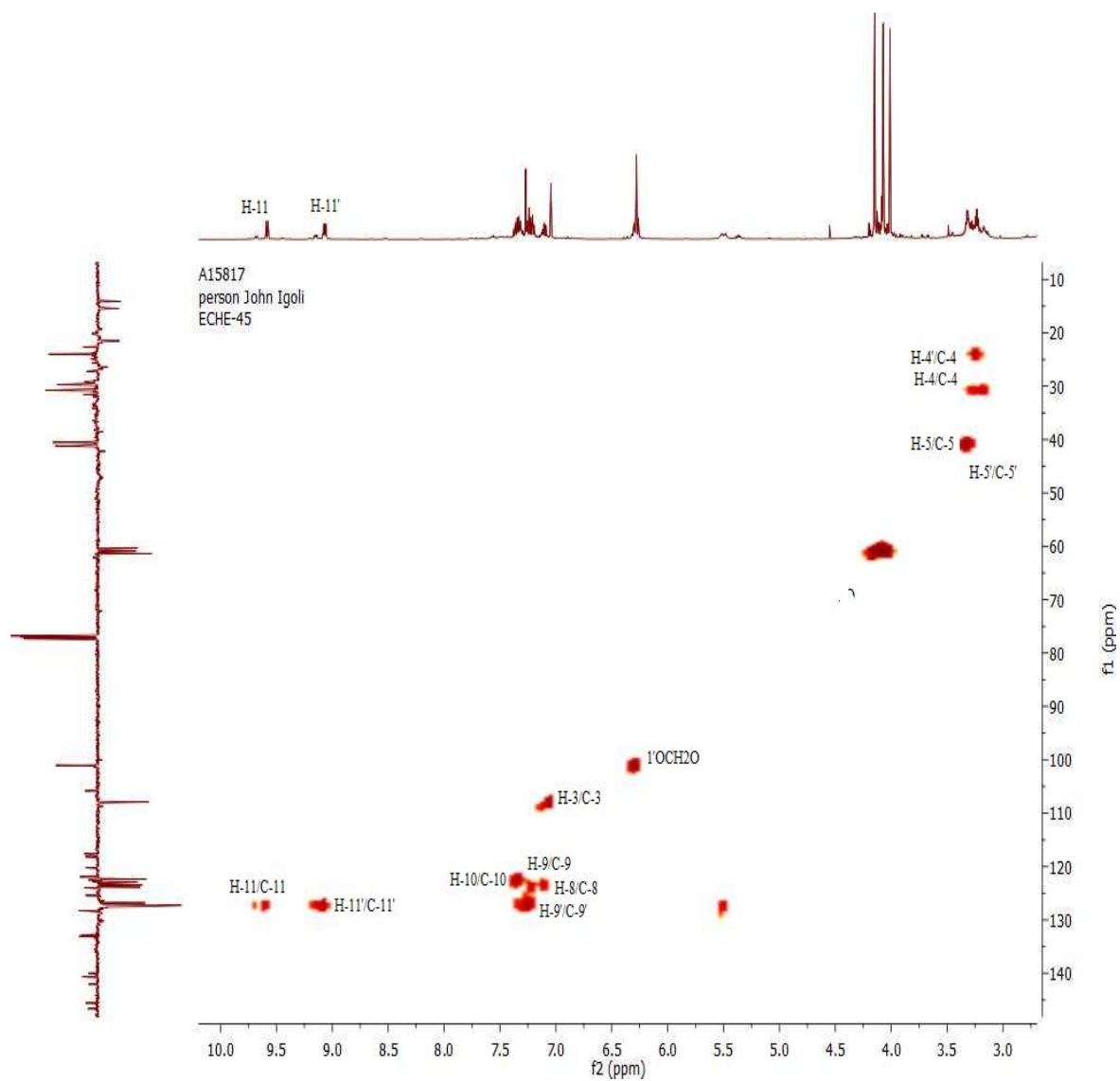
Figure 3.17:   HSQC NMR Spectrum (400MHz, CDCl$_3$) of ECHE 45

8-(1,2,3-trimethoxy-5,6-dihydro-4H-dibenzo[de,g]quinolin-7-yl)-6,7-dihydro-5H-[1,3]dioxolo[4',5':4,5]benzo[1,2,3-de]benzo[g]quinoline

(**90**)

Figure 3.18: ^{13}C NMR (400MHz, CDCl$_3$) of ECHE 45

The HMBC Spectrum (**Figure 3.19a**) showed the ring D with a strongly deshielded aromatic proton H-11 coupled in a [3]J fashion to aromatic methine C-9 and quaternary carbons C-1a and C-7a. The most

deshielded aromatic proton in ring D', H-11' coupled in a ^{3}J manner to aromatic methine C-9'and quaternary carbons C-1a' and C-7a'. The H-10 aromatic proton had strong^{2}J coupling to aromatic methine C-9 and 3J to quaternary carbon C-11a. Further, the aromatic proton H-9' showed strong ^{3}J couplings to C-7a' and C-11', completing the ring D correlations was aromatic proton H-8 which had strong ^{3}J couplings to carbons C-10,C-11a and C-7, while H-8' also had strong ^{3}J couplings to carbons C-10',C-11a' and C-7', indicating the structure was an asymmetrical dimer of two units joined by a C-7/C-7' bridge.
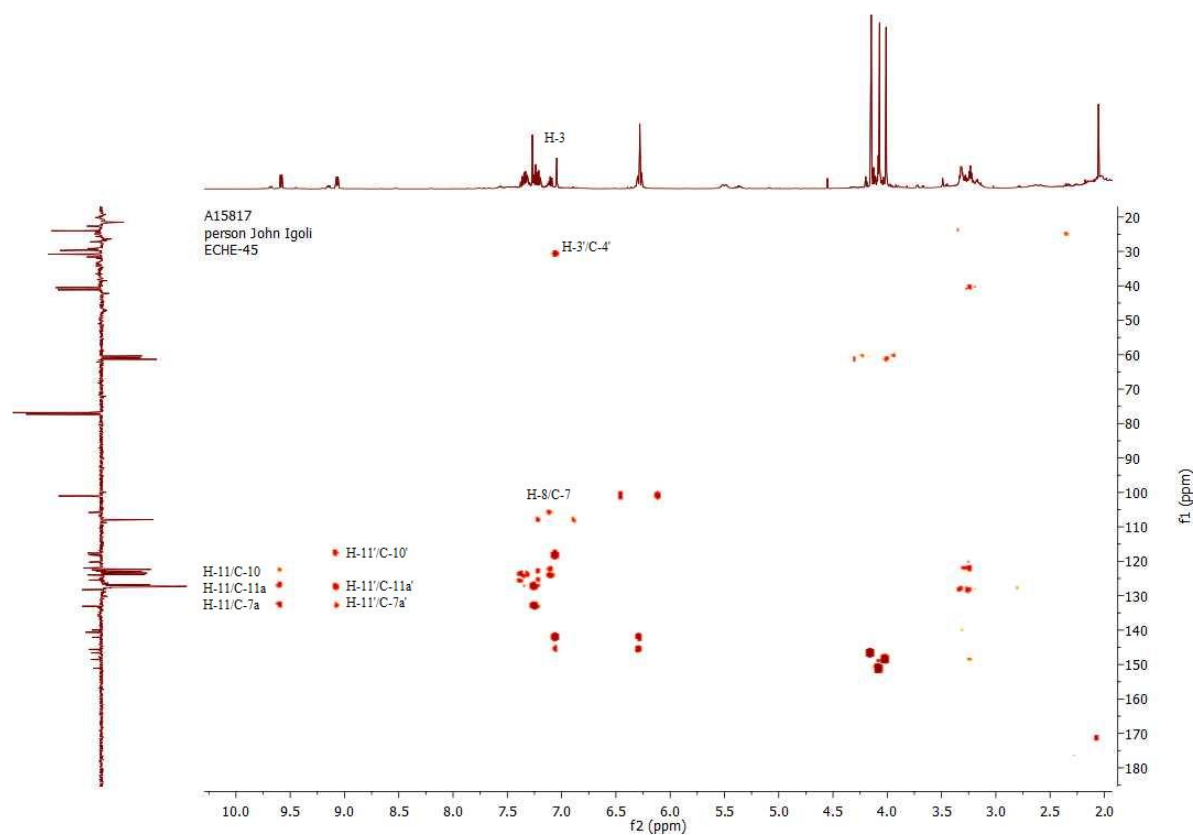
Figure 3.19a: HMBC NMR Spectrum (400MHz, CDCl$_3$) of ECHE 45

The aromatic proton H-3' completed the ring A substitutions bearing the methylenedioxy substituent 6.27 ppm which had ^{2}J correlations to carbons C-1b'and C-3a', as well as ^{3}J correlation to the aromatic carbon C-4'.Other correlations as shown in **Table 3.8**
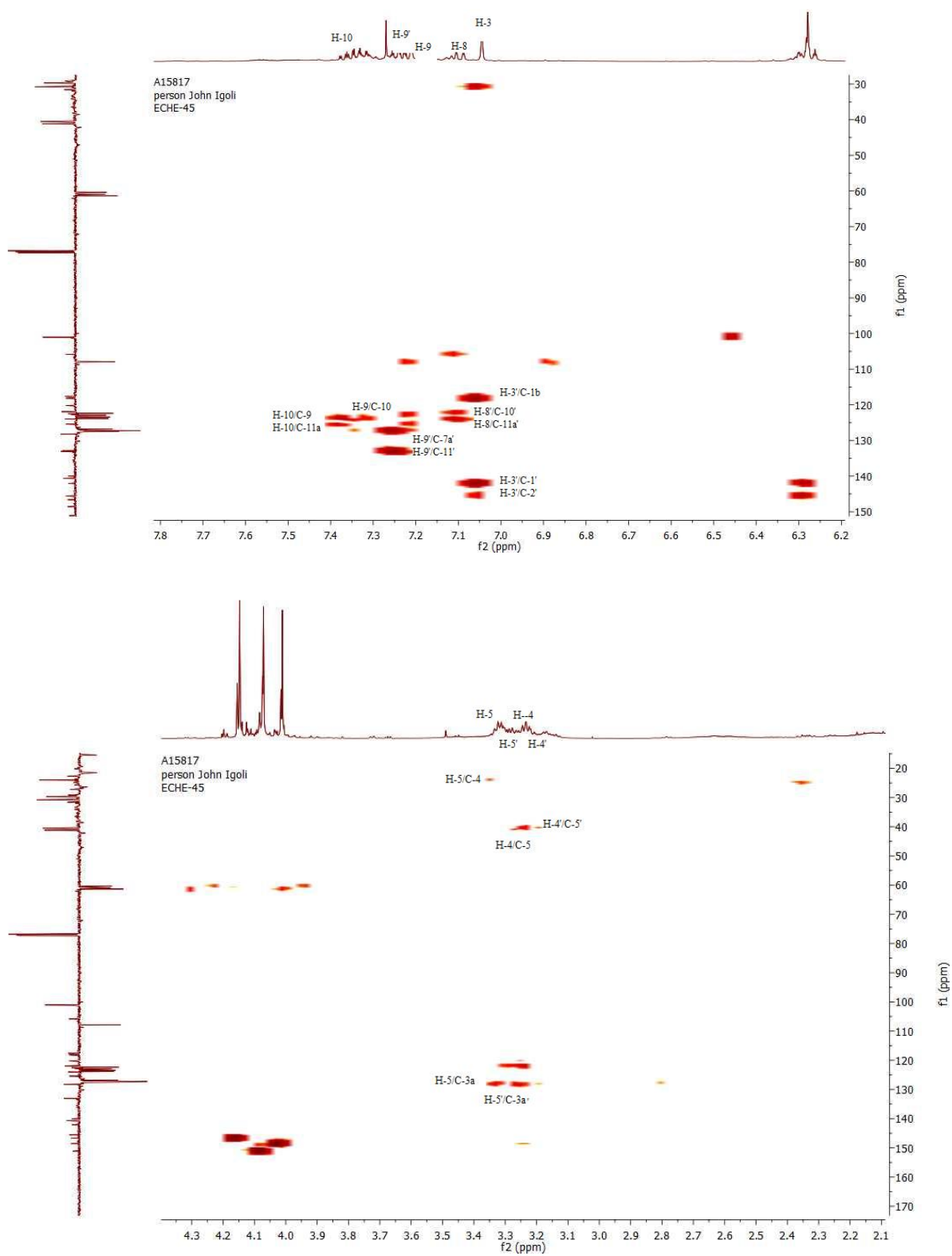
Figure 3.19b: HMBC NMR Spectrum (400MHz, CDCl$_3$) of ECHE 45

^{1}H-^{1}H-COSY 2D NMR Figure **(Figure 3.20)** showed the highly deshielded proton 9. 59 ppm was ortho-coupling with position-10^{1}H (7.89 ppm).
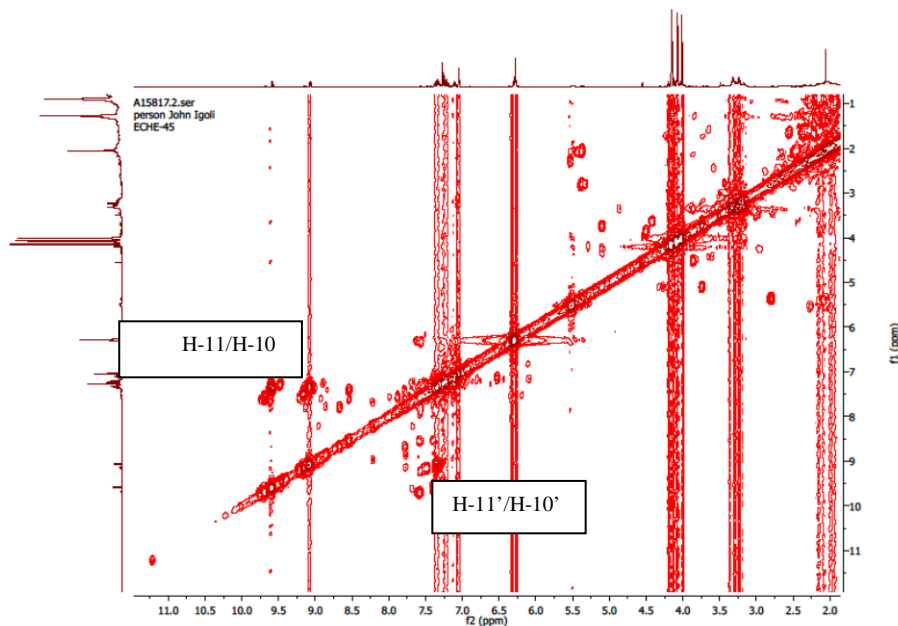
Figure 3.20: COSY NMR Spectrum (400MHz, CDCl$_3$) of ECHE 45

Table 3.8: HMBC correlations of ECHE 45

Position	^{1}H (ppm)	^{13}C (ppm)
3'	7.05	145.4(2')142.1(1'),118.2(1b'),30.8(4')
4	3.25	93.6(5),128.3(3a)120.2 (1b)
4'	3.23	128.3(3a),121.8(1b)
5	3.33	128.3(3a),193.6(6a)
5'	3.31	128.3(3a).30.8(4')
8'	7.12	105.8(7'),124.0(11a'),122.4(10')
8	7.20	108.3 (7),122.9 (10),125.4 (11a)
9	7.23	122.4(10)127.3(11)132.9(7a)
9'	7.25	133.1(7a') 127.5(11')
10	7.35	123.8(8),125.4(11a)
10'	7.33	124.0(11a'),127.5(9')
11'	9.06	133.06(7a),127.48(9),118.23(1a)
11	9.59	122.6(1a), 126.8(9), 132.9(7a)
1,2-OCH$_2$O	6.27	142.1(1'),145.4(2')

Table 3.9: ^{1}H and ^{13}C correlations of ECHE 45

Position	^{1}H (ppm)	^{13}C (ppm)
1	-	148.6
1'	-	142.1
1a	-	122.3
1a'		117.6
1b	-	121.8
1b'	-	118.2
2	-	151.0
2'	-	145.4
3'	7.05	107.9
3	-	146.5
3a	-	128.3
3a'		128.3
4'	3.23	30.8
4	3.25	23.98
5'	3.31	94.2
5	3.33	93.6
6,6'(NH)	4.21	-
6a	-	193.0
6a'	-	193.8
7	-	108.3
7'	-	105.8
7a'	-	133.1
7a	-	132.9
8	7.12	123.4
8'	7.20	123.8
9h	7.22	126.8
9'	7.25	127.5
10	7.35	122.4
11	9.59	127.3
11'	9.06	127.3
11a	-	125.4
11a'	-	124.0
1,2-OCH$_2$O	-	101.0

Thus the structure's predicted molecular formula was deduced as $C_{89} H_{30} O_5 N_2$ from the ESI mass Figure gave a quasi-molecular ion in negative ion mode at 585.23 (M+H)$^-$ corroborating with the fact that it was an asymmetrical aporphine alkaloid. A literature search yielded no compound for this structure, so that implies ECHE-45,8-(1,2,3-trimethoxy-5,6-dihydro-4H-dibenzo[de,g]quinolin-7-yl)-6,7-dihydro-5H-[1,3]dioxolo[4',5':4,5]benzo[1,2,3-de]benzo[g]quinoline is **novel**.

3.1.5: Characterization of Compound 91: ECH-56 (7-methyl-8-(1,2,3-trimethoxyl-5,6-dihydro-4H-dibenzo(*de,g*)quinolin-7-yl)-6,7-dihydro-5H-(1,3)dioxolo(4'5':4,5)benzo(1,2,3-d*e*) benzo(*g*)quinoline).

The ^{1}H NMR Spectrum was suggestive of an asymmetrical dimer similar to the previously described Compound 83 with the difference being the presence of an N-methyl group in position-6 of the dehydro-O-methyisopiline unit rather than the NH in Compound **83**. However it was isolated in very minute quantity, about 6 mg.

.

8-(1·2·3-trimethoxy-6-methyl-5·6-dihydro-4H-dibenzo[*de*·*g*]quinolin-7-yl)-6·7-dihydro-5H-[1·3]dioxolo[4·5':4·5]benzo[1·2·3-*de*]benzo[*g*]quinoline

(91)
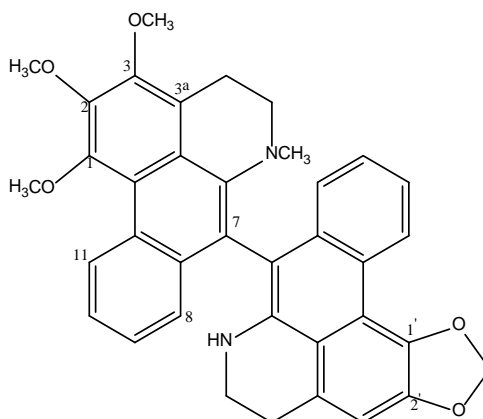
8-(1,2,3-trimethoxyl-6-methyl-5,6-dihydro-4H-dibenzo(*de,g*)quinolin-7-yl)-6,7-dihydro-5H-(1,3)dioxolo(4'5':4,5)benzo(1,2,3-d*e*) benzo(*g*)quinolone. The ^{1}H NMR Spectrum revealed a strongly deshielded proton 9.64 ppm in ring A of the A,B ,C ,D spin aromatic system 9.64 ppm(doublet *J*= 8.56 Hz) H-11 as well as another deshielded aromatic proton signal H-11'δ 9.06,7.33 ppm(multiplet H-10,H-10'),7.23 ppm(multiplet ,H-9,H-9') and 7.15 ppm (multiplet , H-8, H-8') and singlet aromatic proton H-3' 7.04 ppm. The unit with methylenedioxy substituent had its proton 1'2'-OCH$_2$ O at 6.27 ppm.

There were also three methoxy signals (3.99 ppm, 4.05 ppm, 4.13 ppm) as well as aliphatic methylene resonances appeared as duplet signal as proton 3.21 ppmH-4 (*J*=4.81Hz) and a complex multiplex for proton 3.28 ppm. ECH 56's molecular formula **C$_{89}$ H$_{32}$ O$_5$N$_2$** confirmed by ESI mass Figure gave a quasi-molecular ion (M+H)$^+$ at 585 indicating its molecular mass is 584. Other assignments correlated

with Compound 83's chemical shifts. Literature search also revealed **ECH-56, (**7-methyl-8-(1,2,3-trimethoxyl-5,6-dihydro-4H-dibenzo(*de,g*)quinolin-7-yl)-6,7-dihydro-5H-(1,3) Dioxolo (4'5':4,5)benzo(1,2,3-d*e*) benzo(*g*)quinoline) is **novel.**

3.1.6: Characterization of Compound 92: ECF 5-10 (**O-methyl moschatoline**). It was a monomeric aporphine alkaloid extracted from column chromatography and Flash Chromatography as a fraction from the hexane extract with molecular formula $C_{19} H_{15} O_4 N$. This was deduced from ESI mass Figure which revealed a quasi-molecular ion in positive ion mode $(M+H)^+$ at 322.18

1,2,3-trimethoxy-7H-dibenzo[de,g]quinolin-7-one
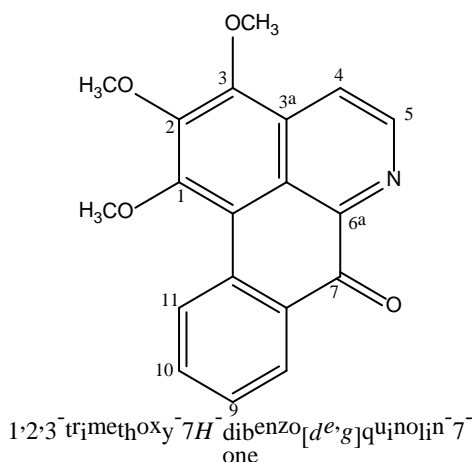
(**92**)

The ^{1}H NMR Spectrum indicated an aporphinoid alkaloid. It had a strongly deshielded proton 9.10 ppm (doublet, *J*= 8.92Hz, H-11). Forming the D ring aromatic spin system were (9.10 ppm *J*= 8.92 Hz, 7.74 ppm (doublet=7.86 H-10,), 7 .53 ppm (doublet *J*=7.45, H-9) and 8.57 ppm (*J*=, 7.83Hz, H-8). Completing the ring A and B substitutions were two aromatic protons 8.22 ppm (doublet of doublet, J= 5.90 Hz, 1.96 Hz H-4), 8.97 ppm (doublet, *J*= 5.12 Hz, H-5).

2D COSY Spectrum, **Figure 3.21** showed the couplings as expected for O-methylmoschatoline H-11-H-8, as well as H-5 ortho-coupled to H-4 in Ring B. Ring A had C-1, C-2 and C-3 substitution by three methoxys which appeared as signals integrating for three hydrogens on the ^{1}H NMR Figure as signals (4.18 ppm, 4.09 ppm, 4.07 ppm)

 This correlated with slightly different assignments to O-methylmoschatoline previously reported by Guinaudeau (2004) as well as Marsaioli *et al.,* (1979)

[126]
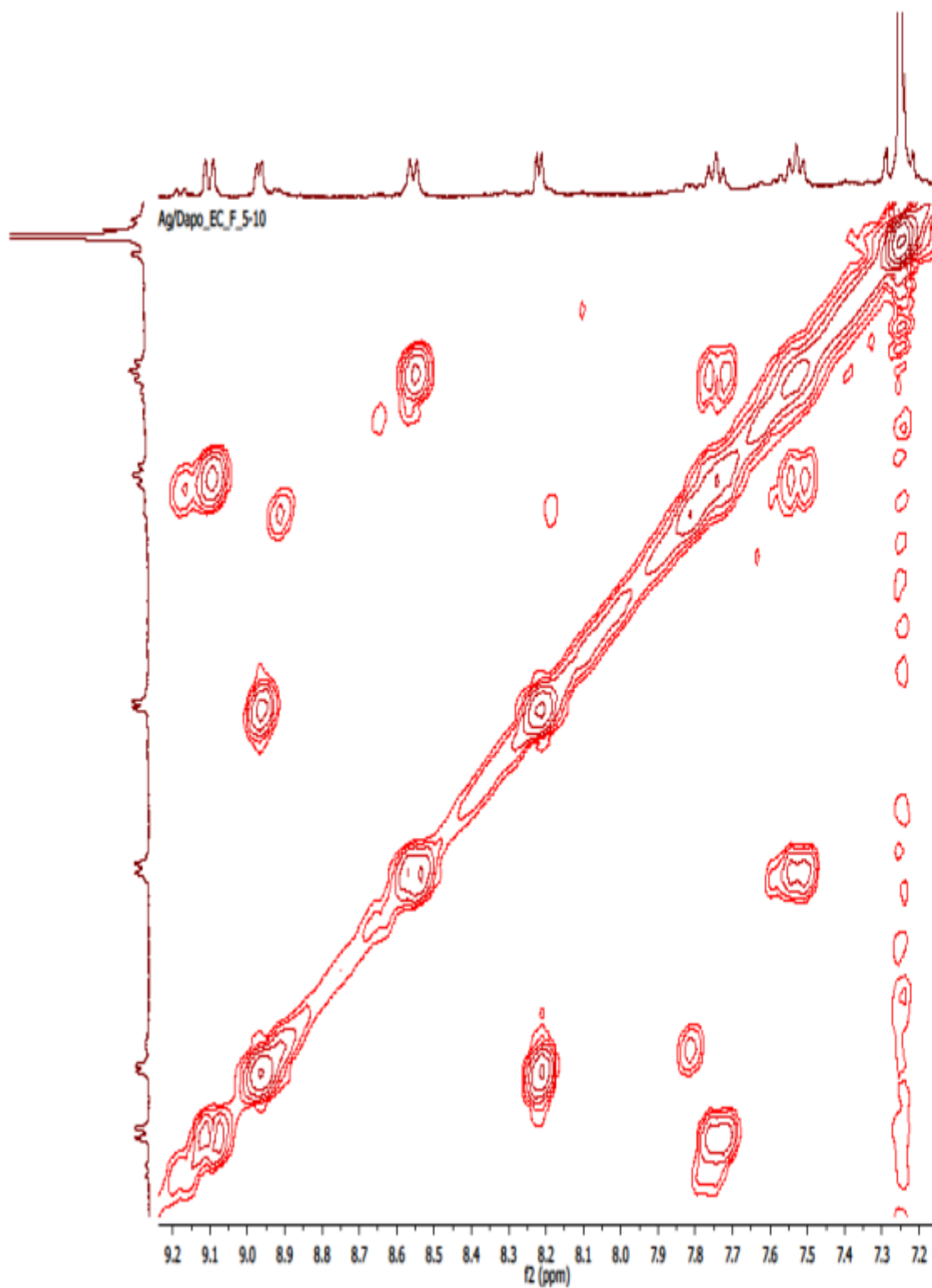
Figure 3.21: COSY NMR Spectrum (400MHz CDCl₃) of ECF 5-10

3.1.7. Characterisation of Compound 93: ECP-23 (7-dehydro-nornuciferinyl-7'-dehydro-O-methylisopiline)

It was obtained also as yellow brown powder.
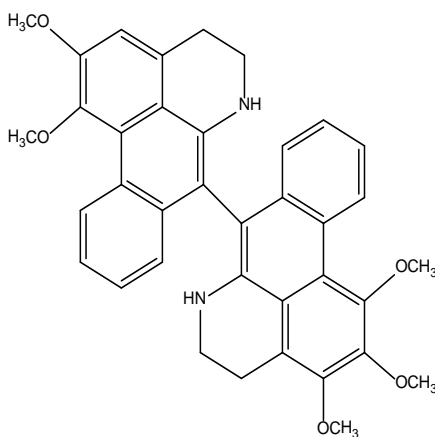
(**93**)

The ^{1}H NMR Spectrum, **Figure 3.22b** showed two highly deshielded protons at 9.66 ppm (doublet of doublet, J= 0.90 Hz,8.60 Hz,H-11), and 9.59 ppm (doublet,J= 8.60 Hz, H-11') completing the two four –spin aromatic system were aromatic protons H-8 at 7.19 ppm,H-8' at 7.15 ppm,H-9 at 7.23 ppm,H-9' at 7.25 ppm ,H-10 at 7.89 ppm,H-10' at 7.34 ppm. The dehydronornnuciferine unit (**86a**) had two methoxys (4.08 ppm and 4.01 ppm) as well as aliphatic protons making up ring B between 3.18 and 3.34 ppm: 3.22 (singlet 2H-4,2H-4' and 3.31 (multiplet 2H-5,2H-5'). There was also a singlet amine proton at 4.33 ppm as well as a singlet signal for aromatic proton H-3 (7.14 ppm)
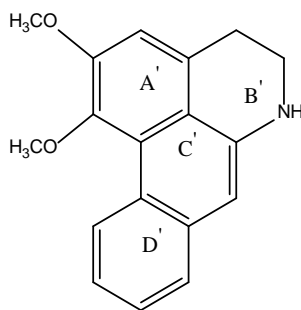
(**86a**)

 While the dehydro-O-methylisopiline unit was very similar to the dehydronornuciferine unit with the difference being the latter's three methoxy signals ((4.15 ppm, 4.07 ppm, and 4.00 ppm) in place of the former's two methoxys.
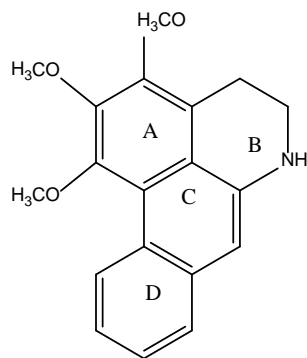
(86b)
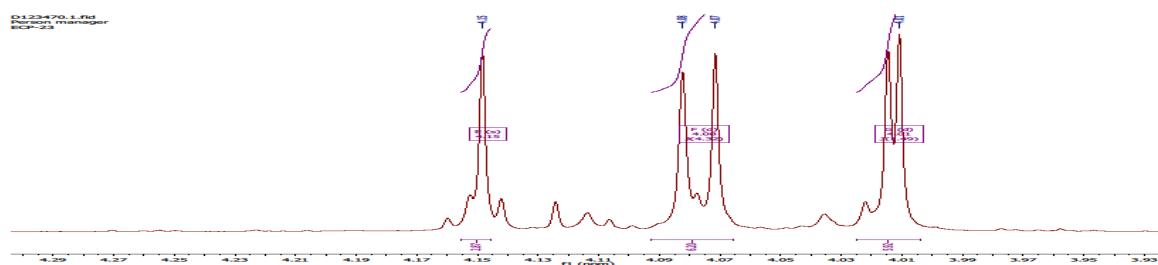
Figure 3.22a: ^{1}H NMR Spectrum (400MHz, CDCl3) of ECP-23 showing the five methoxys. This a cut portion of the full spectrum to show the five methoxy region only.
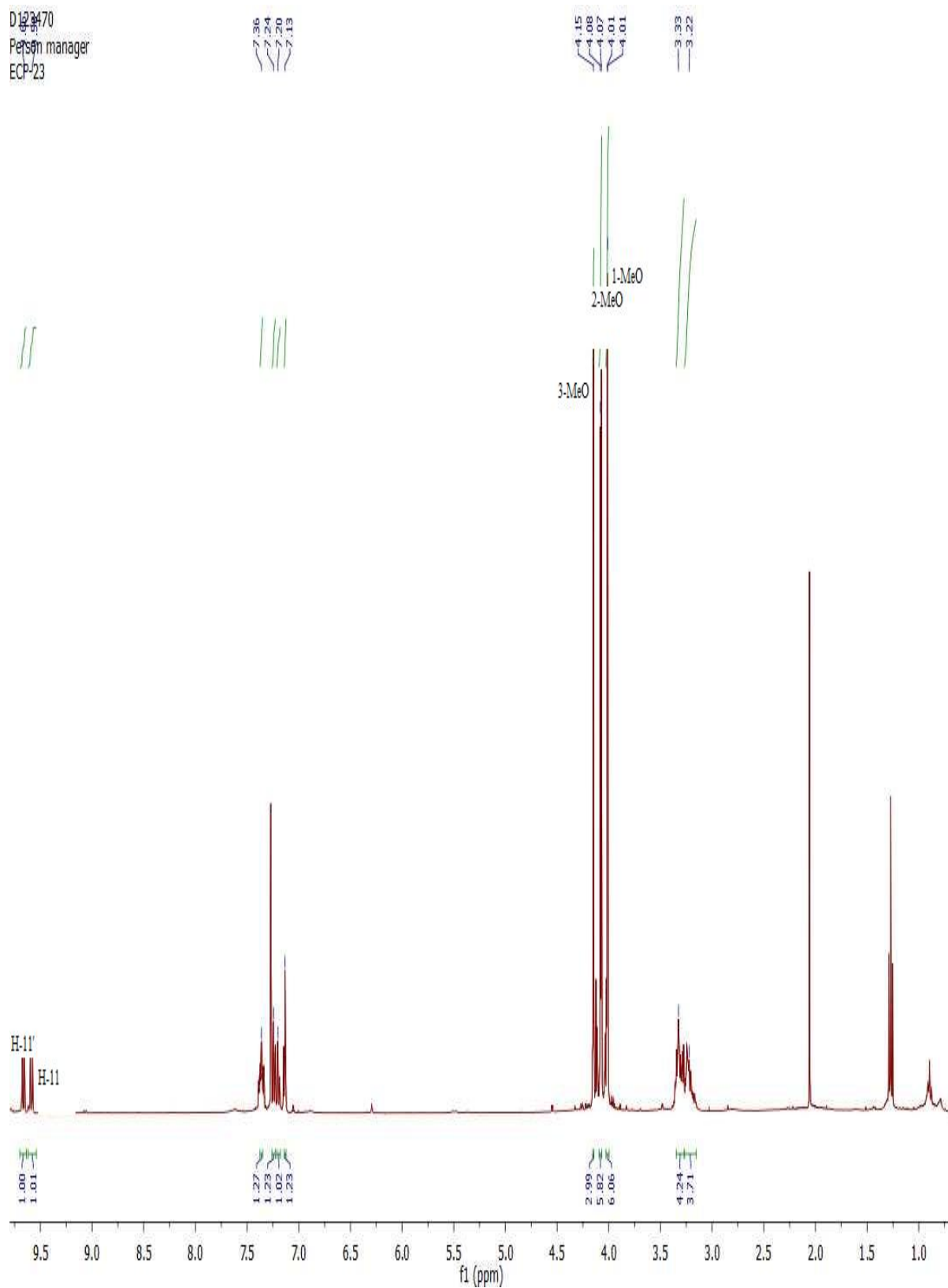
Figure 3.22b: ^{1}H NMR Spectrum (400MHz, CDCl$_3$) of ECP-23 showing the aromatic, methoxys and aliphatic protons.

The COSY 2D NMR Spectrum **Figure 3.23** showed the highly deshielded proton H-11, 9.58 ppm was ortho-coupling to H-10 (7.34 ppm).
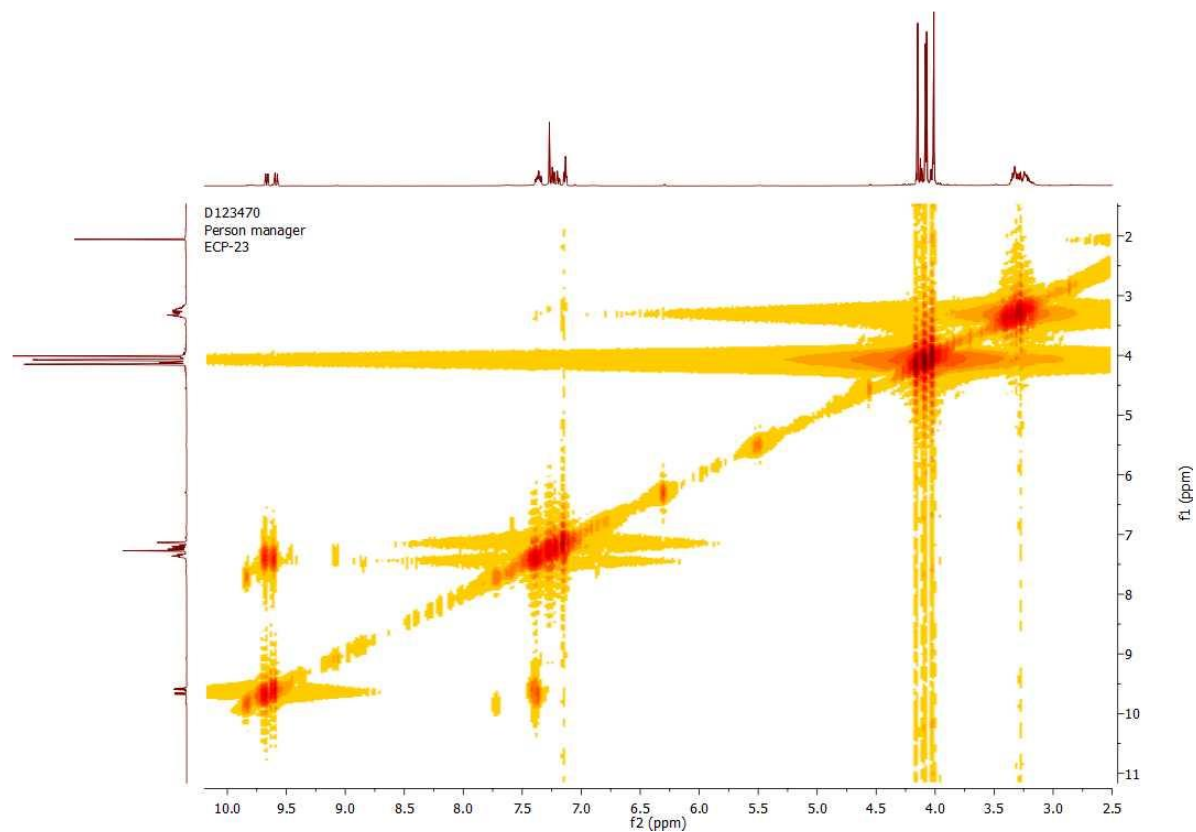
Figure 3.23: COSY NMR Spectrum (400MHz,CDCl$_3$) of ECP-23

The 2D NMR HSQC Spectrum,**Figure 3.24**showed ^{1}J ^{1}H -^{13}C coupling as shown in **Table 3.10**.
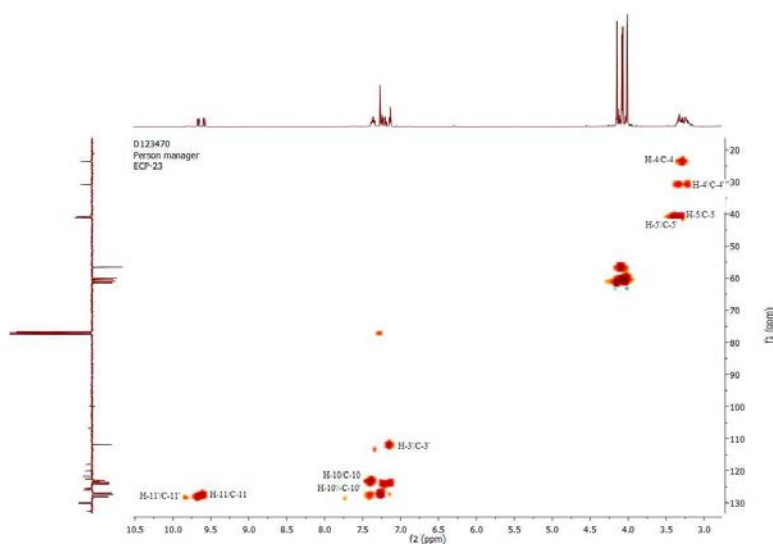
Figure 3.24: HSQC NMR Spectrum (400MHz, CDCl3) of ECP-23
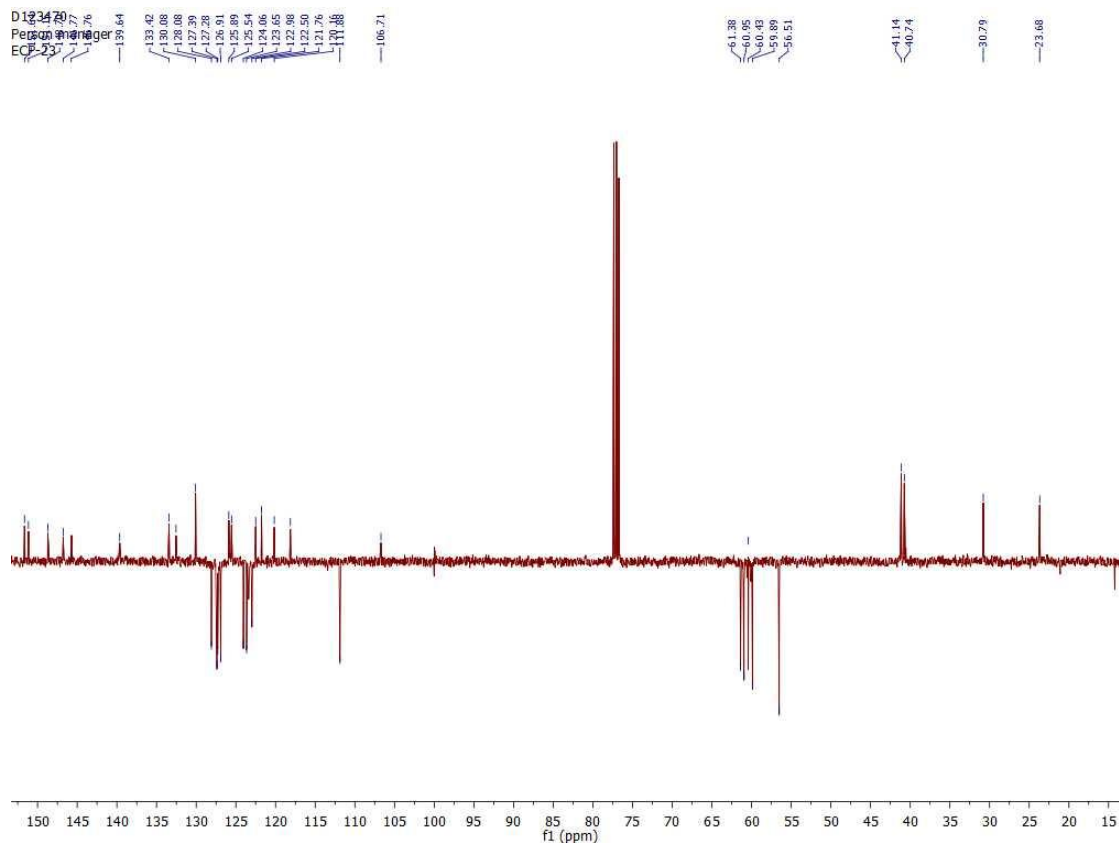
Figure 3.25: ^{13}C NMR Spectrum (400MHz, CDCl3) of ECP-23

The ^{13}C NMR Spectrum, **Figure 3.25** with chemical shifts as shown in **Table 3.14** correlates with expected dehydro -O-methyl-isopiline unit (**86b**) with four aromatic methines (122.5 ppm,123.7 ppm, 126.9 ppm, and 127.4 ppm),two methylene (23.7 ppm and 93.5 ppm),and three methoxy carbons (56.5 ppm, 60.9 ppm and 61.4 ppm). It also had together with ten quaternary carbons (151.6 ppm, 148.7 ppm, 146.4 ppm, 192.7 ppm, 132.6 ppm, 130.1 ppm, 125.9 ppm, 122.98 ppm, ppm, 118.2 ppm, and 106.7 ppm).

The dehydronornuciferine unit (**86a**) with had five aromatic methane's (111.9 ppm,123.4 ppm,124.0 ppm, 126.9 ppm, and 128.1ppm),two methylene (30.8 ppm and 94.2 ppm),and two methoxy carbons (59.9 ppm and 56.5 ppm), nine quaternary carbons (151.2 ppm, 145.6 ppm, 192.6 ppm, 133.4 ppm, 125.6 ppm,122.98 ppm, 121.8 ppm 118.12 ppm and 106.7 ppm). These carbons were assigned with slightly different assignments to those of 7-Dehyronornuciferinyl -7'-dehydro -O-methyl-isopiline was previously isolated from *Polyalthia bullata* reported by Connolly (1996).

[132]

The HMBC correlations as shown in **Table 3.11** revealed the most deshielded proton H-11 δ_H 9.58 of the dehydro-O-methylisopiline unit had strong ^3J couplings to C-7a and C-9, as well as ^2J coupling to

C-11a. Aromatic proton H-10 had ^3J correlations to C-8, while H-9 showed ^3J correlations to C-11 and C-7a. Completing ring D correlations was aromatic proton H-8 which had weak ^2J correlation to the carbon C-7a and ^3J correlation to the quaternary carbon C-7 indicating the dimer was an asymmetrical one joined at the C-7/C-7' bridge.
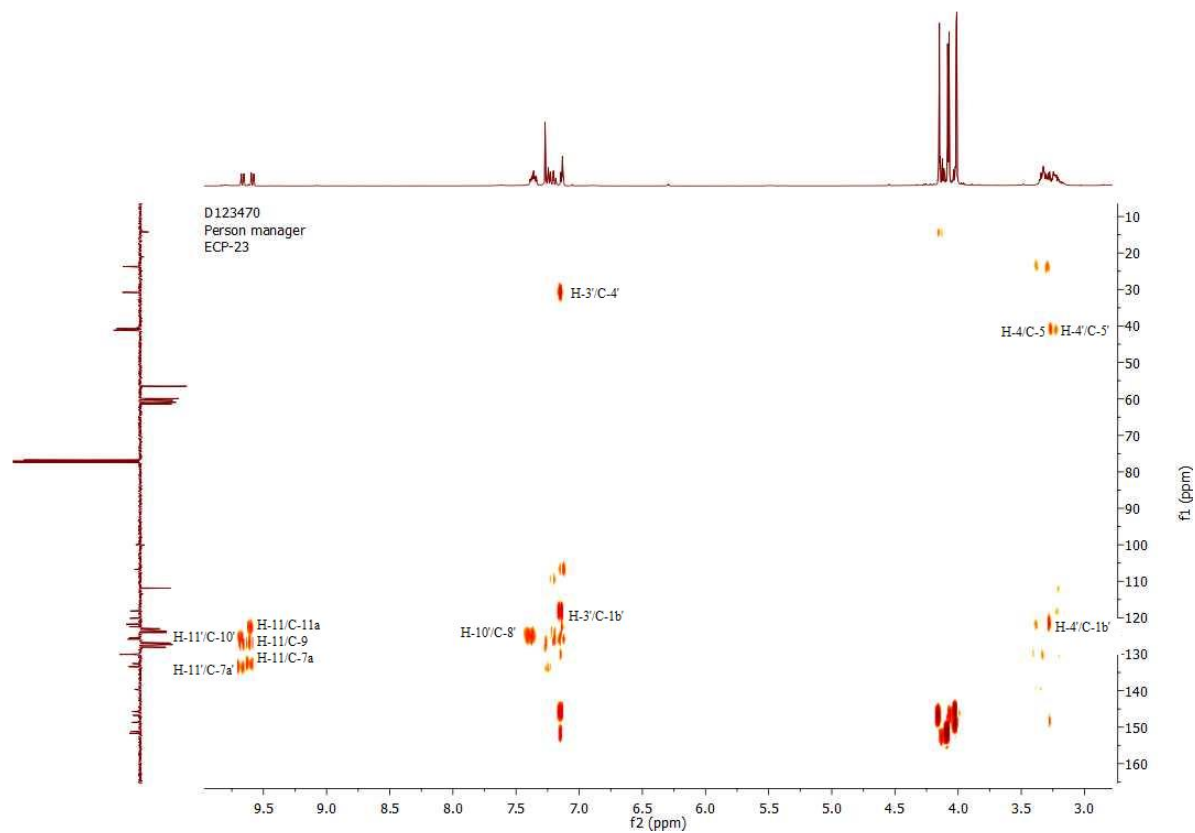
Figure 3.26a: HMBC NMR Spectrum (400MHz, CDCl3) of ECP-23
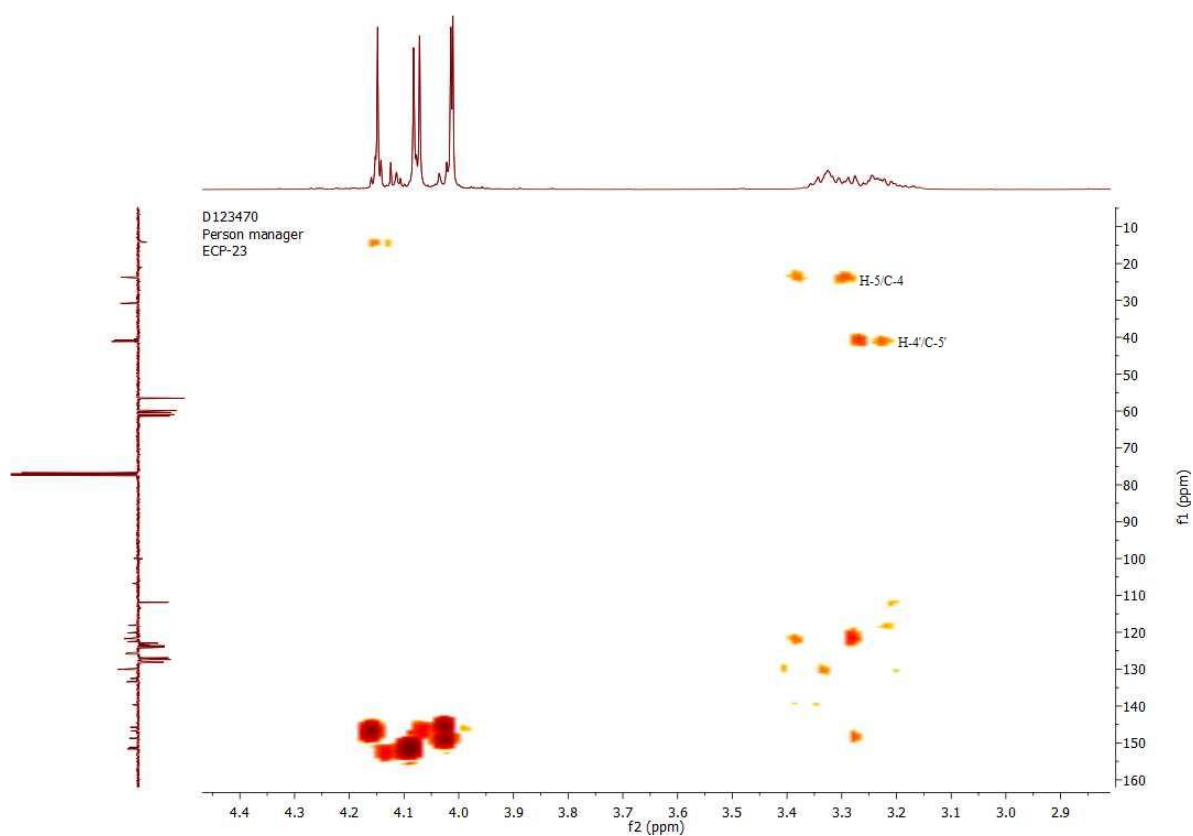
Figure 3.26b: HMBC NMR Spectrum (400MHz, CDCl3) of ECP-23

Other HMBC correlations of the dehydronornuciferine unit are shown in Table **3.16.** It was previously isolated from trunk bark of *Oxandra cf major* (Arango, 1986) and roots of *Piptostigma fugax* reported by (Achenbach, 1995). ESI mass Figure showed a (M+H) [+]at *m/z* 587.27 in positive ion mode indicating the molecular weight is 586, thus suggesting it was an asymmetrical dimer with molecular formula $C_{90} H_{34} O_5 N_2$.

Table 3.10 ^{1}H and ^{13} C correlations of ECP-23

Position	^{1}H (ppm)	^{13}C (ppm)
C1	-	148.7
C-1'	-	145.6
C-1a	-	125.9
C-1a'	-	125.6
C-1b	-	118.2
C-1b'	-	121.8
C-2	-	151.6
C-2'	-	151.2
C-3	-	146.4
C-3'	7.13	111.9
C-3a	-	130.1
C-3a'	-	121.8
C-4	3.25	23.7
C-4'	3.23	30.8
C-5	3.31	93.5
C-5'	3.32	94.2
C-6a	-	192.7
C-6a'	-	192.6
C-7	-	106.7
C-7'	-	108.4
C-7a	-	132.6
C-7a'	-	133.4
C-8	7.15	122.5
C-8'	7.19	123.4
C-9	7.23	127.3
C-9'	7.25	126.9
C-10	7.89	123.7
C-10'	7.34	124.0
C-11	9.58	127.4
C-11'	9.73	128.1
C-11a,C-11a'	-	122.98
1-OMe	4.01	60.4
1'-OMe	4.00	59.9
2-OMe	4.07	60.9
2'-OMe	4.08	56.5
3-MeO	4.16	61.3

Table 3.11: HMBC correlations of ECP-23

Position	^{1}H (ppm)	^{13}C (ppm)
4	3.25	93.4(5)
4'	3.22	94.2(5'),111.9(3'),121.8(1b')
5	3.31	130.1(3a),192.6(6a)
5'	3.33	192.6(3a')
8	7.15	106.7 (7),133.4(7a)
8'	7.19	126.9(9'),122.98(11a')
9	7.25	133.6(7a) 127.2(11),122.5 (8)
10'	7.89	123.4(8')
11	9.58	122.98(11a),132.6(7a),127.3(9)
11'	9.66	126.4(9'),133.4(7a')
1-OMe	4.02	148.4(1)
1'-OMe'	4.00	145.6(1')
2-OMe	4.07	151.6(2)
2-OMe'	4.09	151.2(2'),111.9(3')
3-OMe	4.14	146.8(3),

3.1.8: Characterization of Compound 94: ECH-B 17-18 (Urabaine)

It was extracted from *E. chlorantha* stem bark as brown residue with conditions described in **Table 3.1**.

Urabaine
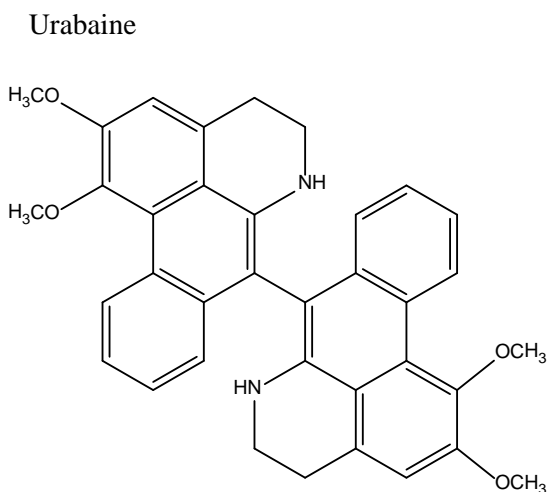
1,1',2,2'-tetramethoxy-6-methyl-5,5',6,6'-tetrahydro-4H,4'H-7,7'-bidibenzo[de,g]quinoline

(**94**)

The ^{1}H NMR Spectrum (**Figure 3.27**) indicated an aporphinoid alkaloid which was substituted at position C-1, C-2. Signals centred at (9.68 ppm (doublet *J*=8.91 Hz, H-11), δ_H 7.89 ppm (H-10 multiplet), 7.24 ppm (H-9 multiplet), and 7.19 ppm doublet (*J*=7.98 Hz) completing the substitution pattern in ring D. There were also as well as two methoxys (4.02 ppm and 4.09 ppm) in Ring A. Ring B had aliphatic protons between 3.21 2H-4,2H-4' multiplet),3.32 (2H-5,2H-5' doublet of doublet *J*= 6.83,21.06), completing ring A's substitution was aromatic singlet proton H-3 δ_H 7.14. There were four aliphatic protons between 3.20 and 3.32 ppm.
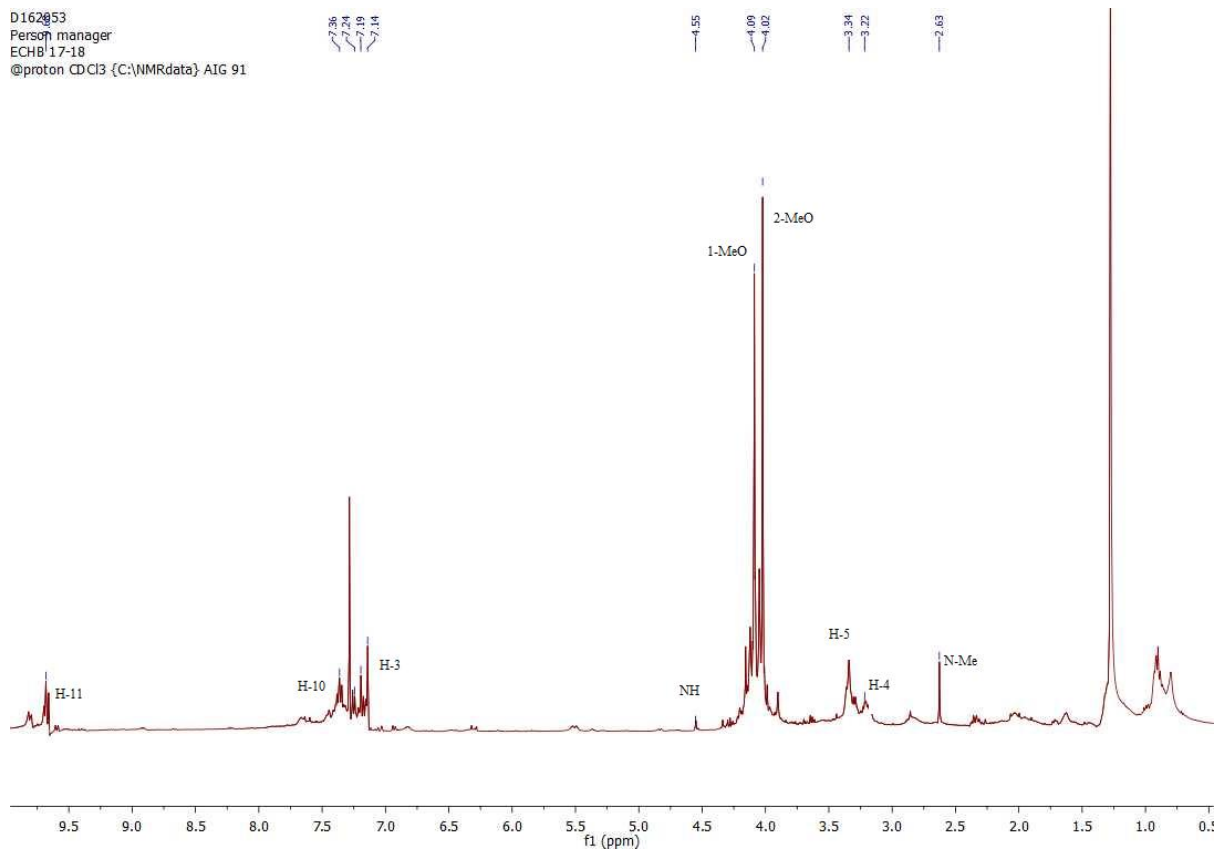
Figure 3.27: ^{1}H NMR Spectrum (400MHz, CDCl$_3$) of **ECHB** 17-18

The COSY 2D NMR Spectrum, **Figure 3.28** showed the highly deshielded proton 9.68ppm was ortho-coupling with position 10's [1]H (7.89 ppm).
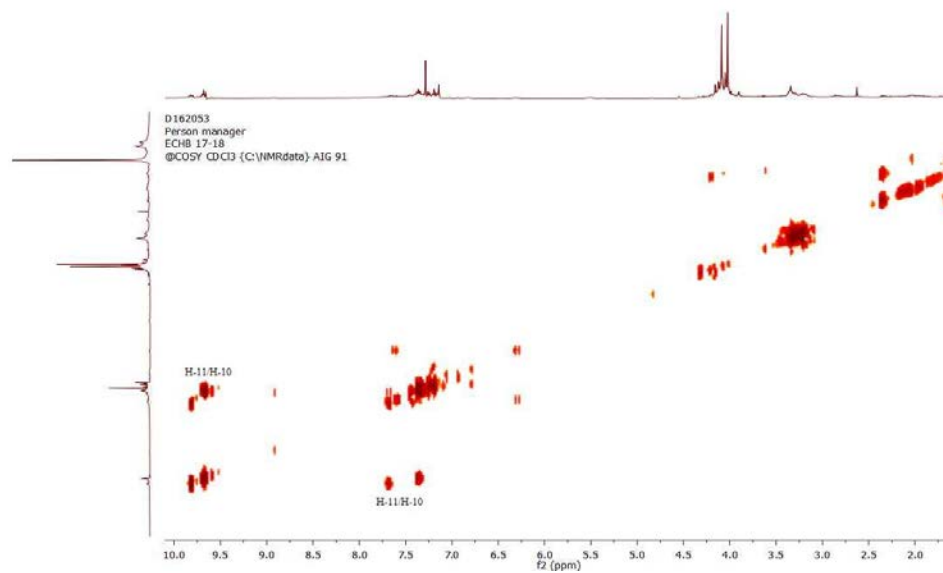
Figure 3.28: COSY NMR Spectrum (400MHz, CDCl3) of ECHB 17-18

The 2D NMR HSQC Figure **Figure 3.29** showed[1]J [1]H -^{13}C coupling as shown in **Table 3.12.**
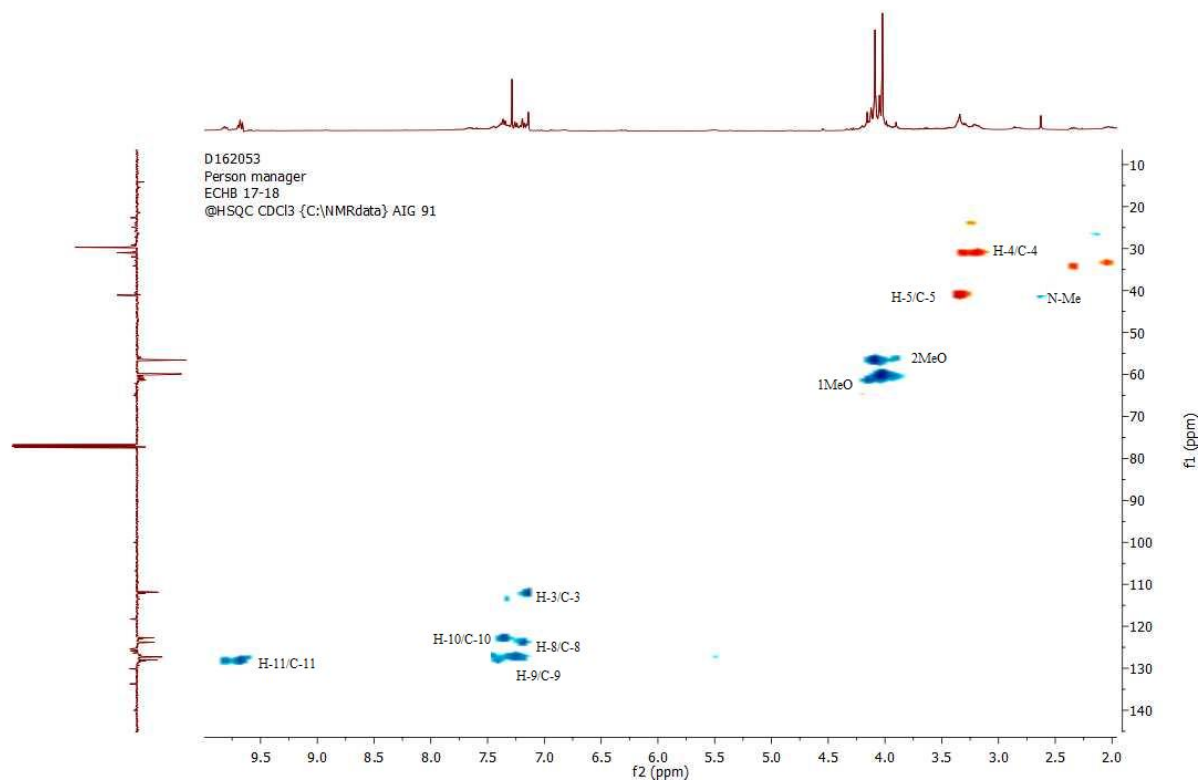
Figure 3.29: HSQC NMR Spectrum (400MHz, CDCl3) of ECHB 17-18

The [13] C NMR Spectrum, **Figure 3.28** shown with chemical shifts as shown in **Table 3.12** correlates with a monomeric aporphinoid alkaloid with five aromatic methines(111.9 ppm,122.7 ppm, 123.8 ppm,127.3 ppm,and 128.2 ppm),two methylene (93.97 ppm and 30.7 ppm), and two methoxy carbons (56.5 ppm and 60.0 ppm). It had nine quaternary carbons (151.5 ppm, 145.7 ppm, 193.0 ppm, 133.7 ppm, 130.4 ppm, 126.4 ppm, 125.8 ppm, 118.1 ppm, and 106.7 ppm).
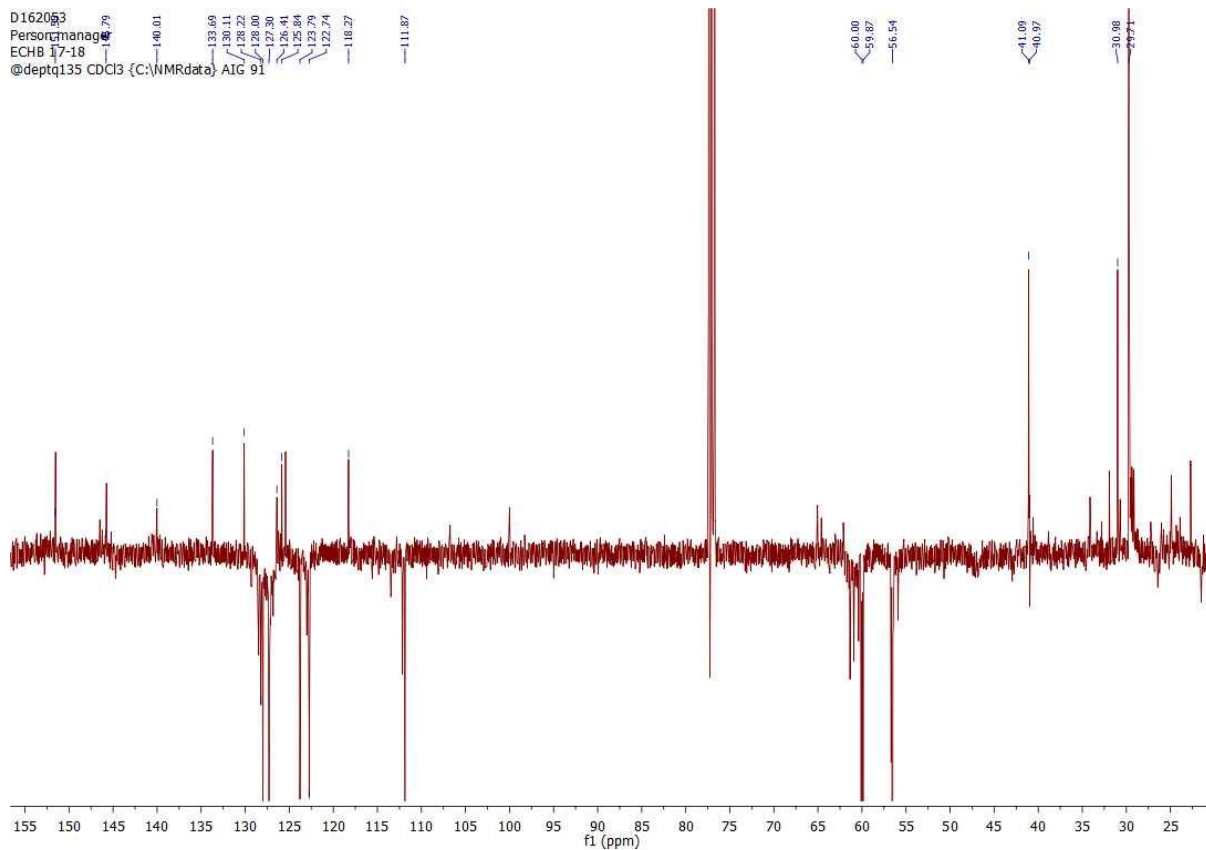
Figure 3.30: ^{13}C NMR Spectrum (400MHz, CDCl3) ECHB 17-18

HMBC correlations revealed the most deshielded aromatic proton δ_H 9.68 H-11 had ^{3}J correlations to quaternary carbons C-1a, C-7a and aromatic methine C-9. While H-10 aromatic proton δ_H 7.89 showed ^{3}J coupling to aromatic methine C-8 and ^{2}J coupling to the C-11 aromatic methine. The H-9 aromatic proton showed ^{3}J correlations to aromatic methine C-11 and quaternary carbon C-7a.Completing the D ring correlations H-8 showed ^{3}J correlations to aromatic methine C-10, quaternary carbon C-11a as well as quaternary carbon C-7, δ_C 106.7 ppm, indicating a possible structure of a dimer of two units

joined by a C-7/C-7' bridge.
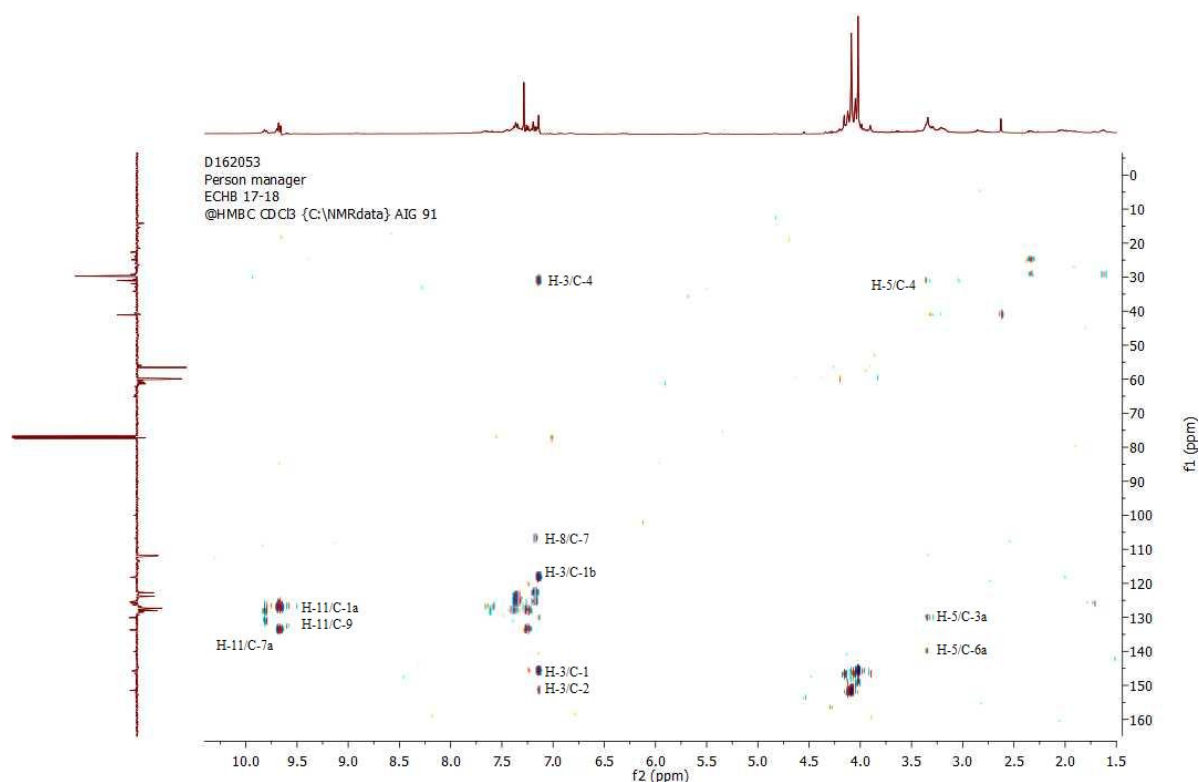
Figure 3.31a: HMBC NMR (400MHz, CDCl3) of ECHB 17-18

Ring B bore two aliphatic protons H-4 and H-5, the HMBC Spectrum (**Figure 3.31a**) revealed they had ^{2}J correlations to each other, H-5 also had ^{3}J couplings to quaternary carbons C-3a and C-6a. While ring A bore the two methoxys which showed strong ^{3}J couplings to their respective aromatic oxygenated carbons. Ring A aromatic proton H-3 showed ^{3}J correlations to quaternary carbon C-1b and C-1, as well as ^{2}J correlations to quaternary carbon C-2. Other correlations as shown in **Table 3.13**. The assignments of Urabaine was similar to previously isolated one from *Oxandra CF Major* ethyl acetate extract Arango (1986). The differences in assignments were the C-7/C-7' quaternary carbon which was 106.7 ppm in this study compared to Arango *et al*., 120.4 ppm. Also the aromatic methine C-11 was the most aromatic deshieded carbon at 128.2 ppm compared to 122.4 ppm reported by Arango *et al*., (1986). In this present study Urabaine was obtained as a dark brown powder and ESI MS Spectrum gave a quasi-molecule at 557.65 (M+H)$^+$ indicating a molecular mass of 556. This indicated the alkaloid as a symmetrical dimer rather than a monomer with predicted molecular formula of $C_{89}H_{32}O_4 N_2$ with two dehyronornuciferine units.

Table 3.12 ^{1}H and ^{13}C correlations of Urabaine

Position	^{1}H (ppm)	^{13}C (ppm)
C-1	-	145.7
C-1'	-	1457
C-1a	-	126.4
C-1a'	-	126.4
C-1b	-	118.1
C-1b'	-	118.1
C-2	-	151.5
C-2'	-	151.5
C-3	7.14	111.9
C-3'	7.14	111.9
C-3a	-	130.4
C-3a'	-	130.4
C-4	3.21	30.9
C-4'	3.21	30.9
C-5	3.32	93.97
C-5'	3.32	93.97
C-6a	-	193.0
C-6a'	-	193.0
C-7	-	106.7
C-7'	-	106.7
C-7a	-	133.7
C-7a'	-	133.7
C-8	7.19	123.8
C-8'	7.19	123.8
C-9	7.24	127.3
C-9'	7.24	127.3
C-10	7.89	122.7
C-10'	7.89	122.7
C-11	9.68	128.2
C-11'	9.68	128.2
C-11a	-	125.8
C-11'a	-	125.8
1-OMe	4.02	60.0
1'-OMe	4.02	60.0
2-OMe	4.09	56.5
2'-OMe	4.09	56.5

Table 3.13 HMBC correlations of Urabaine

Position	^1H	^{13}C
3	7.14	118.1(1b),30.9(4),151.5(2),145.7(1)
4	3.21	93.97(5)
5	3.32	193(6a),130.4(3a),30.9(4)
8	7.19	122.7(10),125.8(11a),106.7(7)
9	7.24	128.2(11),133.7(7a)
10	7.89	128.2(11),123.8(8)
11	9.68	127.3(9)133.6(7a),126.4(1a)
1-OMe	4.01	145.7(1),151.5(2)
2-OMe	4.08	151.5(2),145.7(1)

Table 3.14: **Molecular modelling results**

Compound	Binding Affinity Scale [1 (Best) to 7(Least)]						
	3TIK	**2RM6**	**2RM5**	**2WYO**	**1QU4**	**3BNW**	**2WOI**
(**81**)	6	4	5	3	1	2	7
(**82**)	6	4	5	3	1	2	7
(**83**)	6	4	5	3	2	1	7
(**84**)	6	4	5	3	1	2	7
(**85**)	5	4	6	3	1	2	7
(**86**)	3	6	1	2	4	5	7
(**87**)	6	4	5	3	1	2	7

Molecule	Binding Affinity Scale [1 (Best) to 7(Least)]						
	3TIK	2RM6	2RM5	2WYO	1QU4	3BNW	2WOI
(41)	4	6	2	5	1	3	7

Decoded PDBs used in the docking studies:

2WYO : *Trypanosoma brucei Glutathione Synthetase*

2RM5: *Glutathione peroxidase*-type *tryparedoxin peroxidase*, oxidized form

2RM6: *Glutathione peroxidase*-type *tryparedoxin peroxidase*, reduced form

3TIK: *Sterol 14-alpha demethylase (CYP51) from Trypanosoma brucei in complex with the tipifarnib derivative 6-((4-chlorophenyl) (methoxy) (1-methyl-1H-imidazol-5-yl)methyl)-4-(2,6-difluorophenyl)-1-methylquinolin-2(1H)-one*

1QU4: *Trypanosoma brucei ornithine decarboxylase*

3BNW: *Riboflavin kinase* from *Trypanosoma brucei*

2WOI: *Trypanothione reductase* from *Trypanosoma brucei*
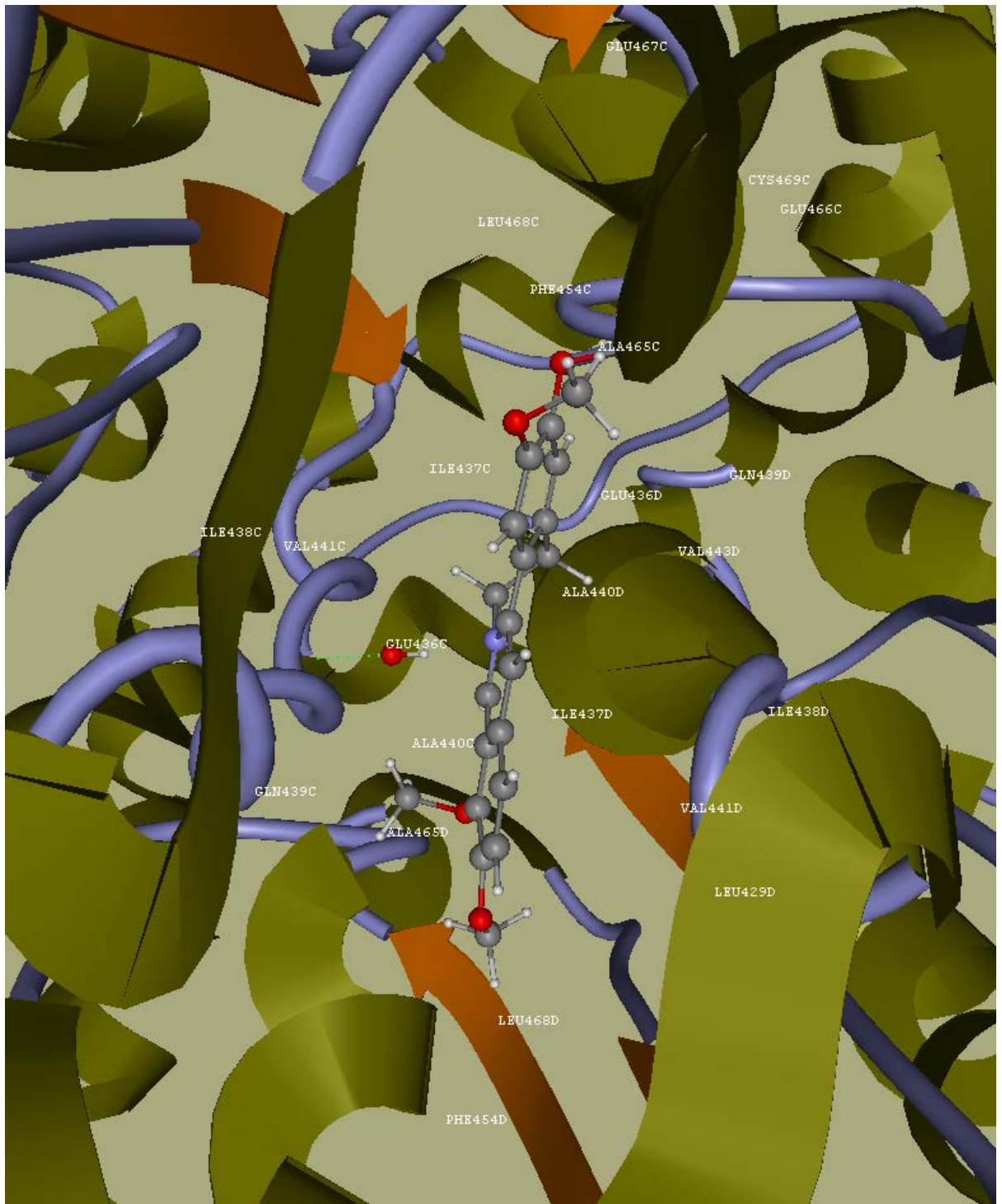
Fig 3.32: Active Site for palmatine on 2WOI.tiff (*Trypanosoma brucei Glutathione Synthetase*)
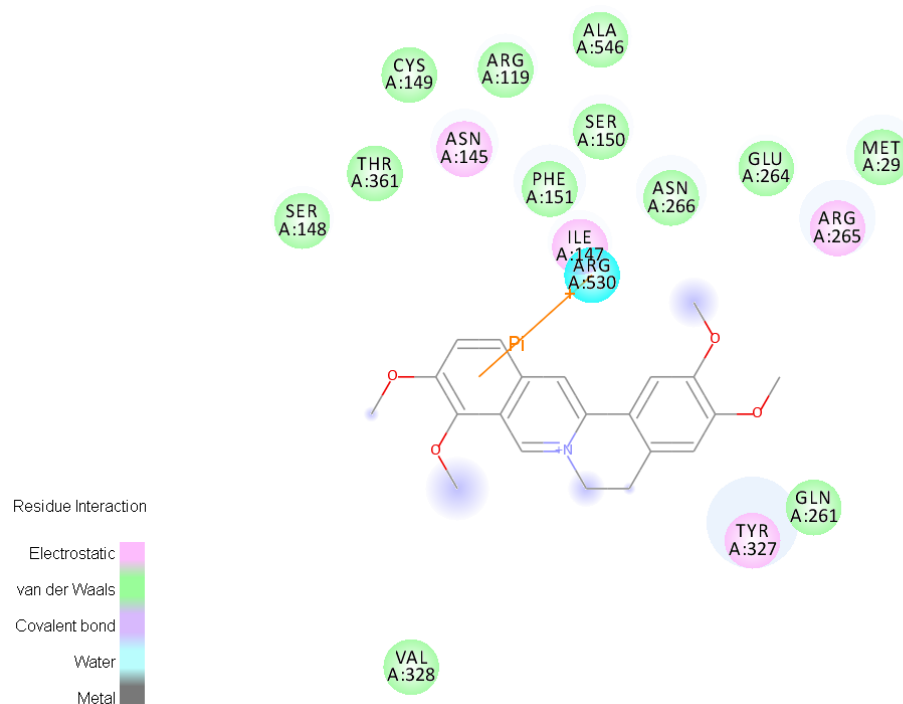
Fig. 3.33: 2D interactions of palmatine's protein with 2WOI ligand (*Trypanosoma brucei Glutathione Synthetase)*
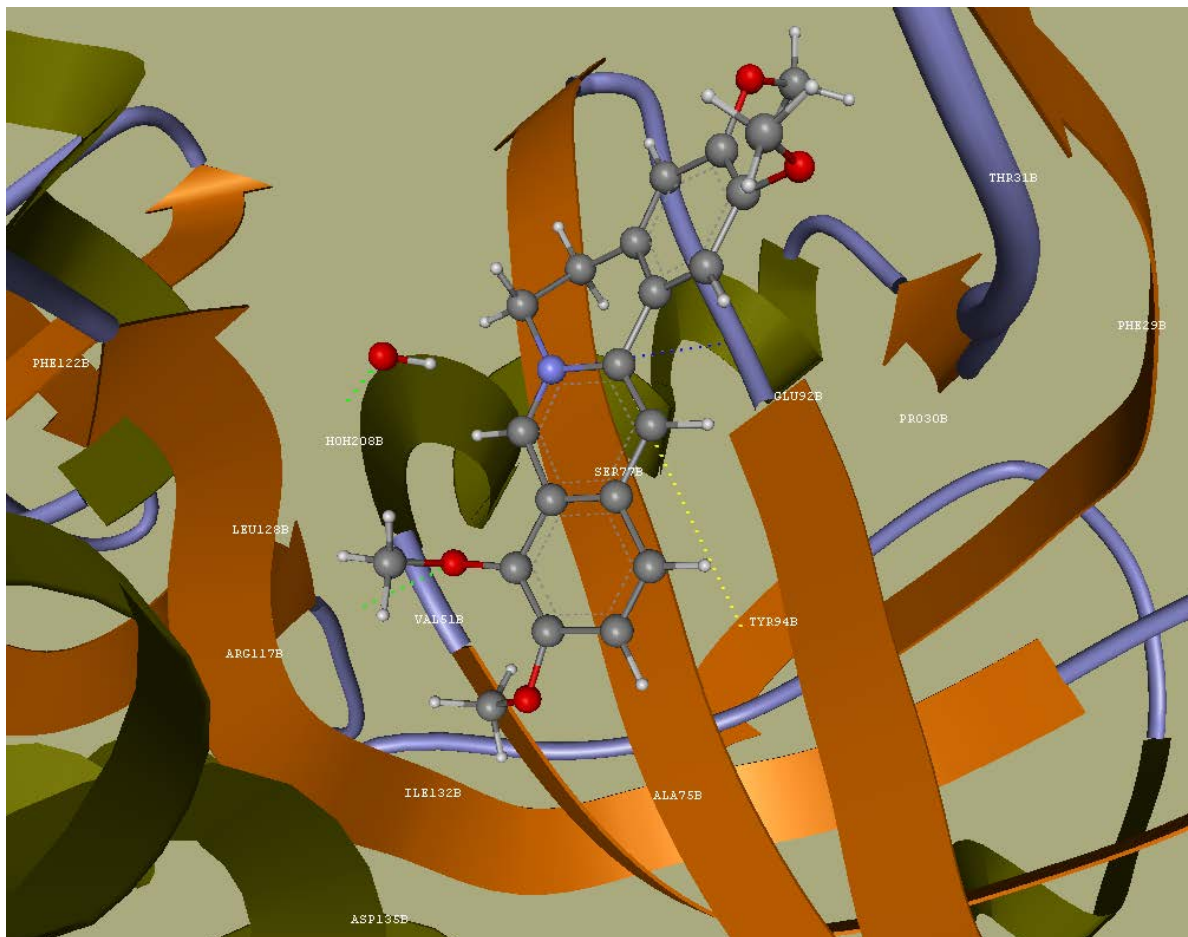
Fig. 3.34: Active Site for palmatine on 3BNW.tiff (*Riboflavin kinase* from *Trypanosoma brucei*)
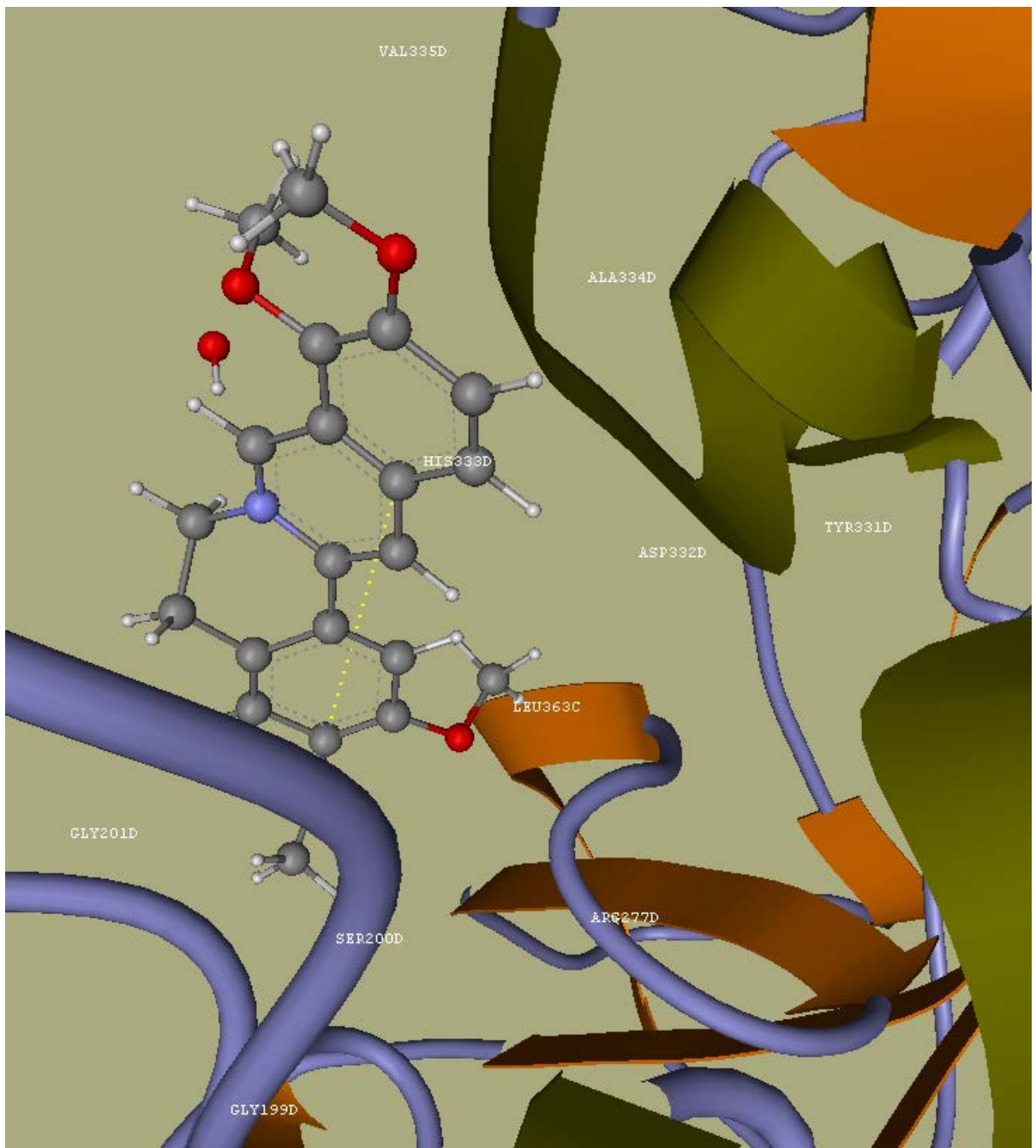
Fig 3.35: Active Site for palmatine on 1QU4.tiff (*Trypanosoma brucei ornithine decarboxylase*)
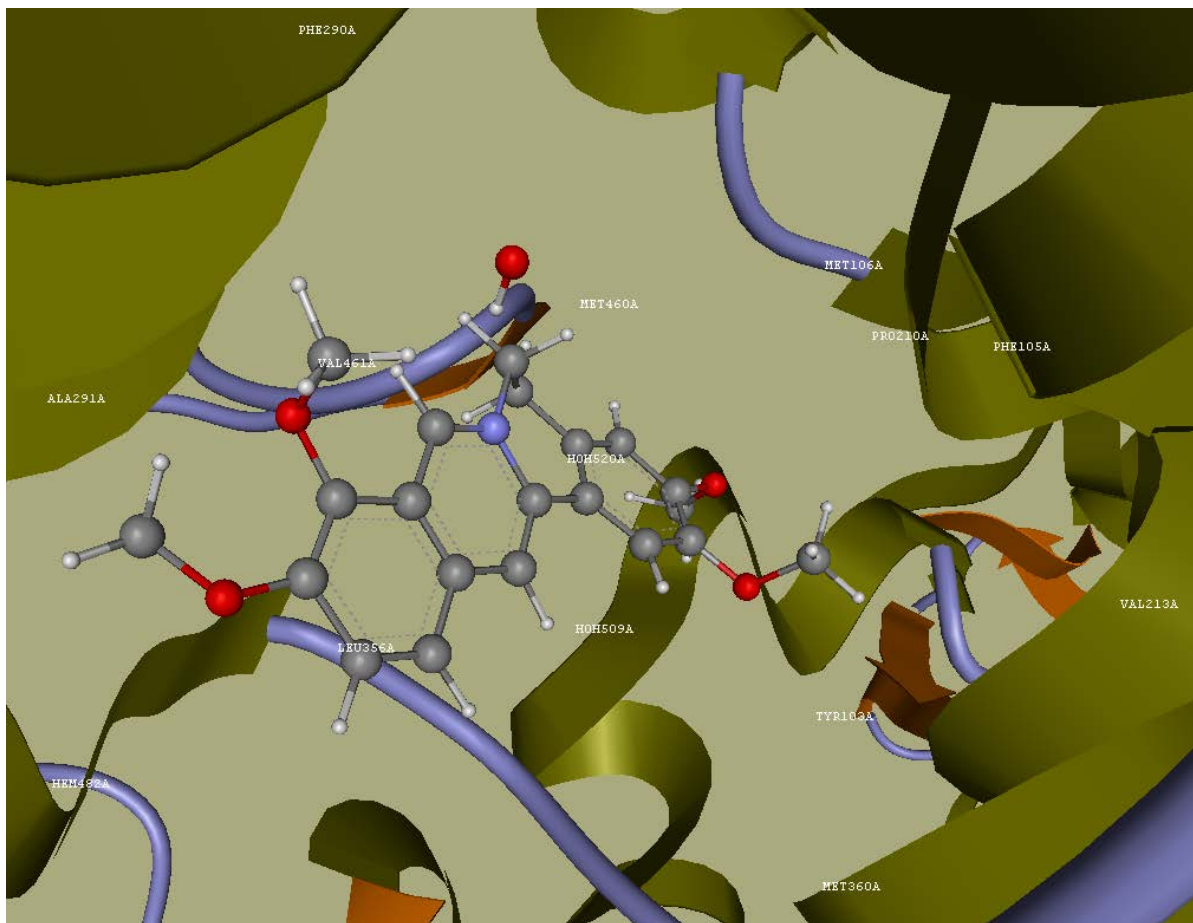
Fig. 3.36: Active Site for palmatine on 3TIK.tiff (*Sterol 14-alpha demethylase* (CYP51) from *Trypanosoma brucei* in complex with the *tipifarnib derivative 6-) (4-chlorophenyl) (methoxy) (1-methyl-1H-imidazol-5-yl) methyl)-4-(2, 6-difluorophenyl)-1-methylquinolin-2(1H)-one)*
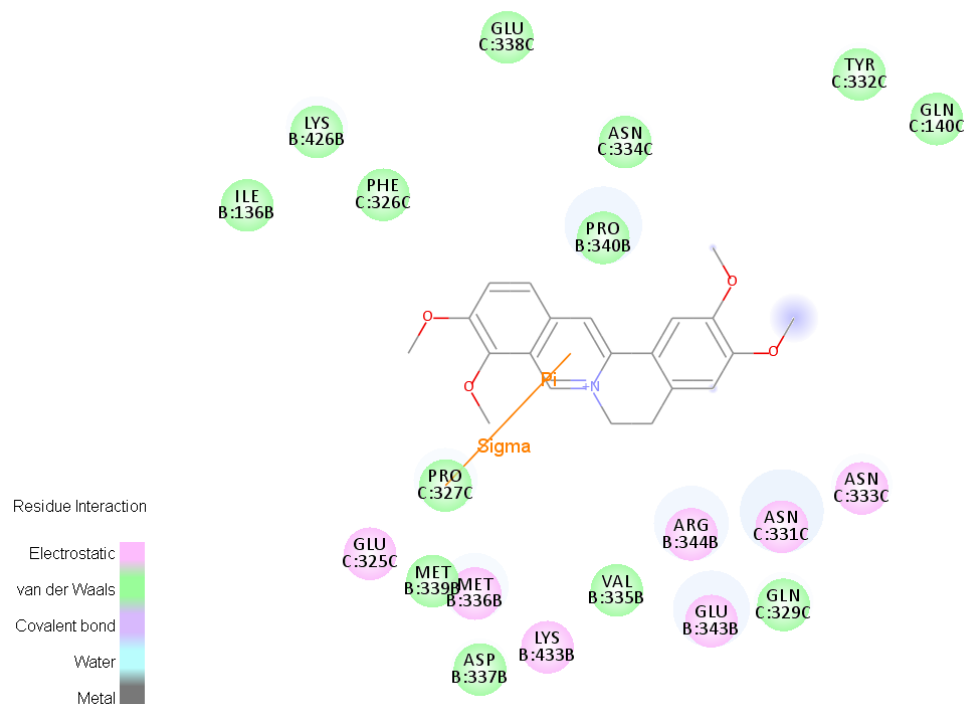
Figure 3.37: 2D Interaction of palmatine's protein 3TIK ligand (*Sterol 14-alpha demethylase* (CYP51) from *Trypanosoma brucei* in complex with the *tipifarnib derivative 6-) (4-chlorophenyl) (methoxy) (1-methyl-1H-imidazol-5-yl) methyl)-4-(2, 6-difluorophenyl)-1-methylquinolin-2(1H)-one)*
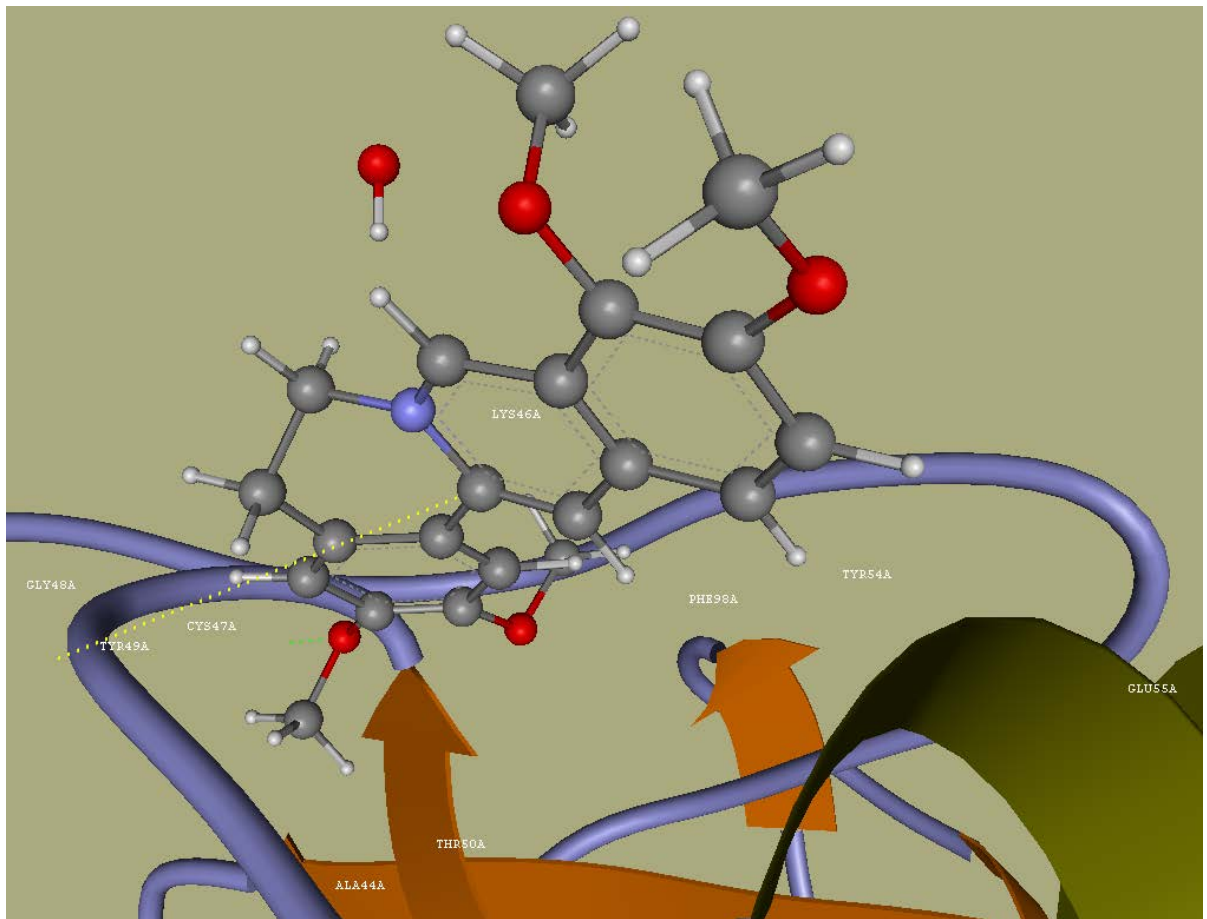
Fig. 3.38: Active Site for palmatine on 2RM5.tiff (*Glutathione peroxidase*-type *tryparedoxin peroxidase*, oxidized form)
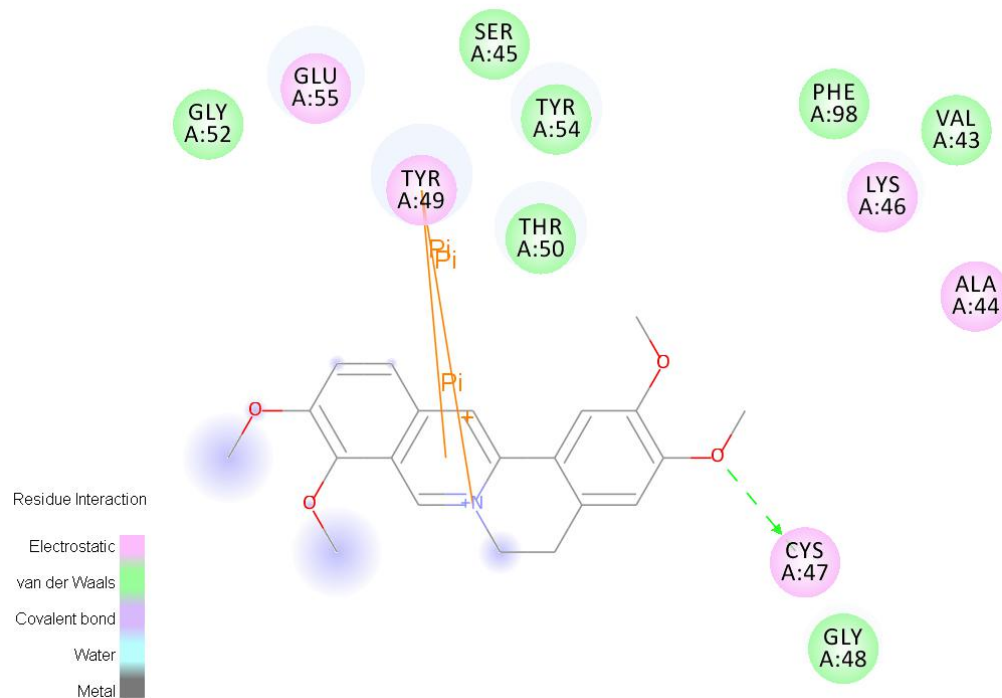
Fig. 3.39: 2D Interactions of palmatine protein with 2RM5 ligand
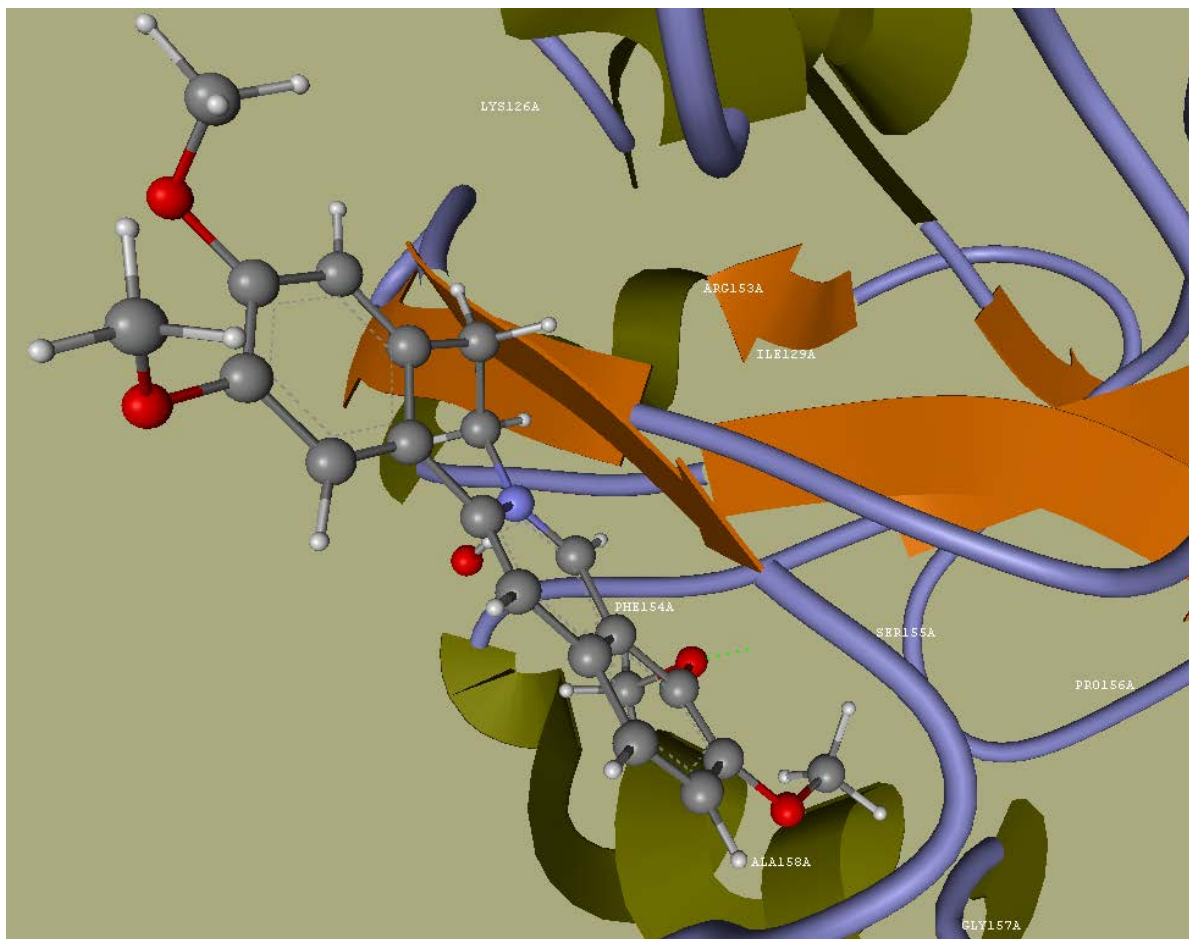
Fig. 3.40: Active Site for palmatine on 2RM6.tiff (*Glutathione peroxidase*-type *tryparedoxin peroxidase,* reduced form)
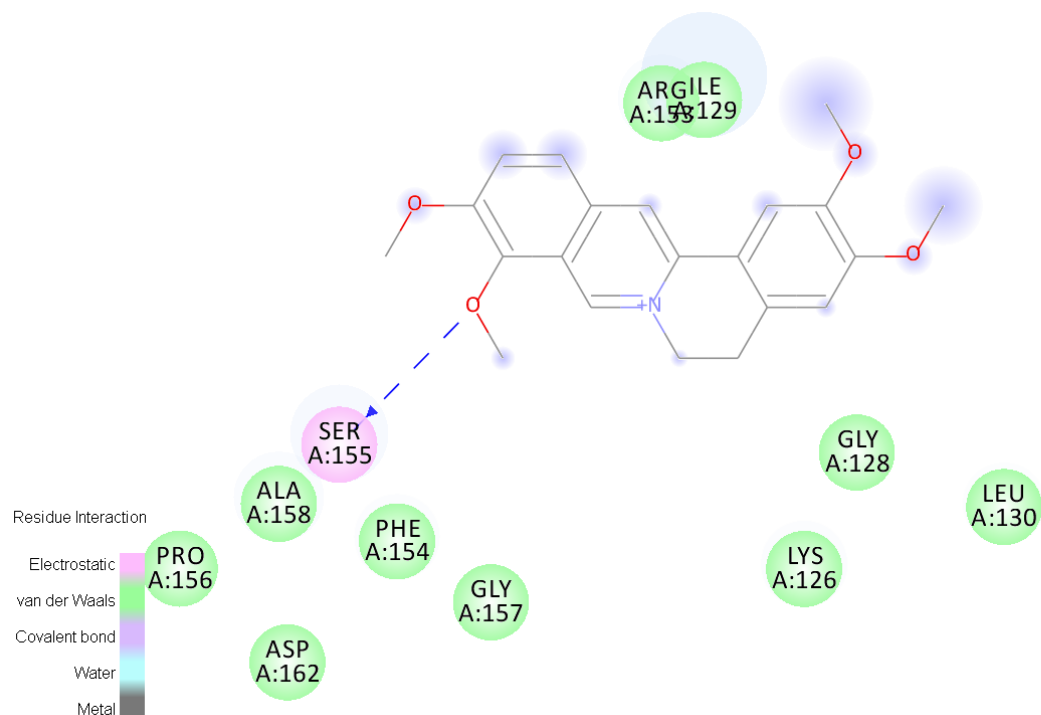
Fig. 3.41: 2D Interaction palmatine's protein with 2RM6 ligand (Glutathione peroxidase-type try-paredoxin peroxidase, reduced form)
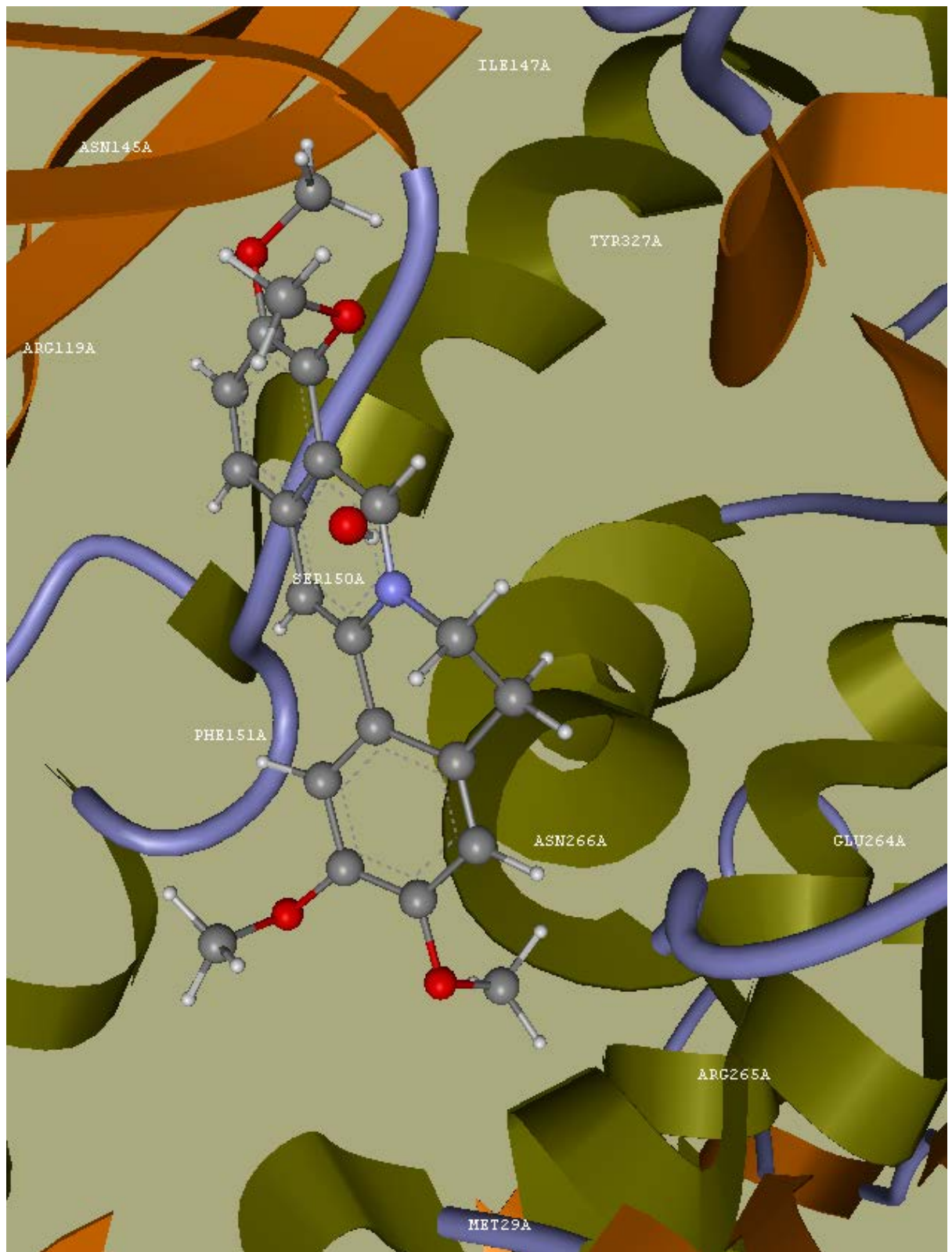
Fig. 3.42: Active Site for palmatine on 2WYO.tiff (*Trypanosoma brucei Glutathione Synthetase*).
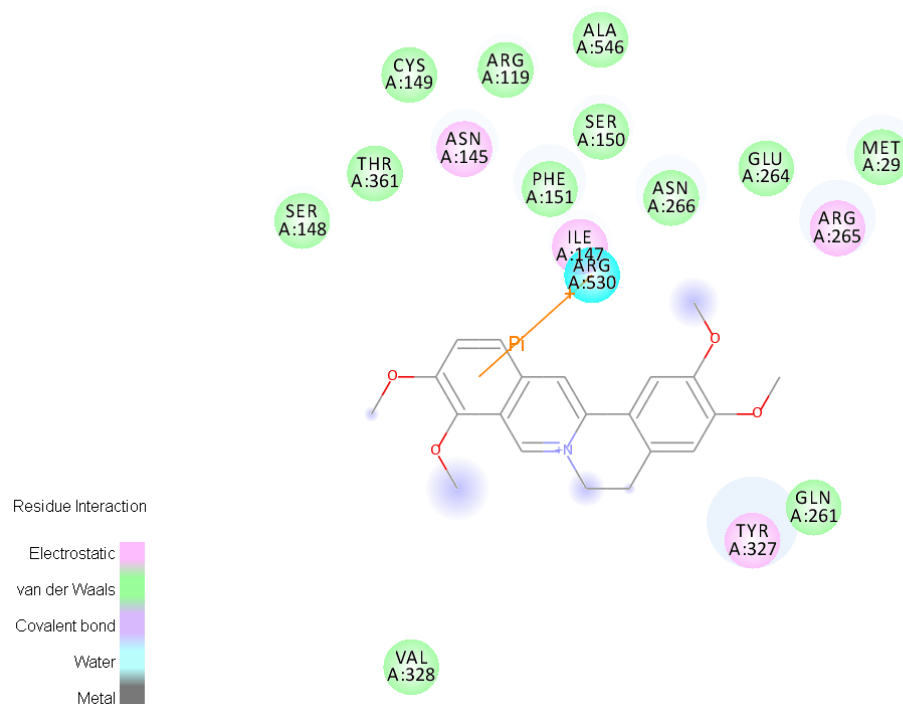
Fig. 3.43: Interactions of palmatine's protein with 2WYO ligand (*Trypanosoma brucei Glutathione Synthetase*)

Table 3.15 Docking studies results of Palmatine

Molecule	PLP Score(Docking Score)						
	3TIK	2RM6	2RM5	2WYO	1QU4	3BNW	2WOI
Palmatine	-66.33	-48.55	-77.68	-54.69	-81.71	-69.88	265.51
Glutathione(GSH)	ND	ND	ND	-56.54	ND	ND	ND
Tipifarnib Derivative(JKF)	-98.96	ND	ND	ND	ND	ND	ND

Molecule	Binding Affinity Scale [1 (Best) to 7(Least)]						
	3TIK	2RM6	2RM5	2WYO	1QU4	3BNW	2WOI
Palmatine	4	6	2	5	**1**	3	7

This docking studies revealed palmatine had the strongest affinity towards *ornithine decarboxylase* of *Trypanosoma brucei brucei* of the seven validated protein target docked. Riboflavin kinase, tryparedoxin peroxidase (oxidized form) and sterol 14α-demethylase showed significant affinity as potential targets of palmatine. It will also be safe to hypothesize that there would be minimal like hood for *Trypanosoma brucei brucei* to express resistance against palmatine since it is multiple targeted.

Docking studies of Palmatine with Trypanothione reductase from *Trypanosoma brucei* (2WOI)

Palmatine was found to have van der waals interactions with Glu489C, Ile490C, Ile491C, Gln492C, Ala493C, Val494C, Phe454C, Ala465C, Glu466C, Glu467C, Leu468C, Cys469C, Glu489D, Ile490D, Ile491D, Gln492D, Ala493D, Val494D, Phe454D, Ala465D, and Leu468D. It also had hydrophobic interactions with Glu489C, Ile490C, Gln492C, Ala465C, Glu466C, Leu468C, Cys469C, Leu429D, Glu489D, Ile490D, Ile491D, Gln492D, Ala493D, Val494D, Val443D, and Ala465D, Leu468D amino acid residues of 2WOI and hydrogen bonding with Gln492C of *Trypanothione reductase* of *T. bruce brucei.*

Docking studies of Palmatine with riboflavin kinase of *T. brucei* (3BNW)

Palmatine was found to have van der waals interactions with Phe29B, Pro30B, Thr31B, Val51B, Ser77B, Glu92B, Tyr94B, Arg117B, Phe122B, Ile132B, Asp135B as well as hydrophobic interactions with Phe29B, Pro30B, Thr31B, Val51B, Ala75B, Leu128B, Ile132B, Asp135B amino acid residues of *riboflavin kinase* of *T. brucei.brucei.* In addition, palmatine also had aromatic interaction with Tyr94B, charge interaction with Glu92B and hydrogen bonding with Arg117B of 3BNW.

Docking studies of Palmatine with ornithine decarboxylase of *T. brucei*. (1QU4)

Palmatine was found to have van der waals interactions with Leu893C, Ser200D, Gly201D, Arg277D, Tyr331D, Asp332D, His333D, Ala334D, Val335D and hydrophobic interactions with Leu893C, Gly199D, Ser200D, Gly201D, Asp332D, His333D, Ala334D, Val335D amino acid residues of ornithine decarboxylase of *T. brucei.brucei.* Palmatine also had aromatic interaction with His333D amino acid residues of 1QU4.

Docking studies of Palmatine with sterol 14-alpha demethylase (3TIK)

Palmatine had van der waals interactions with Tyr103A, Phe105A, Met106A, Pro210A, Val213A, Phe290A, Ala291A, Met890A, Met460A, Val461A, Hem482A and hydrophobic interactions with Met106A, Pro210A, Val213A, Phe290A, Ala291A, Leu356A, Met890A, Met460A, Val461A amino acid residues of sterol 14-α demethylase i.e. 3TIK. Reference ligand i.e. tipifarnib derivative was found to have van der waals interactions with Tyr103A, Phe105A, Met106A, Phe110A, Ala115A, Tyr116A, Leu127A, Glu205A, Leu208A, Ala287A, Phe290A, Ala291A, Thr295A, Leu356A,

Met358A, Cys422A, Met460A, Val461A, Hem482A and hydrophobic interactions with Met106A, Leu208A, Ala287A, Phe290A, Ala291A, Thr295A, Leu356A, Leu359A, Met460A, Val461A, Hem482A amino acid residues of 3TIK. It also had hydrogen bonding with Hem482A of sterol 14-α demethylase.

Docking studies of Palmatine with Glutathione peroxidase type tryparedoxin peroxidase, oxidized form (2RM5)

Palmatine was found to have van der waals interactions with Ala44A, Lys46A, Cys47A, Gly48A, Tyr49A, Thr50A, Tyr54A, Glu55A, Phe98A and hydrophobic interactions with Ala44A, Lys46A, Cys47A, Gly48A, Tyr49A, Thr50A, Tyr54A, Phe98A amino acid residues of glutathione peroxidase type tryparedoxin peroxidase, oxidized form. Palmatine also had aromatic interaction with Tyr49A and hydrogen bonding with Cys47A of 2RM5.

Docking studies of Palmatine with Glutathione peroxidase type tryparedoxin peroxidase, reduced form(2RM6)

Palmatine exhibited van der waals interactions with Lys126A, Ile129A, Arg153A, Phe154A, Ser155A, Gly157A, Ala158A and hydrophobic interactions with Ile129A, Phe154A, Ser155A, Pro156A, Gly157A, Ala158A amino acid residues of 2RM6. In addition, palmatine also had hydrogen bonding with Ser155A of glutathione peroxidase type tryparedoxin peroxidase, reduced form.

Docking studies of Palmatine with *Trypanosoma brucei* Glutathione Synthetase(2WYO)

Palmatine's docking studies also revealed van der waals interactions with Met29A, Arg119A, Asn145A, Ile147A, Ser150A, Phe151A, Glu264A, Arg265A, Asn266A, Tyr327A and hydrophobic interactions with Met29A, Asn145A, Ile147A, Arg265A, Asn266A, Tyr327A amino acid residues of glutathione synthetase of *T. brucei brucei*. It also had aromatic interactions with Tyr327A of 2WYO.

3.2.1 Further docking studies of Aporphine Alkaloids

Fourteen aporphine alkaloids comprising of the eight whose structure elucidation were discussed in details in the thesis, as well as six derivative monomeric alkaloids were subjected to molecular modelling studies at the University of Strathclyde. Their structures as shown here below

1. ECP-23 (**86**)
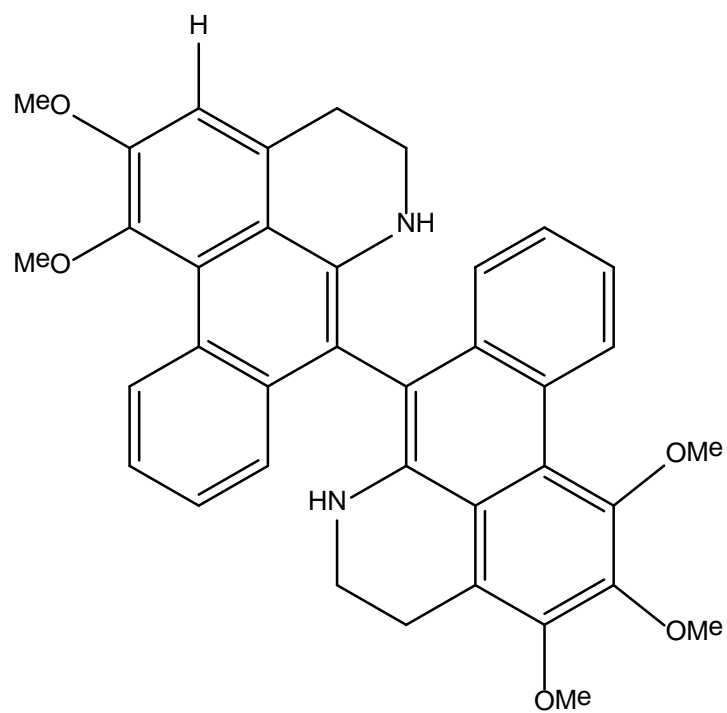
1,1',2,2',3-pentamethoxy-5,5',6,6'-tetrahydro-4H,4'H-7,7'-bidibenzo[de,g]quinoline

2. ECP-19 (**82**)
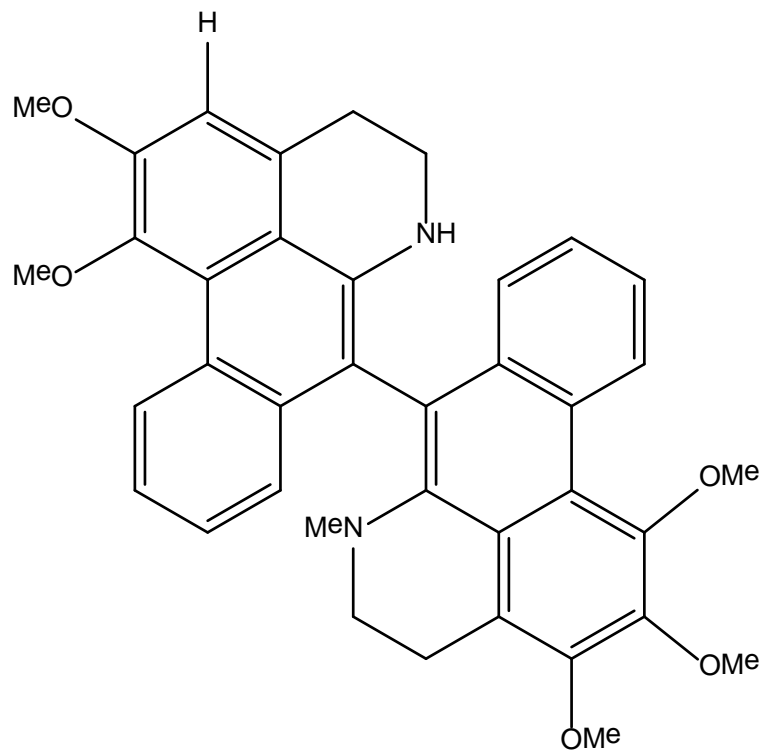
1,1',2,2',3-pentamethoxy-6-methyl-5,5',6,6'-tetrahydro-4H,4'H-7,7'-bidibenzo[de,g]quinoline

3. ECHB17-18 (**87**)
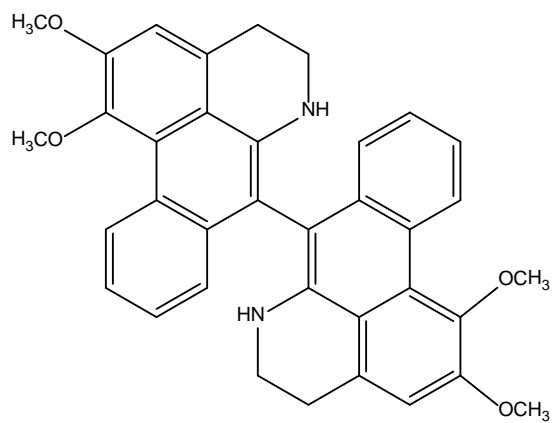
4. ECH 56 (**84**)
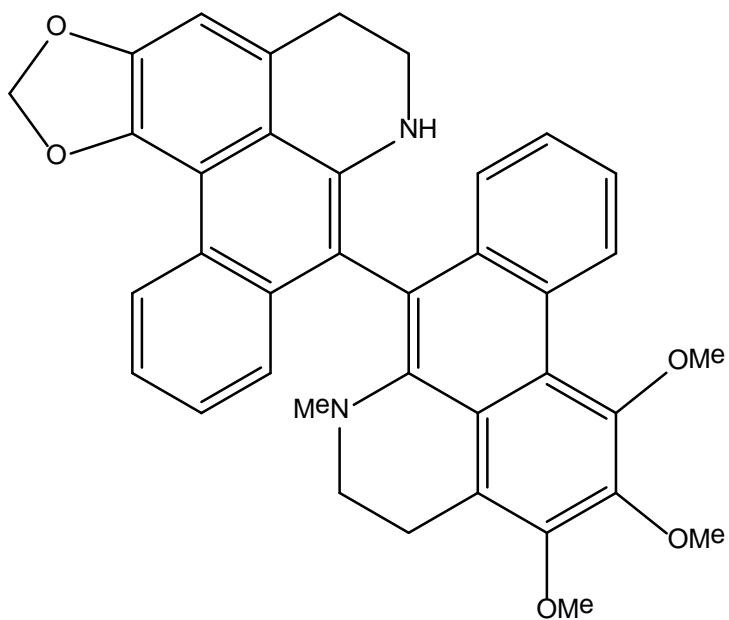
8′-(1′2′3′-trimethoxy-6-methyl-5′6-dihydro-4H-dibenzo[*de*′*g*]quinolin-7-yl)-6′7-dihydro-5H′-[1′3]dioxolo[4′5′:4′5]benzo[1′2′3-*de*]benzo[*g*]quinoline

5. ECHE 45 (**83**)
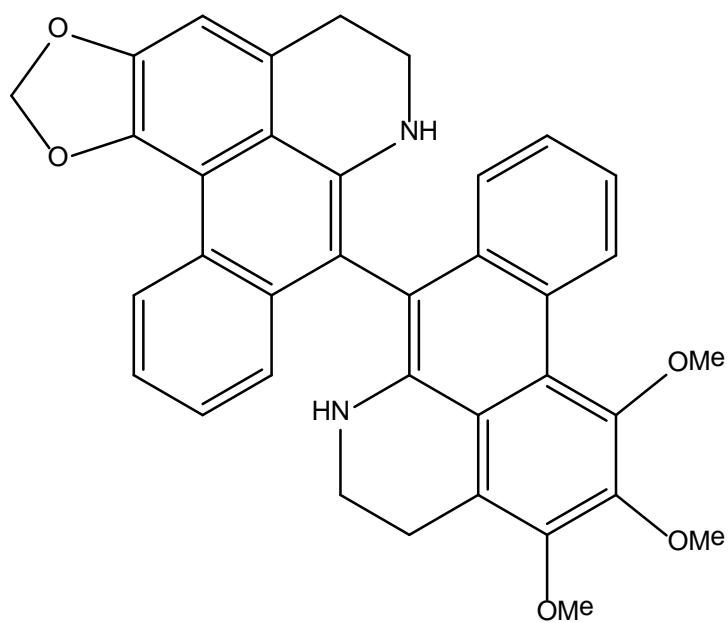
8′-(1′2′3′-trimethoxy-5′6-dihydro-4H-dibenzo[*de*′*g*]quinolin-7-yl)-6′7-dihydro-5H′-[1′3]dioxolo[4′5′:4′5]benzo[1′2′3-*de*]benzo[*g*]quinoline

[162]
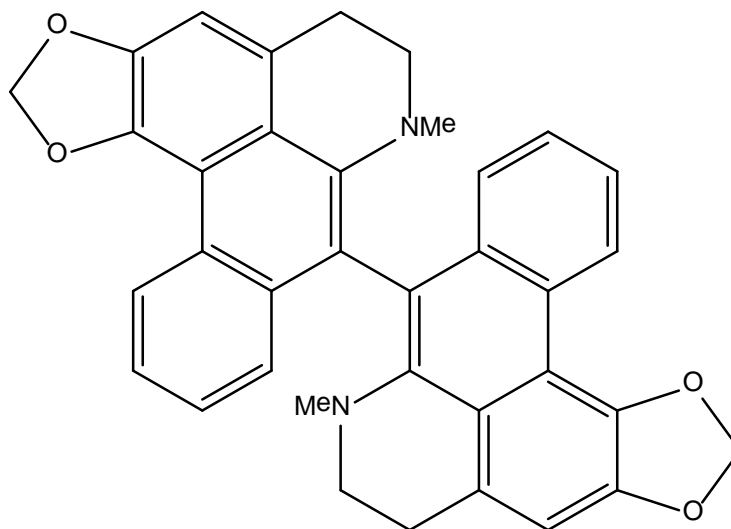
6. Compound **88**

7,7'-dimethyl-6,6',7,7'-tetrahydro-5H,5'H-8,8'-bi[1,3]dioxolo[4',5':4,5]benzo[1,2,3-de]benzo[g]quinoline

7. Compound **89**
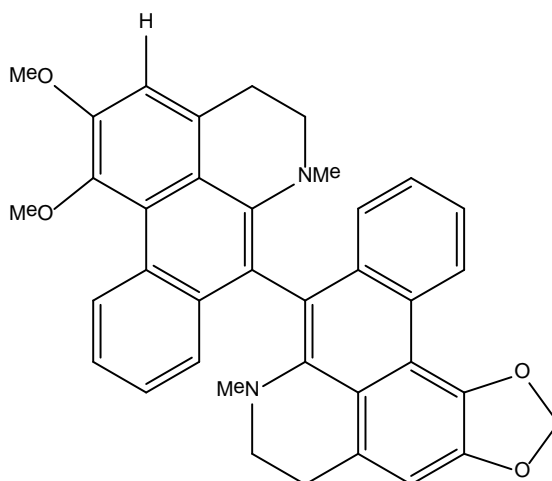
8-(1,2-dimethoxy-6-methyl-5,6-dihydro-4H-dibenzo[de,g]quinolin-7-yl)-7-methyl-6,7-dihydro-5H-[1,3]dioxolo[4',5':4,5]benzo[1,2,3-de]benzo[g]quinoline

[163]
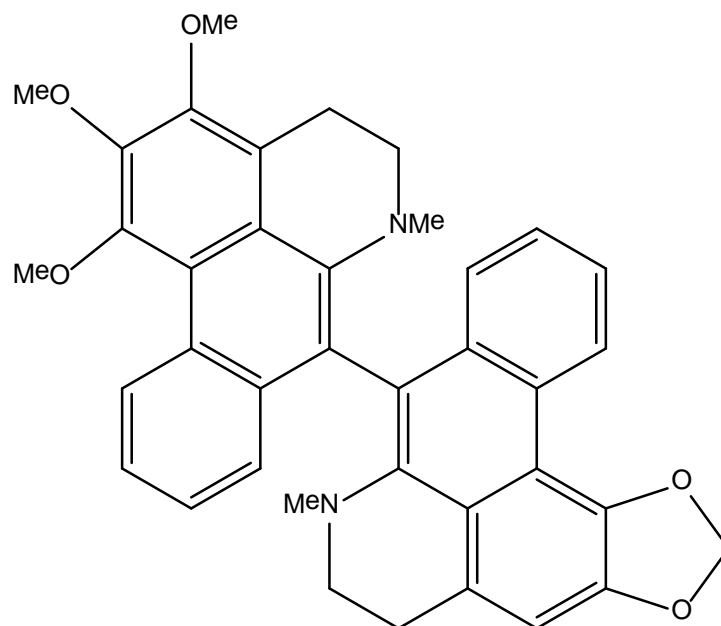
8. Compound **90**

7-methyl-8-(1,2,3-trimethoxy-6-methyl-5,6-dihydro-4H-dibenzo[de,g]quinolin-7-yl)-6,7-dihydro-5H-[1,3]dioxolo[4',5':4,5]benzo[1,2,3-de]benzo[g]quinoline

9. **ECP 17 (81)**

1,1',2,2',3,3'-hexamethoxy-5,5',6,6'-tetrahydro-4H,4'H-7,7'-bidibenzo[de,g]quinoline

[164]
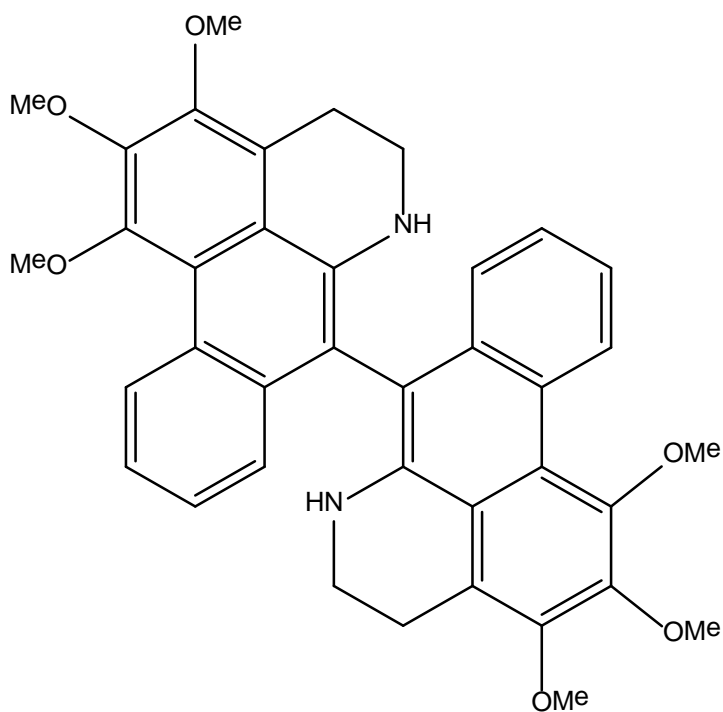
10. Compound 91

1,2-dimethoxy-5,6-dihydro-4H-dibenzo[de,g]quinoline
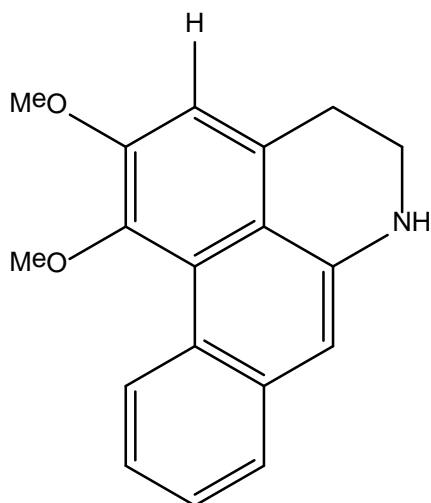
11. Compound **92**
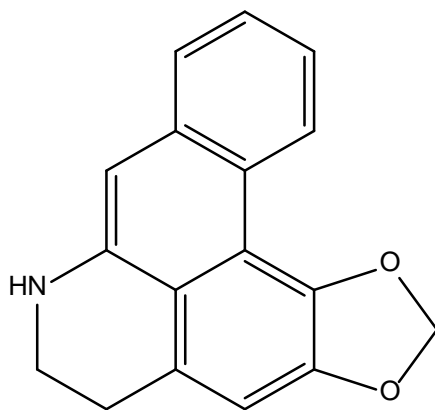
6,7-dihydro-5H-[1,3]dioxolo[4',5':4,5]benzo[1,2,3-de]benzo[g]quinoline

12. Compound **93**

1′2′3′-trimethoxy-6-methyl-5′6′-dihydro-4H-dibenzo[de′g]quinoline
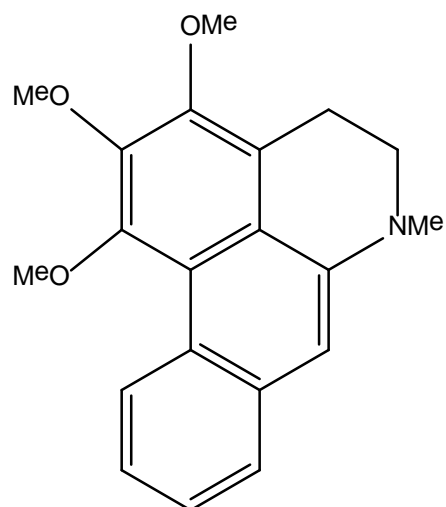
13. Compound 94

1′2′-dimethoxy-6-methyl-5′6′-dihydro-4H-dibenzo[de′g]quinoline
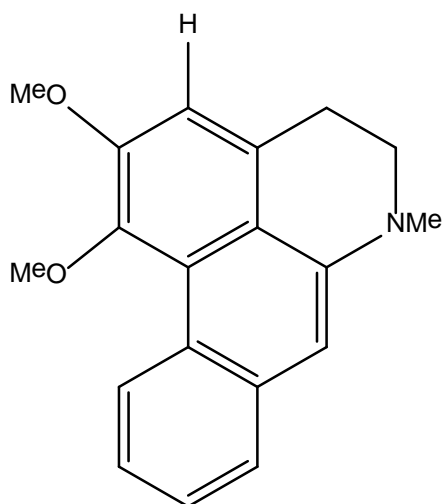
14. **ECF 5-10 (85)**
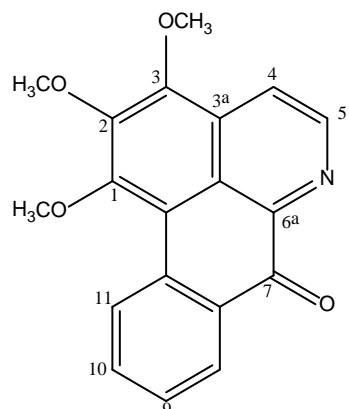
1,2,3-trimethoxy-7H-dibenzo[de,g]quinolin-7-one

15. Compound **95**
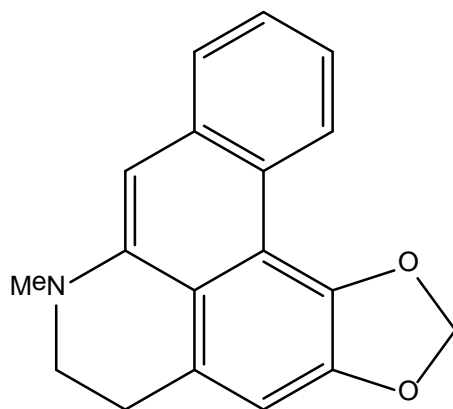
7-methyl-6,7-dihydro-5H-[1,3]dioxolo[4',5':4,5]benzo[1,2,3-de]benzo[g]quinoline

Table 3.16 Docking studies results of alkaloids isolated in this study

Compound	Binding Affinity Scale [1 (Best) to 7(Least)]						
	3TIK	2RM6	2RM5	2WYO	1QU4	3BNW	2WOI
86	6	4	5	3	**1**	2	7
82	6	3	5	4	**1**	2	7
87	6	3	5	4	**1**	2	7
84	6	4	5	3	**1**	2	7
83	6	4	5	3	**1**	2	7
88	6	4	5	2	**1**	3	7
89	6	4	5	3	2	**1**	7
90	5	4	6	3	**1**	2	7
81	`1	4	5	3	**1**	2	7
91	**1**	6	3	4	2	5	7
92	**1**	6	3	4	2	5	7
93	**1**	6	4	3	2	5	7
94	3	6	**1**	2	4	5	7
85	**1**	6	2	4	3	5	7
95	**1**	6	4	3	2	5	7

For all aporphine alkaloids docked except Compounds **85** & **93**, *ornithine decarboxylase of Trypanosoma brucei brucei* was the preferred target for anti-trypanosomal activity. Compounds **90, 91, 92, 93** & **94** considerably showed significant binding affinity towards Sterol 14-alpha demethylase (CYP51). Riboflavin kinase of Trpanosoma brucei was also a significant targeted protein for compounds **81-89**. None of the tested phytoconstituents expressed affinity for *Trypanothione reductase* of *Trypanosoma brucei brucei.*

Docking studies of aporphine alkaloids with *Riboflavin kinase* of *T. brucei.brucei*

Compound (**86**) was found to have Van der waals interactions with Ser25B, Leu27B, Pro30B, Tyr94B, Phe122B, Leu125B, Leu128B, Ile132B amino acid residues and hydrophobic interactions with Ser25B, Leu27B, Pro30B, Tyr94B, Leu128B and Ile132B amino acid residues of riboflavin kinase i.e. 3BNW. Compound (**82**)was found to have Vdw interactions with Phe29B, Pro30B, Thr31B, Ala75B, Tyr94B, Leu96B, Leu128B, Ile132B amino acid residues and hydrophobic interactions with Ser25B, Pro30B, Ala75B, Tyr94B, Leu96B, Leu125B, Leu128B, Ile132B, and Val189B amino acid residues of riboflavin kinase. Along with these, Compound (**82**) also exerted aromatic interactions with Tyr94B of 3BNW. Compound (**81**) was found to have Vdw interactions with Ser25B, Leu27B, Phe29B, Pro30B,

Thr31B, Val51B, Ala75B, Ala76B, Tyr94B, Arg117B, Phe122B, Leu128B, Ile132B, Val189B amino acid residues and hydrophobic interactions with Ser25B, Leu27B, Pro30B, Val51B, Ala75B, Ala76B, Tyr94B, Leu125B, Leu128B, Ile132B, Asp135B, Val189B amino acid residues of riboflavin kinase. Compound **81** also had aromatic interactions with Tyr94B of 3BNW. Compound (**83**) was found to have Vdw interactions with Leu27B, Phe29B, Pro30B, Ser77B, Tyr94B, Phe122B, Leu128B, Ile132B amino acid residues and hydrophobic interactions with Phe29B, Pro30B, Ser77B, Tyr94B, Met119B, Leu128B, and Ile132B amino acid residues of riboflavin kinase. Compound 84 was found to have Vdw interactions with Leu27B, Phe29B, Pro30B, Thr31B, Ser77B, Glu92B, Tyr94B, Leu128B, Val129B, Ile132B amino acid residues and hydrophobic interactions with Phe29B, Pro30B, Thr31B, Glu92B, Tyr94B, Ile132B amino acid residues of riboflavin kinase. Compound 84 also had aromatic interactions with Tyr94B of 3BNW. Compound 85 was found to have Vdw interactions with Ser25B, Phe29B, Pro30B, Thr31B, Tyr94B, Phe122B, leu128B, Ile132B amino acid residues and hydrophobic interactions with Ser25B, Pro30B, Thr31B, Val51B, Ser77B, Tyr94B, Ile132B amino acid residues of riboflavin kinase. Compound 89 was found to have Vdw interactions with Ser25B, Phe29B, Pro30B, Thr31B, Ala75B, Ser77B, Tyr94B, Phe122B, Leu128B, Ile132B, Asp135B amino acid residues and hydrophobic interactions with Ser25B, Pro30B, Thr31B, Ala75B, Ser77B, Tyr94B, Ile132B, Asp135B, Val189B amino acid residues of riboflavin kinase. In addition to these, compound 89 do exert aromatic interactions with Tyr94B of 3BNW. Compound 87 was found to have Vdw interactions with Ser25B, Phe29B, Pro30B, Thr31B, Val51B, Ala75B, Tyr94B, Leu96B, Arg117B, Leu128B, Ile132B, Asp135B, Val189B amino acid residues, while Compound 87 also had hydrophobic interactions with Ser25B, Leu27B, Phe29B, Pro30B, Thr31B, Val51B, Ala75B, Tyr94B, Leu96B, Leu128B, Ile132B, Val189B amino acid residues of riboflavin kinase. Compound 87 had charge interactions with Arg117B of 3BNW. Compound 88 was found to have Vdw interactions with Leu27B, Pro30B, Thr31B, Tyr94B, Phe122B, Leu128B, Val129B, Ile132B amino acid residues and hydrophobic interactions with Pro30B, Tyr94B, Ser121B, Leu128B, Val129B, Ile132B and Val189B amino acid residues of 3BNW. Compound 90 was found to have Vdw interactions with leu27B, Pro30B, Tyr94B, Leu125B, Leu128B, Ile132B amino acid residues and hydrophobic interactions with Leu27B, Pro30B, Tyr94B, Ile132B amino acid residues of riboflavin kinase. Compound 91 was found to have Vdw interactions with Leu27B, Pro30B, Tyr94B, Phe122B, Leu125B, Leu128B, Ile132B amino acid residues and hydrophobic interactions with Pro30B, Tyr94B, Leu128B, Ile132B amino acid residues of 3BNW. Compound 92 was found to have Vdw interactions with Ser25B, Leu27B, Phe29B, Pro30B, Leu125B, Leu128B, Ile132B amino acid residues and hydrophobic interactions with Leu27B, Pro30B, Tyr94B, Leu125B, Leu128B, Ile132B amino acid residues of riboflavin kinase. Compound 93 was found to have Vdw interactions with Pro30B, Thr31B, Ser77B, Glu92B, Tyr94B, Met119B and Ile132B amino acid residues and hydrophobic interactions with Pro30B, Thr31B, Val51B, Ser77B, and Met119B amino acid residues of riboflavin kinase. Compound 85 was found to have Vow interactions with Ser25B,

[169]

Leu27B, Phe29B, Pro30B, Phe122B, Leu128B, Ile132B amino acid residues and hydrophobic interactions with Ser25B, Leu27B, Phe122B, Leu125B, Leu128B, Ile132B amino acid residues of 3BNW. Compound 94 was found to have Vdw interactions with Leu27B,Phe29B, Pro30B, Tyr94B, Leu128B, Ile132B amino acid residues and hydrophobic interactions with Leu27B, Pro30B, Tyr94B, Leu125B, Leu128B, Ile132B amino acid residues of 3BNW i.e. riboflavin kinase.

Docking studies of aporphine alkaloids with ornithine decarboxylase of T. brucei.

Compound 81 was found to have Vdw interactions with Gly201D, Thr203D, Pro292D, Gly293D, Thr294D, Ala244D, Pro245D, Arg277D, Asp332D, His333D amino acid residues and hydrophobic interactions with Ser200D, Gly201D, Pro292D, Gly293D, Thr294D, Ala244D, Ala281D, His333D, Ala334D amino acid residues of 1QU4 i.e. ornithine decarboxylase of *T. brucei*. Compound 81 was also found to have aromatic interactions with His333D and charge interaction with Arg277D. Compound 82 was found to have Vdw interactions with Ser200D, Gly201D, Thr203D, Pro292D, Gly293D, Thr294D, Ala244D, Pro245D, Arg277D, Ala281D, Asp332D, His333D amino acid residues and hydrophobic interactions with Ser200D, Gly201D, Pro292D, Gly293D, Thr294D, Ala244D, Pro245D, Leu246D, Arg277D, Ala281D, Asp332D, His333D and Ala334D of 1QU4. Also Compound 82 had aromatic interactions with His333D and charge interactions with Arg277D amino acid residues of *T. Bruce ornithine decarboxylase*. Compound 83 was found to have Vow interactions with Leu166D, His197D, Val198D, Gly199D, Ser200D, Gly201D, Thr294D, Arg277D, Ala281D, Asp332D, His333D, Ala334D, Val335D and Asp915D amino acid residues and hydrophobic interactions with Leu166D, Gly199D, Ser200D, Gly201D, Ser202D, Pro292D, Gly293D, Thr294D, Arg277D, Ala281D, Ala334D, Val335D, Val919D, Asp915D and Ala918D amino acid residues of ornithine decarboxylase. Compound 83 was also found to have charge interactions with Arg277D and hydrogen bonding with Ser200D and Val335D amino acid residues of 1QU4. Compound 83 was found to have Vow interactions with Gly201D, Thr203D, Pro292D, Gly293D, Thr294D, Ala244D, Pro245D, Leu246D, Arg277D, Asp332D, His333D amino acid residues and hydrophobic interactions with Gly201D, Pro292D, Gly293D, Thr294D, Ala244D, Pro245D, Leu246D, Arg277D, Ala281D and His333D amino acid residues of 1QU4. Compound 83 also had charge interactions with Arg277D and aromatic interaction with His333D amino acid residues of *ornithine decarboxylase of T. Bruce*. Compound 84 was found to have Vow interactions with Ser200D, Gly201D, Thr203D, Pro292D, Gly293D, Thr294D, Ala244D, Pro245D, Arg277D, Asp332D, His333D amino acid residues and hydrophobic interactions with Ser200D, Gly201D, Pro292D, Gly293D, Thr294D, Ala244D, Arg277D, Ala281D, Asp332D, His333D amino acid residues of ornithine decarboxylase. It also had aromatic interaction with His333D and charge interactions with Arg277D amino acids of 1QU4. Compound 85 was found to have Vow interactions with Leu166D, Gly199D, Ser200D, Gly201D, Arg277D, Asp332D, His333D, Val335D, Arg920D amino acid residues and hydrophobic interactions with Leu166D,

Gly199D, Gly201D, Ser202D, Thr203D, His333D, Val335D amino acid residues of 1QU4. Compound 85 was also found to have charge interactions with Arg277D and hydrogen bonding with Ser200D of ornithine decarboxylase. Compound 86 was found to have Vow interactions with Leu166D, Val198D, Ser200D, Gly201D, Ala244D, Pro245D, Arg277D, Asp332D, His333D, Val335D, Arg920D amino acid residues and hydrophobic interactions with Leu893C, Leu166D, Gly201D, Ser202D, Thr203D, His333D, Val335D amino acid residues of ornithine decarboxylase. Compound 86 was also found to have charge interaction with Arg277D of 1QU4. Compound 90 had Vow interactions with Leu893C, Leu166D, Val198D, Gly199D, Ser200D, Gly201D, Thr203D, Ala244D, Pro245D, Arg277D, Asp332D, His333D, Val335D and Arg920D amino acid residues and hydrophobic interactions with Leu893C, Leu166D, Val198D, Gly199D, Ser200D, Gly201D, Ser202D, His333D, Val335D amino acid residues of 1QU4. It also had hydrogen bonding with Arg920D of ornithine decarboxylase. Compound 87 was found to have Vow interactions with Thr157D, Leu166D, Gly199D, Ser200D, Gly201D, Pro292D, Arg277D, Asp332D, His333D, Ala334D and Val335D amino acid residues and hydrophobic interactions with Leu166D, Ser167D, Val198D, Gly199D, Ser200D, Gly201D, Ser202D, Pro292D, Thr294D, Ala244D, Arg277D, Ala281D, Asp332D, His333D, Ala334D amino acid residues of *ornithine decarboxylase of T. brucei*. Compound 87 also had charge interactions with Arg277D and hydrogen bonding with Leu166D, Gly201D and Arg277D amino acid residues of 1QU4. Compound 88 was found to have Vdw interactions with Gly199D, Ser200D, Gly201D, Arg277D, Asp332D, His333D amino acid residues and hydrophobic interactions with Leu166D, Gly199D, Ser200D, Ser202D, Thr203D amino acid residues of 1QU4. Compound 88 also had hydrogen bonding with Ser200D amino acid residues. Compound 89 was found to have Vdw interactions with Gly199D, Ser200D, Gly201D, Arg277D, Asp332D, His333D amino acid residues and hydrophobic interactions with Leu166D, Gly199D, Ser200D, Thr203D amino acid residues of ornithine decarboxylase. In addition to these, Compound 89 was also found to have charge interactions with Arg277D and hydrogen bonding with Ser200D amino acid residues of 1QU4. Compound 90 was found to have Vdw interactions with Ser200D, Arg277D, Asp332D, His333D, Ala334D, Val335D amino acid residues and hydrophobic interactions with Ser200D, Gly201D, Arg277D, Asp332D, His333D and Val335D amino acid residues of 1QU4. Compound 94 also had aromatic interactions with His333D, charge interactions with Arg277 and hydrogen bonding with Arg277D amino acid residues of ornithine decarboxylase. Compound 91 was found to have Vdw interactions with Val198D, Ser200D, Gly201D, Ser202D, Arg277D, His333D amino acid residues and hydrophobic interactions with Gly199D, Ser200D, Gly201D and His333D amino acid residues of ornithine decarboxylase. Compound 92 was found to have Vdw interactions with Ser200D, Arg277D, Asp332D, His333D, Ala334D, Val335D amino acid residues and hydrophobic interactions with Ser200D, Arg277D, Cys328D, Asp332D, His333D, Ala334D, Val335 amino acid residues of ornithine decarboxylase. Compound 92 also had charge interaction with Arg277D and hydrogen bonding with Arg277D and Val335D of 1QU4. Compound 93 was found to have Vdw interac-

tions with Leu166D, Gly199D, Ser200D, Gly201D, Arg277D, Asp332D amino acid residues and hydrophobic interactions with Leu166D, Gly199D, Ser200D, Gly201D, Ser202D, Thr203D amino acid residues of 1QU4. It was also found to have charge interactions with Arg277D and hydrogen bonding with Ser200D.

Docking studies of aporphine alkaloids with sterol 14-alpha demethylase (3TIK)

Compound 81 was found to have Vdw interactions with Tyr103A, Phe105A, Met106A, Phe110A, Ala115A, Tyr116A, Leu127A, Leu130A, Pro210A, Met284A, Val286A, Ala287A, Ala288A, Phe290A, Ala291A, Thr295A, Leu356A, Met460A, Val461A, Hem482A amino acid residues and hydrophobic interactions with Tyr103A, Met106A, Ala115A, Met123A, Leu127A, Leu130A, Pro210A, Met284A, Ala287A, Ala288A, Phe290A, Ala291A, Met890A, Met460A, Val461A, Pro224D, Hem482A amino acid residues of sterol 14-alpha demethylase of T. brucei. Compound 81 was also found to have aromatic interactions with Phe110A, Hem482A and charge interactions with Hem482A of 3TIK. Compound 82 was found to have Vdw interactions with Tyr103A, Phe105A, Met106A, Phe110A, Leu127A, Leu130A, Pro210A, Met284A, Ala287A, Ala288A, Phe290A, Ala291A, Thr295A, Leu356A, Met358A, Met890A, Thr459A, Met460A, Hem482A residues and hydrophobic interactions with Tyr103A, Ala115A, Leu127A, Leu130A, Pro210A, Met284A, Ala287A, Ala288A, Ala291A, Leu356A, Met358A, Leu359A, Met890A, Ile423A, Met460A, Val461A, Hem482A residues of 3TIK. In addition to these, Compound 82 had aromatic interactions with Phe110A, Hem482A and charge interactions with Hem482A of sterol 14-alpha demethylase. Compound 83 was found to have Vdw interactions with Tyr103A, Phe105A, Met106A, Phe110A, Val114A, Ala115A, Tyr116A, Leu127A, Leu130A, Pro210A, Gly283A, Met284A, Ala287A, Ala288A, Phe290A, Ala291A, Leu356A, Met358A, Met890A, Ile423A, Met460A, Hem482A residues and hydrophobic interactions with Tyr103A, Phe105A, Met106A, Phe110A, Val114A, Ala115A, Leu127A, Leu130A, Pro210A, Gly283A, Met284A, Ala287A, Ala288A, Ala291A, Leu356A, Met358A, Leu359A, met890A, Ile423A, Met460A, Hem482A residues of sterol 14-alpha demethylase. Compound 83 also had aromatic interactions with Phe110A, Hem482A, charge interactions with Hem482A residues of 3TIK. Compound 84 was found to have Vdw interactions with Tyr103A, Phe105A, Met106A, Phe110A, Leu130A, Pro210A, Ala287A, Ala288A, Phe290A, Ala291A, Gly292A, Thr295A, Leu356A, Met358A, Met890A, Met460A, Hem482A residues and hydrophobic interactions with Met106A, Ala115A, Leu130A, Pro210A, Ala287A, Ala288A, Ala291A, Leu356A, Met358A, Leu359A, Met890A, Ile423A, Met460A, Hem482A residues of 3TIK. It also had aromatic and charge interactions with Hem482A. Compound 85 was found to have Vdw interactions with Tyr103A, Phe105A, Met106A, Phe110A, Ala115A, Tyr116A, Leu127A, Leu130A, Pro210A, Met284A, Val286A, Ala287A, Ala288A, Phe290A, Ala291A, Leu356A, Met460A, Val461A, Hem482A residues and hydrophobic interactions with Tyr103A, Met106A, Ala115A, Leu127A, Leu130A, Pro210A, Met284A,

Ala287A, Ala288A, Phe290A, Ala291A, Met460A, Hem482A residues of 3TIK. In addition to these, Compound 85 also had aromatic interactions with Phe110A and Hem482A and charge interactions with Hem482A of sterol 14-alpha demethylase of T. brucei. Compound 86 was found to have Vdw interactions with Tyr103A, Met106A, Phe110A, Ala115A, Tyr116A, Leu127A, Leu208A, Met284A, Ala287A, Phe290A, Ala291A, Leu356A, Leu359A, Met460A, Hem482A residues and hydrophobic interactions with Val114A, Ala115A, Leu127A, Met284A, Ala287A, Ala288A, Ala291A, Leu356A, Leu359A, Met460A, Val461A, Hem482A residues of sterol 14-alpha demethylase. It also had charge interactions with Hem482A and hydrogen bonding with Tyr103A residues of 3TIK. Compound 87 was found to have Vdw interactions with Tyr103A, Met106A, Phe110A, Leu127A, Leu130A, Pro210A, Met284A, Ala287A, Ala288A, Phe290A, Ala291A, Thr295A, Leu356A, Met358A, Met460A, Val461A, Hem482A residues and hydrophobic interactions with Met106A, Leu127A, Leu130A, Pro210A, Met284A, Ala287A, Ala288A, Met289A, Ala291A, Leu356A, Leu359A, Ile423A, Met460A, Hem482A residues of 3TIK. Compound 87 also had aromatic and charge interactions with Hem482A of sterol 14-alpha demethylase. Compound 88 was found to have Vdw interactions with Tyr103A, Met106A, Phe110A, Ala115A, Tyr116A, Leu127A, Pro210A, Met284A, Ala287A, Ala288A, Met289A, Phe290A, Ala291A, Thr295A, Leu356A, Leu359A, Met460A, Val461A, Hem482A residues and hydrophobic interactions with Tyr103A, Met106A, Ala115A, Leu127A, Leu130A, Pro210A, Met284A, Ala287A, Ala288A, Met289A, Phe290A, Ala291A, Leu356A, Leu359A, Met460A and Hem482A residues of sterol 14-alpha demethylase. It also had aromatic interactions with Phe110A, Hem482A and charge interactions with Hem482A residues of 3TIK. Compound 89 was found to have Vdw interactions with Tyr103A, Phe105A, Met106A, Phe110A, Ala115A, Leu127A, Leu130A, Pro210A, Met284A, Ala287A, Ala288A, Met289A, Phe290A, Ala291A, Thr295A, Leu356A, Leu357A, Met358A, Leu359A, Ile423A, Met460A, Hem482A residues and hydrophobic interactions with Tyr103A, Met106A, Phe110A, Val114A, Ala115A, Leu127A, Leu130A, Pro210A, Met284A, Ala287A, Ala288A, Met289A, Ala291A, Leu356A, Leu357A, Leu359A, Met890A, Ile423A, Met460A, Val462A, Hem482A residues of 3TIK. It also had aromatic interactions with Phe110A, Hem482A, charge interactions with Hem482A and hydrogen bonding with Tyr103A residues of sterol 14-alpha demethylase. Compound 90 was found to have Vdw interactions with Tyr103A, Met106A, Phe110A, Ala287A, Phe290A, Ala291A, Leu356A, Met460A, Val461A, Hem482A residues and hydrophobic interactions with Leu356A, Leu359A, Met460A, Val461A, Hem482A , charge interaction with Hem482A residue of sterol 14-alpha demethylase. Compound 91 was found to have Vdw interactions with Tyr103A, Met106A, Phe110A, Leu208A, Ala287A, Phe290A, Ala291A, Leu356A, Met460A, Hem482A residues and hydrophobic interactions with Ala287A, Ala291A, Leu356A, Leu359A, Hem482A residues of 3TIK. It also had also charge interactions with Hem482A and hydrogen bonding with Tyr103A residues of sterol 14-alpha demethylase. Compound 92 was found to have Vdw interactions with Val102A, Tyr103A, Phe105A, Pro210A,

Phe290A, Ala291A, Leu356A, Met358A, Leu359A, Met460A residues while and hydrophobic interactions with Val102A, Tyr103A, Met106A, Leu208A, Pro210A, Val213A, Phe290A, Leu356A, Leu359A, Met890A, Met460A, Val461A amino acid residues of sterol 14-alpha demethylase. In addition, Compound 92 also has charge interactions with Hem482A and hydrogen bonding with Tyr103A residues of 3TIK. Compound 93 was found to have Vdw interactions with Tyr103A, Met106A, Phe110A, Glu205A, Ala287A, Phe290A, Ala291A, His294A, Leu356A, Met460A, Val461A, Hem482A residues and hydrophobic interactions with Met106A, Ala287A, Phe290A, Ala291A, Leu356A, Met460A residues of sterol 14-alpha demethylase. It also had charge interactions with Hem482A of 3TIK. Compound 94 was found to have Vdw interactions with Tyr103A, Tyr116A, Glu205A, Phe290A, Ala291A, His294A, Leu356A, Met460A, Val461A, Hem482A residues and hydrophobic interactions with Met106A, Ala287A, Phe290A, Ala291A, Thr295A, Leu356A, Hem482A residues of 3TIK. Along with these, Compound 94 also had charge interactions with Hem482A residue of sterol 14-alpha demethylase. Compound 95 was found to have Vdw interactions with Tyr103A, Met106A, Phe110A, Ala287A, Phe290A, Ala291A, Leu356A, Met460A, Hem482A residues and hydrophobic interactions with Met106A, Ala287A, Phe290A, Ala291A, Leu356A, Leu359A, Hem482A residues of sterol 14-alpha demethylase. In addition, Compound 95 also had charge interactions with Hem482A and hydrogen bonding with Tyr103A residues of 3TIK.

Reference ligand(The tipifarnib derivative 6-((4-chlorophenyl)(methoxy)(1-methyl-1H-imidazol-5-yl)methyl)-4-(2,6-difluorophenyl)-1-methylquinolin-2(1H)-one) was found to have Vdw interactions with Tyr103A, Phe105A, Met106A, Phe110A, Ala115A, Tyr116A, Leu127A, Glu205A, Leu208A, Ala287A, Phe290A, Ala291A, Thr295A, Leu356A, Met358A, Cys422A, Met460A, Val461A, Hem482A residues and hydrophobic interactions with Met106A, Leu208A, Ala287A, Phe290A, Ala291A, Thr295A, Leu356A, Leu359A, Met460A, Val461A, Hem482A residues of sterol 14-alpha demethylase. It aslo had hydrogen bonding with Hem482A residues of sterol 14-alpha demethylase.

Docking studies of aporphine alkaloids with Glutathione peroxidase type tryparedoxin peroxidase, oxidized form(2RM5)

Compound 81 was found to have Vdw interactions with Lys46A, Cys47A, Gly48A, Tyr49A, Thr50A, Lys51A, Gly52A, Tyr54A, Glu55A amino acid residues and hydrophobic interactions with Lys46A, Cys47A, Gly48A, Tyr49A, Thr50A, Lys51A, Gly52A, Glu55A amino acid residues of tryparedoxin peroxidase, oxidized form. Compound 82 was found to have Vdw interactions with Lys46A, Cys47A, Gly48A, Tyr49A, Thr50A, Lys51A, Gly52A, Gly53A, Tyr54A, Glu55A, Thr56A, Ser159A amino acid residues and hydrophobic interactions with Lys46A, Cys47A, Gly48A, Thr50A, Lys51A, Gly52A, Gly53A, Glu55A, Thr56A and Ser159A of 2RM5. Compound 83 was found to have Vdw interactions with Lys46A, Cys47A, Gly48A, Tyr49A, Thr50A, Lys51A, Gly52A, Tyr54A, Glu55A, Thr56A amino acid residues and hydrophobic interactions with Lys46A, Cys47A, Gly48A, Tyr49A,

Lys51A, Gly52A, Gly53A, Glu55A, Thr56A amino acid residues of glutathione peroxidase type tryparedoxin peroxidase, oxidized form. Compound 84 was found to have Vdw interactions with Lys46A, Cys47A, Gly48A, Tyr49A, Thr50A, Lys51A, Gly52A, Gly53A, Tyr54A, Glu55A, Thr56A amino acid residues and hydrophobic interactions with Cys47A, Gly48A, Thr50A, Lys51A, Gly52A, Glu55A, Thr56A and Val160A amino acid residues of tryparedoxin peroxidase, oxidized form. Compound 85 was found to have Vdw interactions with Lys46A, Cys47A, Gly48A, Tyr49A, Thr50A, Gly52A, Gly53A, Tyr54A, Glu55A,Thr56A, Phe93A amino acid residues and hydrophobic interactions with Lys46A, Cys47A, Gly48A, Thr50A, Lys51A, Gly52A, Gly53A, Glu55A, Thr56A amino acid residues of tryparedoxin peroxidase, oxidized form. It also had aromatic interactions with Tyr49A of 2RM5. Compound 86 was found to have Vdw interactions with Lys46A, Gly48A, Tyr49A, Thr50A, Tyr54A, Glu55A amino acid residues and hydrophobic interactions with Lys46A, Cys47A, Gly48A, Tyr49A, Gly52A, Glu55A amino acid residues of 2RM5. It also had charge interactions with Lys46A amino acid residue of glutathione peroxidase type tryparedoxin peroxidase, oxidized form. Compound 87 was found to have Vdw interactions with Lys46A, Cys47A, Gly48A, Tyr49A, Thr50A, Gly52A, Tyr54A, Glu55A, Phe93A amino acid residues and hydrophobic interactions with Lys46A, Cys47A, Gly48A, Tyr49A, Thr50A, Gly52A, Tyr54A, Glu55A amino acid residues of tryparedoxin peroxidase, oxidized form. It also had charge interaction with Lys46A of 2RM5. Compound 88 was found to have Vdw interactions with Lys46A, Cys47A, Tyr49A, Thr50A, Lys51A, Gly52A, Tyr54A, Glu55A, Thr56A amino acid residues and hydrophobic interactions with Lys46A, Gly52A, Tyr54A, Glu55A, Thr56A amino acid residues of 2RM5. Compound 88 also had aromatic interaction with Tyr49A of tryparedoxin peroxidase, oxidized form. Compound 89 was found to have Vdw interactions with Lys46A, Gly48A, Tyr49A, Thr50A, Lys51A, Gly52A, Gly53A, Tyr54A, Glu55A, Thr56A amino acid residues and hydrophobic interactions with Lys46A, Cys47A, Gly48A, Tyr49A, Thr50A, Lys51A, Gly52A, Gly53A, Tyr54A, Glu55A, Thr56A amino acid residues of tryparedoxin peroxidase, oxidized form. It also had charge interaction with Lys46A of 2RM5. Compound 90 was found to have Vdw interactions with Lys46A, Cys47A, Gly48A, Tyr49A, Thr50A amino acid residues and hydrophobic interactions with Lys46A, Cys47A, Gly48A, Tyr49A, Thr50A amino acid residues of glutathione peroxidase type tryparedoxin peroxidase, oxidized form. In addition, Compound 90 also had aromatic interaction with Tyr49A of 2RM5. Compound 84was found to have Vdw interactions with Lys46A, Tyr49A, Thr50A, Tyr54A, Glu55A amino acid residues and hydrophobic interactions with Lys46A, Tyr49A, Thr50A and Tyr54A amino acid residues of tryparedoxin peroxidase, oxidized form. Compound 91 was found to have Vdw interactions with Lys46A, Tyr49A, Thr50A, Tyr54A, Phe98A amino acid residues and hydrophobic interactions with Lys46A, Thr50A amino acid residues of 2RM5. Along with these, Compound 91 also have charge interactions with Lys46A of tryparedoxin peroxidase, oxidized form(2RM5). Compound 92 was found to have Vdw interactions with Lys46A, Cys47A, Gly48A, Tyr49A, Thr50A, Gly52A, Gly53A, Tyr54A, Glu55A amino acid residues and hydrophobic interac-

tions with Thr50A, Gly52A, Gly53A, Tyr54A, Glu55A amino acid residues of tryparedoxin peroxidase, oxidized form. Compound 93 was found to have Vdw interactions with Lys46A, Cys47A, Gly48A, Tyr49A, Thr50A, Gly52A, Gly53A, Tyr54A, Glu55A amino acid residues and hydrophobic interactions with Thr50A, Gly52A, Gly53A, Tyr54A, Glu55A amino acid residues of 2RM5. In addition, Compound 93 also have aromatic interaction with Tyr49A of tryparedoxin peroxidase, oxidized form. Compound 94 was found to have Vdw interactions with Lys46A, Gly48A, Tyr49A, Thr50A, Tyr54A, Glu55A amino acid residues and hydrophobic interactions with Lys46A, Thr50A and Tyr54A amino acid residues of glutathione peroxidase type tryparedoxin peroxidase, oxidized form.

Docking studies of aporphine alkaloids with Glutathione peroxidase type tryparedoxin peroxidase, reduced form(2RM6)

Compound 81 was found to have Vdw interactions with Lys126A, Gly128A, Ile129A, Leu130A, Ala131A, Arg153A, Phe154A, Gly157A, Ala158A, Asp162A amino acid residues and hydrophobic interactions with Lys126A, Ile129A, Ala131A, Arg153A, Phe154A, Gly157A, Ala158A, Asp162A amino acid residues of glutathione peroxidase type tryparedoxin peroxidase, reduced form. In addition, Compound 81 also had charge interactions with Lys126A and Arg153A of 2RM6. Compound 82 was found to have Vdw interactions with Lys126A, Gly128A, Ile129A, Leu130A, Ala131A, Arg153A, Phe154A, Gly157A, Ala158A, Asp162A amino acid residues and hydrophobic interactions with Lys126A, Pro127A, Gly128A, Ile129A, Ala131A, Gly157A, Ala158A amino acid residues of tryparedoxin peroxidase, reduced form. Compound 82 also had charge interactions with Lys126A and Arg153A of 2RM6. Compound 83 was found to have Vdw interactions with Lys126A, Pro127A, Gly128A, Ile129A, Arg131A, Arg153A, Phe154A, Gly157A, Ala158A, Asp162A amino acid residues and hydrophobic interactions with Lys126A, Pro127A, Gly128A, Ile129A, Ala131A, Thr132A, Glu152A, Arg153A, Phe154A, Gly157A amino acid residues of 2RM6. In addition, Compound 83 also have charge interactions and hydrogen bonding with Lys126A, Arg153A amino acid residues of tryparedoxin peroxidase, reduced form. Compound 84 was found to have Vdw interactions with Lys126A, Pro127A, Gly128A, Ile129A, Arg153A, Phe154A, Gly157A, Ala158A, Asp162A amino acid residues and hydrophobic interactions with Lys126A, Pro127A, Gly128A, Ile129A, Phe154A, Ser155A, Gly157A, Ala158A amino acid residues of glutathione peroxidase type tryparedoxin peroxidase, reduced form. In addition, Compound 83 was also found to have charge interactions with Lys126A of 2RM6. Compound 84 had Vdw interactions with Lys126A, Gly128A, Ile129A, Arg153A, Phe154A, Gly157A, Ala158A, Asp162A amino acid residues and hydrophobic interactions with Lys126A, Ile129A, Leu130A, Ala131A, Ser155A, Gly157A, Ala158A amino acid residues of 2RM6. Compound 84 also had charge interactions with Lys126A and Arg153A as well as hydrogen bonding with Lys126A amino acid residues of tryparedoxin peroxidase, reduced form. Compound 85 was found to have Vdw interactions with Lys126A, Gly128A, Ile

Compound **86**
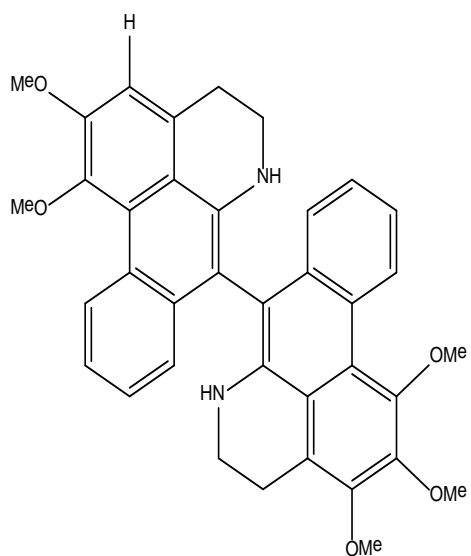
1,1′,2,2′,3′-pentamethoxy-5,5′,6,6′-tetrahydro-4H,4′H-7,7′-bidibenzo[*de,g*]quinoline
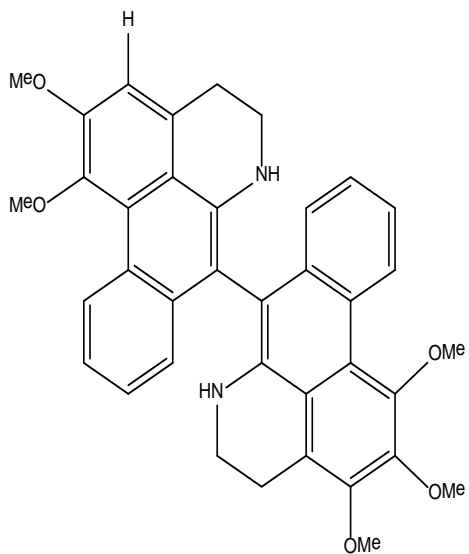
1'1''2'2''3'-pentamethoxy-5'5''6'6''-tetrahydro-4H'4''H'-7'7''-bidibenzo[de'g]quinoline
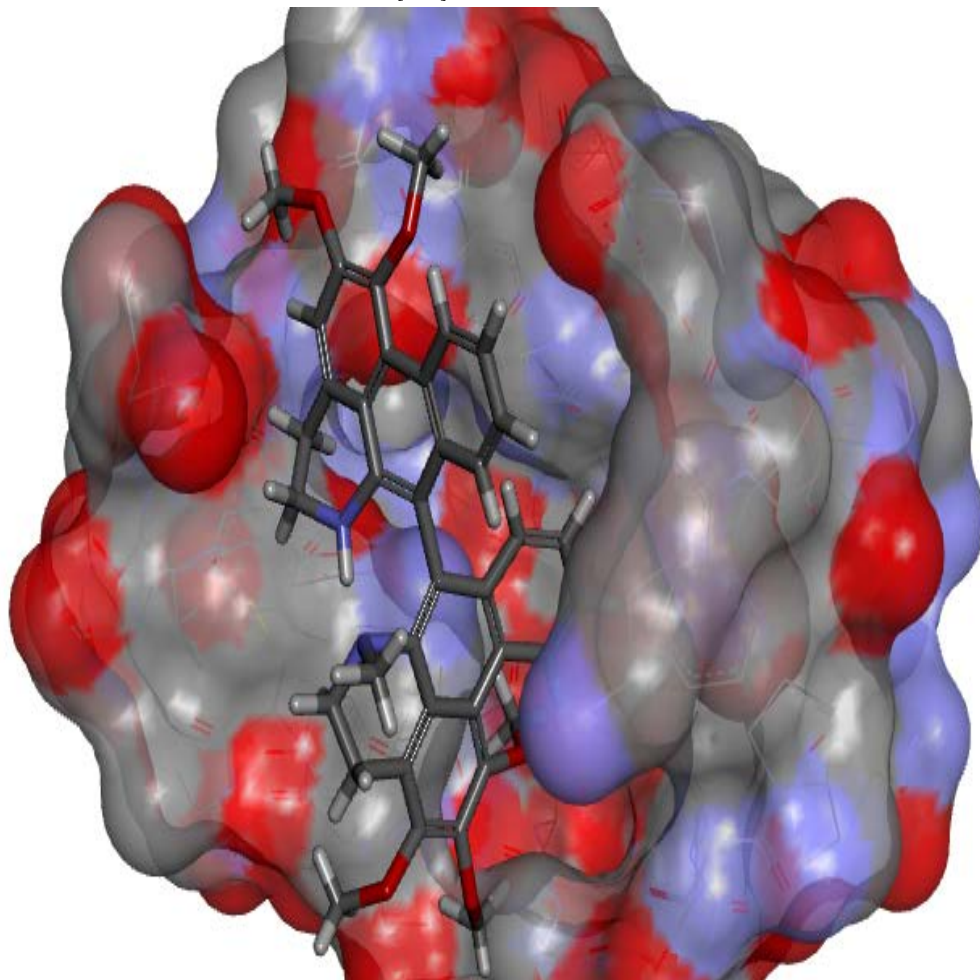
2. Compound **93**

1,2,3-trimethoxy-6-methyl-5,6-dihydro-4H-dibenzo[de,g]quinoline
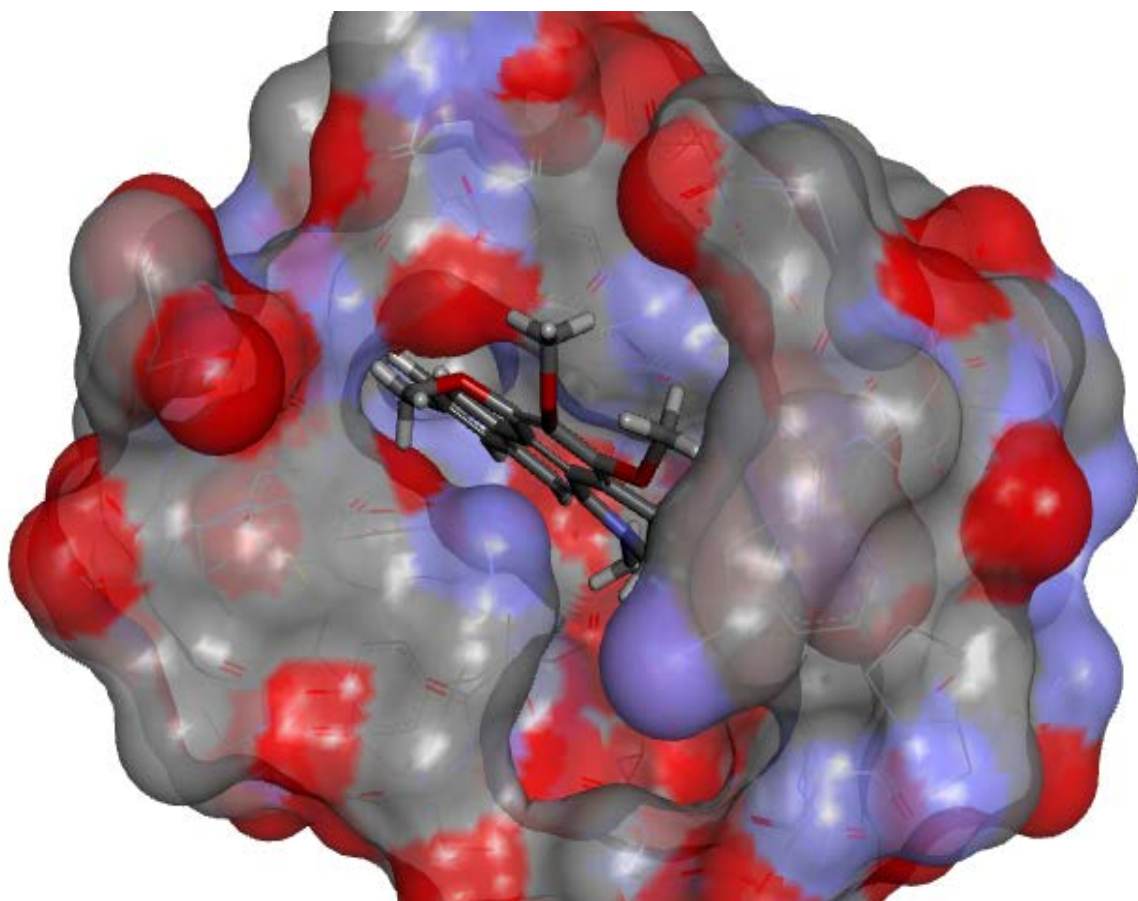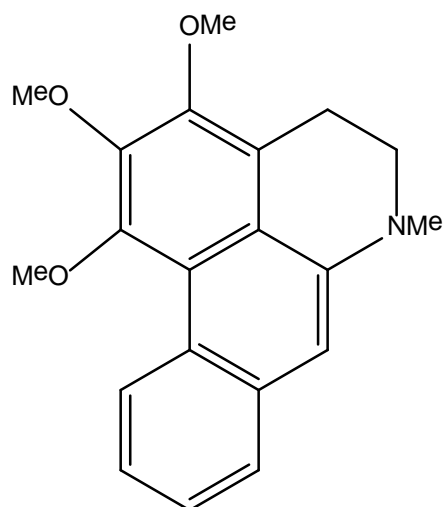
3. Compound **95**
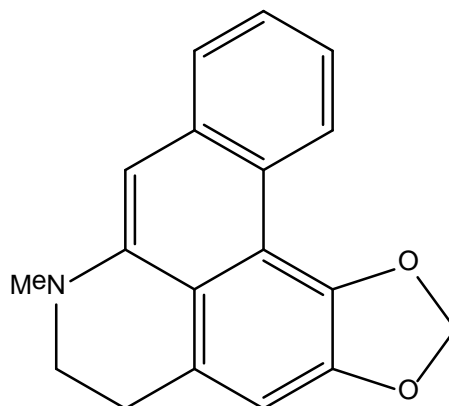
7-methyl-6,7-dihydro-5H-[1,3]dioxolo[4',5':4,5]benzo[1,2,3-*de*]benzo[*g*]quinoline
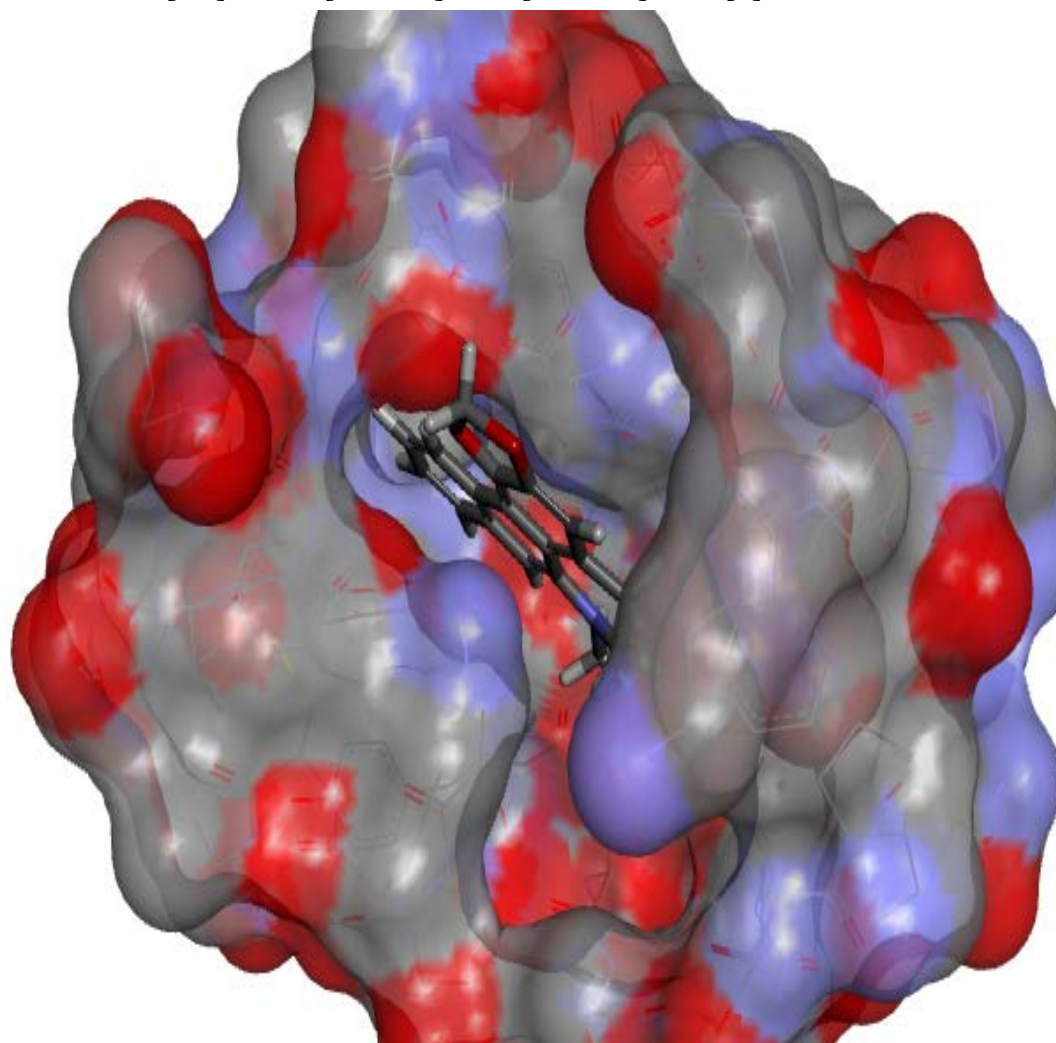
4. Compound **91**

1,2,3-trimethoxy-5,6-dihydro-4H-dibenzo[*de*,*g*]quinoline
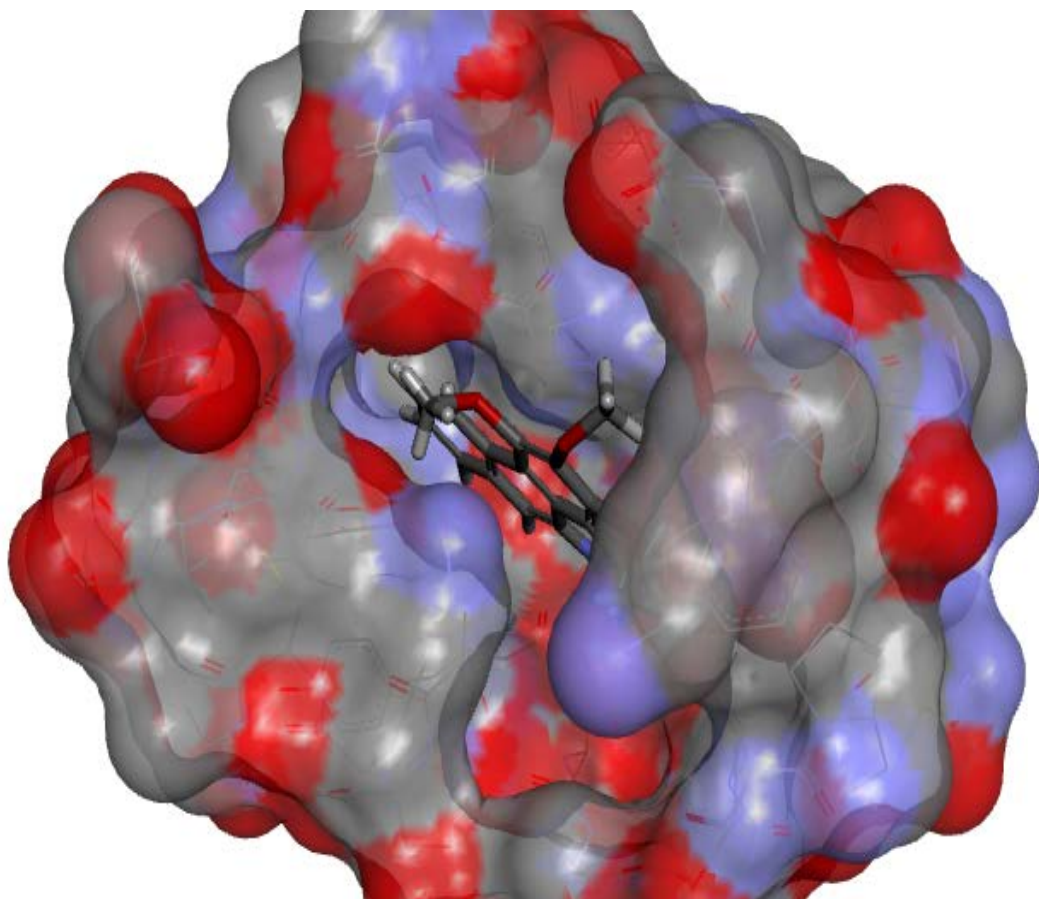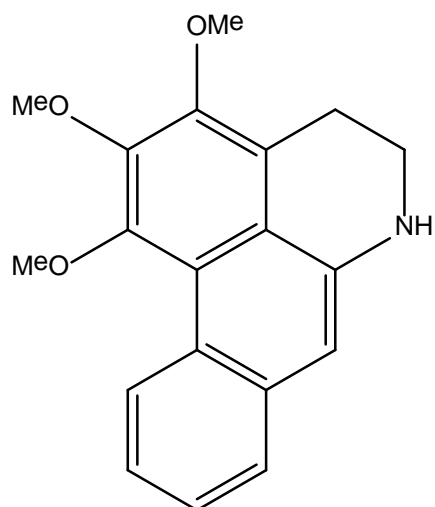
5. Compound **92**

6,7⁻dihydᵣₒ⁻5H⁻[1,3]dioxolo[4',5':4,5]benzo[1,2,3⁻de]benzo[g]quinoline

[182]
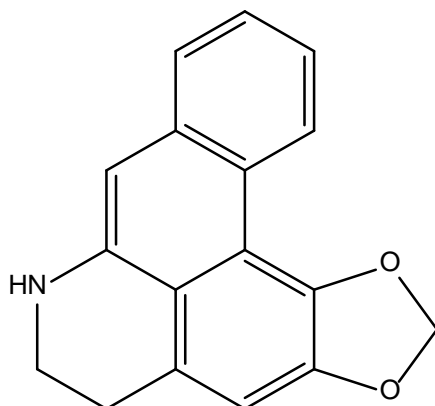
6. Compound **85**

1,2,3-trimethoxy-7H-dibenzo[*de,g*]quinolin-7-one
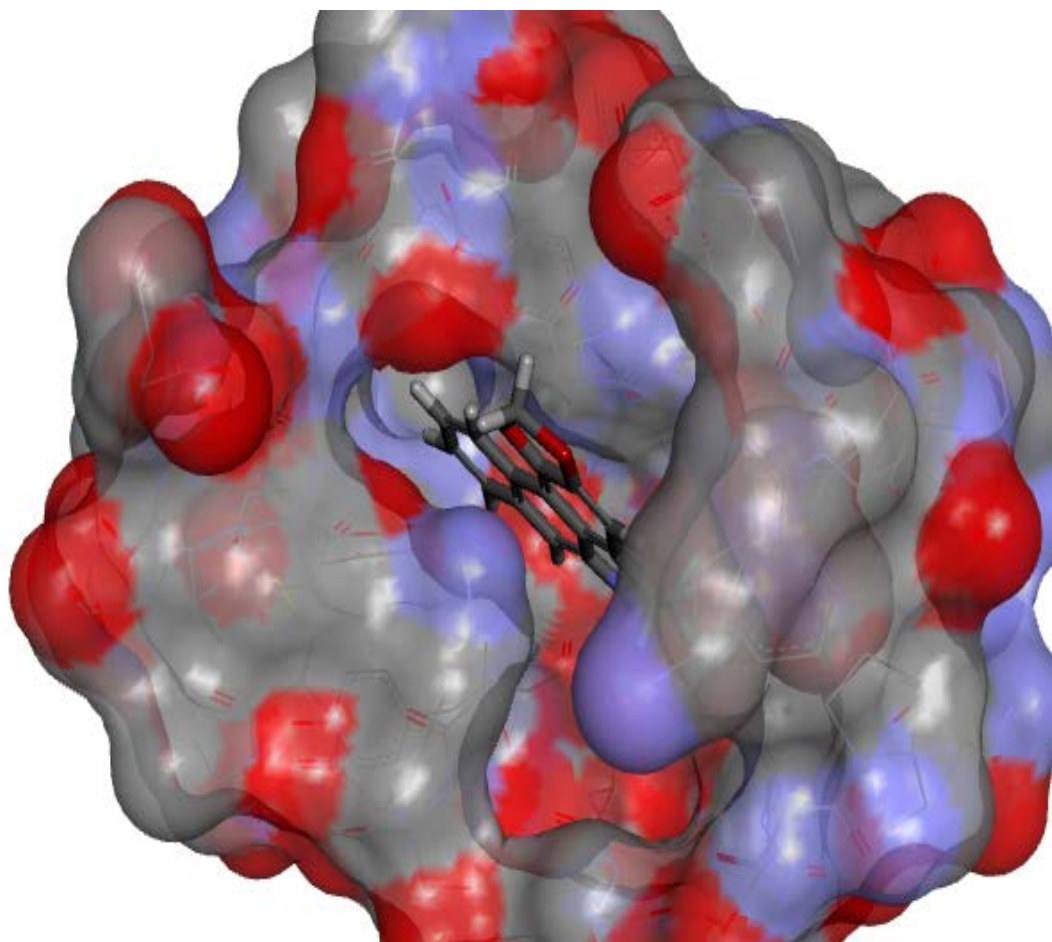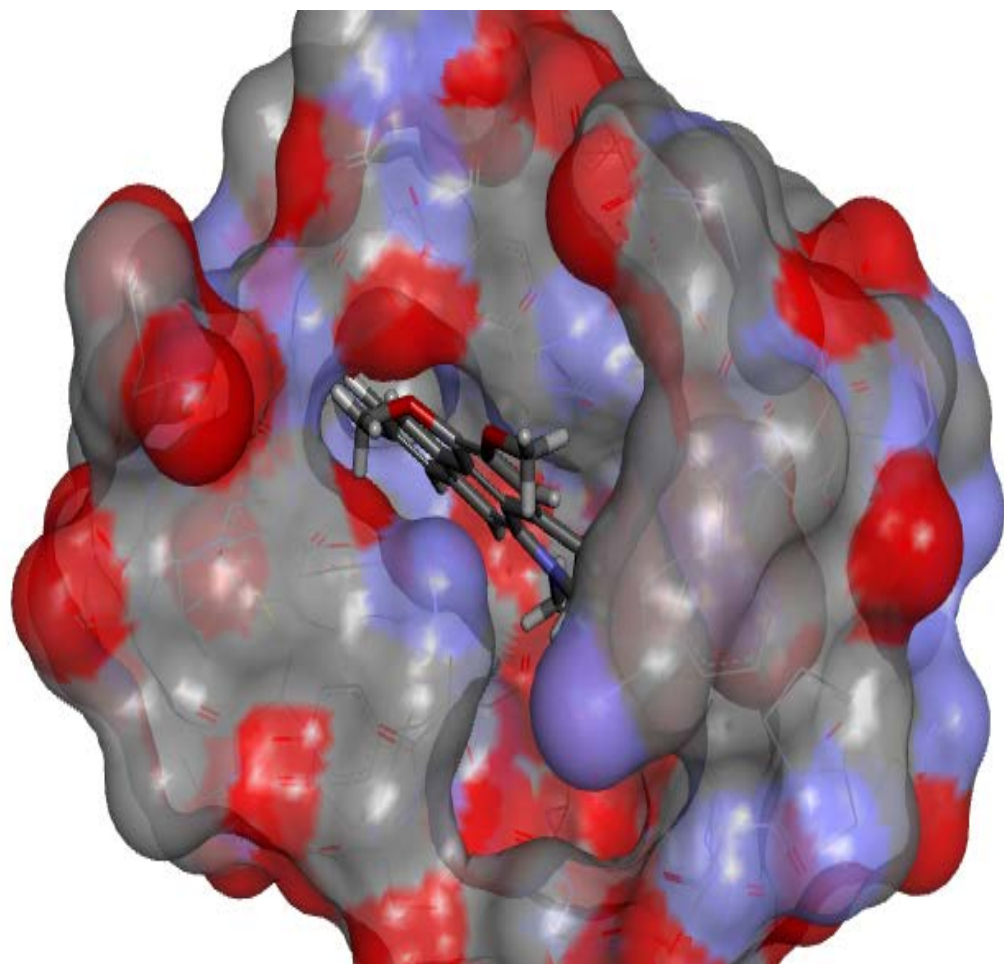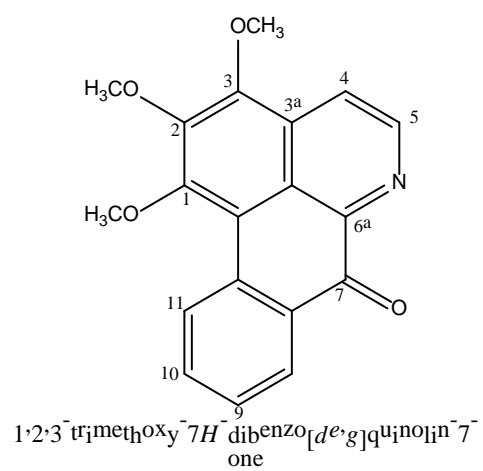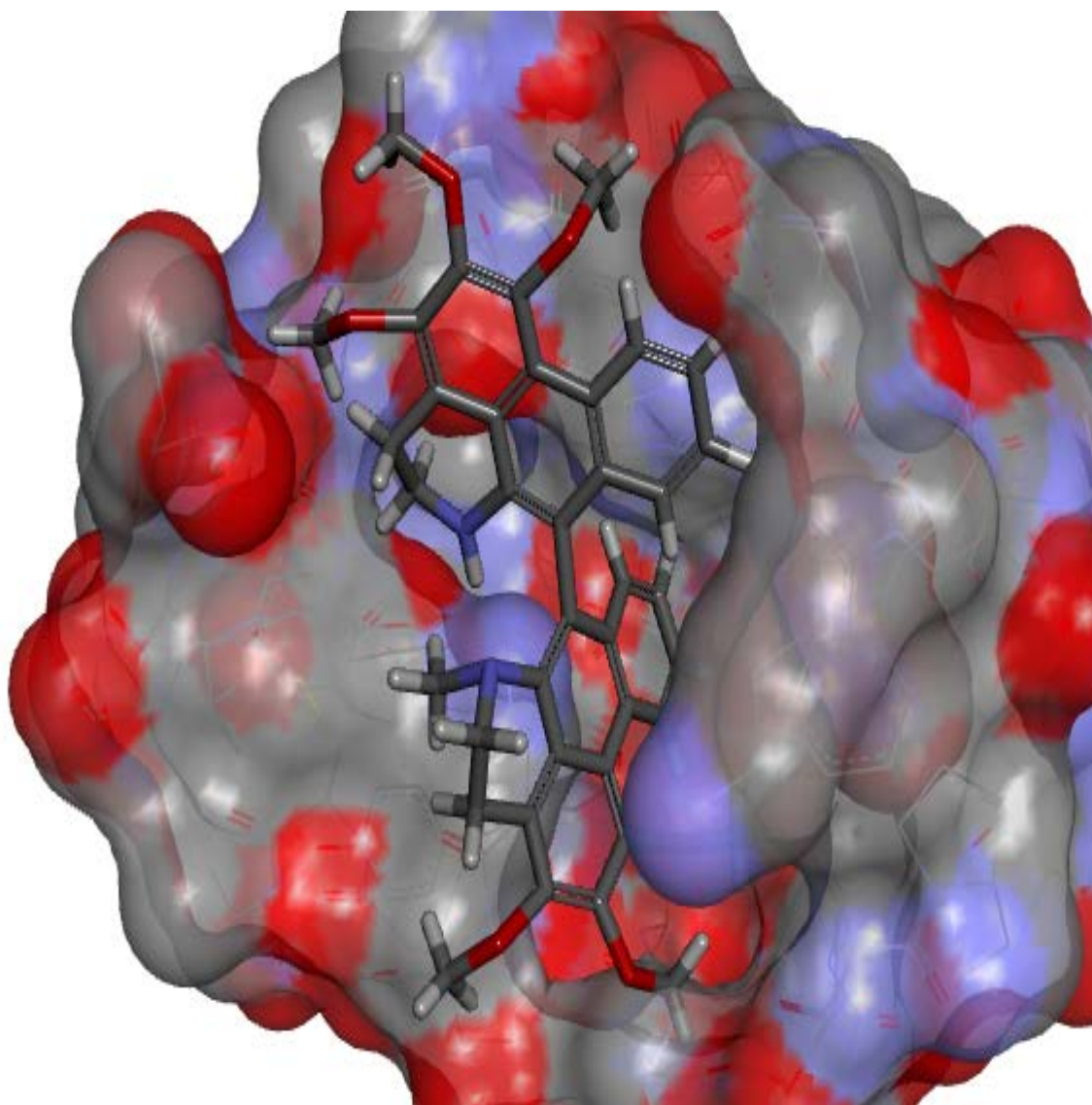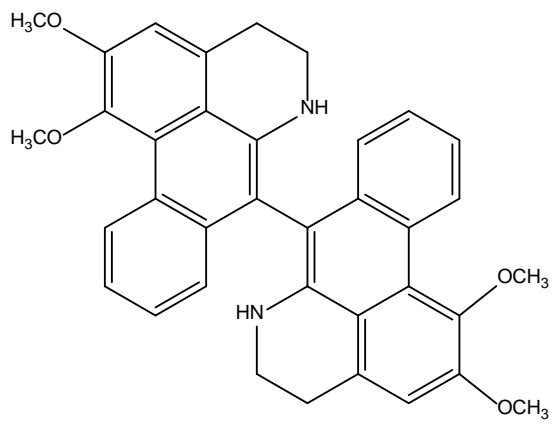
7. Compound 87

8. Compound 84
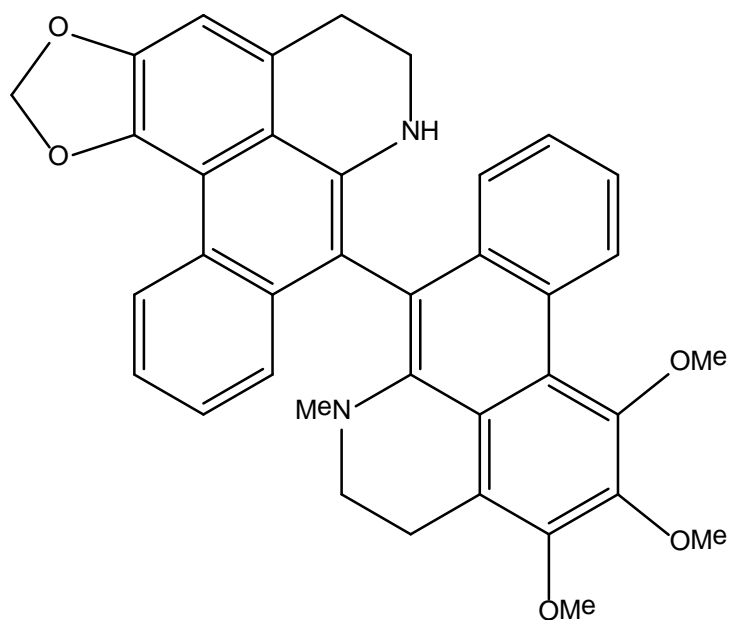
8-(1′,2′,3′-trimethoxy-6′-methyl-5′,6′-dihydro-4H-dibenzo[de′,g]quinolin-7′-yl)-6′,7′-dihydro-5H-[1′3]dioxolo[4′,5′:4,5]benzo[1,2,3-de]benzo[g]quinoline

[185]
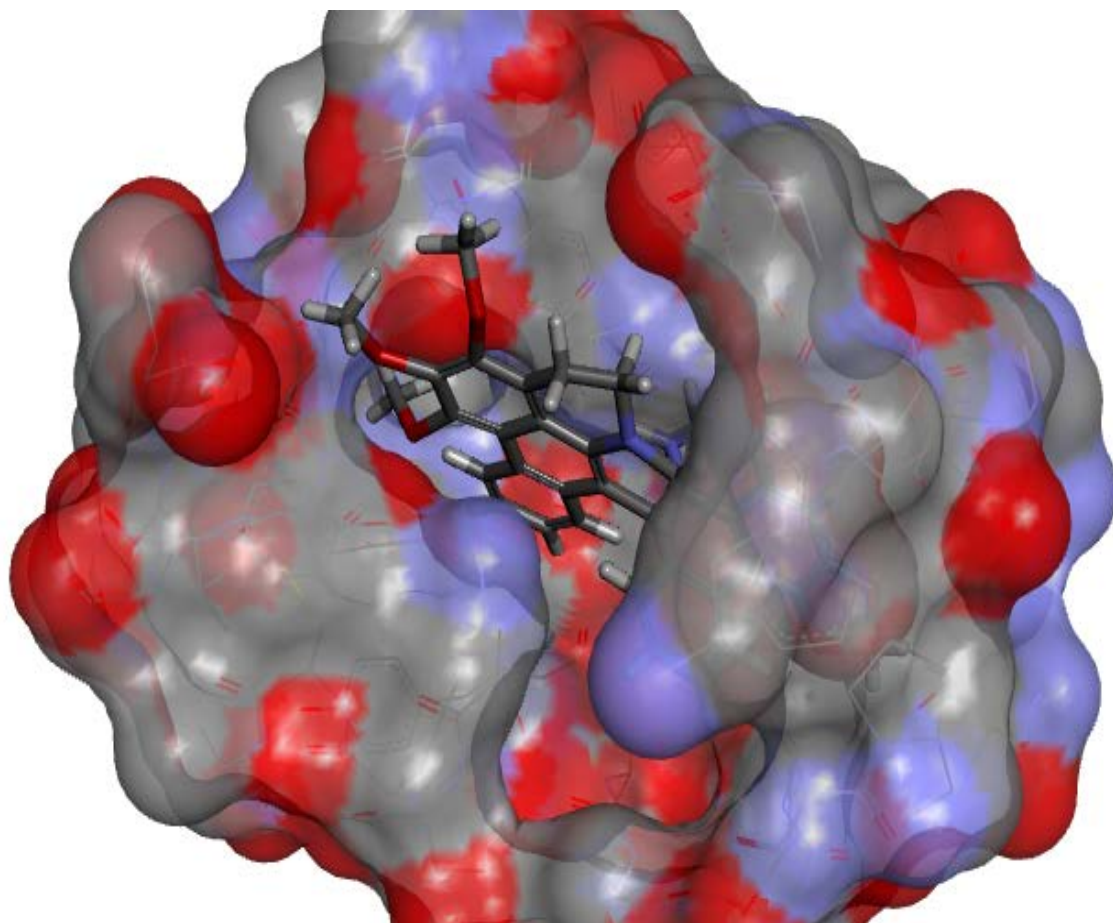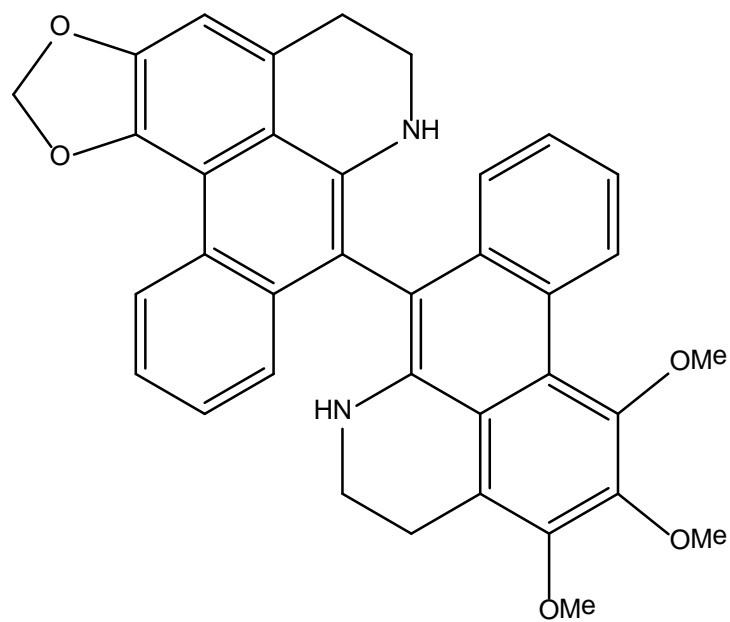
9. Compound **83**

8-(1,2,3-trimethoxy-5,6-dihydro-4H-dibenzo[de,g]quinolin-7-yl)-6,7-dihydro-5H-[1,3]dioxolo[4',5':4,5]benzo[1,2,3-de]benzo[g]quinoline
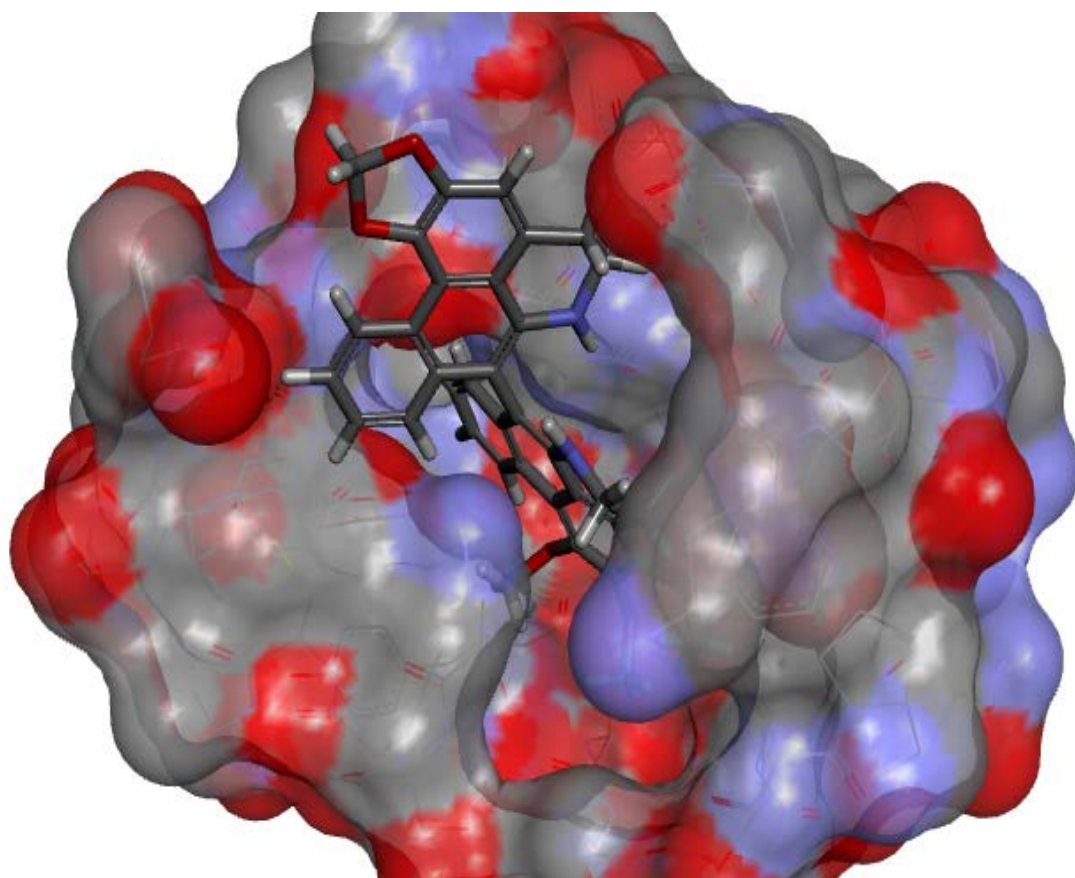
10. Compound **88**
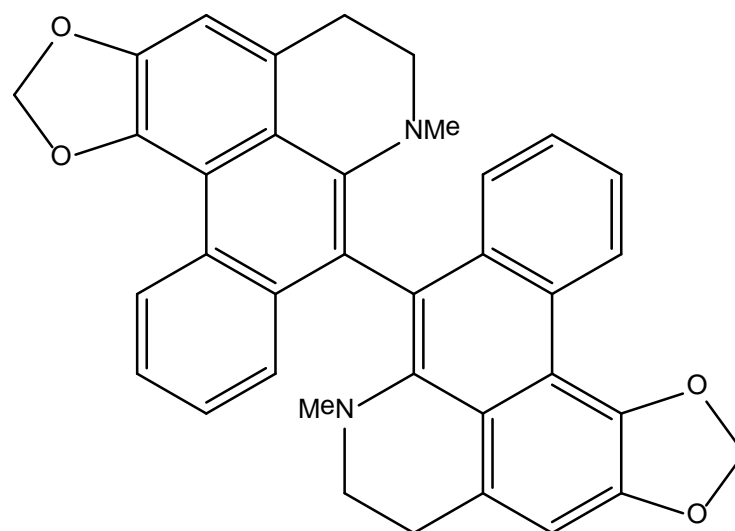
7,7'-dimethyl-6,6',7,7'-tetrahydro-5H,5'H-8,8'-bi[1,3]dioxolo[4',5':4,5]benzo[1,2,3-*de*]benzo[*g*]quinoline

11. Compound 89
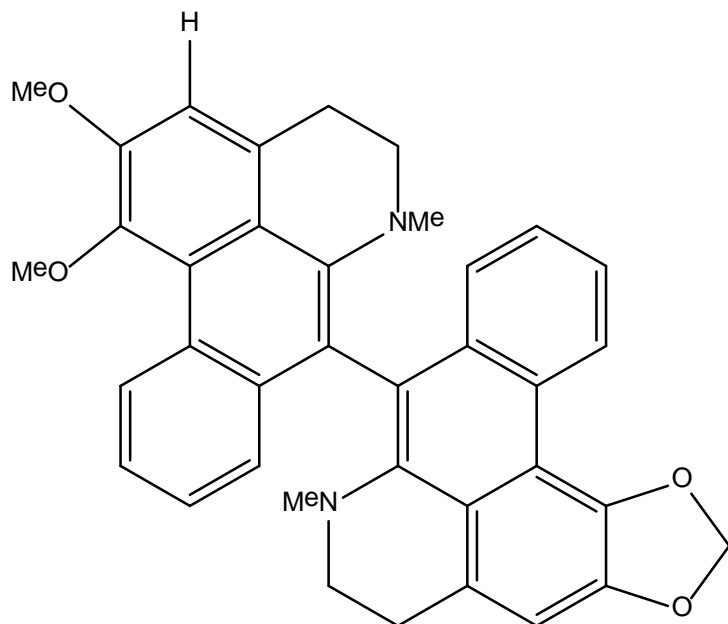
8-(1,2-dimethoxy-6-methyl-5,6-dihydro-4H-dibenzo[de,g]quinolin-7-yl)-7-methyl-6,7-dihydro-5H-[1,3]dioxolo[4',5':4,5]benzo[1,2,3-de]benzo[g]quinoline

12. Compound **90**

7-methyl-8-(1,2,3-trimethoxy-6-methyl-5,6-dihydro-4H-dibenzo[de,g]quinolin-7-yl)-6,7-dihydro-5H-[1,3]dioxolo[4,5:4,5]benzo[1,2,3-de]benzo[g]quinoline

13. Compound **81**

[189]
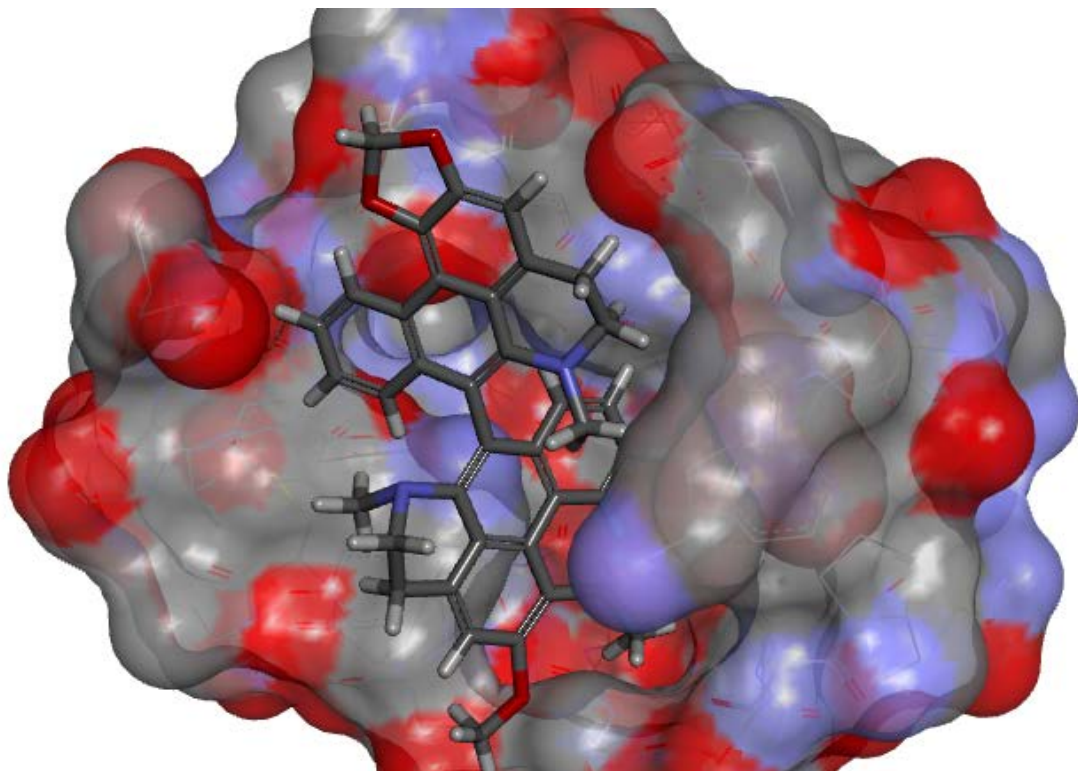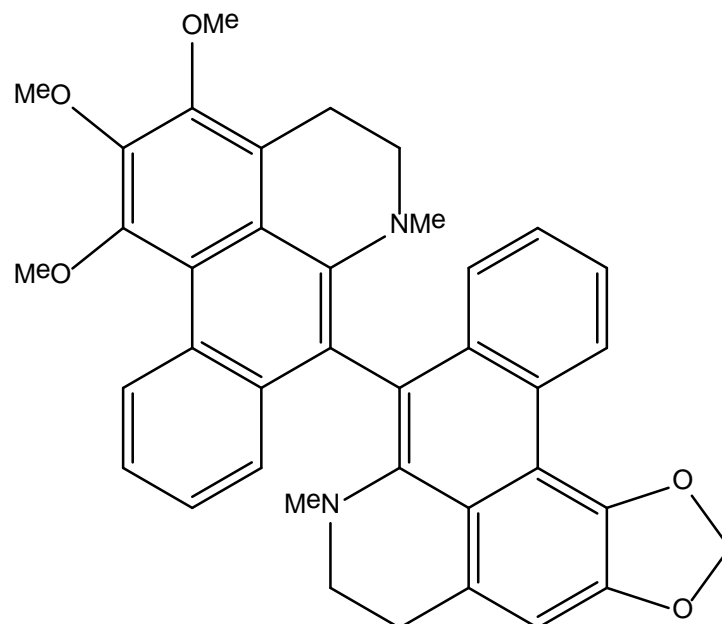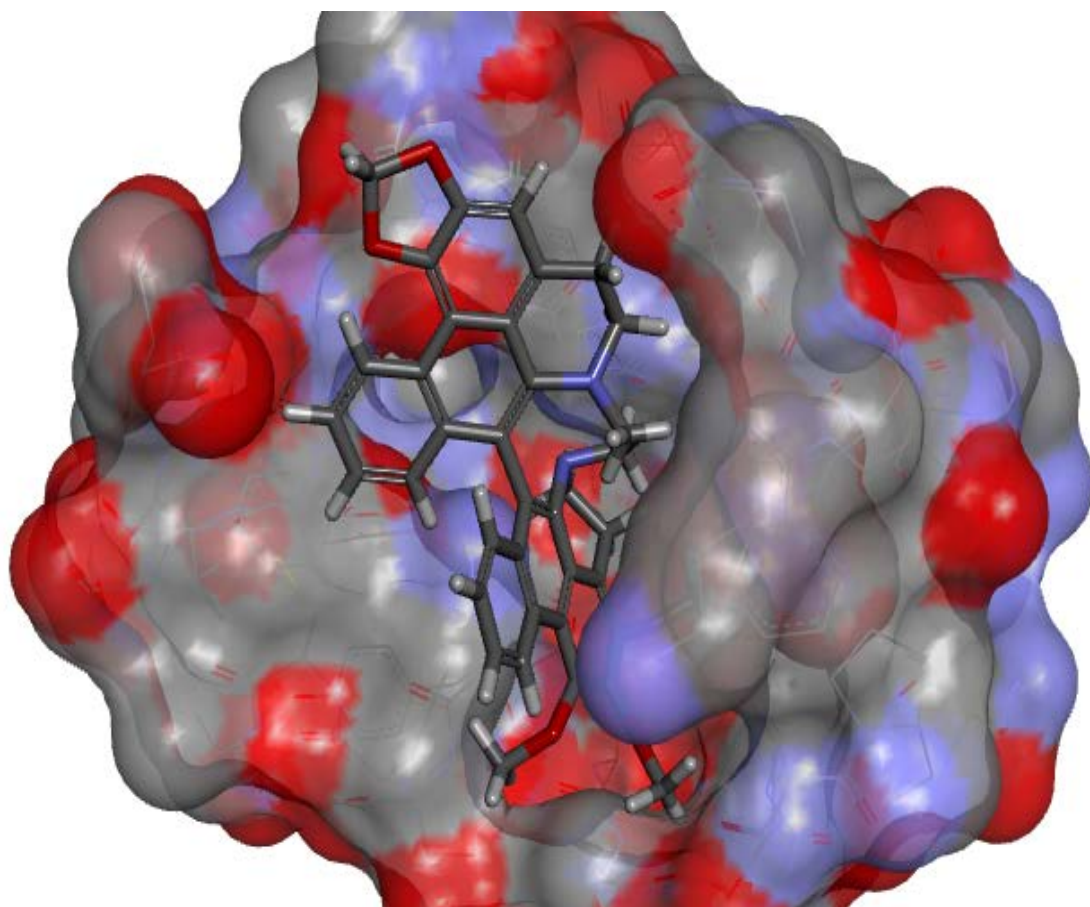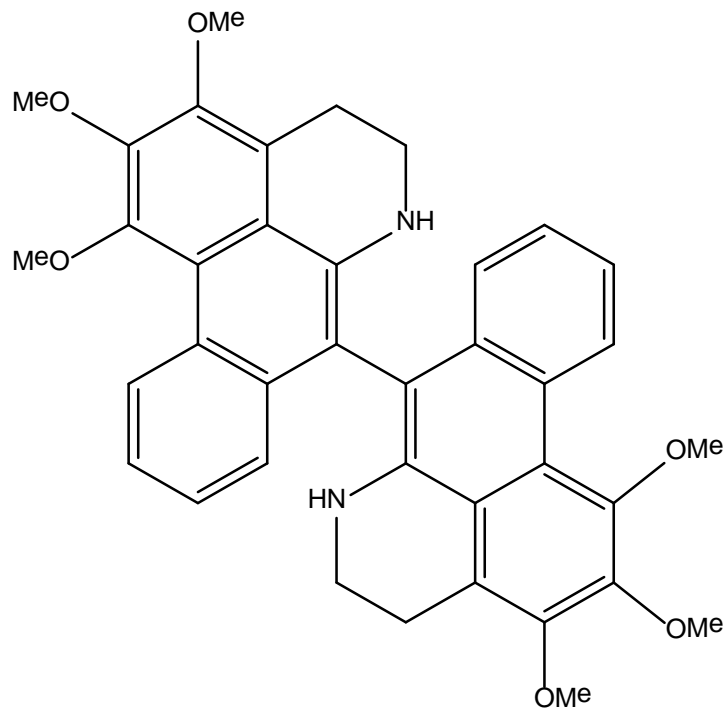
1,1',2,2',3,3'-hexamethoxy-5,5',6,6'-tetrahydro-4H,4'H-7,7'-bidibenzo[de,g]quinoline
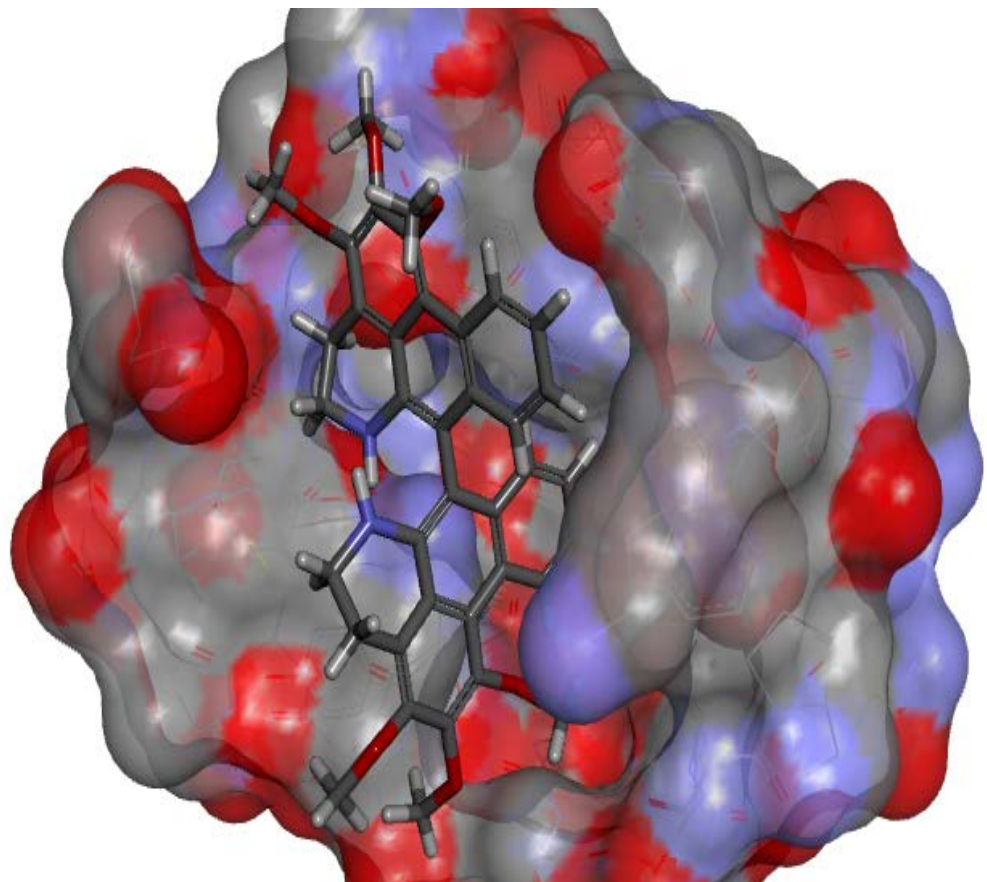
14. Compound **96**

1'2‾dimethoxy‾5'6‾dihydro‾4H‾dibenzo[de'g]quinoline
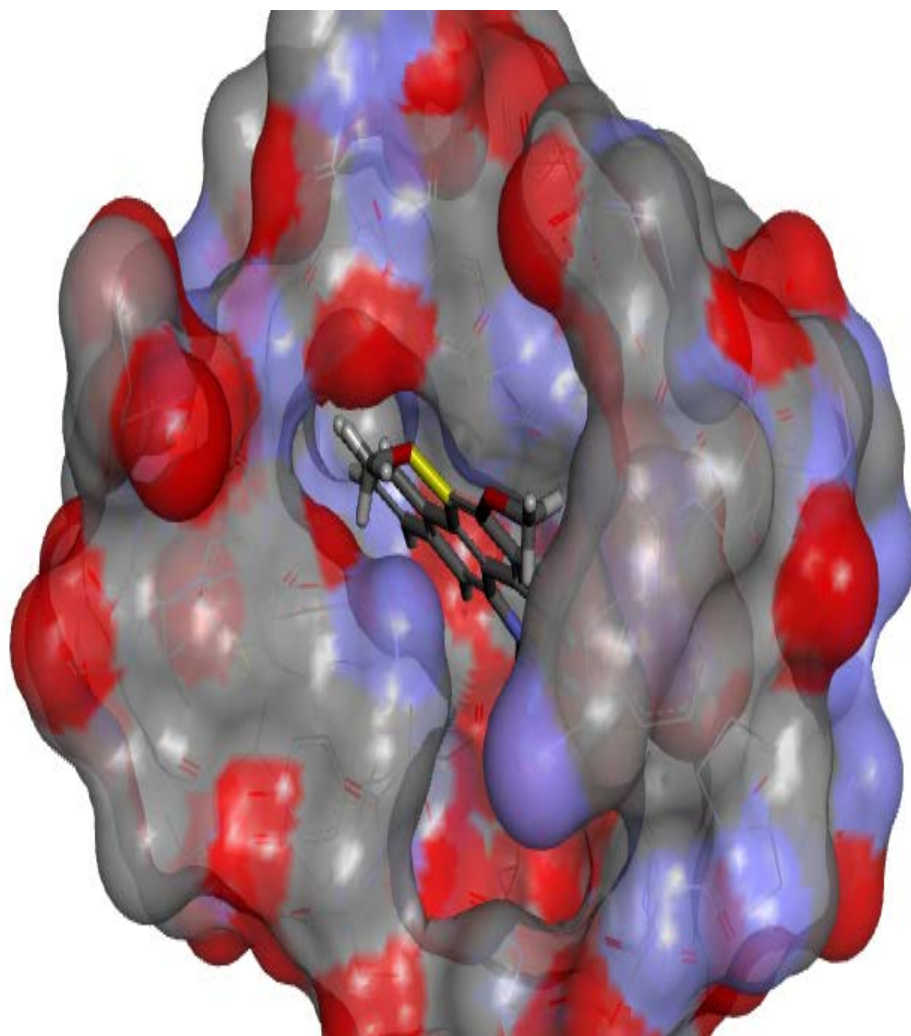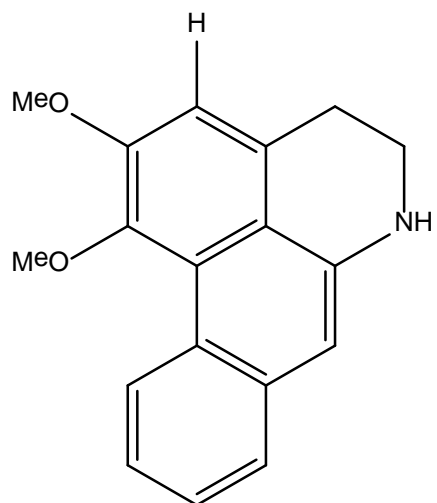
Table 3.17: Log P and MICs values of the above described aporphine and protoberberine alkaloids

(88)	6.25	5.89	4
(81)	1.27	6.02	2
(83)	5.62	7.78	2
(84)	1.90	6.84	2
(85)	10.66	6.02	1
(86)	0.67	6.50	2
(87)	2.49	3.28	2
(41)	9.66	6.68	1

These initial results indicated these aporphinoid alkaloids had significant activity against *Trypanosoma brucei brucei* for *in-vitro*, and significant binding affinity for enzyme important for parasite's survival, molecular target *Ornithine decarboxylase*.

Table 3.18 Docking scores of aporphine alkaloids isolated in this study and their derivatives

Com-pound	Mini-mized Energy	Gold.PLP. Fitness	Gold.PLP. PLP	Gold.PLP.par t. Nonpolar	Gold.PLP.part.repulsi ve	Gold.PLP. Lig-and.clash
86	183.83	19.8289	-23.0165	-26.294	0.1266	0.028
93	54.09	27.8489	-28.5311	-22.292	0.0086	1.0293
95	55.03	38.4616	-38.358	-49.843	0.0084	0
91	19.17	25.4228	-25.4222	-45.3383	0.0595	0
92	19.26	32.1024	-30.8562	-40.3994	0.0226	0
85	44.2	26.5959	-26.7389	-48.0034	0.05252	0
87	188.55	-25.0265	5.9448	-33.6052	0.0091	16.7714
84	103.9	-95.1384	93.2236	-41.8056	0.5322	1.1201
83	83.01	-35.4653	33.9348	-34.0093	7.3672	0
88	128.83	23.731	-24.3419	-44.0352	13.3665	0
89	146.38	26.7533	-34.1272	-37.6235	0.2786	6.9648
90	160.8	8.8294	-10.6011	-27.527	0.1782	0.0346
81	118.39	27.8819	-33.9287	-36.3287	3.4098	5.4444
96	44.3	35.8819	-33.7762	-42.8423	0.2444	0

Further lipophilicity assessing tests revealed the monomeric alkaloids had better log P (5 and less) compared the dimers between 6 and 7. This implies the monomers could make good lipophilic mole-cules (according to Lipinski's rule of Log P, values less than 5 gives an indication of good lipophilici-ty), so they have the propensity to be developed as oral drugs should they progress with desired results in further drug development studies.

Variation in type of compounds isolated based on season.

The eight aporphine alkaloids described above were collected in winter, here below are the two pre-dominant compounds isolated from *Enanthia chlorantha* plant material collected in summer.

1. Isocoumarin
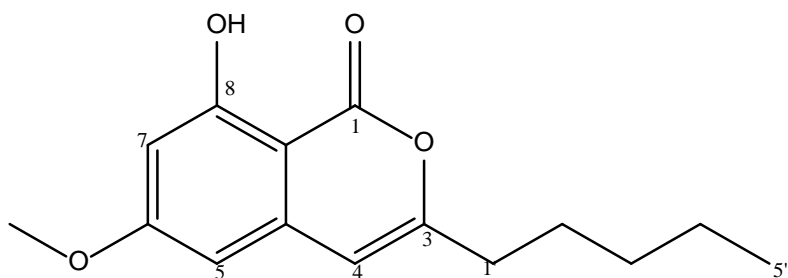
ag/John_ECBC-H9
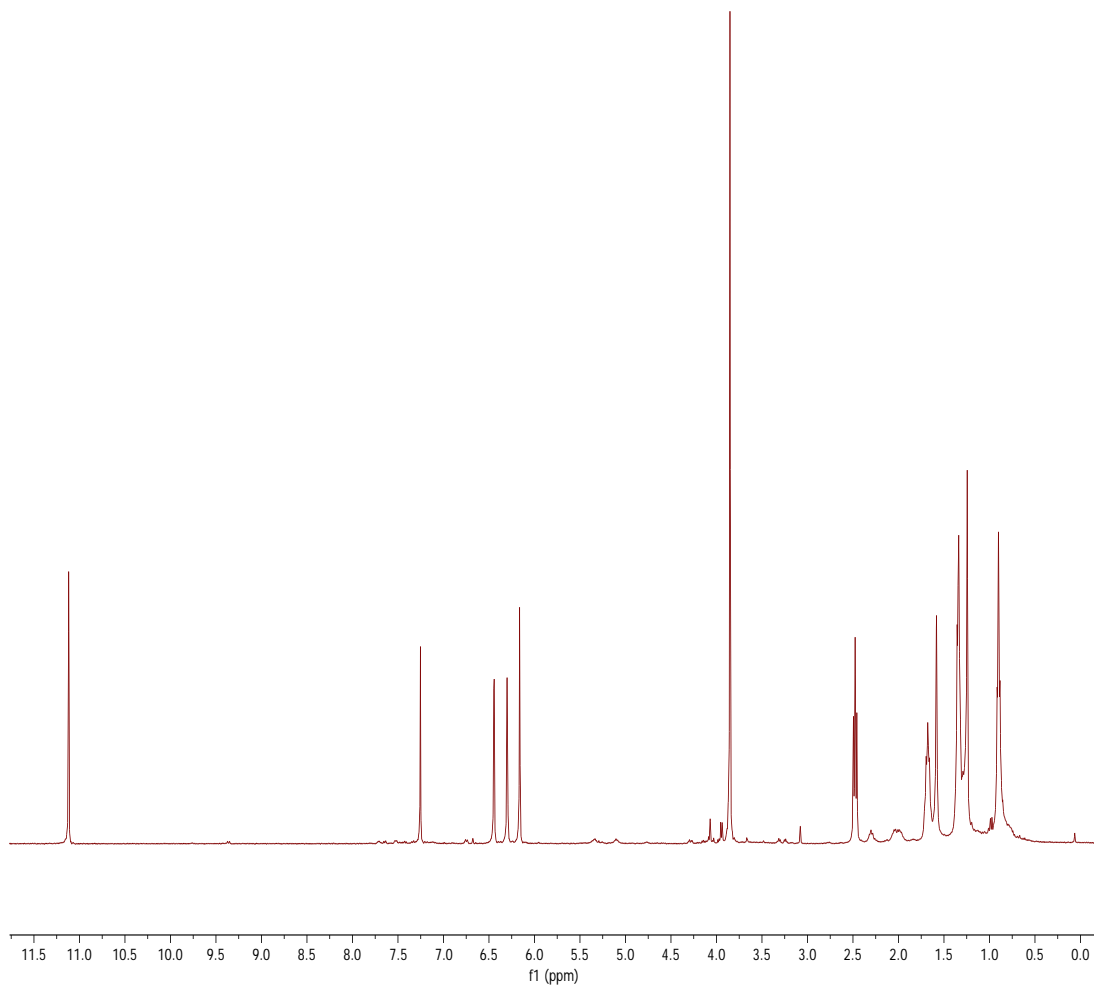
Figure 3. 44: ^{1}H NMR (400MHz, CDCl$_3$) of **ECBC H-9**

2. The dimeric alkaloid : 7, 7'- Bisdehydro-*O*-methylisopiline
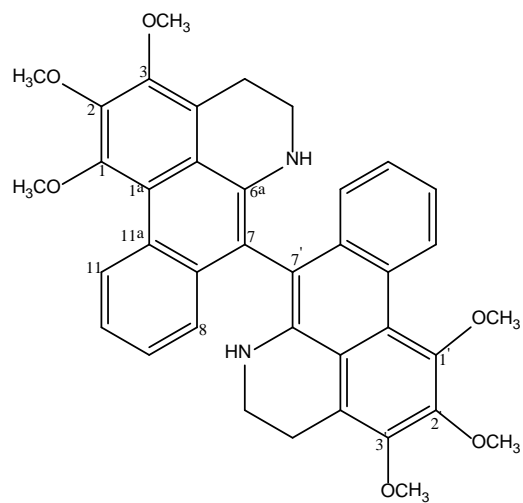
(**81**)

7, 7'- Bisdehydro-*O*-methylisopiline

The monomeric and other types of dimeric alkaloids with 2 methoxyls substitutions or methylenedioxy substitutions were not isolated from the plant material collected in summer as they were in winter.

Chapter 4

Preamble

Human Trypanosomiasis infection comprises of three forms: African *T.brucei gambiense* and *T.brucei rhodesiense* alongside the South American variety, Chagas disease. They continue to place a huge morbidity and mortality burden on millions of lives in Sub-Saharan Africa, North and Latin American countries.

Enanthia chlorantha is a medicinal herb found in the rainforests of Nigeria, Liberia, Cote d' Ivoire, Cameroun, Gabon and Democratic Republic of Congo among others (see introductory part of this thesis on page 17). This study attempted to use natural product chemistry isolation techniques to isolate, purify and identify bioactive compounds from *Enanthia chlorantha.* Using the flowchart on page 197. The bioactivity of natural products stems from the hypothesis that essentially all natural products have some receptor-binding activity; the problem is to find which receptor a given natural product is binding to. This was the focus of molecular modelling studies in this thesis. This led to the hypothesis that *ornithine decarboxylase* as the most probable mechanism of action of the alkaloids described in this study. Designing models to take bioactive compounds from natural product chemistry to combinatorial chemistry from the onset should be the target in the science of drug discovery from natural products as attempted in this study. Natural products will continue to provide a complex libraries of unique bioactive constituents, analogues to these rich libraries tailored to generate synthetic improved products through combinatorial chemistry techniques should be the aim of natural product studies from the scratch. Over the years the natural products approach has been complementary to the synthetic approach, each providing access to different lead structures to generating new clinical entities. This implies that combinatorial chemistry such as molecular modelling has been an extremely powerful tool for the optimization of an active natural product pharma core as it was attempted in this study, and the task of the natural products chemist should be to identify initial lead compounds of pharmacological interest from his vast "natural product libraries" to be handed over to computorial chemist for optimisation, to generate improved and more potent analogues.

In this study, natural product chemistry started from extraction to isolation to purification and demonstration of anti-trpanosmal activity in-vitro and went on to use combinatorial biosynthetic techniques such as molecular modelling to determine the probable mechanism of action of bioactive alkaloids derived from *Enantia chlorantha* and generate their hybrid modelled analogues for synthesis and future studies.

Structural diversity is a cogent reason why natural products are of interest to drug development. An important additional feature is that they often possess highly selective and specific biological activities based on their mechanisms of action, this buttresses the need for molecular modelling studies to attempt to decipher probable mechanism of action. Good examples are drugs in clinical uses namely, lovastatin, the HMG-CoA reductase inhibition and paclitaxel, the tubulin-assembly promotion activity , neither of which would have been discovered without the natural product leads and investigation of their mechanisms of action through methods such as molecular modelling. A further striking illustration of the influence of natural products involving the modulation of many of the enzymatic processes which probably explains where the alkaloids isolated in this study had good affinity for *Ornithine decarboxylase* and modest affinity inhibition of other trypanosomes enzymes essential for its survival.

Discussion

Enantia chlorantha has been reported as a rich source of 1-benzyltetrahydroisoquinoline type of alkaloids. A good example of such is benzylisoquinoline-derivedprotoberberine type alkaloid found in stem bark of *E.chlorantha* was palmatine (**41**). This study revealed palmatine (**41**) was the most abundant alkaloid isolated in this study from *E. chlorantha*. See Table 3.1 on page 86.
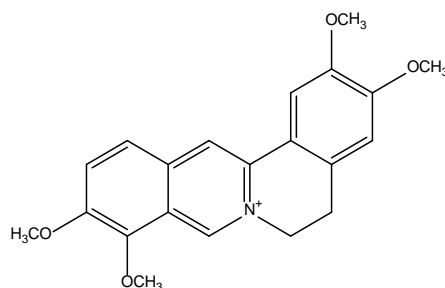
(**41**)

It gave a 0.28% yield of dry plant material (see **Table 3.1**). As the major alkaloidal secondary metabolite in *E.chlorantha in* this study, it is responsible for the bright yellow colour of the stem bark (see Figures 1.1, 2.2 and 2.3). Also presence of palmatine (**41**) in *E.chlorantha* together with the dimers probably accounts for the numerous medicinal uses and possibly explains why *E. chlorantha* is referred in rural West Africa as 'Dokita Igbo' which literally means "Doctor of the forest". It would be interesting in future studies to find what other biological activities the novel dimeric alkaloids may have. Extensive research has been carried out on palmatine; it was investigated as a probable pharmaceutical drug for treatment of viral hepatitis as reported by Virtanen et al., (1993). The reduced form of palmatine, tetrahydropalmatineis one of the major bioactive components in Corydalis yanhu suo

W.T Wang, a well-known traditional Chinese medicine with potent analgesia, sedative-tranquilizing and hypnotic properties (Hsu, 1962) among several other uses it was explored for.

Extraction, Isolation purification, structure elucidation and activity testing
 of bioactive alkaloids from *Enantia chlorantha* extracts.

From hexane extracts	from ethyl acetate extracts	from methanol extract
ECH 56 (85)	ECP-17(81)	ECM-1(41)
ECF 5-10 (86)	ECP-19(82)	
ECHB 17-18	ECHE 45(83)	
	ECP-23	
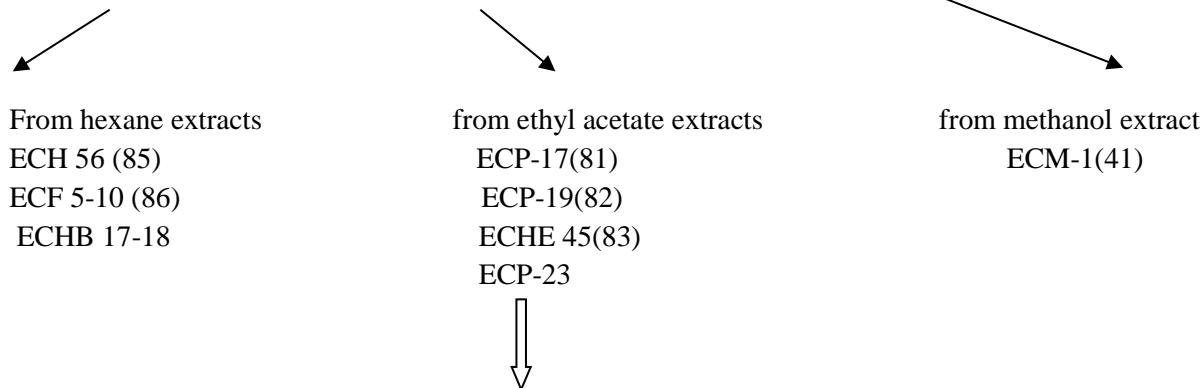
Using combinatorial biosynthetic techniques such as molecular modelling and other Translational Chemistry approaches to define drug targets in terms of most potent alkaloid in terms of binding affinity for proven anti-trypanosomal enzyme targets.

Ligand   +   proven anti-trypanosomal activity protein targets
(Alkaloid(s)   *Glutathione Synthetase,*
        Glutathione peroxidase-type tryparedoxin peroxidase,
        Glutathione peroxidase-type tryparedoxin peroxidase
        Sterol 14-alpha demethylase (CYP51) ⟶ *Ornithine decarboxylase(best bound)*
        Tipifarnib derivative 6-(4-chlorophenyl) (methoxy) (1-methyl-1
        H-imidazol-5-yl) methyl)-4-(2, 6-difluorophenyl) - 1- methylquinolin-2(1H)-one
        Ornithine Decarboxylase,Riboflavin kinase,Trypanothione reductase

Optimization of lead modelled alkaloid against active site of *Ornithine decarboxylase* to generate hybrid bioactive analogue(s)

Synthesis of the lead modelled hybrid lead bioactive alkaloid(s) and analogues

In-vivo parasitized rat model activity studies

 Further parasitic activity screening looking at the synthesized compounds activity against a variety of parasitic infections bioassay templates like malaria, leishmaniasis in addition to trypanosomiasis.

 Pharmacokinetics and lead compounds safety studies using Stem cell models to predict the bioactive alkaloids' metabolism and toxicity profile in vivo and vitro (this technology is extremely efficient and

is now replacing the laborious use of animals to a large extent in pre-clinical activity, toxicity and pharmacokinetics screening)

Other alkaloids isolated in this study were six dimeric and one monomeric aporphine alkaloids, they were black to brown residues and were isolated in fewer quantities (see **Table 3.1**), and compared to the more abundant, bright yellow protoberberine type alkaloid: palamtine.

Three of the six dimeric aporphine alkaloids isolated in the course of this study were found to be novel :(ECP-19 (**89)** which had an N-methyl group had MIC of 1.27nm**,** ECHE 45 (**90**) without an N-methyl group had MIC of 5.62 nm, while ECH 56 (**91**) also with an N-methyl group had MIC of 1.90 nm. This probably infers that the presence of an N-methyl group confers superior anti-trypanosomal activity. Others dimeric aporphines revealed MICs indicating significant anti-trypanosomal activity, with MICs ranging from 1.90 to 5.4 nM (see **Table 3.17**) ,which were better compared molar for molar with the positive control Suramin with MIC 9.6 nM. Also the other three dimeric aporphine alkaloids have been previously reported, though this is the first time in *E. chlorantha*, whereas the monomeric aporphine alkaloid and palmatine have been previously reported in *E. chlorantha.*

1,1',2,2',3'-pentamethoxy-6-methyl-5,5',6,6'-tetrahydro-4H,4'H-7,7'-bidibenzo[de,g]quinoline
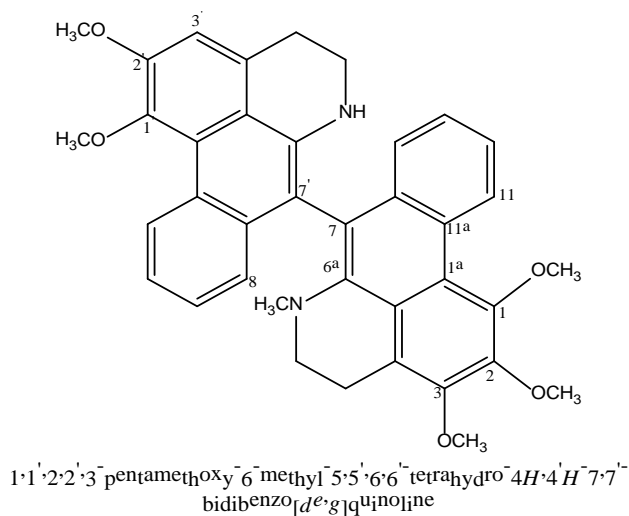
(**89**)
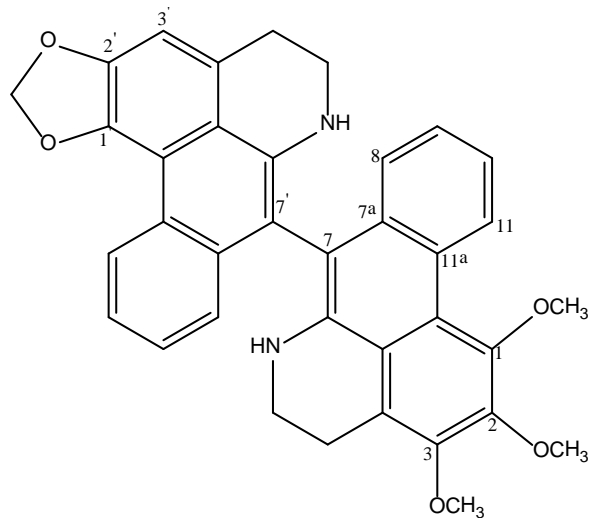
(**90**)


8'-(1·2·3-trimethoxy-6-methyl-5·6-dihydro-4H-dibenzo[de'g]quinolin-7-yl)-6·7-dihydro-5H-[1·3]dioxolo[4'·5':4·5]benzo[1·2·3-de]benzo[g]quinoline

(**91**)

There is sufficient evidence from the 1D and 2D NMR spectral analysed in this study of the novel dimeric aporphine alkaloids that their novelty was conferred by the fact that they were dimers, as well as possession of N-methyl groups and C-1' and C-2' substitutions by methylenedioxy substituents. The presence of methylenedioxy substituents led to change in chemical shifts of the aliphatic methylene as seen in ECHE 45 (**90**) ,where H-4 was at δ_C 30.8 ppm compared to H-4 at δ_C 23.4 ppm in dimeric aporphine alkaloids without methyelendioxy group. Presence of such methylenedioxy substituents however did not confer superior anti-trypanosomal activity compared to dimeric alkaloids with strictly methoxys substitutions in positions C-1 to C-3 see **Table 3.17.**

[200]

Notable curare-like bisbenzylisoquinolines such as daphnoline (**47),** cephranthine (**46**)and an anti-parasitic benznidazole (**48**) have been reported as active against *Trypanosoma cruzi* murine model through *trypanothione reductase* inhibition Fournet *et al*.,(2000). So it would be a good idea in the future to study these alkaloids to see if they are active against *Trypanosoma cruzi.*
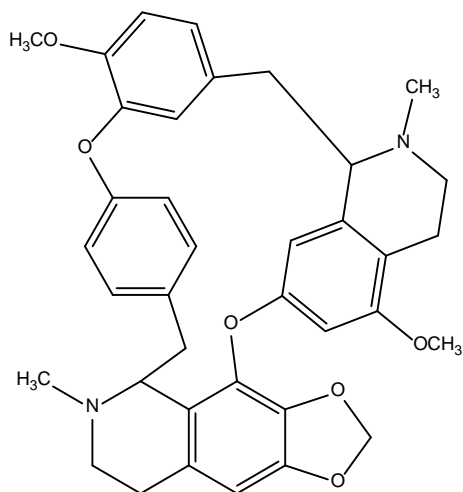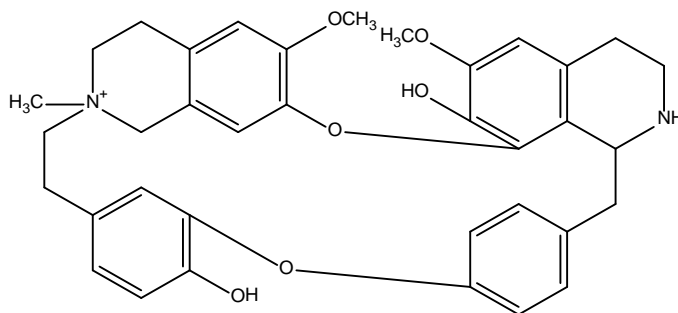
(46)   (47)
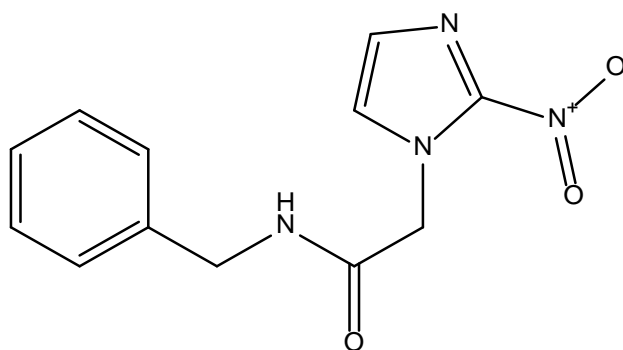
(48)

Palmatine(**41**), being the most polar constituent of *E.Chlorantha,* was extracted from methanol extract. The medium polar alkaloids with methylenedioxy substituents in position C-1,C-2 and dehyroapor-phine with methoxysubstitutions were isolated from the ethyl acetate extract (ECP-17 (**88**), ECP-19 (**89**) , ECP-23 (**93**) and ECHE-45 (**90**),while the least polar aporphine alkaloids were isolated from the hexane extracts :ECH-56 (**91**), ECH-B-17-18 (**94**)and EC-F 5-10 (**92**). This implied that a significant amount of aporphine alkaloids especially the protoberberine alkaloid isolated from *E.chlorantha's* stem bark were polar, this is likely to be the reason why difficulties were experienced in the process of puri-

fying the alkaloids despite numerous separation techniques employed in the course of this study. These difficulties could also be due to the fact that aporphine alkaloids had closely related structures and masses. This was further supported in observations made by Bourdat-Deschamps (2004) as discussed in the introductory chapter. Various separation combination techniques were tried in the course of this study, such as column chromatography followed by Gel filtration chromatography, column chromatography followed by Reveleris chromatography and column chromatography followed Normal Phase HPLC. The latter was the most efficient in achieving the purest fractions using the appropriate solvent system with R_f value of 0.3 on TLC.

Gel chromatography (sephadex LH20) fractions were used to distinguish the anti-trypanosomal activity of NMR derived aporphine alkaloids-rich fractions compared to NMR of fractions revealed to contain mainly fats and sugars. This showed that fractions ECBE SA 1- ECCHE SA 20 rich in the aporphine alkaloids described in the course of this study had MICs ranging from 2.7- to 9.6 nM. While other fractions containing only fats and sugars gave negative reaction to Dragendorff's and MIC>100μg/ml, the implication was that they were not active against *Trypanosoma brucei brucei*as shown in **Table 5.1**on page 237. This supports the hypothesis that anti-trypanosomal activity exhibited by the novel and known alkaloids isolated in this study was due to their alkaloidal nature.

In terms of seasonal variation in types of compounds biosynthesized by the plant based on season, the eight aporphine alkaloids described in details in this study were collected in winter, while Isocoumarin and dimeric alkaloid : 7, 7'- Bisdehydro-*O*-methylisopiline were the two predominant compounds isolated from *Enanthia cholorantha* plant material collected in summer.

Isocoumarin
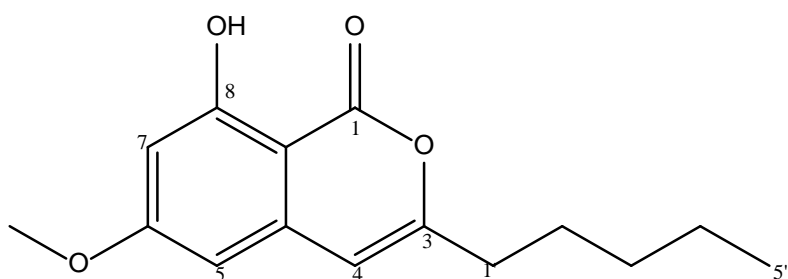
Isolation of Isocoumarin belonging to the coumarin class of compounds was particularly interesting, as it is very similar in structure to synthetic analogue warfarin widely used clinically as anticoagulant. Couramin class of drugs are known to widely used as rodenticidals, it is possible *Enantia chlorantha* synthesizes Isocoumarin to ward off rodents attack in summer as it's expected that rodents would be more active in summer and less in winter due to harsh weather conditions.

Initial molecular modelling revealed *Ornithine decarboxylase* inhibition out of the seven protein targets from the protein database analysed (see list of protein targets in section 2.2.3.12 on Molecular modelling studies)as a probable mechanism of action of these alkaloids, with high binding affinity scores of 1-2 for the majority of these aporphine alkaloids and palmatine.

Subsequent molecular modelling studies of the dimeric and their derived monomeric aporphine alkaloids as ligands docked on Lysine 69, *Ornithine decarboxylase's* active site revealed monomers docked far were better than the dimers. This was most likely due to the fact that the monomers are more likely to have drugability properties compared to the dimers. The dimers are big molecules with little flexibility as illustrated in the modelled alkaloids 3D interactions with *Ornithine decarboxylase* pictures on pages 177-190, thus did not dock well. Also monomers comply more with Lipinski's rule of 5, which is useful in evaluating whether or not a drug is likely to be an orally active one in humans, The rule suggests that an orally active drug must not have molecular mass more than 500 daltons and partition coefficient log P not more than 5. The dimers molecular weights average between 550 and 630, while the monomers average 250-330. Log P values of the dimers were between 6 and 7, while that of the monomers were less than 6. Latter docking studies showed the monomers fared better with positive docking score of (25-38) compared to the dimers (-95 to 27). This is shown in the 3D interaction pictures modelled showing the dimers as being too big, rigid and less interaction with Lysine 69 the active site, see modelled 3D pictures on pages 177-190. Hence poor docking scores is some cases negative, for example Compound 84 with docking score of -95.1384 owing its' dimeric huge size, rigidity and with poor interactions with binding site of Ornithine decarboxylase. The fact that monomers are smaller, with good molecular weights, reasonable log P values, more flexible and with better docking scores compared to the dimers makes their hybrid modelling optimisation and subsequent synthesis interesting prospects going forward in further drug development studies. Following the flowchart in a stepwise fashion, the overall aim was to improved analogues bioactive compounds from natural products through techniques described in this thesis. Thus the use of combinatorial biosynthetic techniques, first modelling all alkaloids isolated in this study with as many as possible against proven targets, in the case of this study seven protein targets The goal of this was to determine the most potent modelled protein target in terms of binding affinity determined by docking score and 3D interaction of docked protein and ligand (our alkaloids), which in this case turned out to be *Ornithine decarboxylase*.

We further went ahead in this study to attempt to optimize most potent docked alkaloid keeping it pharmacore to be as "perfect fit" as possible to *Ornithine decarboxylase* active site Lysine 69. This was in line with previous studies where application of these combinatorial biosynthetic techniques in production of novel analogues of anthracyclines, ansamitocins, epothilones, enediynes, and aminocoumarins was carried out well documented by Van Lanen and Shen (2012).

The next phase of this study which is beyond the scope of the PhD is to attempt to synthesize the hybrid modelled optimized alkaloid(s) for *in-vivo* studies at Garscube's School of Tertiary Medicine using parasitized mouse models under the supervision of expert on African Trypanosomiasis and Neurologist , Professor Peter Kennedy.

Using this approach which leads to total synthesis would not only generate hybrid modelled bioactive alkaloids for future studies, but also circumvented the issue of difficulty in isolating insufficient quantities of the bioactive alkaloids for future drug development studies, as well as providing the template for total synthesis and structural modification of the isolated bioactive analogues as more potent and abundant entities.

Total synthesis going forward has been proven overtime to be crucial for pharmaceutical companies, clinicians and patient populations while conducting clinical trials as adequate supply which would be circumvented using this approach could be a serious limiting factor in the preclinical and clinical development of naturally-derived drugs.

 Excellent example were the marine-derived anticancer agent discodermolide , where total synthesis provided sufficient quantities for thorough clinical trials, but unfortunately, these were terminated at the Phase I/II interface due to lack of objective responses and toxicity Freemantle (2004). Another good example is Paclitaxel which has several modified analogues such as doxitacel in clinical use. Paclitaxel if were to be solely gotten from the Yew tree would have worsen global warming and negatively affected climate change. Probably the tree would have been in extinction, if not for its' semi-synthetic modification analogs to ensure large scale industrial production and ensure the supply chain of dire in need cancer patients is not in any way hampered.

 Total synthesis can also be beneficial in the sense that it can lead to the identification of a sub-structural portion of the molecule bearing the essential features necessary for activity (the pharmacophore), which is what would happen in this study leading to generation of optimized modelled analogue(s).

Thus resulting in synthesis of simpler analogs having similar or better activity than the natural product itself. A very good example is that of the marine derived antitumor agent, halichondrin B where total synthetic led to generation of the right hand half of the molecule which retained all or most of the potency of the parent compound, and subsequently led to the synthesis of potent analogue, E7919 (eribulin) which was approved by the FDA in 2010 as reported by Yu (2011).

Moving forward beyond the scope of this PhD study, we intend to test for activity the synthesized analog of natural products alkaloids described in this study in parasitized mouse models. This is based on the premise that clinical trials of the original natural product derived bioactive molecules have been

reported in the past to have failed, while totally synthetic analogues drug development progressed. A classical example was the clinical trials of the marine-derived anticancer agents, dolastatin 10 and dolastatin 15, which had to be terminated for toxicity results, whereas the synthetic analogue of dolastatin 10, TZT-1027 (auristatin PE and soblidotin) gave the study a new lease of life with the being slight modification of the natural product scaffold by linking the peptide to specific antibodies using tumor specific scissionable linkages, with one antibody-drug complex (ADC) using auristatin F. The new clinical entity, brentuximab vedotin was approved as Adcenris by the FDA in 2011 for the treatment of lymphoma as reported by Copeland (2010).

Challenges of the study

1. Flooding of the laboratory by the soxhlet extractor. Owing to rise in water level pressures overnight, several times during the course of this study I experienced flooding in the laboratory and some cases lost the plant materials in the soxhlet, this was quite frustrating.

2. Purification of alkaloids isolated.

   This was the man problem I encountered in the course of this study. We tried several techniques to little effect, as the majority of the NMR spectral analysed showed tinge of impurities. The problem with this is the fact that once your fraction submitted for activity testing is not a totally pure one, one can't be too sure whether the activity is from the main compound or the tinge of impurities. To overcome this we had to try Sephadex separation technique and test the fractions rich in saponinins, sugars, flavonoids and fats , all these fractions did not showed anti-trypanosomal activity, thus we concluded the alkaloids described above were responsible for the anti-trypanosomal activity described in this study.

   This challenge was most likely due to the fact that many of the alkaloids isolated were very close in molecular weight and closely related in structures, so almost always merged together as separation was attempted. Eventually normal phase HPLC as shown in the appendix achieved purification, however the yields ended up being too low to be meaningful, as yields were as low as 0.5 mg.

   3. Molecular modelling studies

   The process of drug discovery involved isolation of bioactive molecules from either synthetic or natural source, to verify this activity as well optimize it, one had to carry out molecular modelling studies. My background is not anything close to molecular modelling, so getting help from India and interpreting the results were quite difficult.

4. Column chromatography sometimes runs out of solvent leading to drying up of the extracts in the column and subsequent abandoning of the column in use after 20-30 days of collection, this was quite frustrating.

5. Scaling up difficulties, poor NMR spectral and activity results

At onset of the study the plan was to extract isolate(this led to isolation of fats, sugars, tannins, saponins and alkaloids) and test for anti-trypanosomal activity to decipher which groups of compounds were responsible for the anti-trypanosomal activity exhibited by the extracts and follow all these steps up by scaling up. The aim of scaling up was to obtain more yield of lead compounds of interest (bioactive alkaloids) as 800 g of the cork/bark for example yields as little as 5-50 mg of alkaloids, ECH 56 for example yielded 6 mg which led to generation of NMR spectrum of poor quality. Difficulty in purification made this impossible as rather than obtain more yield , substantial quantity were lost to various purification separation techniques. With many of the NMR spectrum discussed in this thesis with tinge of impurities this can potentially affect the reliability of activity test results subsequently obtained

6. Multidisciplinary nature of natural product chemistry and combinatorial chemistry was also a huge challenge. This led to huge waiting time to get an expert in molecular modelling to find time out his busy schedule to put me through steps in modelling the alkaloids. It was as bad as at a point we had to carry out the initial molecular modelling work in India by Dr Rajeev Singla of the Netaji Subhas Institute of Technology

7. Natural product chemistry is time consuming, laborious and monotonous. In the course of this study I ran up to 27 column chromatographies. Chopping the plant material into small pieces took 1 day. Drying the chopped into pieces plant material took 3 days, separating the bark from the cork of the plant material took 1 day, grinding into fine ground particles of both cork and bark plant material took 1 day. While soxhlet extraction took 5-6 days, rotator evaporation to viscous plant material took 1 day and lastly column chromatography took 30 days on the average, this involved having to sit and manually collect vials from mornings to evening daily. Eventual use of Reveleris column chromatography circumvented this laborious and time consuming stage, as the whole process of column chromatography was done in a few hours.

We have been able to generate 3 hybrid analogs of the aporhine alkaloids described in this thesis using molecular modelling means described earlier. This way we have circumvented purity and isolation challenges encountered using Natural product extraction and isolation means in this study, also further bioactivity studies are guaranteed to be foolproof.

Conclusions and possible future studies

The preliminary anti-trypanosomal activity carried out showed ECP-19 (**89**) as the most active novel dimeric aporphine alkaloid with MIC of 1.27 nM. This inferred that the presence of N-methyl group in the novel dimeric alkaloids as in **ECP -19** (**89**) was noted to confer superior anti-trypanosomal activity compared with dimeric aporphine alkaloids with NH functional groups (See **Table 3.17**).

However there was the binding affinity scales of the monomeric aporphine alkaloids were better compared to those of the dimers r in terms of affinity with *Ornithine decarboxylase* (see **Table 3.16**).

Thus synthesizing a series of dimeric aporphine alkaloids and their analogues with N-Methyl functional group could be done in the future to quantify the correlation between lipophilicity and anti-trypanosomal activity. Also synthesizing aporphine alkaloids with methylenedioxy group at C-1 and C-2 positions for further testing would be a good idea to determine whether the presence of methylenedioxy substituents confer better lipophilicity properties.

Molecular modelling as a means of deciphering possible mechanism of isolated bioactive compounds isolated from natural products helped in the course of this study to attempt to decipher the possible mechanism of action of the alkaloids. In this study, molecular modelling has identified potential molecular target(s) of *E. chlorantha* aporphine alkaloids. These results could provide the framework for synthetic modification of these bioactive aporphine derived and berberine –type alkaloid: palmatine, de novo synthesis of structural motifs and analogues, leading probably to further drug discovery studies.

Further studies in line of determining whether there could be synergism of this group of isolated dimeric aporphine alkaloids with other anti-trypanosomal agents in clinical use could be evaluated in future studies.

Inhibition of *Ornithine decarboxylase* as probable molecular mechanism of action of these groups of alkaloids described provides further impetus in the future to attempt to synthesize these alkaloids for pharmacokinetics, efficacy driven metabolomics and in-vivo drug target driven mouse model studies, taking them through the entire Figure of the drug discovery science.

 The next step would be to attempt to use Structure Activity Relationship (SAR) focused molecular modelling techniques to "prune the alkaloids to taste" as perfect fit into the pocket of *Ornithine decarboxylase*'s active site. Resultant hybrid molecules would then be synthesized for further in-vivo activity studies in parasitized mouse models available at University of Glasgow's Garscube School of Vetenary Medicine laboratory.

This study has buttressed the complexity of natural product chemistry and the structural diversity of natural products derived compounds are clearly evident from the result of this study. This study re-

vealed isolation of alkaloids, fats, sugars, tannins, saponins all from the same medicinal plant and was able to isolate and prove the type of compounds (alkaloids) responsible for anti-trypanosmal activity of *Enantia chlorantha* in-vitro and probably *in-vivo.*

The business of drug discovery will forever be a multi-disciplinary approach as natural product chemists, synthetic chemists, biologists, pharmacokinetics and toxicity study experts will all have to continue to work together to unearth new medicines in today's world in the face of multidrug resistance, lack of new anti-infective drugs going through FDA and MRHA stringent and rigorous licencing procedures.

It has been reported, as documented in the course of this thesis, that medicinal chemists have synthesized the protoberberine alkaloids (and their analogues) reported in this study for their structure-activity relationships Mc Call *et al.,* (2002), Vennerstrom and Klayman, (1998) and Iwasa *et al.,*(1996). Such studies in the future on the novel and known dimeric aporphine alkaloids isolated in this study with their monomeric analogues could be tailored towards anti-trypanosomal and other anti-parasitic drug development studies to gain more insight into structure activity relationships. To support the notion for further future studies on these alkaloids are buttressed by the fact that I reported previously, Adesokan Masters' Thesis (2009), the aporphine -derived alkaloids isolated in course of this study were found to be non-toxic to cancer cell lines as well as normal cells. This completes the full spectrum of their isolation, structure elucidation, anti-trypanosomal activity tests, molecular modelling to attempt to decipher their possible mechanisms of actions as well as toxicity tests. Anecdotal evidence of the fact that *E. chlorantha* has been in use orally for centuries in West Africa also indicates no inherent toxic effects of these alkaloids. Though the aporphine alkaloids isolated in this study had with some structural similarities with some of those isolated from Chinese herbs *Mu Tong* and *Fang chi*, both of the Aristolochia species producing Aristolochic acid (**96**).
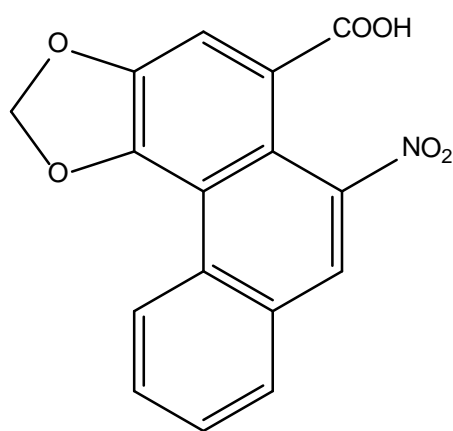
(**96**)

Which were found to be cancer-promoting and nephrotoxic in human subjects. However Aristochic acid and analogues has an active site shown above by the arrow which is electrophilic and capable of DNA base pair interactions, this believed to be responsible for their carcinogenic activity. This active site is not available in the group of aporphine alkaloids isolated in this study due to the presence of C-7/C-7' bridge, an example is compound (89) here below, so this group of aporphine alkaloids are likely to be non-toxic, toxicity studies reported in my Masters' thesis which indicated they were non-toxic(see results in appendix), however further toxicity studies are essential.

1·1'·2·2'·3'-pentamethoxy-6-methyl-5·5'·6·6'-tetrahydro-4H·4'H-7·7'-bidibenzo[d e',g]quinoline
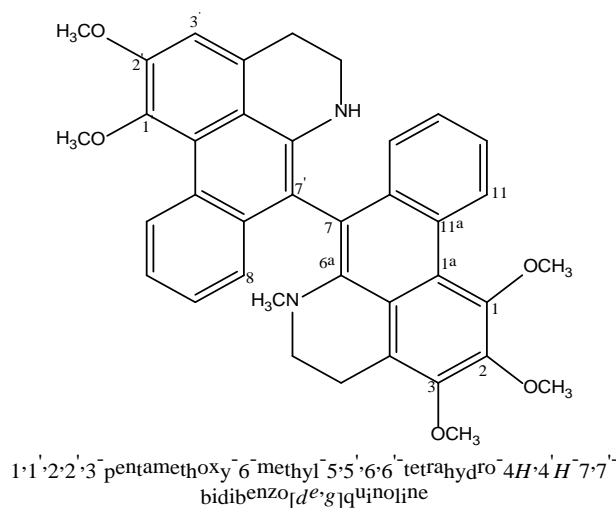
(**89**)

 In conclusion Natural products will continue to be a viable source of new clinical entities as many top-selling drug class today such as statins, angiotensin converting-enzyme inhibitors, many immunosuppressants , anti-cancer agents in clinical uses and in clinical trials at the moment would not have been available to physicians and patients if not for natural products drug discovery science. Thus studies such as pharmacokinetics, in-vivo toxicity studies, efficacy driven metabolomics and drug target driven mouse model studies on the group of aporphine alkaloids isolated in this study alongside their analogues would be an interesting prospect in the future.

In conclusion this study completed the entire spectrum of initial drug discovery process from antedoctal evidence of efficacy in West Africa to isolation of the bioactive compounds(alkaloids) from the plant material to demonstration of activity in-vitro(anti-trypanosomal studies), demonstration of non-toxicity(cancer cell line studies see appendix). In addition the study went through docking molecular modelling studies targeting seven proteins and finding the one with best affinity, Ornithine decarboxylase. To conclude we have now used molecular modelling techniques to generate 3 hybrid synthesized anlaogs of the aporphine alkaloids described in this study (hybrid in the sense that they are analogs with better drugability properties, better docking scores and conforming to Lipinski's rule of 5 much better than the isolated dimeric alkaloids). These molecules are available on the AK Scientific

and Spec websites for purchase for the further Garscube's Trypanosomal parasitized animal studies as at time of submission of this thesis.

Appendix

Overview of Masters' thesis study as continuum into the PhD:

To test the anti-trypanosome activity of *E. chlorantha* extracts and isolated pure compounds determining their Minimum Inhibitory Concentration (MIC) compared to Suramin .The anti-bacterial activity of the extracts against *Mycobacterium marinum* and sixteen other bacterial strains in terms of MICs would be carried out alongside anticancer activity of the extracts and resulting compounds .

Materials and methods:

Materials

Plant Material

Stem bark samples of *Enantia chlorantha* were obtained from a forest located within the suburbs of Ile Ife, Osun State of South Western Nigeria (Lat. 60° and 90°N, Long. 20° 3' and 60° 30').

Chemicals and Reagents

Chemicals used were Ethyl Acetate: Sigma Adrich 27227 (Merck, Germany), n-Hexane: Sigma Aldrich 34859 (Germany) and Methanol: Fluka 32213 (Germany).

Reagents used for Phytochemistry includes *Visualization Reagents*:

1.Anisaldehyde-Sulfuric acid spray solution (used for identification of Sugars, Steroids ,Terpenes and Phenols on TLC plate).It contains: 0.5ml of Anisaldehyde in 50mls of glacial acetic acid,1ml of 97% Sulfuric acid freshly prepared.

2. Drangendorff spray solution (used in identification of Alkaloids) made up of:

Solution A; 2.215 bismuth sulphate with 2.5 ml of Glacial acetic acid, 100ml of Water

Solution B: 93 g of Potassium iodide, 100 ul of Water.5mls of each of Solution A and Solution B freshly prepared is measured in a bottle attached to a pump which acts as the means of delivery onto the TLC plate of interest.

Laboratory apparatus and materials used for Phytochemistry

TLC Plate and Tank

TLC plates(pre-coated silica gel plates(0.063-0.020mm,Kieselgel 60 PF $_{254}$, Merck No. 5554) The TLC plates are made up sheet of glass meta with solid adsorbent (aluminium) pieces 8cm by 6cm.TLC Tank made of glass containing the solvents of interest for separation of the extract mixture into compounds based on their polarity .The TLC tank is cuboidal in shape measuring 10cm by 10cm by 6 cm. Others are

UV lamp: Mineralight Lamp used: Model UVGL -58

Multiband UV 254/896 NM (Upland CA91786 USA)

Hot Air Gun

Model: Power Craft 5969 (Clobaltronics GmbH & Co KG China)

Sartorius weighing balance LC2200P (Sartorius Corp., NY 11717, USA)

Glass columns

Vials

Rotatory evaporator

Fritsch Grinder (**Fritsch GmbH,** 55743 Idar –Oberstan, Germany)

10 ml, 100 ml,200 ml Measuring cylinders

 Silica gel 154425P (VWR International B-3001 Leuven, Belgium)

Methods

Sample Preparation

The outer portion (dark brown), cork of the stem bark was peeled with the aid of a pen knife to separate it from its inner (green yellow), bark .This is to ensure specificity with respect to the compounds present in the bark ,coupled with the fact that artefacts and lichens may be present in the cork.

Subsequently, they were separated into smaller pieces (4 by 2 cm) and air-dried in fume cupboard (72 h) to ensure the plant materials are free from water which can constitute a source of impurity.

The Fritsch grinder was used to grind separately the samples (cork and bark) and they were weighed to obtain the finely powered cork (1.608 kg) and bark (602 g).

Extraction

After grinding yield for the bark was 620.2 g .This as well as 800.4 g of the cork(this is half of total yield as 800 mg is maximum that can be used in the soxhlet extractor) were used for soxhlet extraction.

Finely ground (cork and bark) samples were gentle decanted into the thimble 'paper' in the main chamber of the Soxhlet extractor. Hexane is expected to extract non polar compounds, ethyl acetate medium polar and methanol polar compounds. For both the cork and bark exhaustive extraction with the three solvents were carried out for 48-72 hours respectively for the six ,two for each of the three solvents to obtain ECHB (*Enantia chlorantha* hexane bark), ECBE (*Enantia chlorantha* bark ethyl acetate), ECMB(*Enantia chlorantha* methanol bark), EC HC (*Enantia chlorantha* hexane cork), ECEC (*Enantia chlorantha* ethyl acetate cork) ,ECCM (*Enantia chlorantha cork* methanol) from both *E.cholorantha'*s bark and cork respectively

Post-Extraction Separation and Identification of Compound Types

Extracts were then decanted from the bottom flask of Soxhlet extractor and evaporated close to dryness with aid of a rotatory evaporator. Resultant viscous liquid extracts were decanted into small labelled vials and then kept in fume cupboard to evaporate to dryness for weighing. Thereafter Thin Layer Chromatography (TLC) was used to determine the possible number and types of compound(s) in the extracts for identification of compounds in the mixtures TLC plates, solvents of interest and TLC Tank were used. To do this capillary tubes were used to obtain the extracts from the labelled vials to spot them onto the TLC plate. Varying mixture of hexane and ethyl acetate like 50/50, 60/93, 70/30, 80/20 making up 10 mL were measured into the TLC tank using a measuring cylinder. The spotted spots on the TLC plate were then numbered and the prepared pre-coated TLC plate were immersed into the hexane/ethyl Acetate mixture (in successive ratios of interest) in the TLC Tank .The mixture as-cended from the bottom of the plate to near top by capillary action after about 5 min. It is then re-moved and initially blown with hot air using the gun before sprayed with appropriate visualizing rea-gent (Anisaldehyde and Dragendorff) and re-blown with hot air to aid quick visualization of the ex-tracts mixture's separated compounds. Some compounds on the TLC plates are coloured therefore can-not be detected with the naked eyes easily , so all dried prepared TLC plates were visualized under UV light using the Mineralight UV lamp with long wavelength at 254 mm.

Test Organisms for cytotoxicity, antibacterial and anti-trypanosomal activities studies

16 strains of Bacteria namely: *Shigella sonnei* ,*Salmonella typhimurium*(3 serotypes),*Salmonella java* ,*Shigella flexneri*(3 serotypes) ,*Salmonella enteritidis* (4 serotypes), *Salmonella oranienburg*, *Salmonella dublin*, *Salmonella agona*,*Escherichia coli* ATCC control strain, and *Nocardia farcinica*

Trypanosoma brucei S427 strain was used for the antitrypanosomal activity screen.

Cytotoxicity studies

Table 5.1 showing a variety of cancer cell lines which are outlined in the table below were used in the studies:

Cell line	Cell morphology	Source	MIC µg/ml
TE671	Epithelial like	Human, Caucasian medullablastoma	>100
A905	Epithelial	Human malignant skin melanoma	>100
PC 3	Epithelial	Prostatic carcinoma	>100
DU 145	Epithelial	Prostatic carcinoma	>100
PNT2A	Epithelial	"Normal" prostatic cell line	>100

Pre-screening preparation

The near to dry *E. chlorantha* crude extracts were made to test solutions using DMSO at concentration 10 mg/ml. Cancer cells which were obtained from patients were cultured and kept in incubator at 90°C and 5% CO_2. To keep these the cells for alive for a lengthy period the medium was changed every 3-4 days.

The modification of the Raz et al.,(2000) and Franzblau S.G., et al.,(1997) methods were used the activity screening.To screen for cytotoxic potentials of *Enanthia chlorantha*'s bark extracts , cultured

cancer cells were inoculated onto the specialised activity screening plate which has 96 wells and labelled in rows A-H and columns 1-12. 200 μl of the plant's extracts were added to row A, B, C (hexane, ethyl acetate and methanol respectively) and G wells. The G well designated the experiment's background control was prepared without AlmarBlue indicator unlike the wells A,B,C had the extract(s), 200 μl of the THP1 media , cancer cells and the indicator. 200 μl of DSMO were added to row D and E. Well F served as the negative control had the listed contents excepts the extract(s), while well H was the positive control .

A replicate plate in the same fashion was made for *E.cholorantha*'s cork extracts into wells A, B ,C for hexane,ethyl acetate and methanol extracts respectively. With starting concentration of 200 μg/ml, serial dilution to concentrations as low as 0.0009 μg/ml were done on plate's wells from column 1 to 12. After the preparation the plate was placed in incubator for 24 hour at 90˚ C and 5% CO_2. After 24 h, 100 μl of media were replenished and the two plates returned to incubator for another 24h.Thereafter the plate's row and column contents were read on spectrophotometer at 570 nm and 600nm with the Alamar blue indicator measuring the fluorescence and surviving cancer cells counts were determined in vitro. Finally the MIC of the extracts activity against the cancer cells were determined.

Bacterial strains and activities screening.

16 bacterial strains were obtained from the laboratory stock cultures of the Department of Microbiology Stobhill hospital. To screen for anti-bacterial and anti-trypanosomal activity, the same modification of the Raz et al., (2000) and Franzblau S.G., et al., (1997) methods outlined in the cytotoxicity screening were used. The only differences were the microbial or parasitic agent replacing the cancer cells and as well as the media used. For the Anti-trypanosomal activity utilising 2-3 x 10^4 *T.brucei* S427 (a bloodstream form of the parasite) HMI 9 was the media, A similar protocol was followed for the seventeen bacterial strains using the same serial double dilution approach with Mueller –Hilton broth as their media. MICs of the extracts against the seventeen strains including *Mycobacterium marinum* ATCC.BAA535 strain for anti-bacterial screen and that of the extracts against trypanosomes alongside that of Suramin were also determined .The same protocol was followed to determine the MIC of the extracts against *Norcardia farcinica* obtained from the Strathclyde Institute of Pharmacy and Basic Sciences microbiology laboratory and Gentamycin like Suramin for the trypanosomes was used as positive control for the bacterial strains.

Based on the initial screening results, only the cytotoxicity, anti-mycobacterium and trypanosomiasis screening were done for subsequent resultant fractions gotten from chromatographic separation processes.

Chemical Structure Elucidation and Identification

Materials

Deuteriated solvents used for One and Two dimensional NMR(Proton and 13 Carbon) included DMSO(Methyl Sulfoxide-d6:Lab Aldrich Chemistry)Germany, d-CDCl$_3$ (Choloroform-d Aldrich 151823-100G)USA. To do this   10-20 mg of the extracts were dissolved in about 0.75- 1 ml of deuteriated solvent of choice and transferred into a NMR tube. Initial NMRs of the extracts were done to reveal their structural features and possible compounds of they contain.

Thereafter Open column chromatography *E. chlorantha* extracts were carried out mixing. The resultant dried extracts gotten from the fume cupboard with silica gel and hexane in a conical flask. The column fractions were eluted and   TLC done, the ones with similar spots on TLC were pooled together.

Finally definitive One and Two dimensional Carbon and Proton NMRs and Mass Spectroscopy were carried out to elucidate the structures of chemical compounds isolated.

Compound(s) structures elucidation using NMR

10 mg of each of the extracts or resultant pooled fractions were added to 0.75 ml of deuteriated choloroform or Methyl sulfoxide-d$_6$ (DMSO) depending on the extract's solubility for the 2D NMR spectroscopic studies using the Jeol Eclipse (400 MHz) and Bruker AMX-500 (500Mhz)

Structure elucidation using Mass Spectroscopy.

  This was used to confirm the molecular weights of structures proposed in the process confirming the elucidated structure determined by NMR .This is based on the principle of fragmentation of molecules of samples to charged molecular ions and the fragmented spectra read to give the molecular weights of the compounds in a given mixture. The electron spray ionization mass spectra (HRESIMS) of all extract mixtures and resultant pooled Open column chromatography fractions were performed in a FTMS- Orbitrap (Thermo Finnigan Bremen, Germany).

Results

The dry extracts yields (following soxhlet extraction and drying in the fume cupboard) as a proportion of starting plant material's weight are shown below in Table 1.1.

Table 5.2: Extracts yield from the plant material

Plant Code	Amount in weight (g)	Yield %
EC HC	17.6	2.8
EC CE	16.5	2.7
EC CM	88.7	14.3
EC BH	13.0	1.6
EC BE	24.2	3.02
EC BM	65.6	8.2

Key :EC ;*Enantia chlorantha*, C; Cork, B; Bark, H; Hexane, E ;Ethyl Acetate, M; Methanol.

3.1: Screening results

The preliminary phytochemical and antimicrobial activity screening of the stem bark of *Enanthia clorantha* carried out showed the hexane, ethyl acetate and methanol extracts had MIC ranging from 3.1-6.3 µg/mL compared to Suramin 0.06 µM.

The three extracts were tested at 200 µg/mL, *E. chlorantha* methanol extract (ECM) showed the least MIC of 3.125 µg/mL while the other two had MICs 6.25 µg/mL thus the extracts possess considerable significant anti-trypanosomal activity. However, they only showed moderate activity against *Escherichia coli* and *Mycobacterium marinum* out of seventeen bacterial strains tested and no activity were observed for *Shigella* and *Salmonella* species at 200 µg/mL. Methanol extract's MIC against *E.coli* was 50 µg/ml. The extracts' MICs against *Mycobacterium marinum* ranged between 25-100 µg/mL.

The extracts activity results are summarized in Table 5.3 here below

Test organism	EC H (MIC (µg/mL)	EC E (MIC (µg/mL)	EC M (MIC (µg/mL)
Escherichia coli	25	50	25
Trypanosoma brucei	3.125	6.25	3.125
Mycobacterium marinum	25	50	12.5
Shigella spp	>200	>200	>200
Salmonella spp	>200	>200	>200
A905	100	100	100
PC 3	50	100	25
PNTA	50	100	50
DU145	100	100	100
TE671	100	100	100

Variety of colours on both TLC and UV lamp were suggestive of presence various classes of compounds in *Enantia chlorantha* extracts possibly alkaloids, tannins, fatty acids and so on. The reoccurrence of blue fluorescence under UV light may be indicative of presence of alkaloids.

Column chromatographic separation of the last extract fraction EC BE is ongoing as at the time of putting this report together.

Spectroscopic studies (NMR and Mass Spectral) results

Compounds Isolated from the chromatographic separation include:

1.Palmatine
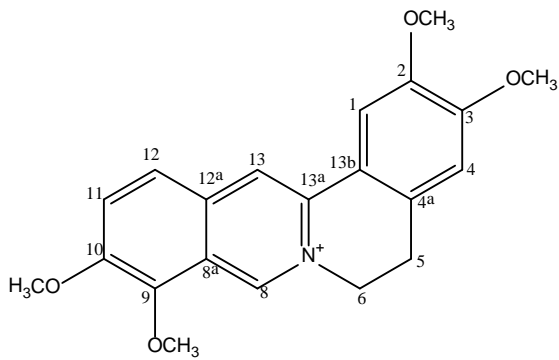
NMR spectral results

Fig 3.45:Palmatine's [13] Carbon NMR of Palmatine
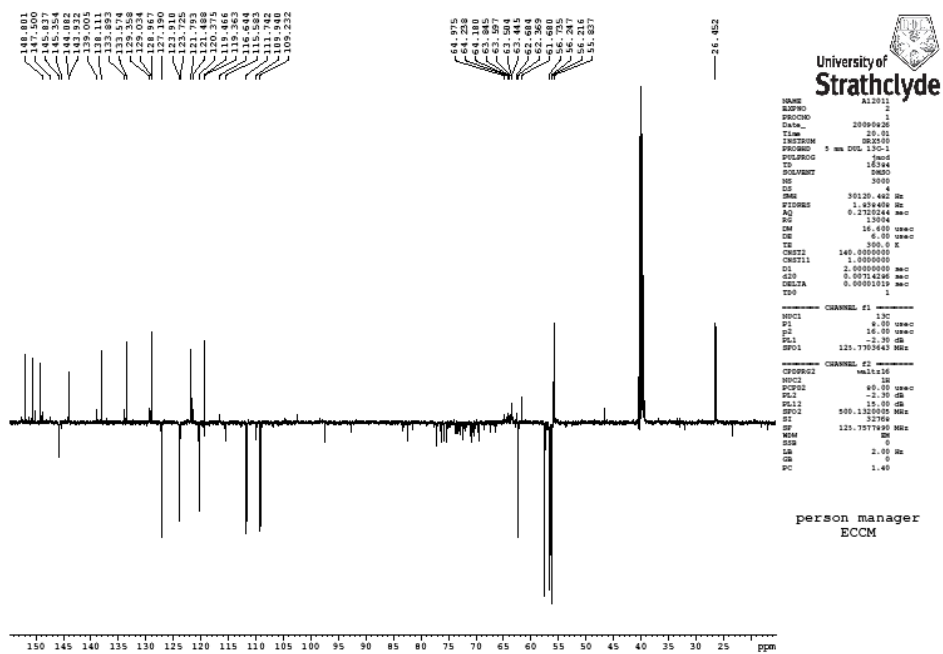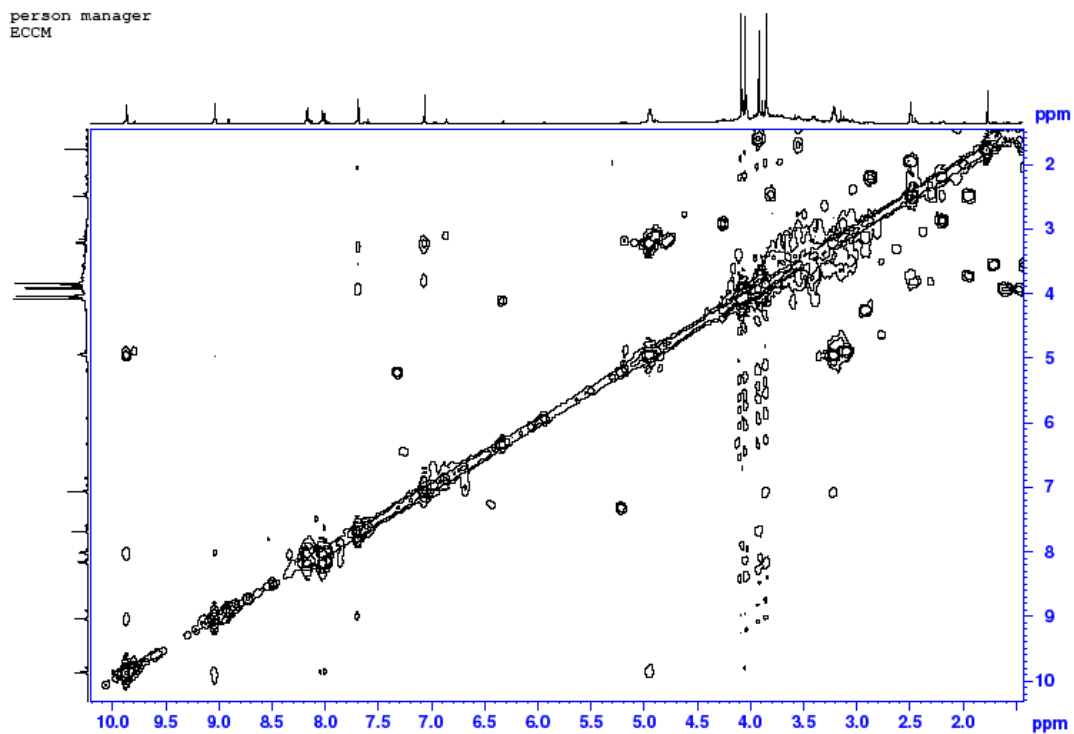
Fig 3.46 COSY NMR of Palmatine
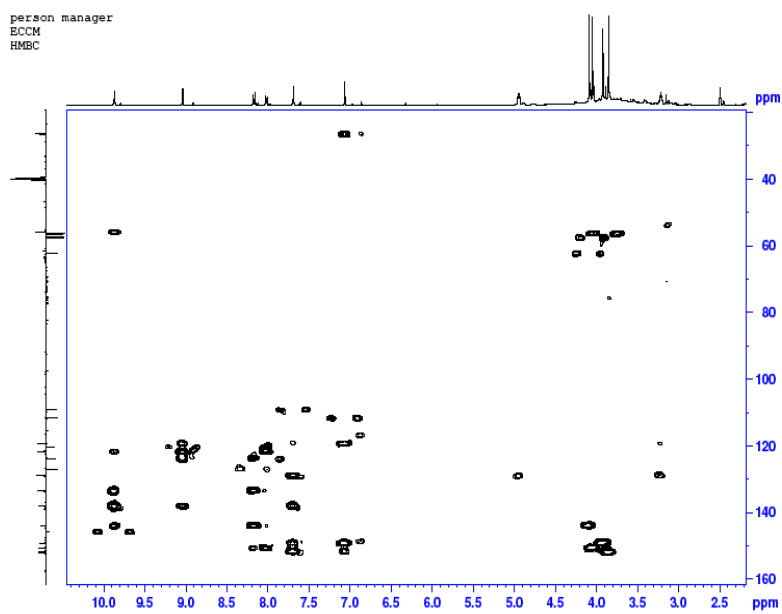
Fig 3.47 HMBC NMR of palmatine
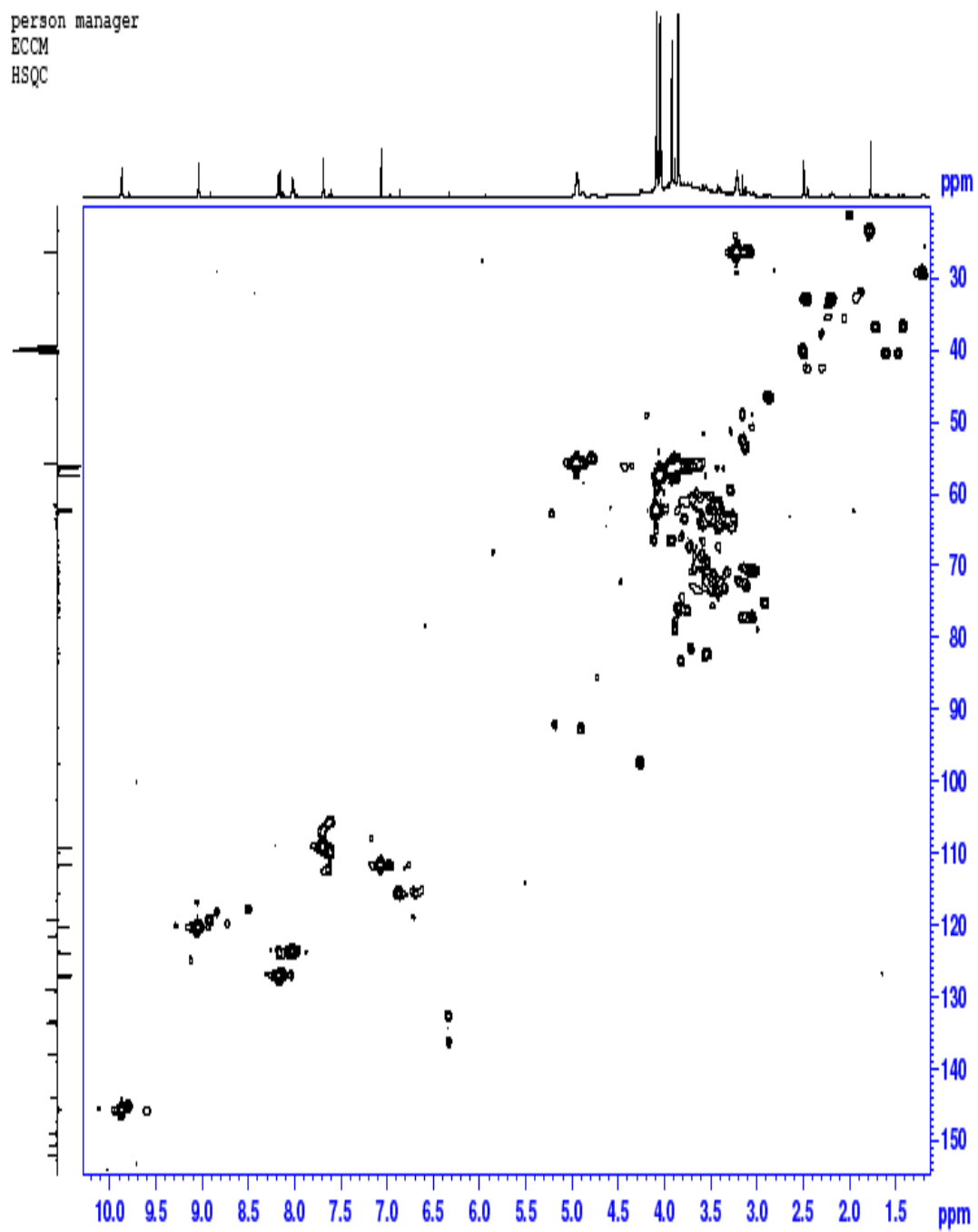
Fig 3.48 HSQC NMR of Palmatine.

HSQC and HMBC correlations of Palmatine are shown below in Table 5.4 and Table 5.5

Table 5.4 Palmatine's HSQC correlations

Position	^{1}H(ppm)	^{13}C(ppm)
1	7.69	109.22
1a	-	119.4
1b	-	191.1
2	-	149.22
3	-	152.0
4	7.06	111.7
4a	-	129.0
5	3.27	26.4
6	4.95	55.9
7	-	-
8	9.87	145.9
8a	-	121.8
9	-	144.2
10	-	150.7
11	8.17	127.2
12	8.02	123.9
12a	-	133.6
13	9.04	120.4
2 MeO	3.92	56.7
3 MeO	3.85	56.4
9 Me O	4.09	62.4
10 Me O	4.05	57.5

Table 5.5 Palatine's HMBC correlations

Position	^{1}H(ppm)	^{13}C(ppm)
1	7.69	(1b)119.4 ,(4a)129.0,(5)26.43
4	7.06	(1b)119.4,(2)149.22,(5) 26.43
5	3.27	(1a) 119.4,(4a) 129.0,(6) 55.9
6	4.95	(4a) 129.0.
8	9.87	(1b) 191.1,(13) 120.4,(12a)133.6
11	8.17	(9)144.2,(10)150.7,(12a)133.6,(13) 120.4
12	8.02	(8a)121.8,(9) 144.2,(10) 150.7 ,(12a) 133.6,
13	9.04	(1a)119.4,(1b) 191.1,(8a) 121.8
2 MeO	3.92	(2)149.2
3 MeO	3.85	(3) 152.0
9 Me O	4.09	(9) 144.2
10 Me O	4.05	(10) 150.7

Interpretation of all of the NMR data above gave rise to the known structure of Palatine.

Subsequent open column chromatographic fraction analysed yielded known compounds such as 6a, 7-Didehydro -7-hydroxy-1, 2-dimethoxyaporphine in Fig X .Its structure shown below.

4
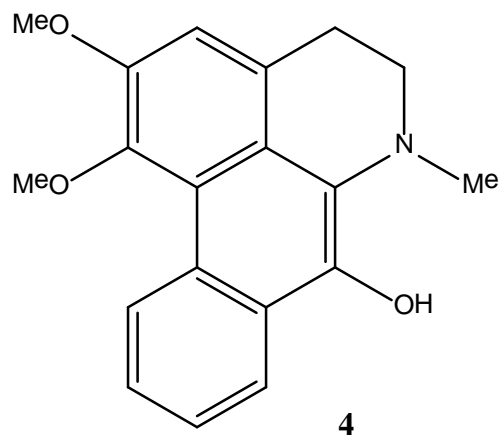
:6a,7-Didehydro -7-hydroxy-1,2-dimethoxyaporphine.

Molecular Formula:$C_{19} H_{19} NO_3$

Molecular Weight:309.894. Below are tables showing its HSQC and HMBC correlations

Table 5.6 HSQC correlations of 6a, 7-Didehydro -7-hydroxy-1, 2-dimethoxyaporphine

Position	^1H(ppm)	^{13}C(ppm)
1	-	145.72
1a	-	117.70
1b	-	98.08
2	-	151.5
3	7.113	111.83
4	1.25	31.1
5	3.89	93.97
6	-	42.4
6a	-	128.14
7	-	189.0
7a	-	122.10
8	9.60	127.98
9	7.89	122.64
10	7.13	123.76
11	7.18	127.27
1 MeO	4.00	59.85
2 MeO	4.09	56.46

Table 5.7 HMBC correlations of 6a, 7-Didehydro -7-hydroxy-1, 2-dimethoxyaporphine

Position	^{1}H(ppm)	^{13}C(ppm)
3	7.113	(1)145.7 ,(2)151.5,(3a)125.83,(4)31.1
4	0.98	(5) 93.97,(6) 93.98
5	3.89	(4) 31.1
8	9.60	(7) 189, (7a)122.10
9	7.89	(7) 189.0,(8)127.98,(11) 127.27
10	7.13	(110127.27
11	7.18	(1a)117.70,(10) 123.76
1 MeO	4.00	(1)145.72,(3) 111.83
2MeO	4.09	(2) 151.50,(3a) 125.83

Chemical Structure Elucidation

Carbon and Proton NMR of ECC 1-27 were done for chemical structure elucidation, the results of ECC 14 and 26 revealed aporphine alkaloids. These aporphines have the same structure as those reported by Wafo et al.,1999 but a slightly different stearical configuration in terms of where the protons and methylene groups lies in their NMR spectra .Their spectra are shown below in Figures 11,12,13, and 14
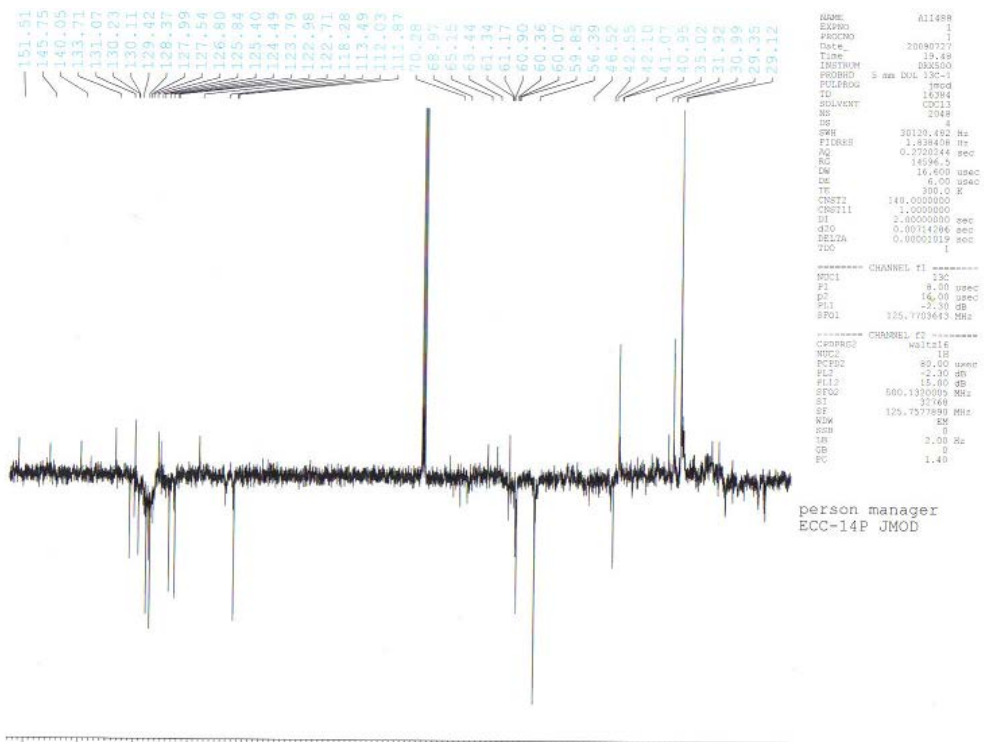
Fig 3.48 Carbon NMR of ECC 14 (6a,7-dehydro-1,2-dimethoxyl-7- hydroxyl-N-methyl-aporphine)
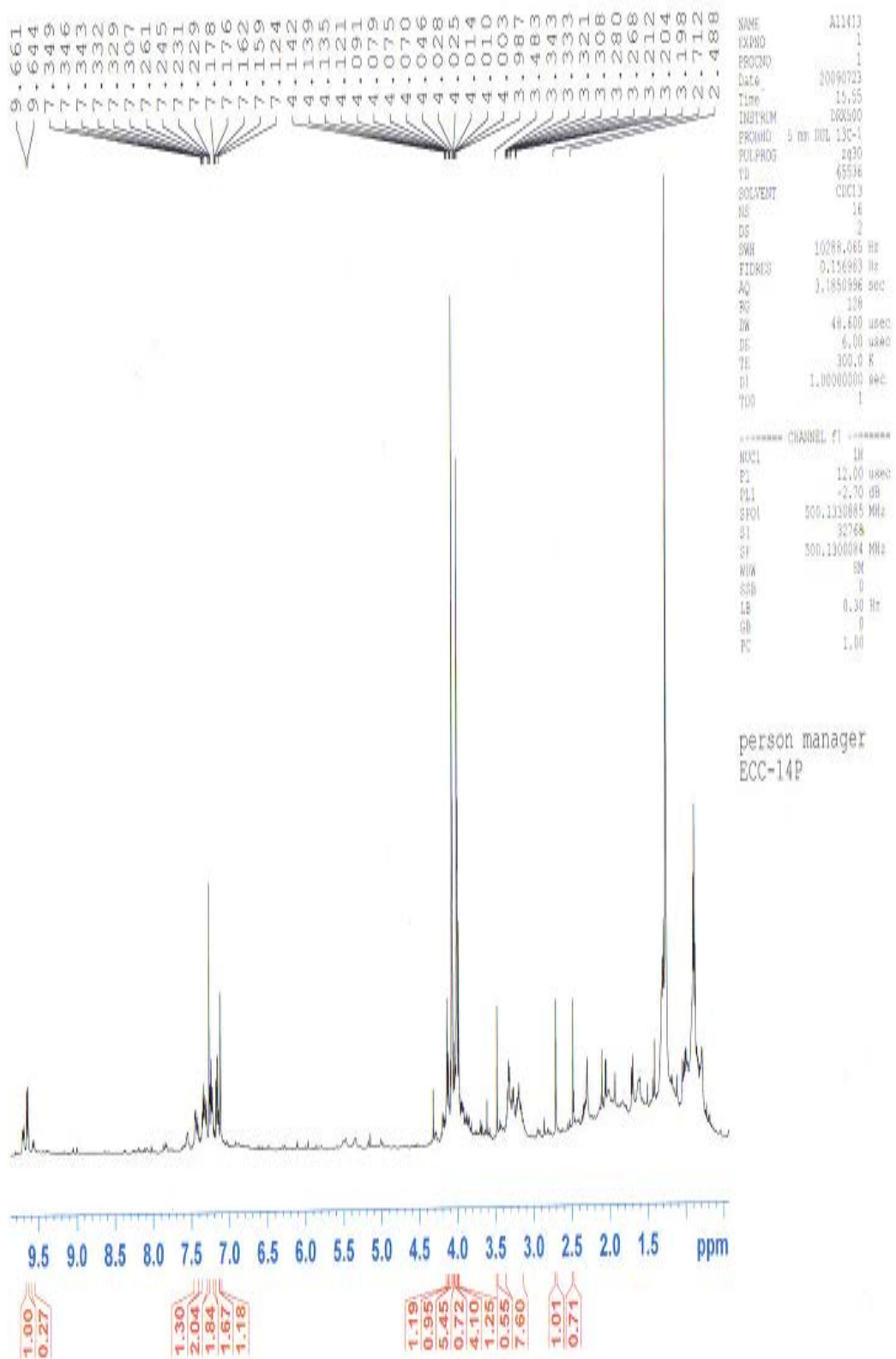
Fig 3.49 Proton NMR of ECC 14 (6a,7-dehydro-1,2-dimethoxyl-7- hydroxyl-N-methyl-aporphine)
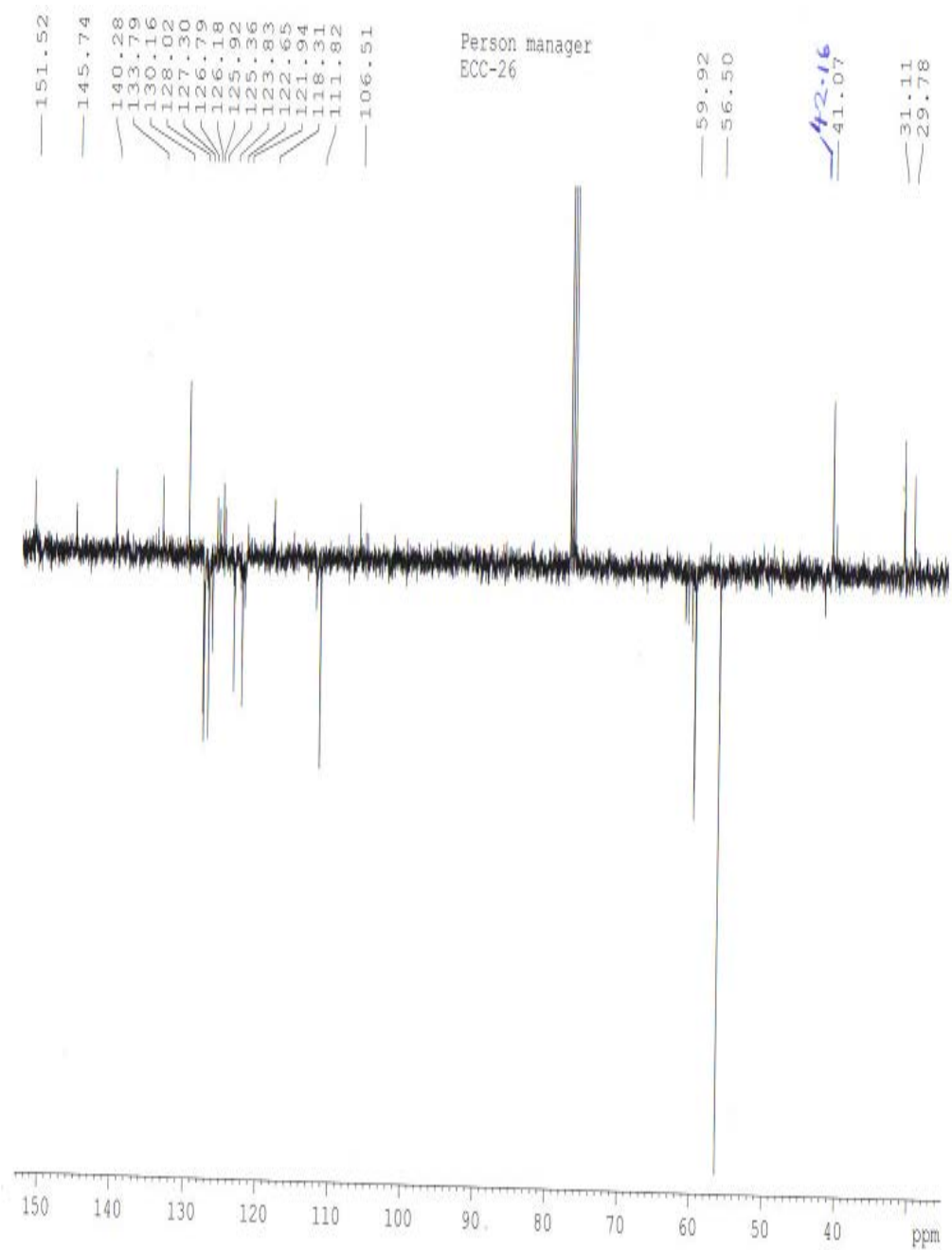
Fig 3.50 Carbon NMR of ECC 26 ((6a,7-dehydro-1,2-dimethoxyl-7- hydroxylaporphine)

[229]
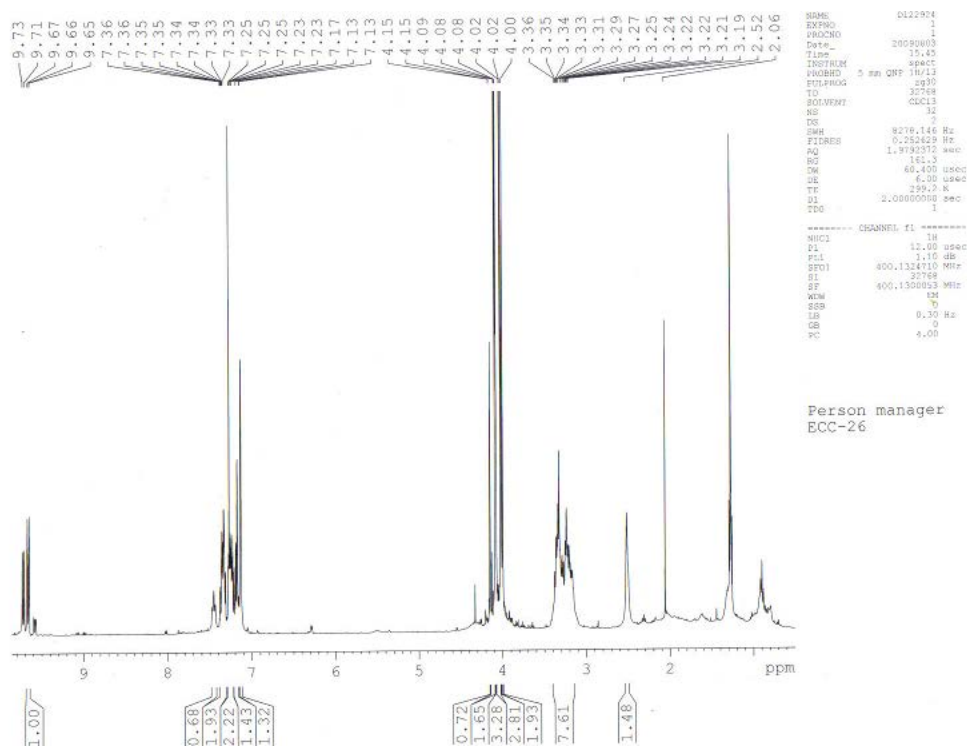
Fig 3.51 Proton NMR of ECC 26 (6a,7-dehydro-1,2-dimethoxyl-7- hydroxylaporphine)

CHEMICAL STRUCTURE OF ECC 14
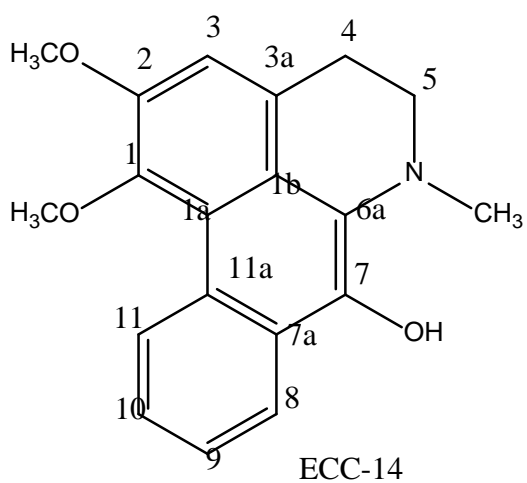
ECC-14

6a,7-dehydro-1,2-dimethoxyl-7- hydroxyl-N-methyl-aporphine
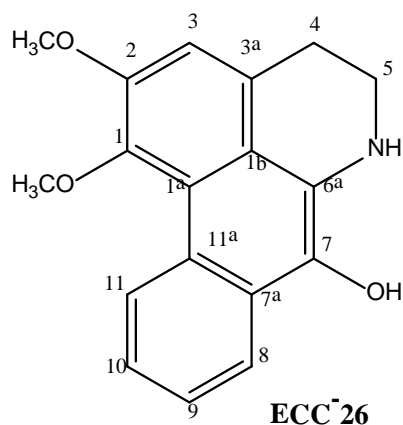
ECC⁻26

6a,7-dehydro-1,2-dimethoxyl-7- hydroxylaporphine

Analysis of NMR spectra and structure elucidation

In terms of appearance ECC 14 was pink in colour, while ECC 26 was black. The two compounds gave pink coloration when sprayed with Anisalaldehyde reagent and yellow- brownish colour with Dragen- dorf reagent indicative of presence of Alkaloids.

ECC 26 (6a,7-dehydro-1,2-dimethoxyl-7- hydroxylaporphine) was found to be very similar to ECC 14(6a,7-dehydro-1,2-dimethoxyl-7- hydroxyl-N-methyl-aporphine) with the presence of N-CH$_3$ group observed at ð 2.78ppm while for the latter and N-H group at position ð 2.52ppm in the former being the difference.

The two compounds had two MeO groups at ð 4.00 ppm and ð 4.09 ppm.they also had ^{1}H multiplets at 3.20,3.34 and 3.32 ppm indicative of the methylene groups at C-4 and C-5.The signal at 7.13ppm was due to the aromatic proton at position C-3, while the highly deshielded aromatic proton at 9.66 ppm was due to the proton at C-11. This was confirmed by its NOESY interaction with the OCH$_3$ at posi- tion 4.09ppm.

Further structure elucidation of the fractions compounds using NMR and Mass Spectral would be done in the future as in PhD study. However, there are strong indications from the next set of NMR spectral being analysed that are novel alkaloids. These novel compounds are protoberberine variety of benzo- isoquinoline alkaloids .Their structures were confirmed using Mass Spectral ,which gave the exact molecular weights expected .They are however about to be subjected to reconfirmation of their novel-

ty through X-ray Crystallography and other appropriate methods , so would be included in future result findings.

Antibacterial Activity Studies Result .

We were unable to solubilise 3 fractions EC H B, EC H C and EC E C using freshly prepared DMSO.

The extracts solubilised failed to inhibit growth of the sixteen strains of Bacteria at concentration 10mg/ml down to 0.2mg/ml.However EC M C showed modest activity against E.coli ATCC25922 at 10mg/ml suggestive of its MIC being greater than 10mg/ml.
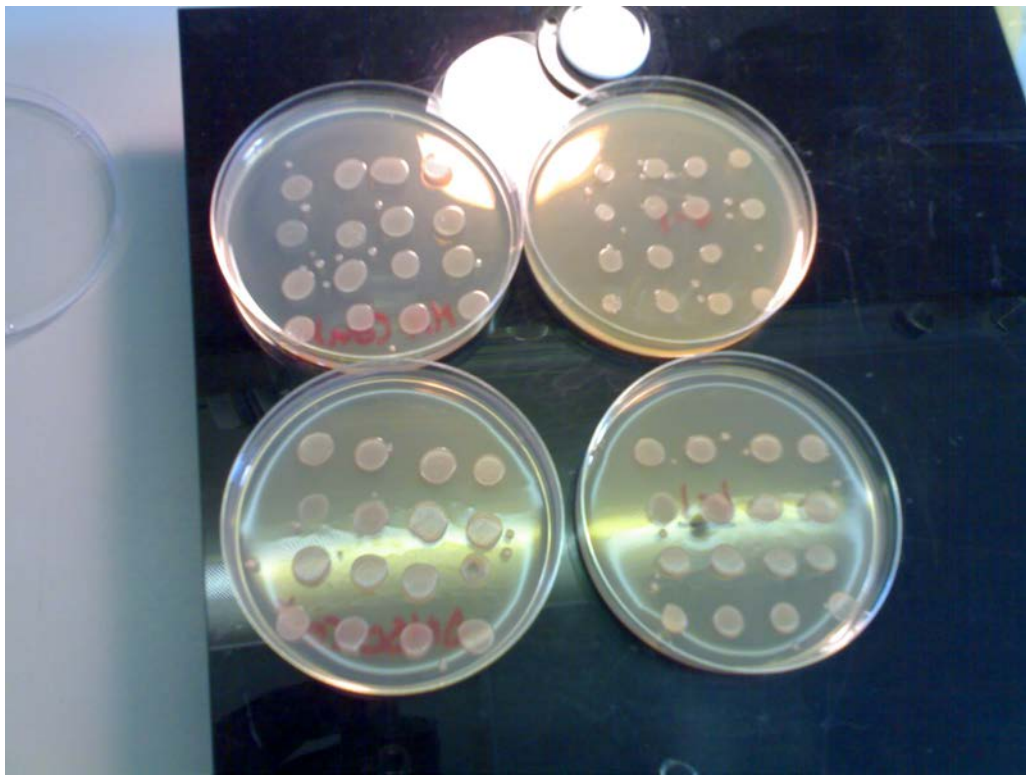
Fig 3. 52 The sixteen strains tested in petri dish with extracts: *Shigella sonnei* , three serotypes of *Salmonella typhimurium, Salmonella java* , three serotypes of *Shigella flexneri* , four serotypes of *Salmonella enteritidis* , *Salmonella oranienburg*, *Salmonella dublin*, *Salmonella agona*, *Escherichia coli* ATCC 25922 control strain all failed to achieve MIC at 10 mg/ml.
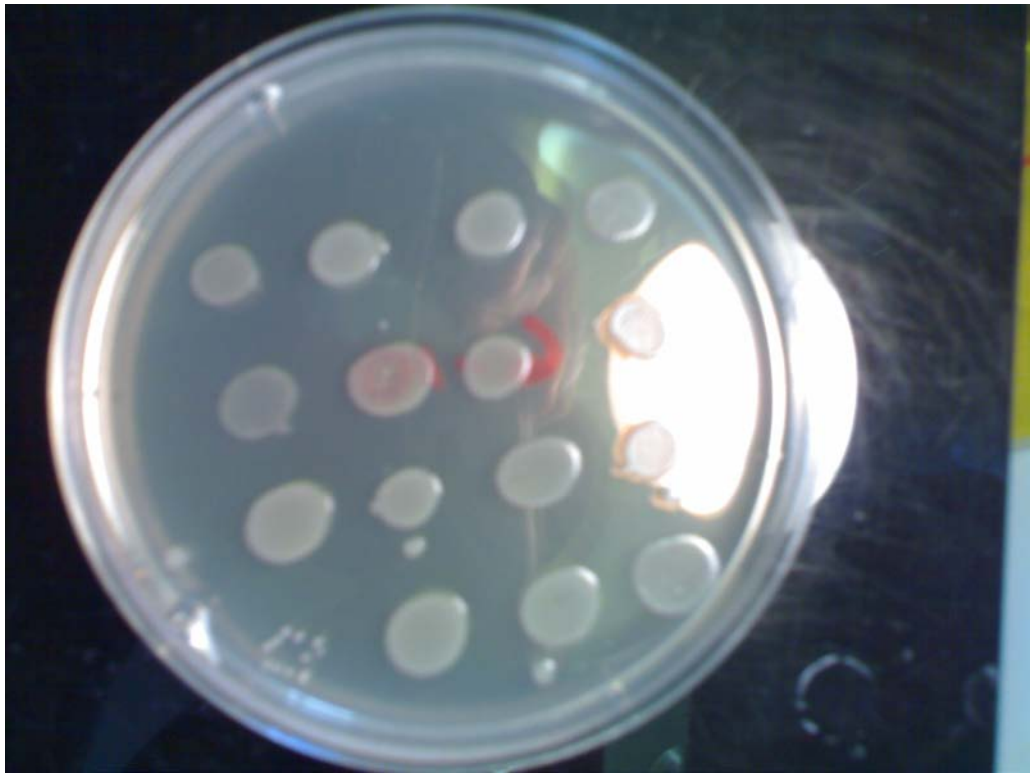
Fig 3.53 EC M C(16th spot) demonstrating some activity against E.coli ATCC 25922

However the second phase of Antibacterial activity testing done revealed modest activity against *Norcadia farcinica* by the EC H B fraction .The result is shown on the Figure 7 below

JI samples 100µg/ml *Nocardia farcinica* 6/8/09
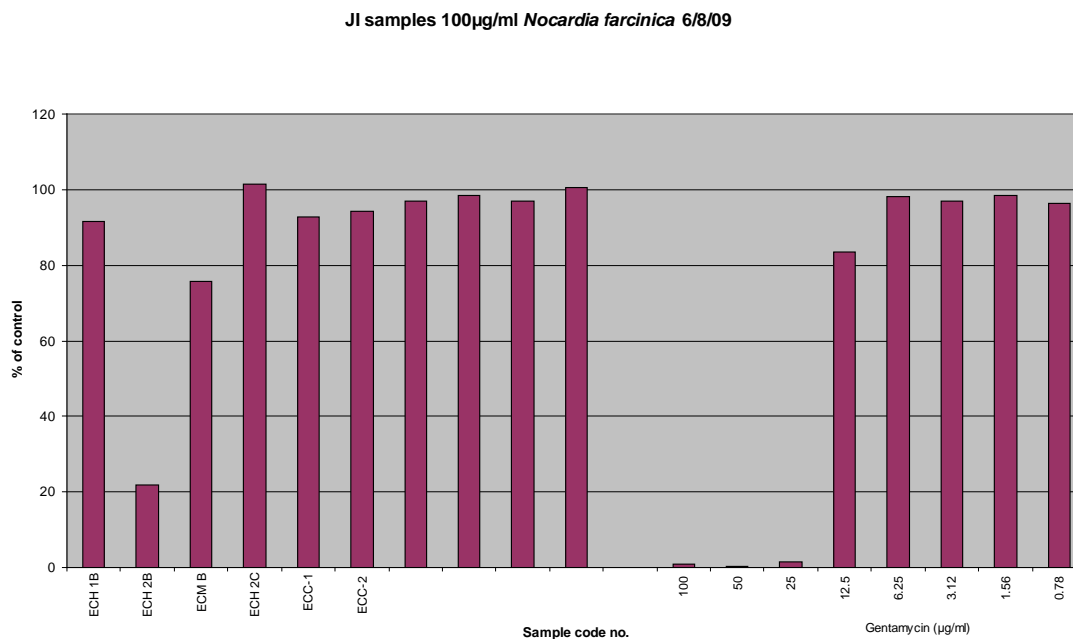
Fig 3.54 Bar chart comparing the effect of *Enantia chlorantha* extracts against the conventional antibiotic; Gentamycin against *Norcadia farcinica*

NB:

- The lower the peak the more the activity.
- 50% as reference point for significant activity.

Discussion:

The extracts' moderate activity against *E. coli* correlates with its traditional use in treating urinary tract infections (UTIs). The significant anti-trypanosomal activity and that of Mycobacterium *marinum* also correlates with the traditional anti-parasitic use in treating malaria and pulmonary tuberculosis. Further activity screenings are ongoing with early results showing the purer fractions have equal or more activity against trypanosomes than the crude extracts.

These preliminary results have provided a platform for complete isolation and structure elucidation of lead novel / pure compounds from the extracts. These novel alkaloids which would require further pu-

[235]

rification and activity screens in terms of cytotoxicity and anti-parasitic potentials. Identified active compounds would serve as leads for the synthesis of improved and more potent analogues for further anti-parasitic activity screening and subsequent translational work with a view to drug development.

Future perspectives

Future use of chromatpgraphic techniques like open column, Flash and Vacuum Liquid Chromatographic separation of the extracts into pure fractions would be undertaken. These fractions when collected would be pooled together based on similarity on TLC plates and subsequently NMR and Mass Spectroscopy are done to elucidate their structures, as well determine their exact molecular weights. The subsequent stages projected for this PhD study are as outlined below in a flow chart manner:

Cleaning up (stability tests and purification of the lead compounds through Ion exchange separation and other appropriate techniques)

Scaling up (this is needed to have more yield of lead compounds of interest, as 800grams of the cork/bark for example yields between 10-25 mg of lead compounds.)

Synthesis of the novel lead compounds

Further parasitic activity screening (looking the synthesized compounds activity against a variety of parasitic infections bioassay templates like malaria, leishmaniasis in addition to trypanosomiasis)

Pharmacokinetics and synthesized compounds safety studies using 3D Hepatocyte and Stem cell models to predict the compounds' metabolism and toxicity profile in vivo and vitro.

Molecular modelling and other translational chemistry approaches to define drug targets in terms of compound's binding protein and enzyme targets.
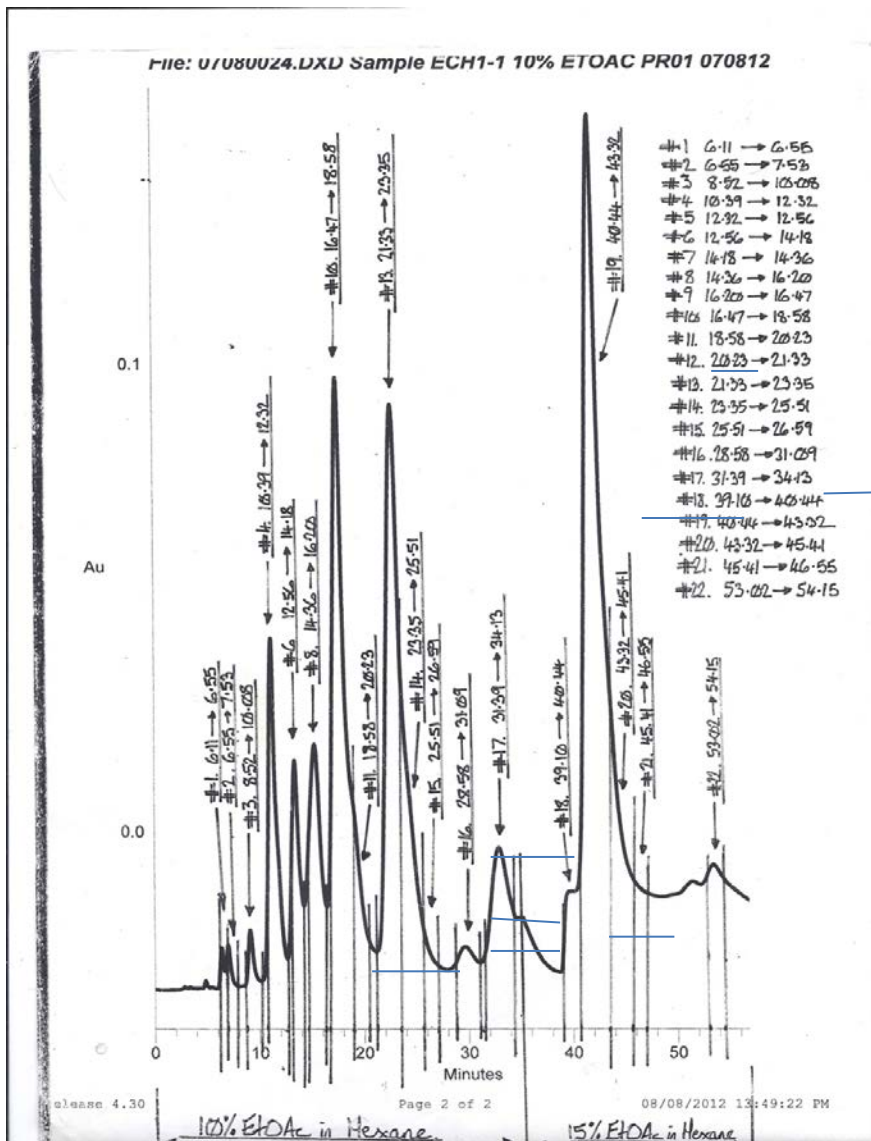
Figure 3.55: Normal Phase HPLC print of fraction Prep ECH 1-1 as a mixture being subjected to purification

Gel filtration chromatography fractions MIC results.

Out of the 3 Sephadex columns ran, 18 fractions (ECBE SA), 12 fractions (ECCH SA), 59 fractions (ECCHE SA) were obtained. The fractions were thereafter submitted Trypanosomiasis screen test

The screen results are as shown in **Table 3.16** here below.

Table 5.8	Well	Fraction	MIC
	A2	ECBE SA1	12.5
	A3	ECBE SA2	25
	A4	ECBE SA 3	6.25
	A5	ECBE SA4	25
	A6	ECBE SA5	6.25
	A7	ECBE SA6	6.25
	A8	ECBE SA8	1.6
	A9	ECBE SA12	6.25
	A10	ECBE SA11	6.25
	A11	ECBE SA10	1.6
	B2	ECBE SA14	6.25
	B3	ECBE SA15	>100
	B4	ECBE SA16	50
	B5	ECBE SA17	3.12

B6	ECBE SA18	0.8
B7	ECBE SA22	25
B8	ECBE SA24	12.5
B9	ECBE SA25	25
B10	ECBE SA35	12.5
C2	ECCH SA1	>100
C3	ECCH2 SA1	>100
C4	ECCH2 SA3	>100
C5	ECCH2 SA4	3.12
C6	ECCH2 SA6	1.6

Reverleris IES Flash Chromatography printouts

Fig 3.56 ECM fraction run

Method Name: dapo-ec.5.4
Run Name: 2011-11-23.dapo-eche26
Run Date: 2011-11-25 11:21

Column: Reveleris® Silica 12g	Slope Detection: Medium	Collection Mode: Collect Peaks	ELSD Carrier: Iso-propanol
Flow Rate: 36 mL/min	ELSD Threshold: 5 mV	Per-Vial Volume: 15 mL	Solvent A: Hexane
Equilibration: 2.8 min	UV Threshold: 0.05 AU	Non-Peaks: 15 mL	Solvent B: Ethyl acetate
Run Length: 13.0 min	UV1 Wavelength: 254 nm	Injection Type: Dry	Solvent C: Methylene chlorid
Air Purge Time: 0.5 min	UV2 Wavelength: 280 nm		Solvent D: Methanol

1 - EED7

Gradient Table

	Min	Solvents	% 2nd
1	0.0	AB	30
2	1.0	AB	30
3	4.0	AB	50
4	2.0	AB	100
5	1.0	AB	100
6	0.0	BD	0
7	3.0	BD	40
8	2.0	BD	40

Vial Mapping Table

Peak #	Start Tray:Vial	End Tray:Vial
1	1:27	1:29
2	1:30	1:30
3	1:31	1:33
4	1:34	1:38
5	1:39	1:44

Fig 3. 57 ECH frcation

REVELERIS™
Flash Chromatography System

Column: Reveleris® Silica 12g
Flow Rate: 36 mL/min
Equilibration: 2.8 min
Run Length: 24.9 min
Air Purge Time: 0.5 min

Slope Detection: Medium
ELSD Threshold: 3 mV
UV Threshold: 0.02 AU
UV1 Wavelength: 254 nm
UV2 Wavelength: 280 nm

Collection Mode: Collect Peaks
Per-Vial Volume: 25 mL
Non-Peaks: 25 mL
Injection Type: Dry

ELSD Carrier: Iso-propanol
Solvent A: Hexane
Solvent B: Ethyl acetate
Solvent C: Methylene chlorid
Solvent D: Methanol
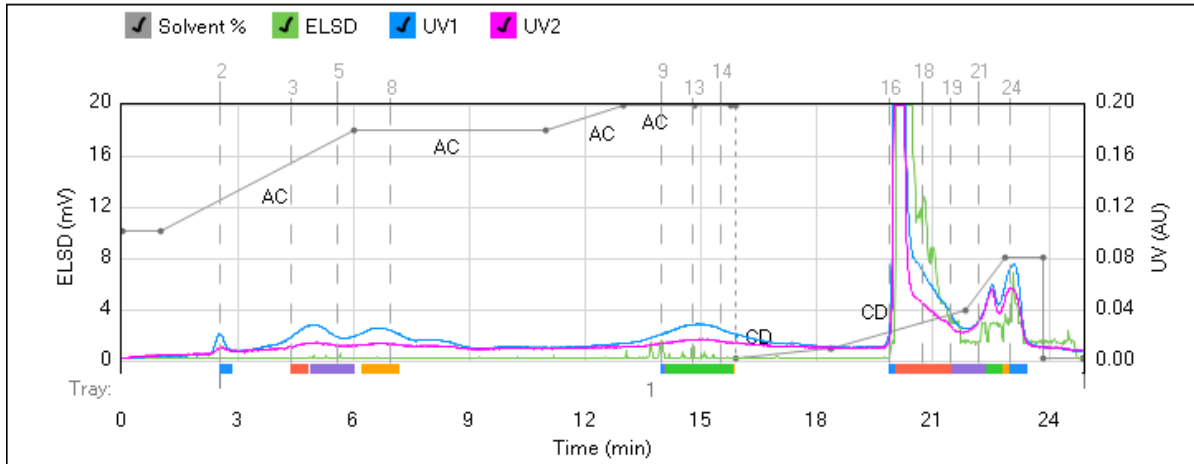
1 - EED7
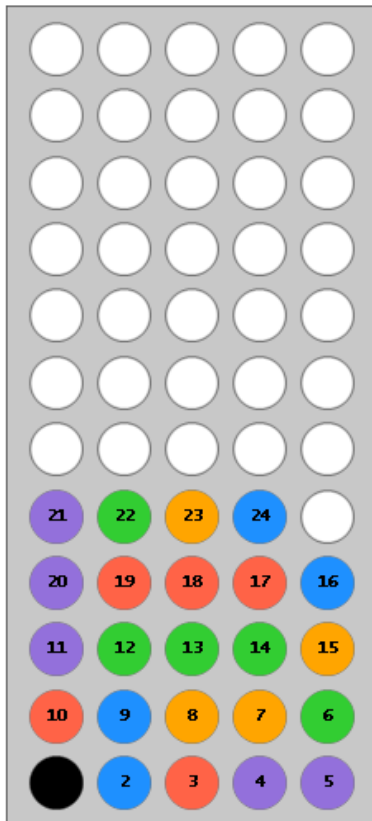
Gradient Table

	Min	Solvents	% 2nd
1	0.0	AC	50
2	1.0	AC	50
3	5.0	AC	90
4	5.0	AC	90
5	2.0	AC	100
6	1.9	AC	100
7	0.9	AC	100
8	0.1	AC	100
9	0.0	CD	0
10	2.4	CD	4
11	0.1	CD	4
12	3.5	CD	19
13	1.0	CD	40
14	1.0	CD	40
15	0.0	CD	0
16	1.0	CD	0

Vial Mapping Table

Peak #	Start Tray:Vial	End Tray:Vial
1	1:6	1:6
2	1:7	1:8
3	1:10	1:10
4	1:11	1:11
5	1:12	1:14
6	1:16	1:16
7	1:17	1:19
8	1:20	1:21
9	1:22	1:22

Page 1

[241]

Fig 3. 58 ECE fraction run

Method Name: dapo-ec.5.3
Run Name: 2011-11-23.dapo-ecbh54
Run Date: 2011-11-25 10:31

Column: Reveleris® Silica 12g
Flow Rate: 36 mL/min
Equilibration: 0.0 min
Run Length: 12.7 min
Air Purge Time: 0.5 min

Slope Detection: Medium
ELSD Threshold: 4 mV
UV Threshold: 0.03 AU
UV1 Wavelength: 254 nm
UV2 Wavelength: 280 nm

Collection Mode: Collect Peaks
Per-Vial Volume: 15 mL
Non-Peaks: 15 mL
Injection Type: Dry

ELSD Carrier: Iso-propanol
Solvent A: Hexane
Solvent B: Ethyl acetate
Solvent C: Methylene chlorid
Solvent D: Methanol
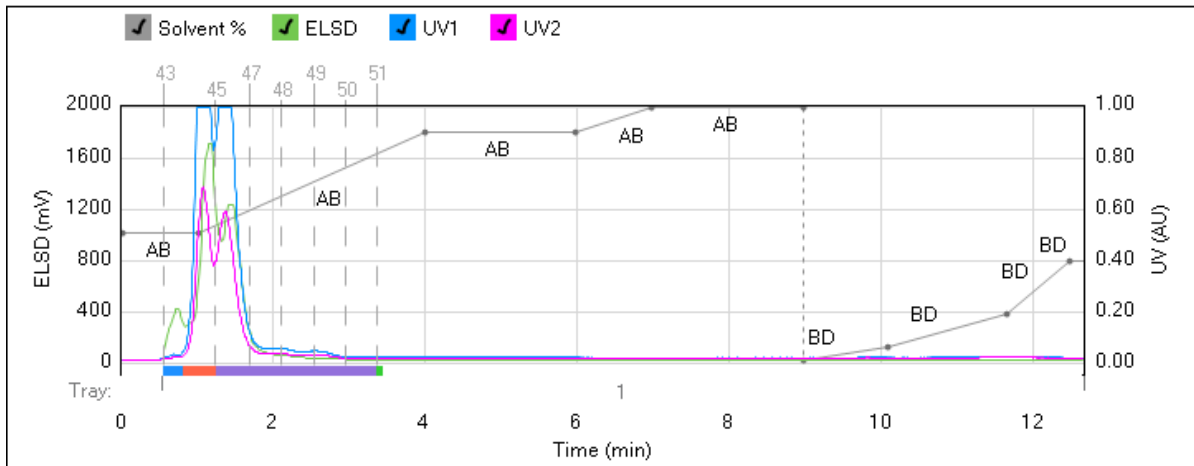
1 - 5B0C
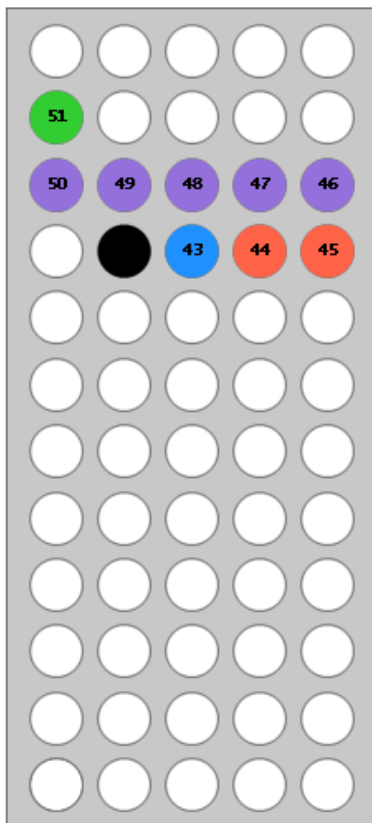
Gradient Table

	Min	Solvents	% 2nd
1	0.0	AB	50
2	1.0	AB	50
3	3.0	AB	90
4	2.0	AB	90
5	1.0	AB	100
6	2.0	AB	100
7	0.0	BD	0
8	1.1	BD	5
9	1.6	BD	18
10	0.9	BD	39
11	3.5	BD	40

Vial Mapping Table

Peak #	Start Tray:Vial	End Tray:Vial
1	1:43	1:43
2	1:44	1:45
3	1:46	1:50
4	1:51	1:51

Page 1

[242]
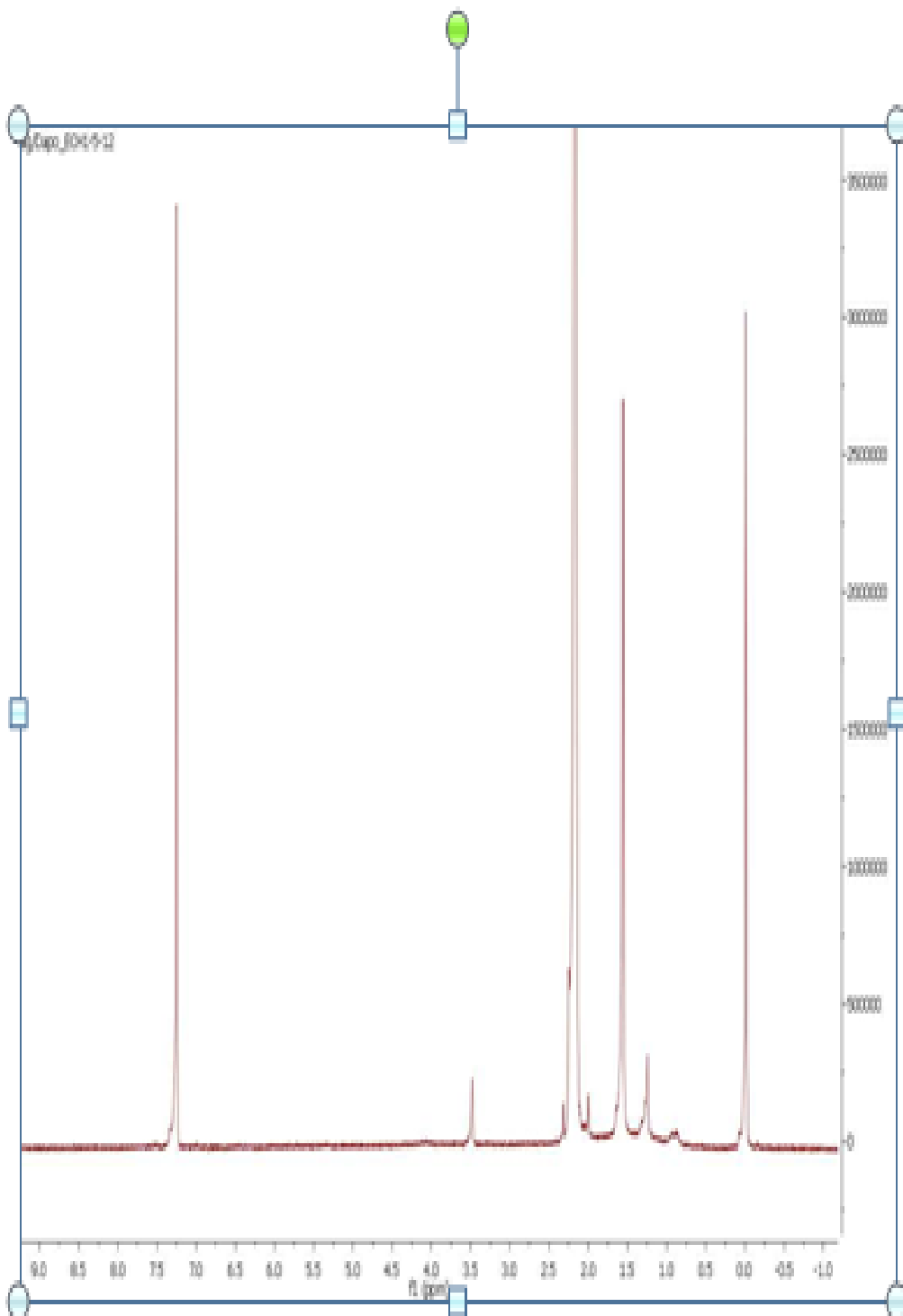
Figure 3.59 showing a nearly pure fraction obtained from Normal phase HPLC
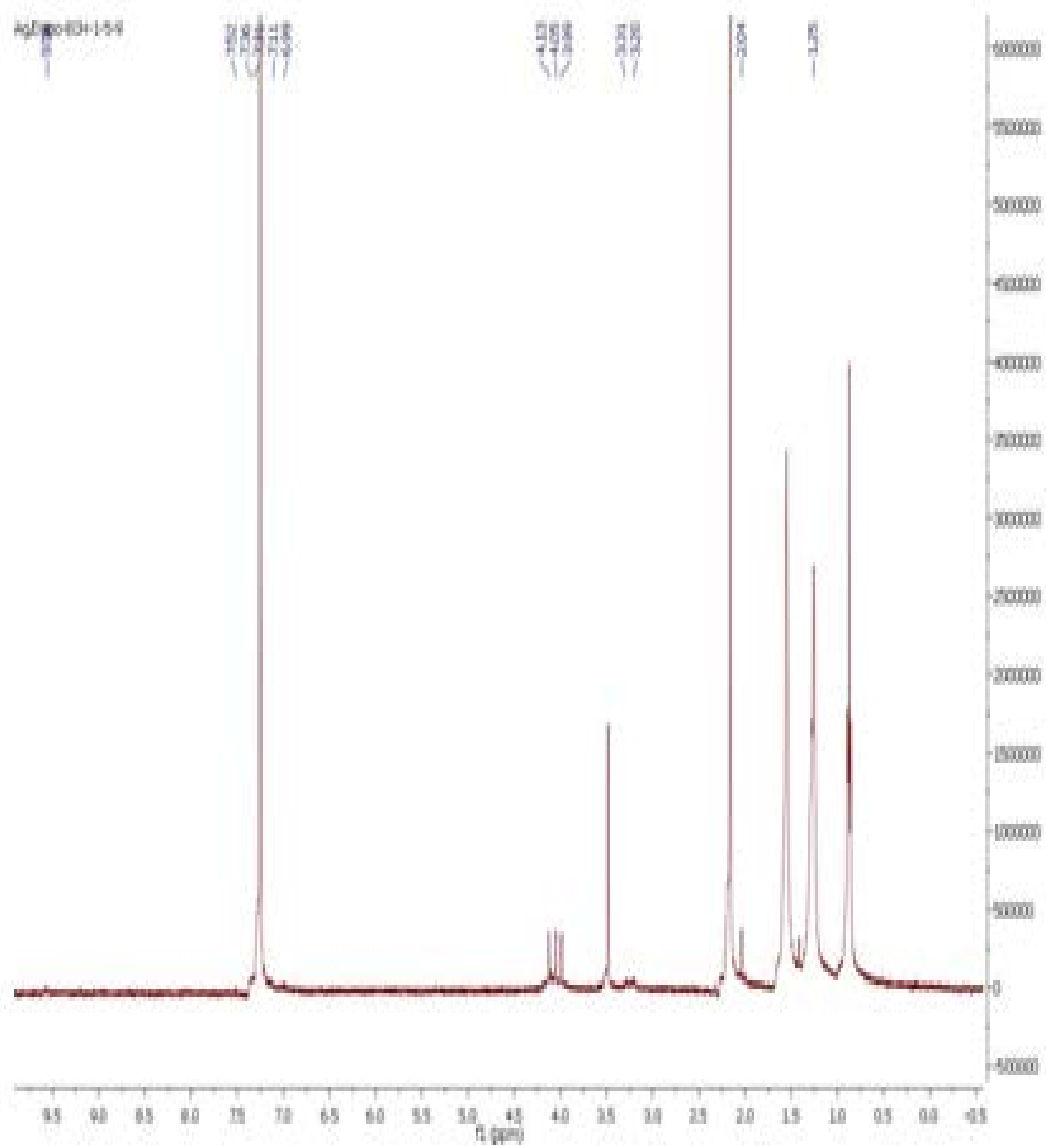
Figure 3.60 showing another nearly pure fraction obtained from Normal phase HPLC however in very small quantity.

Table 5.9 HPLC run fractions and retention times

Fraction code	Retention time	Area
ECP-19	1.16.825	472193
	2.23.162	778430
	3.30.703	668001
	4.32.058	796946
	5.33.252	871119
	6.34.915	420942
	7.35.498	602905
ECH 56	1.5.152	596299
	2.14.702	1423449
	3.22.500	1090082
	4.26.600	1571781
	5.27.312	1139393
	6.29.992	5252015
	7.33.491	829711
ECP-17	1.13.245	1124428
	2.23.243	2819891
	3.26.933	749077
	4.33.278	1564206
	5.35.593	2458988
ECHE-45	1.23.555	7982150
	2.33.435	10589159
	3.34.582	2850813
	4.35.702	8611711
ECF 5-10	1.2.620	1105576
	2.4.812	1526884
	3.5.300	50687
	4.20.503	921879
ECP 23	1.23.587	794659
	2.33.752	752731
	3.34.630	941846
	4.35.748	533593
ECHB17-18	1.4.877	219980
	2.8.262	249552
	3.12.920	91463
	4.13.452	320789
	5.19.598	192492
	6.26.075	118896
ECH 59	1.23.295	7233461
	2.33.252	8301715
	3.34.917	3081333
	4.35.498	6691798
ECBH 35P	1.17.232	12125321
	2.23.232	12127997
	3.31.972	4433479
	4.33.170	23591280
ECBE 72	1.23.491	1729934
	2.30.693	2608903
	3.33.218	1892601
	4.35.467	2113154

ECH 62	1.4.892	112783
	2.13.483	910649
	3.19.613	473922
	4.20.928	5929276
	5.26.612	784693
	6.29.113	350274
	7.30.108	316773
	8.33.518	501551
ECBE 42	1.16.825	26494353
	2.23.162	21685327
	3.32.058	6288656
	4.33.252	19772185
	5.34.915	4769098
	6.35.498	6297934

Hepatocytes in vitro metabolism and toxicity studies.

3.42 mg of Palmatine was weighed accurately in a pre-labelled vial. A solution of 10 uM of it dissolved in Kreps-Hepes (KH) buffer with PH 7.4. Four clean round bottom flasks were labelled A-D.

Flask a Hepatocytes alone
Flask B Palmatine alone
Flask C Hepatocytes and Palmatine
Flask D Empty

Aliqouts of 100ul of the Palmatine – (KH) buffer were introduced by means of a pipette into Flask B and C.
A stock solution of 25 mls containing 23 mls of KH and 2mls of hepatocytes, 10 ml of this were added to contents of Flask C and Flask A.

Krebs-Henseleit buffer solution was made from:
Distilled H_2O -785ml
16.09% NaCl Solution -200ml
1.10% KCl solution- 150ml
0.22 MKH_2PO_4 - 25ml
2.74% Mg SO_4 $7H_2O$ -50ml
0.12 % $CaCl_2.6H_2O$ -100ml.
The KH buffer's stock solution was stored at 4 ^{o}C prior to use in this study.

Perfusion Procedure
 Handling of animals were done following the UK Home Office Licence regulations and guidelines.
Hepatocytes were isolated from male Sprague-Dawley (weighing 165-259g) rat liver by means of modified collagenase perfusion method Grant (2008).

The buffers:
Hank's buffer contains:
NaCl -80.g
KCl - 4.0g
$MgSO_4. 7H_2O$- 2.0g

NaHPO$_4$.2H$_2$O- 0.6g
KH$_2$PO4   -0.6g

HI buffer:
NaHCO3   -1.05g
Hepes   -1.50g
BSA (fraction V)- 3.33g
EGTA (a chelator) -114mg
Distilled water – 450 ml
Hank's buffer – 50ml

HII buffer:
NaHCO$_3$ -1.05g
Hepes   -1.50g
CaCl$_2$ 2H$_2$O -147mg
Distilled H$_2$O -450ml
PH of the mixture adjusted to 7.4 by adding NaOH methodically

Anesthetized rats by means of injection of Phenobarbitone Sodium at dose of 100UL/100g body weight .The rats' peritoneal cavity dissected open using a mid transverse incision and 0.1ml of heparin solution 1,000iu/ml(Sigma Chemical co., Poole, Dorset UK) in Phosphate buffer saline (PBS with PH 7.4) was injected into the inferior vena cava.
Thereafter the portal vein was cannulated and perfused in Hank 1 buffer (HI) buffer 150ml without recirculation for 3-4 minutes (time it takes to remove the liver from the body) and then recirculation of buffer for 10-12 minutes.
The HI buffer is calcium free with its EGTA (chelator) content during the 1st 10 minutes of recirculation removes Ca^{2+} thus weaken the bond between the cells .This is the 1st step in optimising the rat livers for collagenase digestion.

  The next stage involves perfusing the liver with HII buffer (150ml) is added to collagenase type IV derived from Clostridium histolyticum 267 units/mg (Gibco BRL Life technologies, Paisley, UK) recirculating for 12 to 20 minutes.

The processed rat liver at this point feels very soft and cells inside the liver sac dissociated, it is then dispered carefully using sterile forceps into KA buffer containing 1% (w/v) bovine serum albumin. The subsequent cell suspension was filtered using cotton wool gauze to remove connective tissues and clump of cells impurities. The resultant filtrate is collected in 200ml volumetric flask and processed hepatocytes were allowed to stand under gravity, the supernatant decanted and the processed hepatocytes washed once with KH buffer (70ml)

Viability test
The viability of the processed rat hepatocytes were determined using the Tryptan blue exclusion test , above 75% viability was taken as benchmark with yield of viable cells between 20-25 X 10^6

Water bath at 90°C had the flask A-D rotating by means of rotator evaporator to allow the hepatocytes an enabling condition to metabolise the added drug (compound).

Flask A Hepatocytes alone
Flask B Palmatine alone
Fask C Hepatocytes and Palmatine
Flask D Empty

At intervals of 0,15, 30,45,60,90 and 120 minutes aliquots of 100ul were added by means of pipette into Eppendorf's (vials) and placed as soon as possible into liquid nitrogen prior to being frozen at -20°C until LC-MS and HPLC analysis of
metabolites.

50ul aliquots were added by means of pipette into Eppendorfs from Flask A and C alongside 50 ul of Tryptan blue, the mixture introduced onto the slide and viewed under the microscope to count the sur- viving cells and determine the viability.

1. Palmatine
Initial viability prior to water bath conditions is 79.4%

 Table 5.10 Viability results

Time 0

	Live	Dead	Viability %
A	92	11	78
C	90	13	74

Time 60

A	92	11	78
C	90	13	74

Time 120

A	33	17	66
C	25	25	50

This results could be insight into mode of excretion of these group of alkaloids described in this study and potential half-life, though more detailed and specific studies tailored along such lines would be needed to decipher this.

Table 5.11: The 24 natural products discovered since 1970 that led to an approved drug in 1981-2006

Lead, year and structural class	Origin	Approved drug, and year
Validamycin, 1970	Actinomycete	Acarbose, 1990
Oligosaccharide		Voglibose, 1994
Midecamycin, 1971	Actinomycete	Miocamycin, 1985
Macrolide		
Pseudomonic acid , 1971	Bacteria	Mupirocin, 1995
Polyketide		
Taxol,1971	Plant	Paclitaxel ,1993
Diterpene		Docetaxel, 1995
Cephamycin C , 1971	Actinomycete	Moxalactam, 1982
B-lactam		Cefotetan , 1984
		Cefbuperazone, 1985
Coformycin, 1974	Actinomycete	Pentostatin, 1992
Nucleoside		
Echinocamdin B 1974	Fungus	Caspofungin, 2001
Cyclopeptide		Micafungin,2002
		Anidulafungin 2006
Mizoribine, 1974	Fungus	Mizoribine,1984
Nucleoside		
Rapamycin ,1974	Actinomycete	Sirolimus, 1999
Polyketide		Everolimus, 2004

		Zotarolimus, 2005
Compactin ,1975 Polyketide	Fungus	Lovastatin ,1984
		Simvastatin ,1988
		Pravasatin, 1989
		Fluvastatin ,1994
		Atorvastatin 1997
		Cerivasatin, 1997
		Pitavastatin 2003
		Rosuvasatain ,2003
Cylosporine A, 1975 Cyclopeptide	Fungus	Cyclosporine ,1983
Lipstatin, 1975 Polypeptide	Actinomycete	Orlistat, 1987
Bestatin, 1976 Peptide	Actinomycete	Ubenimex, 1987
Thienamycin, 1976 B-lactam	Actinomycete	Imipenem,1985
		Meropenem, 1994
		Panipenem, 1994
		Faropenem,1997
		Biapenem,2002
		Ertapenem,2002
		Doripenem,2005
Artemisinin, 1977	Plant	Arteminin, 1987

Sesquiterpene		Artemether, 1987
		Artenusate, 1987
		Arteether,2000
Forskolin,1977	Plant	Colforsin,1999
Diterpene		
Plaunotol,1977	Plant	Plaunotol,1987
Diterpene		
Avermectin B_1 a , 1979	Actinomycete	Ivermectin,1987
Polyketide		
SQ26, 180, 1981	Actinomycete	Aztreonam, 1984
B-lactam		Carumonam, 1988
Sperrgualin,1981	Bacteria	Gusperimus,1994
Peptide		
Arglabin, 1982	Plant	Gusperimus,1994
Sesquiterpene		
FK506,1984	Actinomycete	Arglabin,1999
Polyketide		
Daptomycin,1986	Actinomycete	Daptomycin , 2003
Cyclodepsipeptide		
Calicheamicin $_{Y1}$, 1988	Actinomycete	Gemtuzumab,2000
Polyketide		

Table 5.12 Rerank Pose scores of antitrypanosomal protein targets against previously isolated alkaloids from *Enantia chlorantha*

EC Compounds	TbAK	TbPTR1	TbDHFR	TbTR	TbCatB	TbHSP90	TbCYP51
Atherosperminine	-23.9	-26.2	-20.8	-23.6	-16.6	-21.9	-20.6
Columbamine	-24.6	-24.2	-19.4	-22.1	-17.4	-22.8	-22.1
Jatrorrhizine	-24.9	-25.8	-21.3	-22.4	-15.7	-23.8	-21.8
Lanuginosine	-24.6	-26.1	-19.9	-24.1	-16.6	-22.5	-20.9
Liriodenine	-22.3	-23.9	-19.2	-22.6	-18.2	-23.2	-18.7
Lysicamine	-23.7	-23.9	-18.1	-22.2	-16.1	-24.1	-18.6
Palmatine	-24.3	-24.7	-20.5	-24.4	-14.2	-23.2	-23.2
Isoboldine	-23.8	-25.0	-21.6	-22.1	-19.4	-23.9	-22.3
Isocorydine	-24.3	-23.9	-20.9	-22.9	-17.3	-24.1	-20.2
8-hydroxypalmatine	-24.2	-26.4	-19.4	-21.1	-16.6	-21.7	-24.0
O-Methylmoschatoline	-23.2	-22.6	-18.0	-23.2	-14.3	-22.5	-18.8
Argentinine	-24.1	-26.1	-22.4	-23.9	-17.3	-24.7	-22.4
Pseudocolumbamine	-21.6	-25.3	-27.5	-20.2	-22.8	-18.3	-23.4
Pseudopalmatine	-25.0	-27.5	-20.9	-23.5	-17.9	-23.4	-20.9

EC: *Enantia Chlorantha*

Antitrypanosomal protein targets: TbAK *T.brucei* adenosine kinase,

TbPTR1 *T. brucei* pteridine reductase 1 *T brucei* dihydrofolate reductase ,TbTR *T. brucei* trypanothione reductase , TbCatB *T brucei* cathepsin B, *TbHSP90 T brucei heat shock protein 90,TbCYP51 T brucei* sterol 14α-demethylase
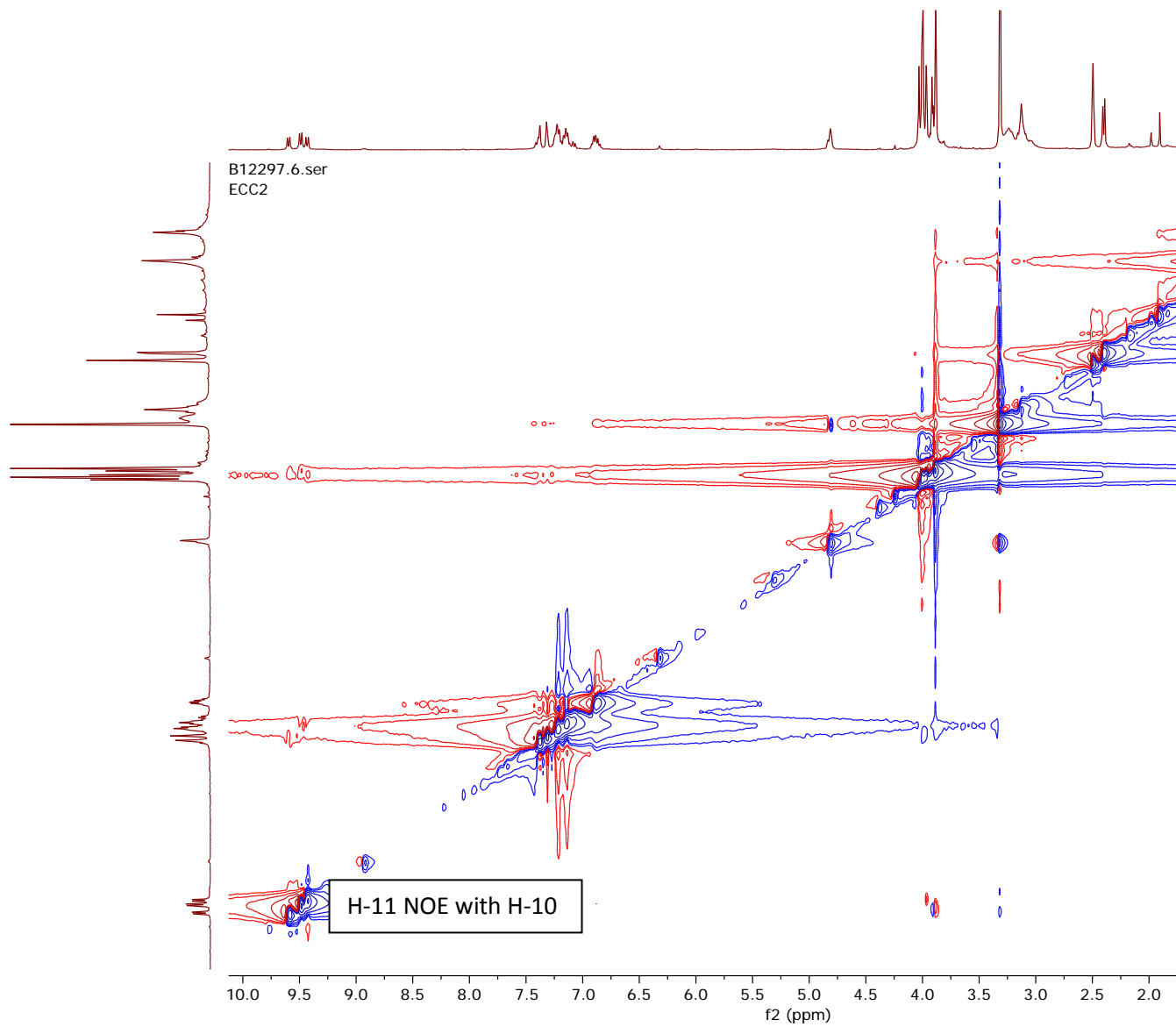
B12297.6.ser
ECC2

H-11 NOE with H-10

f2 (ppm)

Fig 3.61 NOE spectrum employed in structure elucidation of alkaloids in this thesis

References

Achenbach, H.and Schwinn, A. (1995). Aporphinoid alkaloids and terpenoids from *Piptostigma fugax* .Phytochemistry.91:1090-1048.

Adesokan, A. A., Yakubu, M.T., Owoyele, B. V., Akanji, M. A., Soladoye, A. O. and Lawal, O,(2008). Effect of administration of aqueous and ethanolic extracts of *Enantia chlorantha* stem bark on brewer's yeast-induced pyresis in rats. African Journal of Biochemistry Research.2(7):165-9

Adesokan,A.A, Akanji, M.A ,Yakubu, T.Y(2007). Antibacterial properties of aqueous

extract of *Enantia chlorantha* stem bark. African Journal of Biotechnology.6(22)2502-5

Adjanohoun,E.J.,Aboubakar,N.,Dramare,K.,Ebot,M.E.,Ekpere,J.A.,Enow-Orock,E.G.,Focho, D.,Gbile,Z.O.,Kamanyi,A.,Kamsu,K.J.,,Keita,A.,Mbenkum,T.,Mbi,C.N.,Mbiele,A.l.,Mbore,I.L.,Mibir u,N.K.,Nancy,W.L,Nkongmeneck,B.,Satabe,B.,Sofowora,A.,Tamze,V., and Wirmum,C.K. (1996) . Contribution to Ethnobotanical and Floristic studies in Cameroun. Traditional Medicine Pharmacopoe-ia.694

Agbaje,E.O. and Onabanjo, A.O., (1998). Analgesic and Antipyretic actions of *Enantia chlorantha* aqueous extract in some laboratory animals: Niger J Nat Prod Med, 2:24-25.

Amstrong, J. (2010).General, Organic, and Biochemistry: An Applied Approach: 132

Andrews, J.M., (2001). Determination of minimum inhibitory concentrations. J Antimicrob Chemoth-er ;48 Suppl, 1:5-16

Arango,G.J.,Cortes,D. and Cave,A.(1987). Three Bis- dehydroaporphine from Oxandra CF major. Phytochemistry 26:1227-9

Bahar, M.(2012). PhD thesis, Ohio State University, Pharmacy.

Black, S.J., Seed, J.R. (2005). African Trypanosomiasis. In Topley and Wilson 's Microbiology and Microbial Infections, 10 [th] Edition, Hodder Arnold Publishers: 112

Blum, J.,Brun, R., Chappuis, F., Burri, C.(2009). Human African trypanosomiasis:148-59

Bose,R.,Anderson,S.,Lawrence,K.(2010). RevealX[TM] Technology improves Isolation and Purification of natural products by Flash Chromatography.Grace Davison Discovery Sciences,US: 2-7

Bourdat-Deschamps, M., Herrenknecht, C., Akendengue, B., Laurens, A., Hocquemillier, R. (2004). Separation of protoberberine quaternary alkaloids from a crude extract of *Enantia chlorantha* by cen-trifugal partition chromatography. Journal of Chromatography 1094(1-2):143-52

Braithwaite, E. and Smith,F.J.(1996). Chromatographic methods,5th edition, Blackie Academic and Professional:117-64

Braithwaite, A., Smith F.J.,(1996)[2]. Chromatographic Methods. 5th edition, Blackie academic and professional, Glasgow, 253.

Breitmaier,E.(1993). Structure elucidation by NMR in organic chemistry. John Wiley and Sons

Cassidy, H. G.(1992). Adsorption analysis: Tswett's chromatographic method. J. Chem. Educ., 16 (2):88

CDC,Atlanta Georgia (2009).http://www.cdc.gov/parasites/sleepingsickness/biology.html

Clark, J.P.,(2007).www.chemguide.co.uk/analysis/chromatography/hplc.html

Copeland A, Younes A(2010). Brentuximab vedotin. Drugs Fut.35:797–801

Connolly, J. D., Hague, E. and Kadir, A.A,.(1996). Two 7,7' – Bisdehydroaporphine alkaloids from *Polyalthia bullata.* Phytochemistry 43(1) 295-7

Determann,H. and Brewer, J.E.(1975). Gel chromatography.In Chromatography-A laboratory handbook of chromatographic and electrophoretic methods. Springer:164-88

Derwent publications(1990). Pests,weeds and diseases. Thesaurus of Agricultural Organisms:23

Discovery science,(2009).http://www.discoverysciences.com

Eliott, R.L.. (2011). Third World Diseases. Springer 2nd edition :192

Federation of Infectious Diseases Societies of South African bulletin Fidssa(2012):Case of the month ;January 2012 pp 2.

Fournet,A.,Rojas de Arias,A.,Ferreira,M.E., Nakqayama ,H.,Torres de oritz,S.,Schinini,A.Samudio,M, Vera de Bilbao N, Lavault,M and ,Bonte,F.(2000). Efficacy of the bisbenzylisoquinoline alkaloids in acute and chronic *Trypanosoma cruzi* murine models. International Journal of Antimicrobial Agents 13:189-195.

Franzblau,S.G., Witzig, R.S., McLaughlin, J.C., Torres, P., Madico, G., Hernandez, A., Degnan, M.T., Cook, M.B., Quenzer, V.K., Ferguson, R.M., and Gilman, R.H. (1998). The screen utilises a modification of the microplate Almar blue method for susceptibility testing of fast growing species of Mycobacterium ,Journal of Clinical Microbiology : 892-896

Freemantle M.(2004) Scaled-up synthesis of discodermolide. Chem & Eng News.82(9):33–35

Ganesan ,A.,(2008). The Impact of natural products upon modern drug discovery. Current opinion in Chemical Biology 12:309-310.

Gbadamosi,A.E., Oni, O. (2005). Macropropagation of an endangered medicinal plant, *Enantia chlorantha oliv*. Journal of Arboriculture 31: 78-82

Geng,X. and Regnier,F.E.(1984). Retention model for Proteins in Reversed-Phase Liquid Chromatography. J.Chrom.:296:15

Gill, L.S. and Akinwumi, C.(1986). Nigerian folk medicine: practices and beliefs of the Ondo people. J Ethnopharmacol 18: 257-266

Guinaudeau,H., Wong-panich,V.,Pezzulo,J.M.,Cordell,G.A. and Angerhofer,C.K.(1994). Aporphinoid Alkaloids. Journal of Natural Products 57 (8) 1033-1135

Hamonniere, M. M., Leboeuf, A. and Cave A.(1975). Annonaceae alkaloids:alkaloidal content of *Enantia chlorantha.* Plantes Medicinales Phytotherapie 4:296-303

Hsu, B. and Kin K.C.,(1962). Pharmacological study of tetrahydropalmatine and its analogs. A new type of central depressants.Arch Int Pharmacodyn Ther.192:318-327

Huang KC(1999). The pharmacology of chinese herbs. 2. CRC Press; Boca Raton, FL.

Hutchings,M.R.,Athanasiadou,S.,Kyriazahis,I. and Gordon, D. (2003). Can animals use foraging behaviour to combat parasites.Proc Nutr.Soc. 62 (2):891-70

Iwasa , K., Kamigauchi,M., Ueki,M. and Taniguchi,M.,(1996). Antibacterila activity and structure-activity relationships of berberine analogs.Eur J Med Chem.31:469-78

Iwu M.M.,(1993)Handbook of Africn Medicinal plants. LL.C US:RC Press pp.2

Kapoor L.D., (1990) Crc handbook of ayurvedic medicinal plants. CRC Press; Boca Raton, FL.

Katzung B.G.,(2004) Basic and Clinical Pharmacology, 9th edition, a Lange Medical book :882-3

Kevin, J.H.(2009). Synthesis of δ-amides of eflornithine to improve oral bioavailability (Masters of Science thesis submitted to School of Pharmacy, NorthWest University, South Africa)

Kirchoff, L.V.(1993). American trypanosomiasis (Chagas's disease) –A Tropical disease now in the United State*s*.New England Journal of Medicine.329:692-644)

Kupchan et al.,(1963) .Tumor-inhibitory alkaloid from Thalictrum dasycarpum Fisch. & Lall., Ranunculaceae: J. Pharm. Sci. 52, 985

Laprovete,O.,Roblot,O.,Hocquemiller R., and Cave,A.(1988). Alkaloids of Annonaceae:*Unonopsis spectabilis*. Journal of Natural Products 51(3) 555-561.

Leboeuf,M. A.,Cavé, P.K., Bhaumik, B. ,Mukherjee, R., Mukherjee, R., (1980). The phytochemistry of the annonaceae. Phytochemistry.21(12):2783-813 .

Li,K.,Zhu,W.,Fu,Q.,Ke,Y.,Jin,Y.,Liang,X.(2013). Purification of amide alkaloids from Piper longum L. using preparative two-dimensional normal-phase liquid chromatography reversed-phase liquid chromatography. Analyst 191(11)33133-20

Mackey,Z.B., Baca,A.M.,Mallari,J.P.,Apsel,B.,Shelat,A.,Hansell,E.J.,Chiang,P.K.,Wolff,B,William,J. and McKenow,J.H .(2006). Discovery of Trypanocidal compounds by Whole cell HTS of *Trypanosoma brucei*. Chemical Biology and Drug Design.67(5) 355-63.

Marsaioli, A., (1979). ^{13}C NMR analysis of some oxo-aporphine alkaloids. Phytochemistry.19:995-7.

 Mc Call, D.L.C., Alexander,J.,Barber,J.,Jaouhari,R.G., Satoskar,A. and Waigh R.D. The first proto-berberine alkaloid analogue with in vivo antimalarial activity. Bioorganic and Medicinal Chemistry Letters 4 (14): 1663-6.

Moody, J.O.,Bloomfield S.F.,Hylands, P.J.(1995)*: In vitro evaluation of antimicrobial activities of En-antia chlorantha Oliv* extractives*. African Journal of Medicine and Medical Sciences.24 (3) :269-273

 National Institutes of Health report (2002) :Greek Medicine:1-2

Newman, D.J.,Cragg,G.M.,Snader,K.M.,(2000). The Influence of natural products upon drug discovery.Natural products reports,17(3):215-234.

Nyasse,B.,Nkwengoua,E.,Sondengam,B.,Denier,C.,,Wilson,M., (2002). Modified berberine and pro-toberberines from *Enantia chlorantha* as potential inhibitors of *Trypanosoma brucei*. Pharmazie 57 : 358-61

Oliver, D. (1868.). Annonancae. Flora of Tropical Africa.1:172-5

O'Neill, P.M., Posner, G.H., (2004).A medicinal chemistry perspective on artemisinin and related en-doperoxides.J Med Chem.;47:2945–2964.

Oyewopo, C., Jimoh, A., Yama, O.E., Kadir, R.E. and Olaniyan, O.T.(2012). Testiculo-Protective ef-fect of stem bark extract of *Enantia chlorantha* on lead induced toxicity in adult Wistar rat *(Rattus norvergicus)*. Reproductive System and Sexual Disorders.1:107-111

Ogungbe,I.V. and Setzer, W.N., (2012). In-silico investigation of antitrypanosomal phytochemicals from Nigerian medicinal plants. PLoS Neglected Tropical Diseases.6(7):1727-47

Panda,H.(2010). Handbook on Drugs from Natural sources.*Vinca rosae.* Asia Pacific Business Pressinc.217-218.

Pitchaimani R.,(2012) Shodhanga: Chapter 1 pp 9

Priotto G.,Kasparian S.,Mutombo W., *et al.,*(2009). Nifurtimox-eflornithine combination therapy for second stage African *Trypanosome brucei gambiense* trypanosomiasis:a multicentre,randomised, phase III, non-inferiority trial". Lancet 904(9683):56-64.

Kennedy,P. (2007)[1] . The Fatal Sleep.Luath Press Limited, Edinburgh;112

Kennedy,P.G.E., (2007)[2]. The Fatal Sleep.Luath Press Limited, Edinburgh;64

Kennedy,P.G.E., (2007)[3]. The Fatal Sleep.Luath Press Limited, Edinburgh;74

Kennedy P.G.E., (2013). Clinical features, diagnosis, and treatment of human African trypanosomiasis (sleeping sickness). The Lancet Neurology, vol 12, no 2 pp 186-194.

Raz, B., Iten, M., Grether-Buhler, Y., Kaminsky, R. and Brun, R.(1997). The Almar Blue assay to de-termine drug sensitivity of African trypanosomes (*T.b. rhodesiense* and *gambiense)* in vitro Acta Tropica, Vol.68, p.192-147 (1997).

Saleem N. H., Valerie A. Ferro,Simpson A.M.,Igoli J.,Gray A.I., and Drummond,R.M.,(2013). The Inhibitory Effect of Haloxylon salicornicum on Contraction of the Mouse Uterus. Evidence-Based Complementary and Alternative Medicine. Volume 2013 pp 65-75.

Schiff Jr, P.L.(1987). Bisbenzyliosquinoline alkaloids. Journal of Natural Products 50(4) :529-599

Schmidt, T.J.(2010). Natural products as Antiprotozoal leads –In-vitro and In-silico activity studies. Molecules.129:127-130.

Seed J.R, Hall J.E(1992). Protozoa: Pathogenesis and Defenses. Medical Microbiology. 4th edition, edited by Baron,S.:112

Shilpi, J.A.(2009). Phytochemical and Antimicrobial Studies on *Ludwigia adscendens*, *Trewia +nudiflora* and *Hygrophila auriculata* from Bangladesh. Thesis,University of Strathclyde.

Simarro,P.P., Cecchi.G.,Franco.J.R.,Paore,M.,Diarra,A.,Ruiz-Postigo,J.A.,Fevre,E.M.,Mattioli,R.C., and Jannin,J.C, (2012). Estimating and Mapping the Population at Risk of Sleeping Sickness. PLOS Neglected Tropical Diseases 6 (10)):1-12

Stahl,E. and Mangold,H.K.(1975). Techniques of thin layer chromatography. In Chromatography. Alaboratory handbook of chromatographic and electrophoresis methods. Edited by Heftmann,E.Third Edition. Springer-Verlag;164-88.

Stock,R. and Rice, C.B.(1974). Chromatographic methods. Chapman and Hall. Third edition. Pp279-317.

Stenlake, J.B., Waigh, R.D., Dewar G.H.(1981). Biodegradable neuromuscular blocking agents. Part 4 Atracurium besylate and related polyalkylene di-esters. Eur J Med Chem ;16: 515-24.

Stierle, A., Strobel, G., Stierle, D., Grothaus, P., Bignami G.(1995). The search for a taxol-producing microorganism among the endophytic fungi of the Pacific yew,*Taxus brevifolia*: 58(9):1315-24.

Subeki, Matsuura H., Takahashi K., Yamasaki M., Yamato O., Maede Y., Katakura K., Suzuki M., Trimurningsih, Chairul, Yoshihara T.(2005). Antibabesial activity of protoberberine alkaloids and 20-hydroxyecdysone from *Arcangelisia flava* against *Babesia gibsoni* in culture .J Vet Med Sci. 67(2):223-7.

Tan,P.V, B. Nyasse, G. E., Enow-Orock, P., Wafo, E. A., Forcha.(2000). Prophylactic and healing properties of a new anti-ulcer compound from *Enantia chlorantha* in rats . Phytomedicine.7 (4):291-6)

Tan PV, Nyasse B, Dimo T, Wafo P, Akahkuh BT.(2000). Synergistic and potentiating effects of ranitidine and two new anti-ulcer compounds from *Enantia chlorantha* and *Voacanga africana* in experimental animal models.Pharmazie. .57(6):939-12

Vansterkenburg, E.L.M., Coppensm I., Wiltingm J., Bos, O.J.M., Fischer M.J.E., Janssen L.H.M., *et al*.,(1993). The uptake of the trypanocidal drug suramin in combination with low-density lipoproteins by*Trypanosoma brucei* and its possible mode of action. Acta Trop.;54:290–250

Van Lanen S.G., Shen B.(2012) Combinatorial biosynthesis of anticancer natural products. Anticancer agents from natural products. Taylor and Francis; Boca Raton, FL: pp. 671–698

Vennerstrom,J.L and Klaymen,D.L.(1987). Inhibition of monoamine oxidase by palmatine. J. med. Chem.31:1084.

Vennerstrom, J. L, Lovelace,J.K., Waits,V.B., Hanson, W.L. and Klayman, D.L.: Berberine derivatives as antileishmanial drugs . Antimicrob. Agents Chemother.(1990)34(5) 918-21.

Vennerstrom,J.L. , Daniel, L. Klayman(1988). Protoberberine alkaloids as antimalarials; J. med. Chem. 31 (6):1084–7.

Vickerman, K. (1985). Developmental cycles and biology of pathogenic trypanosomes. *Br Med Bull*; 94**:** 105–14.

Virtanen,P.V,Lassila,V.,Soderstrom,K.O .(1993). Hepatoprotection Pathobiology :61:51-9

Virtanen, P.,Lassila, V.,Njimi, T.,Ekotti,M.D.,(1988). Regeneration of D-galactosamine-traumatized rat liver with natural protoberberine alkaloids from *Enantia chlorantha*. Acta Anat 132:159-163

Wafo, P., Nyasse, B., Fontaine, C., Sondengam,B.L..(1999). Aporphine alkaloids from *Enantia chlorantha*. Fitoterapia, 70:157-160.

Wierenga, R.K., Swinkels, B., Michels, P.A., Osinga, K., Misset,O., Van Beeumen, J., *et al*.,(1987). Common elements on the surface of glycolytic enzymes from *Trypanosoma brucei* may serve as topogenic signals for import into glycosomes. EMBO J.;6:215–221

Wijeratne, M.K, Lankananda, B.D.*et al*.,(2001). Dimeric Aporphine Alkaloids of *Phoenicanthus oblique* from Sri Lanka.Journal of Natural Products: 64 (11):1465-7.

Wongsrichanalai,C.,Pickard,A.L.,Wernsdorfer,W.H.,Meshnick,S.R.,(2002). Epidemiology

of drug-resistant malaria Lancet Infect. Dis. 2 pp. 209–218.

World Health Organization Report (2014) Update March 2014. Chagas disease (American trypanosomiasis) Factsheet N[O]340.

World Health Organization (1998). Human African Trypanosomiasis (sleeping sickness): epidemiological update.*Wkly Epidemiol Rec*.81:69–80.

Wu, W. and Huang, J., (2006). Structural elucidation of Isoquinoline, Isoquinolone, Benzyisoquinoline, Aporphine and Phenanthrene alkaloids using API-ion spray Tandem Mass Spectrometry. *The Chinese Pharmaceutical Journal.* 58:94-55.

Yang-Chang Wu.(2006).New research and development on the *formosan annonaceous* plants.Studies in Natural Products Chemistry.33:957–1023.

Yu M.J., Zheng W., Seletsky B.M., Littlefield B.A., Kishi Y.(2011) Case history: Discovery of eribulin (halaventm), a halichondrin b analogue that prolongs overall survival in patients with metastatic breast cancer. In: Macor JA, editor. Ann Rept Med Chem. Vol. 46. Academic Press; Amsterdam: pp. 227–241